N° d'ordre : D.U. : 2689
EDSPIC : 752

Université Blaise-Pascal - Clermont II

Ecole Doctorale
Sciences Pour l'Ingénieur de Clermont-Ferrand

Thèse

présentée par

William FAURIAT
Ingénieur IFMA

en vue d'obtenir le grade de :

Docteur d'Université
Spécialité : Génie Mécanique

Modélisation stochastique des sollicitations provenant de la route pour l'estimation de la fiabilité du châssis et des composants du véhicule par la simulation

Soutenue publiquement le 26 Avril 2016 devant le jury composé de :

Pr. Aléxis BEAKOU	IFMA, Clermont-Ferrand	Co-directeur de Thèse
Pr. Pierre-Alain BOUCARD	ENS, Cachan	Président du jury et Rapporteur
Dr. André BIGNNONET	AB Consulting, Beaulieu-sur-Layon	Invité
Dr. Thierry CEMBRZYNSKI	Renault, Guyancourt	Examinateur
Mr. Bruno COLIN	Nexter Systems, Versailles	Invité
Dr. Nicolas GAYTON	IFMA, Clermont-Ferrand	Co-directeur de Thèse
Dr. Cécile MATTRAND	IFMA, Clermont-Ferrand	Co-encadrante
Pr. Franck MOREL	Arts et Métiers ParisTech, Angers	Rapporteur

Institut Pascal - Axe Mécanique Matériaux et Structures
Université Blaise Pascal et Institut Français de Mécanique Avancée

Stochastic modeling of road-induced loads for reliability assessment of chassis and vehicle components through simulation

A thesis submitted in partial fulfillment
of the requirements for the degree of

Doctor of Philosophy
(Mechanical Engineering)

by

William FAURIAT

Blaise-Pascal University - Clermont II

defended on April 26th 2016 before the following jury:

Pr. Aléxis BEAKOU	IFMA, Clermont-Ferrand	Supervisor
Dr. André BIGNNONET	AB Consulting, Beaulieu-sur-Layon	Guest
Pr. Pierre-Alain BOUCARD	ENS, Cachan	President of the jury and Reviewer
Dr. Thierry CEMBRZYNSKI	Renault, Guyancourt	Examiner
Mr. Bruno COLIN	Nexter Systems, Versailles	Guest
Dr. Nicolas GAYTON	IFMA, Clermont-Ferrand	Supervisor
Dr. Cécile MATTRAND	IFMA, Clermont-Ferrand	Assistant Supervisor
Pr. Franck MOREL	Arts et Métiers ParisTech, Angers	Reviewer

Abstract

In order to design vehicle components that will achieve a prescribed reliability target, it is imperative to possess a precise description of the variability of the loads to which such components may be subjected within the environment in which they are used. The strong diversity of the loads imposed on different vehicles by different customers, or on a particular vehicle throughout its life, constitutes a formidable statistical challenge. Generally, the acquisition of information about the load variability experienced by vehicle components is based on the use of load measurement campaigns. The complexity, duration and cost of such campaigns naturally limit the size of the statistical samples that may be collected. Moreover, the recorded load histories are inevitably dependent on the vehicle used for the measurements.

The work presented within this manuscript explores the possibility of a fundamental change in the approach to load characterisation. The objective is to make use of simulation rather than measurements and focus statistical analysis efforts not directly on load variability itself but on the variability of the factors that determine such loads. Stochastic models are proposed to describe the evolution of the geometry of road surfaces covered by vehicles, as well as the evolution of vehicles' speed on those road surfaces. The characterisation of the variability of such factors is performed in combination with the use of life situations. The latter may be employed to divide the load histories associated to different vehicles, within a population of customers, and analyse their variation more easily. Eventually, the dynamic response of the vehicle to the excitation imposed by the road can be derived through simulation.

Statistical data on the variation of the road and speed factors obviously have to be acquired in order to apply the methodology. For example, road-related information may be obtained through the use of a road profile estimation algorithm proposed within the framework of this manuscript. Such information may then be exploited to constitute, through simulation, an arbitrarily large set of load histories at a very low cost and for any vehicle whose mechanical characteristics are known.

The proposed methodology based on simulation enables us to study more extensively the variability of road-induced fatigue loads, the influence of the different factors that determine such loads, as well as the effect they have on the reliability of any considered vehicle component.

Keywords: road-induced loads, stochastic modeling, vehicle dynamics simulation, fatigue, reliability of vehicle components, durability, operating profile

Résumé

Concevoir un composant automobile et s'assurer que celui-ci atteindra un niveau de fiabilité cible requière une connaissance précise de la variabilité des chargements que ce composant est susceptible de rencontrer dans son environnement d'utilisation. La grande diversité des chargements appliqués à différents véhicules par différents clients, ou à un même véhicule tout au long de son historique d'utilisation, représente un défi statistique majeur. Généralement, l'acquisition d'information relative à la variabilité des chargements imposés aux composants des véhicules, repose sur la réalisation de campagnes de mesures. La complexité, la durée et le coût de telles campagnes limite naturellement la taille des échantillons statistiques constitués et les chargements enregistrés sont inévitablement dépendants du véhicule utilisé pour la mesure.

Le travail présenté dans ce manuscrit explore la possibilité de changer fondamentalement d'approche, en se basant sur la simulation plutôt que sur la mesure et en concentrant l'effort d'analyse statistique non pas directement sur la variabilité des chargements mais sur la variabilité des facteurs qui les déterminent. Dans ce but, des modèles stochastiques sont proposés pour décrire l'évolution de la géométrie des surfaces de routes rencontrées par les véhicules ainsi que l'évolution de la vitesse à laquelle les conducteurs les parcourent. La caractérisation de la variabilité de ces facteurs est couplée à la notion de situations de vie. Ces dernières permettent de segmenter l'historique d'utilisation des véhicules, afin de faciliter l'analyse statistique de leur évolution au sein d'une population de clients. Pour finir, la réponse dynamique du véhicule à l'excitation générée par la route est déduite par la simulation.

Des données statistiques relatives à la variabilité des facteurs de route et de vitesse sont évidemment nécessaires. L'information sur les routes parcourues peut par exemple être acquise à moindre coût au moyen d'une méthode d'estimation des profils de route proposée dans ce manuscrit. Cette information peut ensuite être exploitée afin de constituer, par la simulation, à un coût très faible et pour n'importe quel véhicule dont les caractéristiques sont connues, un échantillon d'historiques de chargements aussi important que souhaité.

Cette méthodologie basée sur la simulation offre la possibilité d'analyser plus largement la variabilité des chargements de fatigue provenant de la route, l'influence des différents facteurs qui les déterminent ainsi que l'effet sur la fiabilité des composants du véhicule étudié.

Mots-clés : chargements provenant de la route, modélisation stochastique, simulation de la dynamique véhicule, fatigue, fiabilité des composants automobiles, durabilité, profil de mission

Remerciements

Au cours de ces trois années passées en grande partie sur le site du Technocentre Renault de Guyancourt, j'ai eu la chance de vivre une expérience forte en enseignements techniques, humains et personnels. Celle-ci n'aurait tout d'abord pas été possible sans la confiance que m'ont accordé Thierry CEMBRZYSKI, statisticien au sein de Renault, ainsi que mon co-directeur de thèse Alexis BEAKOU. Je salue ici leur implication dans la construction de ce projet commun entre Renault et l'Institut Français de Mécanique Avancée (IFMA), aujourd'hui SIGMA Clermont-Ferrand, à qui je souhaite réussite et longévité.

Je tiens à remercier chaleureusement messieurs Pierre-Alain BOUCARD et Franck MOREL d'avoir accepté d'évaluer la qualité de ce manuscrit, ainsi que pour l'intérêt qu'ils manifestent envers mon travail. J'aspire à penser que la lecture de ce manuscrit fera naître des réflexions productives et sera un témoin de ma modeste contribution à l'édifice scientifique. Ma gratitude va évidemment à l'ensemble des membres du jury qui me font l'honneur d'évaluer mon travail.

Je souhaite témoigner ma reconnaissance à mes co-directeurs de thèse Alexis BEAKOU et Nicolas GAYTON ainsi qu'à mon encadrante de thèse Cécile MATTRAND. Leurs conseils, leur expérience, leurs implications et contributions respectives, en dépit d'emplois du temps chargés, mais également leurs compliments et leurs encouragements, ont été grandement appréciés tout au long de cette thèse. Je souhaite aussi reconnaître leur capacité à critiquer (dans le sens positif du terme) mon travail lorsque cela était nécessaire, afin d'en améliorer encore la qualité et la clarté. Ceci m'a permis de perfectionner ma réflexion et mon argumentation au cours de discussions très intéressantes. Votre exigence témoigne également de votre attachement à la réussite de cette expérience.

J'adresse des remerciements particulièrement mérités à mon encadrante de thèse Cécile, pour son travail de correction très détaillé, que ce soit pour ce manuscrit ou pour les différentes publications réalisées. Ta disponibilité, tes conseils et nos discussions techniques ont été d'une aide précieuse.

Pour son accueil chez Renault et son soucis permanent quant au bon déroulement de mon expérience de thèse, je remercie amicalement mon tuteur Renault, Thierry CEMBRZYNSKI. Je te suis reconnaissant pour ta bienveillance.

L'organisation est un être changeant et je tiens à remercier les différents clients et responsables hiérarchiques qui se sont succédé au sein de Renault, madame Christine LE-HUR, monsieur Thierry BAILLIEZ, monsieur Jean-Sébastien BLAZY et plus particulièrement madame Isabelle CHAYE-MAUVARIN pour m'avoir offert l'opportunité de cette expérience de thèse en environnement industriel, très formatrice et certainement déterminante dans mon parcours. Chacun a apporté la contribution que le temps lui permettait, mais tous ont été encourageants et ont cru en mon autonomie.

Je ne peux me montrer exhaustif mais je remercie tous ceux qui ont contribué par leurs conseils, leur travail, leur aide ou leur pilotage, à l'avancée de ce sujet de recherche et m'ont permis d'obtenir un résultat scientifique de qualité. Merci à François, Jean-Marc, Eric, Thierry, Paul, Loic, Reynald, Michel, Nathalie, Laurent, etc...

Je remercie également Joffroy et Maxime, les deux stagiaires BAC+5 qui ont apporté leur contribution à ce travail de recherche. J'espère que cette expérience partagée a été interessante et profitable pour eux autant qu'elle l'a été pour moi. Je leur souhaite le meilleur dans leur vie professionnelle et privée.

Ces trois années de thèse n'auraient pas été les mêmes sans mes collègues Ludovic, Philippe et Stéphane, ainsi que ceux qui sont partis vers d'autres horizons, Jean et Nicolas. Pour leur humour, leur bonne humeur et parfois un brin de folie, je leur dis merci et leur souhaite une heureuse continuation de carrière (ou de retraite).

Pour les bons moments passés durant les conférences, à l'IFMA, chez Renault, ou en dehors. Pour avoir partagé nos expériences respectives et les complaintes traditionnelles du thésard. Chers collègues thésards, chers Simon (D), Simon (B), Antoine, Paul, Paula, Mathieu, diplômés déjà ou encore entrain de bûcher, je vous salue bien bas.

Enfin, ces remerciements seraient vains s'ils ne reconnaissaient pas mon soutien principal au cours de ces années bien remplies, mon amour et future épouse Axelle. Tu as su être là quand il le fallait, tu as été patiente et compréhensive, tu n'as pas craqué sous la pression quand je la transmettais et tu as cru en moi dès le début. Pour ce soutien sans failles et ton amour, je te suis infiniment reconnaissant.

A ma mère. Mes accomplissements sont aussi le résultat de tes efforts.

Contents

Abstract **i**

Résumé **ii**

Remerciements **iii**

Résumé étendu **xv**

1 Introduction **1**

2 Reliable design of vehicle components subjected to variable loads **7**
2.1 Fatigue phenomenon in the context of load variability 8
2.1.1 High-cycle fatigue and fatigue strength of a material 8
2.1.2 Fatigue life assessment under variable amplitude loads 10
2.1.3 Damage equivalent load for analysis and testing 11
2.2 Design of vehicle components and reliability requirements 15
2.2.1 Vehicle development process 15
2.2.2 characterisation of load variability 17
2.2.3 Design, testing and assessment of reliability in practice 21
2.3 Simulation of the loads acting on vehicle components 25
2.3.1 Vehicle dynamics and vertical responses 25
2.3.2 Architecture of the vehicle and vertical dynamics modelling 26
2.3.3 Solving of the equations of vertical dynamics 28

3 Estimation of road profiles from a vehicle's dynamic responses **32**
3.1 Introduction 33
3.2 Extracting road-related information from a vehicle's responses 34
3.2.1 Overview on road roughness characterisation 34
3.2.2 Road profiles and vehicle dynamics 36
3.2.3 Existing methods for the processing of vehicle's responses 37
3.2.4 Selected algorithm for the estimation of road profiles 38
3.3 Estimation of the excitation acting on a system: an inverse problem 39
3.3.1 Inverse problems and related mathematical difficulties 39
3.3.2 Regularisation of inverse problems 42

3.3.3 Illustration on an example . . . 43
3.4 An excitation estimation algorithm based on Kalman filtering theory . . . 44
3.4.1 The linear Kalman filter . . . 44
3.4.2 A state augmented Kalman filter for excitation estimation . . . 48
3.4.3 Regularisation through the Kalman filtering framework . . . 50
3.5 Implementation of the algorithm for the estimation of road profiles . . . 52
3.5.1 Choice of a vehicle model for the estimation algorithm . . . 53
3.5.2 Semi-empirical tuning of the estimation algorithm . . . 56
3.6 Testing of the road estimation algorithm . . . 61
3.6.1 Testing framework and objective scalar criteria . . . 61
3.6.2 Numerical testing of the road estimation algorithm . . . 63
3.6.3 Physical testing of the road estimation algorithm . . . 69
3.6.4 Sensitivity and limits of the algorithm . . . 72
3.6.5 Discussion on the applicability of the algorithm . . . 77
3.7 Synthesis and conclusion . . . 80

4 Stochastic modelling of road and speed profiles 84
4.1 Introduction . . . 85
4.2 Principal elements of stochastic process theory . . . 86
4.2.1 Randomness, random variables and stochastic processes . . . 86
4.2.2 Spectral representation of stochastic processes . . . 88
4.2.3 Identification of a stationary process and generation of trajectories . 90
4.3 Stochastic modelling of road profiles . . . 92
4.3.1 Road roughness, road profiles and vertical excitations . . . 92
4.3.2 Stochastic models for road profiles in literature . . . 93
4.3.3 Proposed candidate model structures and parameter identification . 97
4.4 Stochastic modelling of speed profiles . . . 104
4.4.1 Speed of the vehicle and its evolution . . . 104
4.4.2 Stochastic models for speed profiles . . . 106
4.4.3 Proposed candidate model structures and parameter identification . 107
4.5 Exploitation of available data: testing of the considered models . . . 113
4.5.1 Example of data acquisition from load measurement campaigns . . . 114
4.5.2 Statistical characteristics of the estimated road profiles . . . 117
4.5.3 Selection of representative stochastic models for road and speed . . . 120
4.6 Synthesis and conclusion . . . 126

5 Stochastic simulation of road-induced fatigue loads 130
5.1 Introduction . . . 131
5.2 Proposed methodology for load characterisation . . . 132
5.2.1 Variability of loads and reliability concerns . . . 132
5.2.2 On the characterisation of loads: diversity and life situations . . . 132
5.2.3 Proposed methodology: stochastic simulation of road-induced loads 135
5.3 Testing of the proposed stochastic simulation methodology . . . 140
5.3.1 Available data for testing and statistics on input parameters . . . 140

5.3.2 Comparison of predicted and observed (measured) load variability . 144
5.3.3 Comparison of predicted and observed load sensitivity 149
5.4 Prediction of the load life of vehicles 153
5.4.1 Statistical analysis and extrapolation 154
5.4.2 Study of extrapolation hypotheses 160
5.4.3 Prediction of the life of a population of vehicles 163
5.5 Application of stochastic simulation for reliability analysis 167
5.5.1 Design of reliable components and vehicle development process . . . 167
5.5.2 Realisation of different stochastic simulation campaigns 168
5.5.3 Modifications of influential factors and reliability assessment 170
5.6 Synthesis and conclusion 172

6 Conclusions and perspectives 176

Bibliography 189

Index 190

A Notations 191

B Additional vehicle models 194
B.1 Non-linear (2-DOF) quarter-car model 194
B.2 Linear bicycle model 195
B.3 Linear full-vehicle model 195

C Modelling and influence of the tyre/road contact 198
C.1 Tyre modelling and tyre/road contact 198
C.2 Limitations of the road estimation method 199
C.3 Limitations of the simulation with a linear tyre model 201

D Experimentations and testing of the estimation algorithm 203
D.1 Numerical testing of the road estimation algorithm 204
D.1.1 Experiments involving a 2-DOF non-linear quarter-car model 204
D.1.2 Experiments involving a detailed Mutli-Body model 210
D.2 Physical testing of the road estimation algorithm 213
D.3 Study of the influence of tuning parameters 216
D.4 Study of the influence of mechanical characteristics 218
D.5 Study of the influence of vehicle speed 220
D.6 Study of more complex models 221
D.6.1 Models with more DOF 222
D.6.2 Non-linear model 224

E Algorithm for the division in constant speed segments 225

F Testing and validation of stochastic simulation 227

F.1 Comparison of the predicted and observed (measured) load variability . . . 228
F.2 Comparison of the predicted and measured load sensitivity 235
F.3 Comparison of the predicted and measured load lives of vehicles 236

List of Figures

1 Processus de développement d'un nouveau véhicule xvi
2 Division et caractérisation de la vie des véhicules xvii
3 Utilisation de l'information acquise sur la variabilité de chargements xviii
4 Principe de la méthodologie de simulation stochastique xix
5 Illustration d'un résultat d'estimation de route xxi
6 Résultats du traitement d'une campagne de mesures xxii
7 Exemple de profil de route généré aléatoirement xxii
8 Exemple de profils de vitesses généré aléatoirement et mesuré xxiii
9 Modèle linéaire quart-de-véhicule utilisé pour la simulation xxiv
10 Résultats des comparaisons entre hauts quantiles (95%) xxv
11 Influence de divers facteurs sur la variabilité de chargements xxvii

1.1 Outline of the manuscript 5

2.1 Constant amplitude fatigue strength test and Wöhler curve 9
2.2 Vehicle development process 17
2.3 Distribution representing load variability 18
2.4 Use of the information on load variability 22
2.5 Quarter-car model of the vehicle 27
2.6 Typical architecture of front and rear suspension systems 27
2.7 Highly detailed multi-body model in an MBS software 28

3.1 'Direct' road measurement methods 35
3.2 Illustration of the need for regularisation 44
3.3 Principle of the Kalman filter: prediction-correction scheme 46
3.4 Quarter-car model of the vehicle 53
3.5 Empirical estimation of the state noise's strength 57
3.6 Empirical estimation of the measurement noise's strength 58
3.7 Illustration of the four-post vertical test rig 69

4.1 Example of randomly generated profiles, using ISO PSD model 95
4.2 Two band PSD model identified on a measured profile 96
4.3 Non-stationary character of a real road 99
4.4 Normalized variances r_j, comparison of empirical and Gamma CDFs 100

4.5 Random realisation of a non-stationary profile 101
4.6 Generated road profile comprising transients 102
4.7 Calibration of transient detection criterion 103
4.8 Identification of transient related distributions 104
4.9 Vertical excitations for two different speed signals 105
4.10 Comparison of several drivers on the same route 107
4.11 Measured vehicle speed and constant speed sections 108
4.12 Distributions of length and speed of different segments 109
4.13 Example of a randomly generated speed profile 110
4.14 Observed 'correlation' between vehicle's speed and the road profile 111
4.15 Influence of the speed stochastic model on damage accumulation 112
4.16 Results of the processing of the route imposed campaign 115
4.17 Results of the processing of the route free campaign 116
4.18 Statistical characteristics for a city road profile (V) 118
4.19 Statistical characteristics for a country road profile (R) 118
4.20 Statistical characteristics for a highway profile (A) 119
4.21 Variability of PSD parameters for 20 profiles of 3 road categories 120
4.22 Limits of the PSD-based description 121
4.23 Validation procedure for a given modelling hypothesis 123
4.24 Comparison of candidate models: mean damage criterion 124
4.25 Comparison of candidate models: q_{90} damage criterion 124

5.1 Division and characterisation of vehicles' load life 134
5.2 Illustration of the heterogeneity of strata 136
5.3 Principle of the stochastic simulation methodology 137
5.4 Variation of the constituting parameters: country A 141
5.5 Variation of the constituting parameters: country B 142
5.6 Variation of the constituting parameters: waviness (w_1,w_2) 143
5.7 Validation of the methodology: compared loads 146
5.8 Comparisons of predicted and measured distributions: Susp. disp. 147
5.9 Coefficients of simulation and measurement-based response surfaces 152
5.10 Simulation and measurement based response surfaces 154
5.11 Correlation between constituting parameters: example (S_1, v_m) 157
5.12 Extrapolation using independent realisations of damage values 160
5.13 Scatter in damage over increasingly longer segments 161
5.14 Evolution of cumulated damage over long segments 161
5.15 Comparison of extrapolation strategies and load history lengths 162
5.16 Relative proportion of different life situations 164
5.17 Predicted variability of the load lives of vehicles 165
5.18 Sensitivity of high quantiles to influential factors 170
5.19 Sensitivity of failure probability to influential factors 172

B.1 Non-linear (2-DOF) quarter-car model 195
B.2 Characteristics of the non-linear suspension 196

B.3 Linear bicycle model 197
B.4 Linear full-vehicle model 197

C.1 Comparison of the road geometry with a realistic vertical excitation 200
C.2 Geometric filtering of rough pavement track 200
C.3 Comparison between vertical excitation and rolling tyre 202

D.1 Data from 2-DOF model: Road estimate 204
D.2 Data from 2-DOF model: PSD of road estimate 204
D.3 Data from 2-DOF model: Road estimate (no high-pass filtering) 205
D.4 Data from 2-DOF model: PSD of road estimate (no high-pass filtering) . . 205
D.5 Data from 2-DOF model: suspension displacement 206
D.6 Data from 2-DOF model: sprung mass acceleration 206
D.7 Data from 2-DOF model: unsprung mass acceleration 207
D.8 Data from 2-DOF model: suspension displacement PSD and LC 207
D.9 Data from 2-DOF model: sprung mass acceleration PSD and LC 208
D.10 Data from 2-DOF model: unsprung mass acceleration PSD and LC 208
D.11 Data from 2-DOF model: convergence to the 'true' profile 208
D.12 Data from 2-DOF model: unsprung mass acceleration (no regularisation) . 209
D.13 Data set 1 from detailed (MBS) model: road estimate 210
D.14 Data set 1 from detailed (MBS) model: PSD of road estimate 210
D.15 Data set 2 from detailed (MBS) model: road estimate 211
D.16 Data set 2 from detailed (MBS) model: suspension displacement 211
D.17 Data set 3 from detailed (MBS) model: road estimate 212
D.18 Data set 3 from detailed (MBS) model: PSD of road estimate 212
D.19 Data set 1 from test-rig measurement: road estimate 213
D.20 Data set 1 from test-rig measurement: PSD of road estimate 213
D.21 Data set 1 from test-rig measurement: unsprung mass acceleration 214
D.22 Data set 1 from test-rig measurement: result with no regularisation 214
D.23 Study of the influence of sampling time on the estimation 215
D.24 Data set 2 from test-rig measurement: road estimate 215
D.25 Data set 2 from test-rig measurement: PSD of road estimate 216
D.26 Influence of tuning on the low frequency content (LF) 217
D.27 Influence of tuning on the medium frequency content (MF) 217
D.28 Influence of tuning on the high frequency content (HF) 217
D.29 Influence of the regularisation coefficient 218
D.30 Influence of knowledge on mechanical characteristics: LF 219
D.31 Influence of knowledge on mechanical characteristics: MF 219
D.32 Influence of knowledge on mechanical characteristics: HF 219
D.33 Influence of knowledge on mechanical characteristics: MBS data 220
D.34 Influence of vehicle's speed on the estimation 220
D.35 Sensibility of the estimation to vehicle's speed 221
D.36 Comparison of estimates obtained with different vehicle models 222
D.37 Comparison of estimates yielded by a linear and non-linear algorithm 224

E.1 Identification of constant speed sections 226

F.1 Comparisons of predicted and measured distributions: Susp. disp. 228
F.2 Comparisons of predicted and measured distributions: Sprung acc. 228
F.3 Comparisons of predicted and measured distributions: Unsprung acc. 229
F.4 Overall quality of the methodology: suspension displacement 229
F.5 Overall quality of the methodology: Sprung acc. 230
F.6 Overall quality of the methodology: Unsprung acc. 230
F.7 Testing of the methodology: comparison of mean values, country A 231
F.8 Testing of the methodology: comparison of 95% quantiles, country A 231
F.9 Testing of the methodology: comparison of mean values, country B 232
F.10 Testing of the methodology: comparison of 95% quantiles, country B 232
F.11 Coefficients of simulation and measurement-based response surfaces 235
F.12 Coefficients of simulation and measurement-based response surfaces 235
F.13 Coefficients of simulation and measurement-based response surfaces 236
F.14 Predicted load life: suspension displacement 236
F.15 Predicted load life: sprung acceleration 237
F.16 Predicted load life: unsprung acceleration 237

List of Tables

3.1 Semi-empirical assessment of the state noise's strength 59
3.2 Semi-empirical assessment of the measurement noise's strength 59
3.3 Data from 2-DOF model: result of the estimation 64
3.4 Data set 1 from detailed (MBS) model: result of the estimation 66
3.5 Data set 2 from detailed (MBS) model: result of the estimation 67
3.6 Data set 3 from detailed (MBS) model: result of the estimation 68
3.7 Data set 1 from test-rig measurement: result of the estimation 70
3.8 Data set 1 from test-rig measurement: result with no regularisation 71
3.9 Data set 2 from test-rig measurement: result of the estimation 72
3.10 Correspondence between spatial and time frequency of the excitation 75

4.1 Different candidate stochastic road models 103
4.2 Different candidate stochastic speed models 113
4.3 Validation procedure: comparison of DEA criteria 123

5.1 Testing of the methodology: comparison of mean values, country A 147
5.2 Testing of the methodology: comparison of 95% quantiles, country A 148
5.3 Coefficients of simulation and measurement-based response surfaces 153
5.4 Comparison of predicted load lives: Country A 164
5.5 Comparison of predicted load lives: Country B 165
5.6 Mean and standard deviation of the gamma distributions 169
5.7 Reference vehicle characteristics 169

A.1 Notations: fatigue, load variability and reliability 191
A.2 Notations: vehicle dynamics and inverse problem 192
A.3 Notations: Stochastic modelling, road and speed 192
A.4 Table of acronyms 193
A.5 Life situations designations 193

C.1 Road estimate compared to filtered profile 201
C.2 Comparison of the road geometry with a realistic vertical excitation 201

D.1 Data from 2-DOF model: result of the estimation (no regularisation) 209
D.2 Design of experiments: influence of tuning parameters 216
D.3 Design of experiments: influence of the mechanical characteristics 218

D.4 Influence of vehicle's speed on road roughness estimation 221
D.5 Comparison of estimates obtained from different vehicle models 223
D.6 Comparison of estimates yielded by a linear and non-linear algorithm 224

F.1 Testing of the methodology: comparison of mean values, country A 233
F.2 Testing of the methodology: comparison of 95% quantiles, country A 233
F.3 Testing of the methodology: comparison of mean values, country B 234
F.4 Testing of the methodology: comparison of 95% quantiles, country B 234

Résumé étendu

Contexte

Les constructeurs automobiles se doivent de maîtriser la fiabilité des véhicules afin d'assurer la sécurité des passagers, de ne pas générer d'insatisfaction pour le client ou de ne pas engendrer de coûts de réparation, qu'ils soient supportés par le client ou par le constructeur. Les objectifs de fiabilité définis pour les différents composants du véhicule dépendent de la gravité des conséquences de la défaillance de ces derniers.

Le contexte considéré ici concerne les défaillances dues à l'endommagement par fatigue. L'évaluation de la probabilité de défaillance d'un composant dépend simultanément de la variabilité des chargements appliqués à celui-ci ainsi que de sa capacité de résistance. L'objectif principal de ce travail de recherche se concentre sur la première partie du problème, à savoir **l'étude de la variabilité des chargements appliqués aux différents composants du véhicule**.

Le travail proposé dans ce manuscrit s'insère dans le cadre de la fatigue des structures soumises à des chargements aléatoires. La particularité des chargements étudiés ici; qui seront limités aux conséquences de l'excitation verticale due aux profils de routes parcourus; est que la variabilité à caractériser est extrêmement forte. En effet, différents clients peuvent utiliser leur véhicule de façons très diverses, en sélectionnant des routes différentes et en imposant des styles de conduite différents. Une analyse statistique approfondie est donc nécessaire pour le traitement de cette problématique.

En pratique lors du développement d'un nouveau véhicule, illustré en figure 1, **il est impératif de posséder une connaissance quantifiée de la variabilité des chargements appliqués à chacun des composants du véhicule**. Par suite, le travail de conception et de validation consiste à procurer aux composants la capacité de résistance suffisante (choix des matériaux, géométrie des composants, assemblages des composants, répartitions des efforts) compte tenu des chargements qu'ils sont susceptibles de rencontrer, et à s'assurer que celle-ci permet d'atteindre les objectifs de fiabilité préalablement définis.

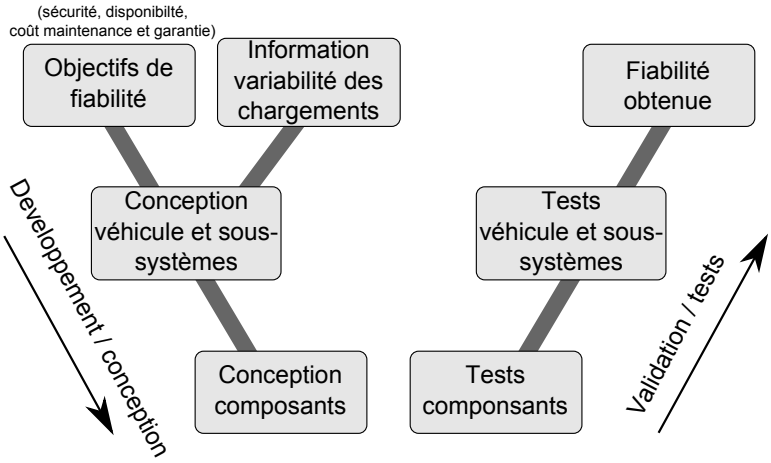

Figure 1: Processus de développement d'un nouveau véhicule.

Approche conventionnelle de caractérisation de la diversité des chargements

Acquérir de l'information relative à la variabilité des chargements impose nécessairement de **collecter des historiques de chargements**. Les historiques collectés sont souvent exprimé sous la forme simplifiée d'une grandeur scalaire ou 'pseudo-dommage', dont la variabilité peut être étudiée plus simplement.

Pour la grande majorité des constructeurs automobiles, cette collecte d'information s'appuie sur la mise en place de campagnes de mesures pour lesquelles un véhicule instrumenté est placé entre les mains de différents conducteurs et dans son contexte d'utilisation. Ces campagnes sont généralement **complexes** (matériel de mesure), **coûteuses et longues**, ce qui limite naturellement la possibilité de constituer des échantillons statistiques importants et confère peu de flexibilité pour analyser l'influence des différents facteurs qui peuvent impacter les chargements. De plus, la longueur des chargements enregistrés est forcement limitée par rapport à la vie complète d'un véhicule. Ainsi et au vue de la diversité des utilisations possibles pour les véhicules au sein d'une population de clients, le choix et le traitement des échantillons acquis constitue un challenge statistique important.

Il est possible de collecter plus efficacement de l'information en procédant à une **division de la vie des véhicules en un certain nombre de situations** (identifiables) **de vie**. Dans cette optique, les clients sont questionnés par sondage à propos du pourcentage d'utilisation qu'ils consacrent aux différentes situations de vie. En parallèle, des historiques de chargements sont collectés pour chacune de ces situations. Techniquement, la 'population de chargements' est divisée en un ensemble de 'strates' et l'analyse statistique de la variabilité des chargements s'obtient par 'échantillonnage stratifié'. Une illustration de la notion d'échantillonnage et de la division de la vie des véhicule est donnée en figure 2.

Par ailleurs, dans le cadre de l'utilisation de campagnes de mesures, tout résultat acquis est **dépendant des caractéristiques du véhicule utilisé pour la mesure**.

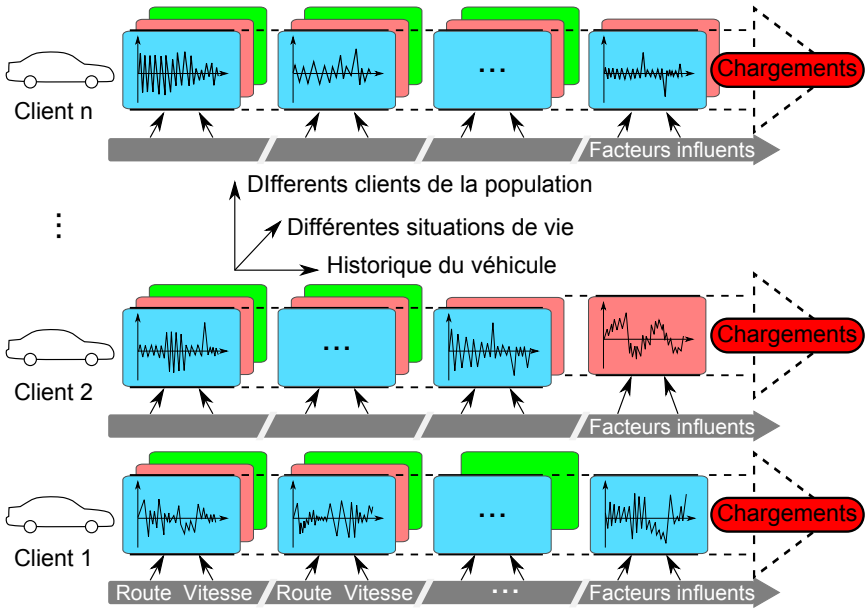

Figure 2: Division et caractérisation de la vie des véhicules.

Ceci représente un problème lorsque l'objectif est de concevoir un nouveau véhicule pour lequel aucune instrumentation n'est encore possible. De plus, les chargements appliqués à un composant donné peuvent être fortement dépendants des caractéristiques du véhicule (par exemple la raideur de pneu ou l'amortissement des suspensions). Deux solutions peuvent alors être envisagées.

Premièrement, on peut utiliser un véhicule existant dont les caractéristiques mécaniques sont aussi proche que possible du nouveau véhicule conçu. Deuxièmement, on peut avoir recours à un **profil d'excitation déterministe** qui sera utilisé (en phase de développement) afin d'évaluer les chargements appliqués aux différents composants par l'intermédiaire de la simulation (donc pour n'importe quel véhicule). Ce profil d'excitation (quasi-deterministe) est généralement basé sur l'utilisation de pistes de validation spécifiques aux différents constructeurs (mauvais pavés, bosses, nids de poules) et qui ont été numérisées afin de pouvoir être utilisées en simulation. Dans les deux cas, une hypothèse forte doit être émise, soit sur la pertinence d'utiliser des chargements acquis sur un véhicule aux caractéristiques différentes, soit sur le positionnement du profil d'excitation deterministe par rapport à la variabilité constatée dans la population de clients. En général, ce positionnement est obtenu à partir de campagnes de mesures réalisées précédemment (c'est-à-dire hors du délai de développement du véhicule, voir figure 1) . Une illustration de ces concepts est donnée en figure 3.

Le profil d'excitation déterministe choisi correspond généralement à un client sévère ou sévérisé. Souvent, ce profil déterministe est également utilisé afin de **déterminer la résistance d'un composant par des tests sur un banc d'essai et valider ou invalider de fait la conception.** Quelle que soit l'utilisation faite du profil d'excitation

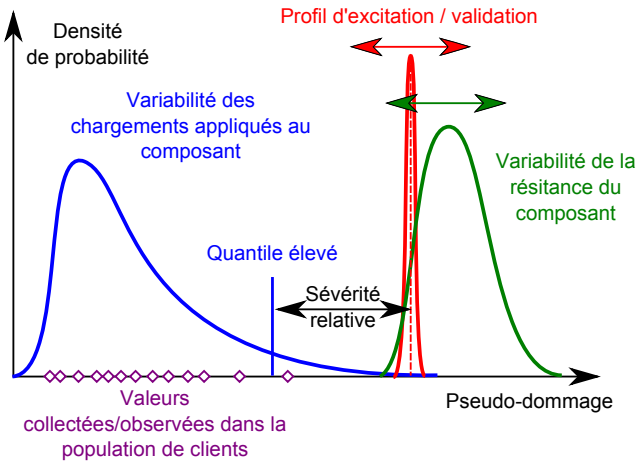

Figure 3: Utilisation de l'information acquise sur la variabilité de chargements.

déterministe choisi, il est **indispensable de disposer d'une information quantifiée sur sa relation avec la variabilité de chargement dans la population de clients** avant de pouvoir réaliser une estimation de fiabilité, voir figure 3, ou afin de s'assurer que les objectifs de dimensionnement/validation utilisés en pratique sont adaptés.

Caractérisation de la variabilité des chargements par simulation stochastique

Principe de la méthodologie proposée

L'objectif de la méthodologie développée dans ce manuscrit est de permettre une caractérisation de la variabilité des chargements appliqués aux différents composants des véhicules par une population de clients donnée. La méthodologie proposée vise à changer fondamentalement d'approche en obtenant les (échantillons statistiques) historiques de chargements **par la simulation plutôt que par la mesure**.

Le principe sous-jacent à cette approche est le suivant. Il est préférable de **concentrer l'effort d'analyse statistique sur la variabilité des facteurs influents** (entrées) qui déterminent les chargements, à savoir la **géométrie de route et la vitesse du véhicule**, plutôt que directement sur les chargements (sorties). Ce principe représente le fondement conceptuel autour duquel s'articule ce travail de recherche.

En pratique, des profils de routes et de vitesses sont générés aléatoirement à partir de modèles stochastiques et ensuite utilisés pour obtenir, par la simulation de la dynamique verticale du véhicule, un ensemble d'historiques de chargements. Ce procédé est décrit schématiquement par la figure 4. La méthodologie est couplée ici avec la notion de situations de vie, dans le cadre desquelles la variabilité des facteurs influents est généralement plus réduite.

L'intérêt de concentrer l'effort d'analyse sur la variabilité des facteurs influents est

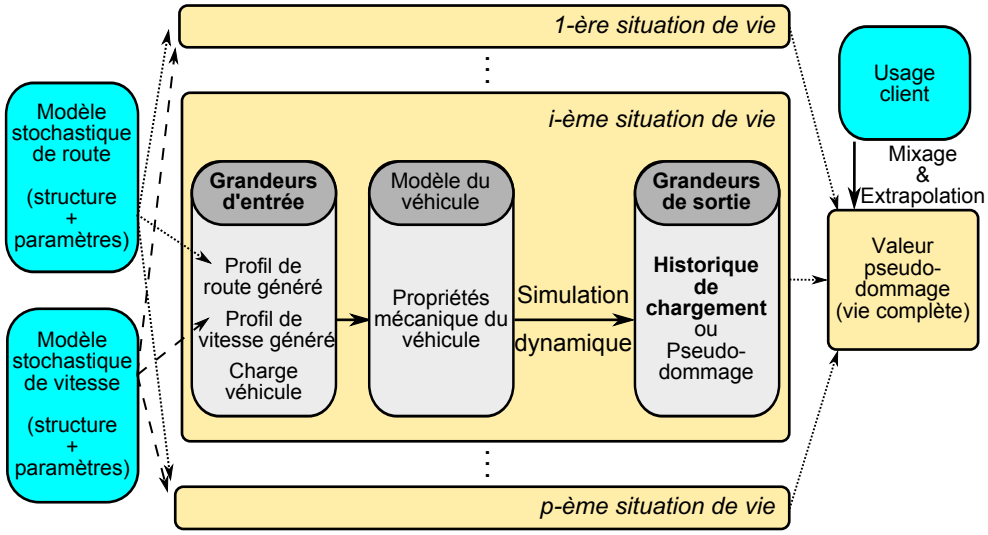

Figure 4: Principe de la méthodologie de simulation stochastique.

que lorsque l'on dispose de suffisamment d'information statistique sur ces derniers, il est possible de générer autant d'historiques de chargements que souhaité, rapidement, à un coût faible et pour tout véhicule dont les caractéristiques mécaniques sont connues.

La qualité des résultats de la méthodologie dépend de la **capacité à pouvoir générer des trajectoires représentatives des profils de routes et de vitesses** qui auraient pu être mesurés en pratique (et relativement à la population de clients considérés). La sélection et la validation des modèles stochastiques est un objectif majeur du travail de recherche présenté ici. Par ailleurs, tout résultat de simulation est évidemment dépendant de la **qualité de l'outil de simulation utilisé** et de la fidélité du modèle de véhicule employé.

Etude et modélisation de la variabilité des facteurs influents

Afin de pouvoir utiliser la méthodologie proposée, il est **impératif d'acquérir de l'information sur la variabilité des facteurs influents** (route et vitesse). Ici cette information est acquise à partir de campagnes de mesures existantes. Bien que cette approche ne soit pas la plus directe (les profils de routes pourraient être directement mesurés), les données de campagnes de mesures constituent la seule source importante d'information statistique disponible dans le cadre de ce travail.

Dans ce manuscrit, des structures mathématiques sont proposées pour les modèles stochastiques permettant de générer des trajectoires représentatives des profils de routes et de vitesses. Les paramètres qui déterminent complètement ces structures, appelés ici '**paramètres constituants**', sont utilisés afin de simplifier l'analyse de la variabilité des facteurs influents (route et vitesse). En effet, ils permettent de réaliser une 'projection' d'une gardeur complexe et continuellement variable (un profil de $10km$ dans le cadre de ce manuscrit) sur un vecteur de dimension réduit. Il est ensuite plus facile d'étudier

statistiquement **la variation de ces quelques paramètres tout au long de la vie d'un véhicule ou entre plusieurs véhicules d'une population étudiée**, voir figure 2. Réciproquement, pour un jeu de paramètres donné et une structure de modèle correspondante, il est possible de générer autant de profils que souhaité, dans le but de réaliser des simulations.

L'étude de la variation de ces paramètres constituants demeure un problème statistique complexe. La question de l'extrapolation à partir d'historiques courts vers la vie complète des véhicules, est discutée dans le cadre de ce travail. L'utilisation du concept de situations de vie décrit précédemment et des informations acquises par sondage dans la population de clients, peuvent par ailleurs permettre une description plus pertinente de la variabilité des facteurs influents dans cette population.

Acquisition d'information sur les profils de routes et vitesses

Un algorithme d'**estimation des profils de routes à partir de mesures de réponses sur un véhicule instrumenté** a été développé et testé et constitue une contribution importante de ce travail de recherche. Il permet d'extraire de l'information sur la variabilité de route à partir de campagnes de mesures existantes (et donc à un coup négligeable) réalisées par Renault dans différents pays. D'autre part, les profils de vitesses sont directement mesurés.

L'algorithme d'estimation de route est basé sur la résolution d'un problème inverse. La méthode cherche l'excitation la plus probable compte tenu des réponses observées sur le véhicule, à savoir les débattements de suspension et les accélérations verticales de la roue et de la caisse. Elle s'appuie sur le principe du filtre de Kalman et sur un modèle linéaire dit 'quart-de-véhicule' (voir figure 9). L'algorithme est **rapide** et permet le traitement de gros volumes de données. Il permet aussi de combiner facilement l'information qui provient de différentes sources (capteurs). Enfin, il peut être 'réglé' pour obtenir une **bonne qualité d'estimation des profils de routes** malgré la simplicité du modèle de véhicule utilisé. Une illustration de l'expérimentation de l'algorithme, réalisée à partir d'un véhicule monté sur un banc d'essai vibratoire vertical, est donnée en figure 5.

Dans ce manuscrit, deux campagnes menées dans deux pays différents sont utilisées et traitées (quelques miliers de kilomètres au total). Ces campagnes sont réalisées à partir de circuits imposés appartenant à différentes catégories de routes (différentes situations de vie). Le traitement par la méthode d'estimation de route permet d'obtenir un ensemble de profils de routes et de vitesses (excitations de route), correspondant à chaque enregistrement disponible. Les paramÃÍtres constituants liés aux structures de modèles choisies sont ensuite identifiés Ãă partir des profils obtenus. Sur la figure 6, chaque point correspond à un enregistrement de $10km$ pour lequel le type de route est connu à l'avance.

Une réduction de la variabilité des **paramètres constituants** des modèles de route et de vitesse (partitions de l'espace sur la figure 6) peut être observée dans le cadre des différentes situations de vie. Dans le contexte présent, la description de la variabilité de ces paramètres constituants constitue le cœur de **l'information statistique** qui doit être maîtrisée afin de pouvoir réaliser *in fine* des prédictions de la variabilité de chargement.

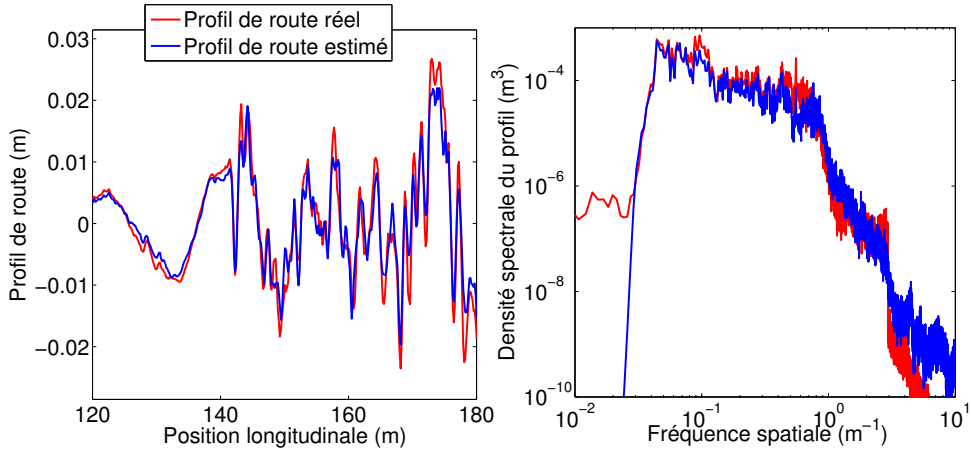

Figure 5: Illustration d'un résultat de d'estimation de route. Expérimentation sur un banc d'essai vibratoire vertical pour lequel l'excitation injectée est parfaitement connue et peut être comparée au résultat de l'estimation.

Sélection et test des modèles stochastiques de route et vitesse

A partir des profils de routes et de vitesses obtenus grâce au traitement des campagnes existantes, mais également à partir des travaux disponibles sur le sujet dans la littérature, un certain nombre de modèles stochastiques candidats sont considérés. Ces derniers sont testés au regard des données disponibles.

Plus précisément, pour un ensemble de profils (estimés) pris comme une référence, des profils sont générés aléatoirement à partir des modèles stochastiques candidats et ensuite comparés à ces profils (réels) de référence. Les comparaisons sont effectuées tant sur la base des **caractéristiques statistiques** des profils qu'en considérant les **réponses** que ceux-ci provoquent sur les véhicules. Dans ce dernier cas, le but est de s'assurer que l'information prédite en termes de variabilité des chargements qui s'appliquent aux composants du véhicule est représentative.

Pour la modélisation de la géométrie de route ou '**rugosité de route**', tous les modèles s'appuient sur une description fréquentielle (spatiale) du contenu du profil. Le modèle de route retenu, provenant de la littérature, utilise une forme analytique basée sur deux fonctions puissances décroissantes pour décrire la densité spectrale de puissance (DSP) du processus stochastique. Sur cette base, une approche par 'filtres formateurs' est proposée pour générer des trajectoires. Le modèle de non-stationnarité, repris de la littérature, consiste à moduler la variance du profil sur différentes sections de longueur constante ($200m$) à l'aide de réalisations d'une loi gamma de moyenne unitaire. La DSP évaluée sur la longueur totale du profil est inchangé par cette modulation, mais le profil est ainsi composé de différents de 'niveaux de rugosité'. Le modèle de route retenu ne prend pas en considération d'éléments transitoires du type 'nids de poule' ou 'bosses'. En effet, le modèle proposé et testé dans ce manuscrit pour décrire ces phénomènes ne permet pas

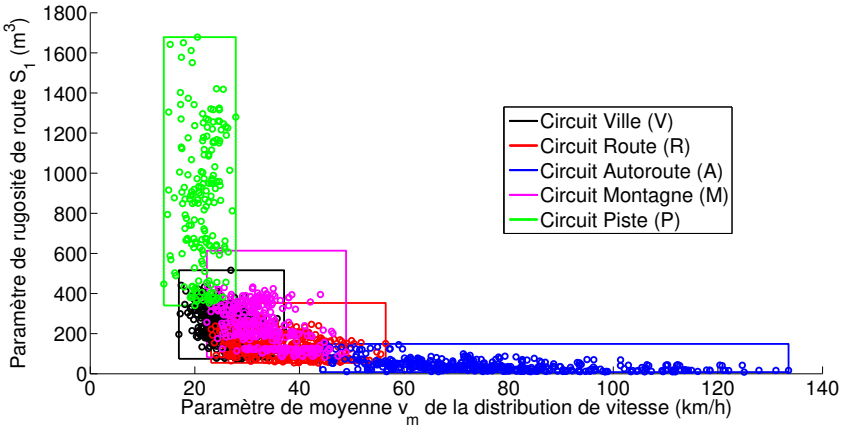

Figure 6: Résultats du traitement d'une campagne de mesures.

d'atteindre des résultats satisfaisants. Un exemple de profil de route non-stationnaire généré aléatoirement selon le modèle retenu est donné en figure 7.

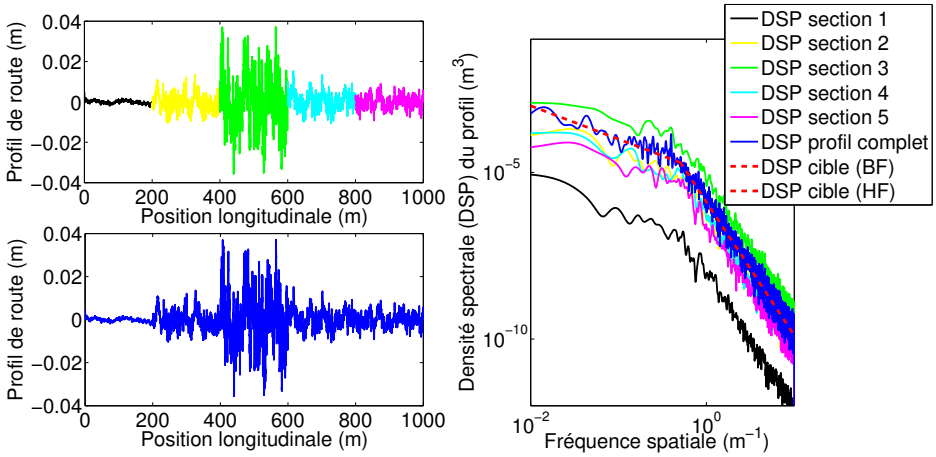

Figure 7: Exemple de profil de route généré aléatoirement à l'aide d'un modèle à 4 paramètres.

Pour la modélisation du profil de vitesse, le modèle retenu est basé sur un processus constant par morceaux. En effet, l'évolution de la vitesse semble varier entre des états quasi-constants pour lesquels la consigne de vitesse dépend à la fois du comportement du conducteur (agressivité, contrainte de temps, économie de carburant, préservation de la durée de vie du véhicule, etc.) et d'éléments extérieurs (trafic, limitations de vitesse, signalisations, topologie de la route, conditions météo, etc.). Le modèle retenu est défini par deux distributions. La longueur d'une section à vitesse constante est distribuée selon une loi exponentielle (un paramètre). La vitesse sur une section est distribuée selon une loi

normale (deux paramètres). Les deux distributions (marginales) sont liées par une copule Gaussienne. Un exemple de profil de vitesse généré aléatoirement a partir du modèle retenu est donné en figure 8.

L'étude de la corrélation entre profil de route et profil de vitesse a été menée et il a été constaté qu'une corrélation forte apparaît surtout au voisinage des éléments transitoires (nids de poule, bosses). Le modèle de vitesse retenu ne prend pas en compte de corrélation entre profil de route et profil de vitesse car le modèle retenu pour la géométrie de route n'intègre pas d'éléments transitoires.

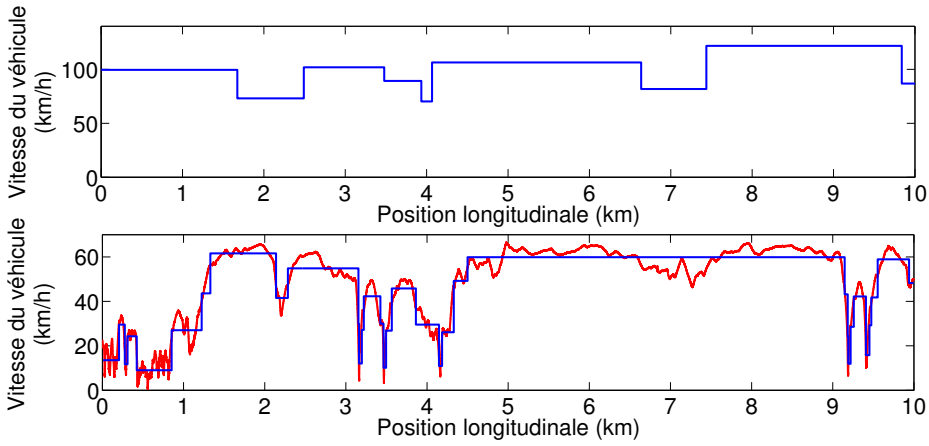

Figure 8: Exemple d'un profil de vitesse généré aléatoirement (haut) à l'aide d'un modèle à 4 paramètre et d'un profil mesuré (bas) pour lequel des sections à vitesse quasi-constante ont été identifiées.

Pour résumer, **les deux structures de modèles stochastiques retenues sont celles qui permettent de générer les trajectoires les plus représentatives, au regard des critères et des profils de références (réels) considérés dans cette étude expérimentale**. Elles sont chacune complètement détermines par 4 paramètres constituants et chaque jeu de paramètres permet de générer autant de trajectoires de $10km$ que souhaité. La variabilité de 2 de ces paramètres constituants, observée à partir des données de profils de routes et vitesses (réels) disponibles et de l'identification de ces paramètres en rapport avec les structures de modèle choisies, est illustrée en figure 6.

Une fois les structures de modèles choisies, les paramètres constituants de ces modèles peuvent être utilisés pour faciliter l'étude de la variabilité des facteurs influents (route et vitesse) au cours de la vie d'un véhicule et pour différents véhicules d'une même population.

Test de la méthodologie de simulation stochastique et analyse des résultats

Expérimentation menée

La méthodologie proposée a été testée en utilisant les structures de modèles stochastiques sélectionnées précédemment. Afin de procéder à des comparaisons exploitables, il est important que ces dernières soient **basées sur la même information statistique en ce qui concerne la variabilité des 'facteurs influents'**. Ainsi, les profils de routes et de vitesses utilisés sont générés à partir de modèles stochastiques dont les paramètres constituants sont tirés aléatoirement par un ré-échantillonnage de l'ensemble de paramètres constituants identifiés lors du traitement des campagnes de mesures (voir par exemple figure 6). Dans ce contexte, l'utilisation de campagnes existantes est un avantage car elle permet de comparer la variabilité de chargement prédite (par simulation stochastique) à la variabilité observée par la mesure; et donc de **vérifier la pertinence de la méthodologie.**

Dans le détail, pour les différentes situations de vie, un vecteur de paramètres constituants est tiré aléatoirement dans l'ensemble des vecteurs (de dimension 8) disponibles, puis utilisé pour générer une excitation aléatoire (profil de route + profil de vitesse). Cette excitation est ensuite appliquée pour simuler la réponse d'un modèle linéaire quart-de-véhicule présenté sur la figure 9. Les voies de réponses comparées sont les débattements de suspension ($z_s - z_t$), les accélérations de la caisse ($\ddot{z}_s$) et les accélération de la roue ($\ddot{z}_t$).

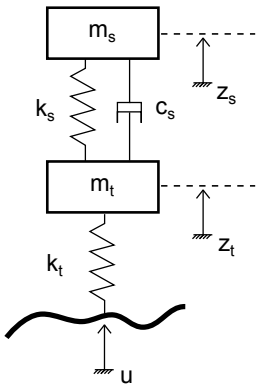

Figure 9: Modèle linéaire quart-de-véhicule utilisé pour la simulation.

Comparaisons réalisées

Premièrement, les résultats de simulations stochastiques sont comparés aux réponses simulées à partir du même modèle de véhicule mais en utilisant directement les profils (réels) obtenus à partir de la méthode d'estimation de route et du traitement des données de mesure disponibles. Ces comparaisons permettent de **tester la qualité des modèles stochastiques et de vérifier que les profils générés aléatoirement sont représen-**

tatifs des profils 'réels' qui ont été utilisés pour identifier les paramètres de ces modèles stochastiques. Elles donnent donc une indication directe de la **pertinence de l'implémentation choisie (modèles choisis) pour l'application de la méthodologie**.

Deuxièmement, les réponses résultant de la simulation des profils estimés (réels) peuvent également être comparées aux réponses mesurés sur le véhicule. Dans ce cas, il convient de noter que les écarts peuvent être important du fait de la modélisation simple choisie pour la dynamique du véhicule. Pour faire simple, même si la qualité des modèles stochastiques permettaient de générer des trajectoires parfaitement représentatives des profils réels, la précision serait limitée par la fidélité de l'outil de simulation.

Enfin, les comparaisons directes entre résultats de simulations stochastiques et réponses mesurées sur le véhicule instrumenté doivent être effectuées avec prudence car celles-ci peuvent mêler les erreurs de nature stochastique avec les défauts de fidélité de la simulation.

Au delà des comparaisons réalisées pour chaque situation de vie et en relation avec des profils de $10km$ (voir figure 10), des comparaisons ont également été réalisées après sommation des différentes contributions de chaque situation de vie (mixage) et utilisation d'une règle d'extrapolation à un objectif kilométrique élevé ($200000km$). Afin de ne pas biaiser la comparaison, l'extrapolation (à partir de profils de $10km$) a été réalisée selon la même règle que ce soit pour les réponses issues de la mesure ou de la simulation.

Analyse des résultats

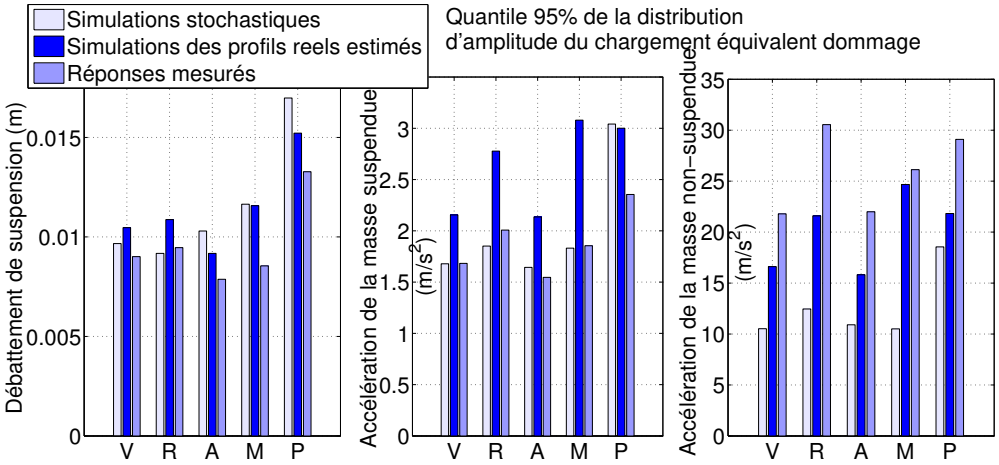

Figure 10: Résultats des comparaisons entre hauts quantiles (95%) des distributions correspondants aux différentes réponses. Les résultats sont donnés en termes d'amplitude de chargement équivalent en (pseudo-)dommage. Les résultats sont donnés pour les cinq situations de vie considérées. Pour chaque situation des ensembles de 500 historiques de chargements constituent les distributions de dommage étudiées.

Les résultats obtenus lors des comparaisons entre simulations stochastiques et simu-

lations des profils estimés, voir figure 10, montrent que les modèles stochastiques choisis présentent des insuffisances notables. La cause majeure d'écart identifiée est liée à la non prise en compte des événements transitoires (nids de poule, ralentisseurs, etc.) et de la corrélation entre profil de route et profil de vitesse qui est observée dans leur voisinage.

Il est discuté dans le manuscrit qu'à la connaissance de l'auteur, il n'existe pas de solution adaptée dans la littérature pour ce problème complexe mais également que toute amélioration de la représentativité des modèles stochastiques sur ce point s'accompagnerait vraisemblablement d'une forte augmentation de la complexité des modèles, tant les formes de motifs transitoires tout comme les comportements des conducteurs sont divers. Proposer des modèles plus complexes nécessiterait également un volume d'information statistique important.

Il convient donc de se montrer prudent lors de l'utilisation des résultats obtenus à partir de l'implémentation choisie ici (modèle choisis) pour la méthodologie proposée.

Capacité de la méthodologie à prédire les tendances et sensibilités

Les excitations de route estimées (route+vitesse) correspondant aux réponses mesurées sur le véhicule instrumenté, ont été utilisées afin d'identifier les paramètres constituants associés à celles-ci. La sensibilité des chargements mesurés a ces paramètres a ensuite pu être étudiée. En parallèle, à partir d'un tirage aléatoire (ré-échantillonnage) parmi cet ensemble de paramètres, des chargements ont été calculés par simulations stochastiques afin d'étudier la sensibilité qui peut être prédite par l'utilisation de la méthodologie.

En utilisant une analyse de sensibilité/tendance basée sur des surfaces de réponses, il a été constaté que l'adéquation est bonne entre les résultats obtenus à partir des historiques mesurés et les résultats obtenus à partir de simulations stochastiques. La méthodologie semble donc être pertinente pour analyser les tendances/sensibilités aux paramètres constituants.

En clair, elle permet d'**extraire de l'information quantitative sur la variabilité de chargements à partir de la connaissance disponible quant à la variabilité des facteurs influents**, même si la précision peut être limité du fait de la difficulté à modéliser ces mêmes facteurs influents (route et vitesse).

Exemple d'application et utilisation de la méthodologie en contexte industriel

La méthodologie est particulièrement intéressante lorsque l'on dispose d'une information statistique étendue sur la variabilité des facteurs influents dans un environnement d'utilisation donné, par exemple pour un nouveau pays de commercialisation ou une nouvelle population cible de clients. Dans le cadre de ce travail de recherche, la méthodologie a été élaborée et testée en utilisant les ensembles de données statistiques de taille assez modeste (au regard de la variabilité statistique dans la population) qui étaient disponibles. La méthodologie présente un plus grand potentiel d'application quand la quantité d'information statistique à traiter est importante.

A titre d'illustration, un exemple concret d'application de la méthodologie a été proposé. Pour l'exemple, l'information quant à la variabilité des facteurs influents est supposée connue *a priori*. Afin d'émuler l'effet d'un changement de pays de commercialisation, de population cible de clients ou de changements notables des caractéristiques du véhicule, plusieurs campagnes ont été réalisées en appliquant des modifications (raisonnables et déterminées par l'expérience) pour les facteurs influents. L'effet sur un haut quantile (95%) de la distribution de pseudo-dommage, pour plusieurs réponses sur le véhicule, est illustré sur la figure 11.

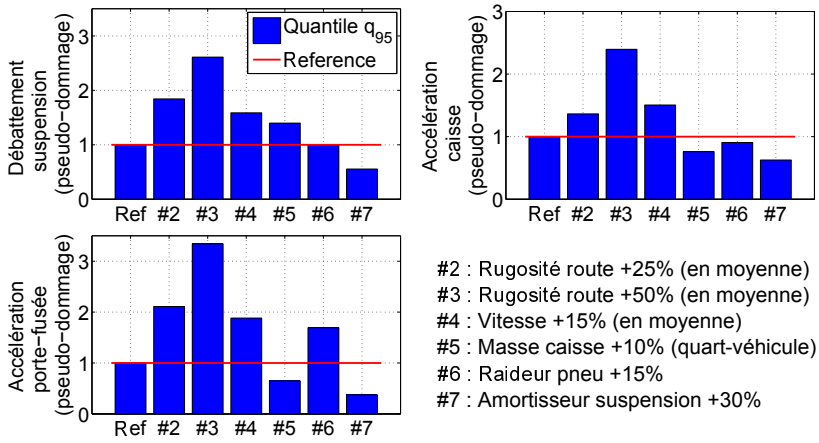

Figure 11: Exemple d'étude de l'influence de divers facteurs sur la variabilité de chargements. La campagne prise comme référence est affichée. Pour toutes les autres campagnes, un seul facteur est modifié à la fois.

Dans un contexte industriel, l'utilisation la plus pertinente de ce type d'approche consiste à analyser objectivement et quantitativement l'effet de la modification de ces différents facteurs sur la variabilité de chargement. En pratique, un niveau suffisant d'information statistique doit être disponible. Cette analyse objective peut permettre d'**aider à la résolution de problèmes décisionnels**, par exemple, en relation avec à la nécessité de planifier de nouvelles campagnes de mesures spécifiques (coûteuses) ou de considérer une modification (par l'intermédiaire de mesures spécifiques) des objectifs de dimensionnement/validation utilisés lors du développement du véhicule. **Avoir une information exploitable rapidement et à un coup raisonnable afin d'anticiper de telles modifications et agir en conséquence, est beaucoup plus difficile par la mesure que par la simulation**.

Il convient aussi de noter que l'algorithme d'estimation de route proposé dans ce manuscrit est un moyen intéressant pour valoriser des bases de données de mesures existantes à faible coût et obtenir de l'information sur la variabilité des profils de routes. A l'avenir, cet algorithme pourrait être utilisé dans le cadre de **l'acquisition de données en masse**, en tirant profit de l'instrumentation croissante qui apparaît sur les véhicules vendus aux particuliers.

Limites et Perspectives

Les résultats des comparaisons expérimentales entre chargements issus de simulations stochastiques et chargements obtenus à partir de profils réels révèlent le manque de représentativité des modèles stochastiques choisis ici pour les facteurs de route et de vitesse (notamment dans le cadre d'éléments rares et sévères comme les nids de poules et bosses). Néanmoins, l'analyse de ces écarts tend également à montrer qu'une amélioration de la représentativité des modèles s'accompagnerait naturellement d'une augmentation significative de leur complexité et de la difficulté à valider leur pertinence (tant la variabilité est grande en pratique). **Un compromis doit donc être trouvé entre précision et complexité** en fonction du niveau de précision nécessaire pour l'étude considérée. Dans ce manuscrit, des structures de modèles 'raisonnablement simple' ont été choisies et la quantité d'information disponible pour les valider est relativement modeste (par rapport à la variabilité qu'on peut attendre dans la population de clients).

Du point de vue de la modélisation de la dynamique véhicule, le même compromis entre précision et complexité (temps de calcul) doit être trouvé. Des modèles plus représentatifs existent mais la **représentativité des profils d'excitation de route générés aléatoirement est un prérequis à l'amélioration des résultats**, qui constitue davantage le cœur de ce manuscrit.

Il a également été noté qu'une partie importante du problème concerne la capacité à décrire **la variabilité des facteurs influents au cours de la vie de différents véhicules** de la population. Lors de l'utilisation d'une approche basée uniquement sur la mesure d'historiques de chargements de longueurs limitées (au plus quelques centaines de kilomètres), cette difficulté est liée à la question de **l'extrapolation** (qui en découle, voir figure 2). Il semble que pour progresser sur ce point extrêmement influant par rapport à l'information obtenu *in fine* quant à la variabilité de chargement, il est préférable de s'intéresser aux facteurs influents que directement aux chargements. Ainsi, la méthodologie proposée est vraisemblablement la solution la plus pertinente pour obtenir une connaissance plus large de la variabilité de chargement dans la population de clients.

Il convient de rappeler l'importance de **maîtriser quantitativement la variabilité de chargement, car sa connaissance conditionne lourdement toute prédiction de fiabilité qui pourrait être réalisée**. Or, la variabilité prédite est fortement impactée par l'hypothèse d'extrapolation ainsi que par le choix et la taille des échantillons constitués (limité en mesure) en termes d'historiques de chargements.

Le travail de recherche mené a permis de **formaliser les difficultés liées à la description probabiliste de la variabilité de chargement** observée en pratique. Néanmoins, **le problème est avant tout 'statistique' et toute amélioration de la connaissance est forcement dépendante de la quantité d'information à disposition**. Cette remarque est valable simultanément pour la simulation stochastique et pour les campagnes de mesures. Le philosophie de la méthodologie proposée est avant tout de **tirer le meilleur parti de l'information disponible**. Cette méthodologie constitue un cadre pertinent pour la recherche d'une compréhension plus large de la variabilité de chargement au sein de la population de clients et pour **l'amélioration des prédictions de fiabilité.**

Chapter 1

Introduction

Context

Reliability requirements and load variability

Essentially, reliability evaluation relates to the statistical analysis of the expected number of failed individuals within a population of components, given that they may be subjected to different loads and that their capacity to support such loads without failing is scattered. Reliability requirements are determined by the analysis of the gravity of potential failures. This may involve concerns about passengers safety, warranty costs for the car manufacturer or customer satisfaction.

In order to design vehicle components that meet specific reliability requirements, it is imperative to possess a precise description of the variability of the loads applied on such components. Different design choices may subsequently be adopted in order to provide the components with the necessary strength to support such loads, thus determining the reliability of the said components.

The variability of the loads experienced by vehicle components is arguably extremely strong due to the multiple possible usages of the vehicle, *e.g.* covered road surfaces or driver behaviours. Consequently, the issue of the of load variability constitutes a formidable statistical challenge.

Variability of road-induced fatigue loads

When a vehicle covers a road surface at a given speed, this surface represents a time-varying boundary constraint on the wheels of the vehicle, which in turn produces a dynamic response on the vehicle and therefore imposes loads on its different components. Arguably, for many components, road-induced vertical loads constitute the most important contributor to failure. Therefore, **the focus is put on road-induced vertical loads in this**

manuscript.

The time-varying vertical loads applied on vehicle components generate stress cycles inside the material(s) of these components and a progressive degradation due to the (high-cycle) fatigue phenomenon. In order to make a prediction for the fatigue life of a component, it is necessary to know the cumulative history of the stress states that the component has experienced. The use of the fatigue damage value (scalar) is very convenient when working with load variability. This value represents a quantitative description of the cumulative (at a given time) 'quantity of load' or 'level of solicitations' to which a particular component has been subjected. In this context, *i.e.* with scalar values, it is easier to perform statistical analyses on the diversity of loads among a population of vehicles (customers) and for different components.

Characterisation of load variability and vehicle development process

In order to study load variability, it is necessary to collect samples of load histories within the population of vehicles. For car manufacturers such as Renault, this is generally performed through the use of load measurement campaigns, where an instrumented vehicle is placed into the loading environment for which it is designed and in the hands of different drivers.

Such campaigns are complex, long and costly and this imposes a practical limitation on the size of the statistical samples of load histories that can be collected. In this context, it may not be easy to acquire extensive information on the diversity of loads within a population of vehicles or analyse and anticipate (sufficiently rapidly) the differences between different populations, *e.g.* for a different market (country).

Also, any load history acquired through such campaigns is **dependent on the characteristics of the vehicle used for the measurement**, as it is related to the vehicle's response to the road excitation. In early design stages of the development of a new vehicle, a physical prototype may not be available to perform such measurement campaigns. This is a problem since the loads that are applied on certain components may be strongly influenced by the characteristics of the vehicle, which determine the load path that extends from the road, through the wheels, and toward the studied components.

It is thus necessary to either realise the measurement campaign with a vehicle (of the previous generation) with relatively similar characteristics or to make use of a (deterministic) digitalized company-specific proving ground in order to perform multi-body simulations corresponding to the new vehicle, early in the design process. Both approaches imply strong hypotheses either on the relevance of acquiring loads on a different vehicle or on the relationship between the company-specific proving ground and the population of vehicles.

Consequently, when considering a measurement-based approach for the characterisation of load variability, it is neither possible to directly gather statistical information that is adapted to a new vehicle (being designed), nor achievable to carry out very extensive

characterisations within a reasonable time frame and at an acceptable cost. In this context it is relevant to fundamentally change the current approach to the characterisation of load variability.

Objectives and proposed methodology

The main objective of the presented research work is to provide an efficient solution to acquire a quantitative description of the load variability experienced by any given component within any given population of vehicles (and their related customers), with the objective of performing reliability assessments.

Recreating load histories through stochastic modelling and simulation

Here, the fundamental change that is proposed with respect to the characterisation of load variability, consists in **simulating load histories rather than only measuring them**. The underlying principle associated to the proposed methodology is the following. **It is preferable to concentrate efforts, in terms of statistical analysis, not directly on the variability of loads themselves but on the variability of the factors that determine such loads, which will be labelled as influential factors.** If stochastic models can be proposed for the evolution of such factors, then an arbitrarily large sample of load histories may be derived through simulation for any given vehicle and component.

The attention is restricted here to **road-induced vertical loads** and it is thus necessary to propose stochastic models (*i.e.* probabilistic descriptions) for the evolution of the geometry of the covered road surfaces and for the evolution of the speed of the vehicle on these surfaces, which should be viewed as the main influential factors. Multiple random realisations of road and speed profiles can then be generated and applied to a model of the considered vehicle in order to calculate, through vertical dynamics simulation, a desired set of load histories (or responses of the vehicle).

Obviously, it is only possible to generate representative load histories if two conditions are satisfied. First, the randomly generated road and speed profiles must be representative (in the statistical sense) of the road and speed profiles that could have been measured in practice. Second, any result based on simulation is dependent on the fidelity of simulation and of the selected vehicle model.

The main interests that naturally originate from a simulation-based framework are its ability to **generate an arbitrarily large set of load histories at a low cost and time, and for any component on a given vehicle with known mechanical characteristics**. Thus, the information obtained on load variability can both be an extensive description of the large diversity of loads within the population of customers and be adapted to any new vehicle being designed.

In this manuscript the principle of the proposed methodology is precisely described. Its practical implementation is discussed, tested and analysed. To this purpose, the issue of the variability of influential factors (road and speed) is addressed and specific stochastic models are selected to describe such quantities. **The selection and validation of representative stochastic models constitute a central objective of the present work**.

Variability of influential factors, acquisition of statistical data and use of life situations

In order to analyse the variability of road and speed profiles and propose relevant stochastic models, **it is imperative to acquire (extensive) statistical information on such profiles**. Here this information is extracted from existing load measurement campaigns. Arguably this is not the most straightforward approach (indeed road profiles could be directly measured) since one objective of the methodology is to avoid a costly measurement campaign. Yet the use of an existing measurement campaign is an interesting framework to test the methodology and compare simulated load histories with measured load histories. Also, in the context of this research work, it represents the only available and extensive source of statistical information about road and speed factors.

Speed profiles are readily accessible as they are directly measured. Conversely road profiles are not. **An efficient road estimation algorithm is proposed in this manuscript in order to extract the information on the covered road profiles from the responses of the vehicle to such profiles**. This road estimation algorithm is described and tested within the present manuscript. It is used to extract road-related statistical information at a very insignificant cost from existing datasets gathered by Renault in different countries. This information is then put to use to select and test stochastic models for road and speed profiles.

Furthermore, the variation of influential factors within the population of vehicles can be more thoroughly analysed through the concept of life situations. The life of vehicles is divided into multiple identifiable segments, *e.g.* city, country or highway travels (or routes), for which the variation of influential factors is naturally reduced and may thus be more easily described. The concept of life situations is introduced in order to make use of valuable information about the variation of influential factors throughout the lives of vehicles. This information may be gathered rather inexpensively through surveys carried out among customers. The implied division of the 'population of loads' into different categories or 'strata' may be seen as an application of stratified sampling. Additionally, the processed datasets (existing measurement campaigns) from which statistical information is extracted here, have also been acquired using such a division into different life situations.

Essentially, the proposed methodology may thus be conceptually seen as a combination of vehicle dynamics simulation, stochastic modelling of influential factors and stratified sampling.

Research framework

The research work developed within this manuscript has been initiated at the request of Renault with the objective of providing a better assessment and control of the reliability of its different vehicles and their constituents, as early as possible in the vehicle development process and in adequacy with customer requirements in its different markets. This work is financed by Renault and by the French "Association Nationale de la Recherche et de la Technologie" (ANRT), in the context of a "Convention Industrielle de Formation par la REcherche" (CIFRE) and under the supervision of the "Institut Pascal CNRS / UBP / IFMA."

The datasets acquired on instrumented vehicles in various countries and on Renault's different proving grounds, which are processed and analysed throughout this manuscript, have been provided by Renault along with the detailed multi-body simulation tool.

Outline of the manuscript

The outline of the manuscript is illustrated in figure 1.1.

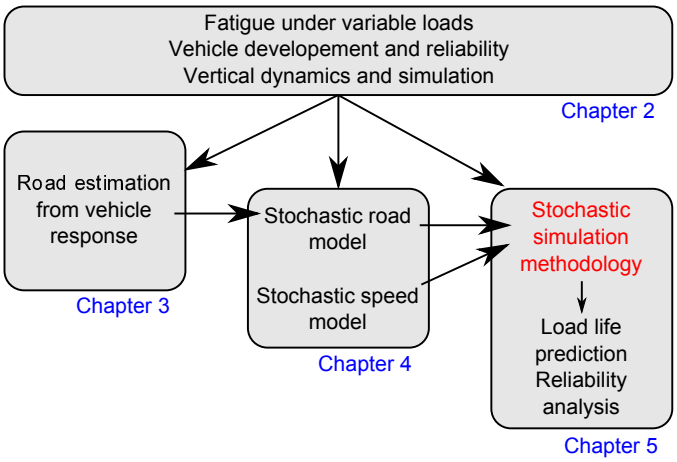

Figure 1.1: Outline of the manuscript.

Chapter 2 introduces the main concepts related to the fatigue of structures submitted to variable loads, which constitutes the underlying framework of this manuscript. The practical simplifications that are applied in order to quantify load variability more easily are detailed. The industrial context of vehicle development and the specific difficulties related to the issue of load characterisation that the present work aims to address are also discussed. Eventually, some elements about the simulation of the vertical response of a vehicle submitted to a road excitation are given.

Chapter 3 is slightly more independent than other chapters. It discusses the issue

of the estimation of road profiles from vehicle responses, which constitutes an inverse problem. An efficient algorithm is proposed to solve such a problem. It is tested using several experimentations and its quality and limitations are analysed.

Chapter 4 briefly introduces some important notions of stochastic process theory. It discusses potential candidates for road and speed models, based on the analysis of literature and on the information collected through the application of the road estimation algorithm on existing datasets. A study is carried out in order to select the best model, according to specifically defined criteria and in view of the available data.

Chapter 5 then precisely **details the proposed stochastic simulation methodology** and the concept of life situations (stratified sampling). The methodology is tested through the comparison of simulated campaigns with existing load measurement campaigns. Also, several statistical questions and difficulties relative to the variability of influential factors throughout the life of different vehicles of a population are discussed and analysed within this chapter. An application of the methodology is eventually proposed in order to illustrate its usefulness in an industrial setting, in particular, to study the effect of modifications in the loading environment (*e.g.* loads corresponding to a different market or a vehicle with different characteristics) and enquire whether design and validation targets should be adapted.

The main contributions of this research work and the results of the different experimentations are summarized in chapter 6. The overall quality of the proposed implementation for the proposed stochastic simulation methodology is analysed. Limitations and perspectives for improvement are discussed.

Chapter 2

Reliable design of vehicle components subjected to variable loads

Contents

2.1 Fatigue phenomenon in the context of load variability 8
2.1.1 High-cycle fatigue and fatigue strength of a material 8
2.1.2 Fatigue life assessment under variable amplitude loads 10
2.1.3 Damage equivalent load for analysis and testing 11
2.2 Design of vehicle components and reliability requirements 15
2.2.1 Vehicle development process 15
2.2.2 characterisation of load variability 17
2.2.3 Design, testing and assessment of reliability in practice 21
2.3 Simulation of the loads acting on vehicle components 25
2.3.1 Vehicle dynamics and vertical responses 25
2.3.2 Architecture of the vehicle and vertical dynamics modelling 26
2.3.3 Solving of the equations of vertical dynamics 28

"And thus, the actions of life often not allowing any delay, it is a truth very certain that, when it is not in our power to determine the most true opinions we ought to follow the most probable."
René Descartes

All the research work described in the present manuscript constitutes a particular instance of a larger issue, namely the reliability evaluation of mechanical structures subjected to variable loads. In this chapter, several elements of this framework are detailed in order to put the content of the manuscript into perspective and precisely define its boundaries and specificities.

The fundamental concepts of fatigue analysis are recalled in section 2.1 and practical approaches to load variability are introduced. In section 2.2, the design and validation processes that are applied in order to meet reliability requirements are discussed. Also, the industrial framework of vehicle development is detailed. Eventually, as it is a large part of the issue that is addressed in this manuscript, the description of vertical vehicle dynamics is discussed in section 2.3.

These different elements, both theoretical and practical, are used throughout the manuscript, either to run specific calculations and experiments or to analyse and discuss the obtained results.

2.1 Fatigue phenomenon in the context of load variability

Before describing the fatigue phenomenon, let us acknowledge that other factors may cause a degradation of the material, namely corrosion or ageing of the material due to thermal and/or humidity cycles. Such factors are not considered in this research work, even if their action should not be fully disregarded when studying the reliability of vehicle components. Also, brittle fracture due to stress levels that exceed the yield stress of the material, which can be encountered with extreme and non-standard operating conditions, *e.g.* severe shocks or accidents, are not considered here.

2.1.1 High-cycle fatigue and fatigue strength of a material

The fatigue phenomenon describes the **progressive degradation of a given material subjected to a time-varying mechanical load**. In the context of high-cycle fatigue, the material is subjected to a large number of stress cycles, whose levels are inferior to the yield strength of the material and which cause irreversible modifications in the micro-structure of the said material. Taken individually, these cycles are not sufficient to trigger a fracture of the material, but their cumulative effects over time eventually leads to such a fracture, see *e.g.* [Dirlik, 1985, Lalanne, 2010]. Hence, **fatigue is a cumulative and time-dependant phenomenon.**

The objective of the design against fatigue failure is to choose a material and select dimensions for the structure so that the latter is able to withstand the accumulation of stress cycles, during a predefined time frame (life of the structure), without failing.

In order to determine the quantity of stress cycles that a component or structure is able to withstand, named **fatigue strength**, experimental characterisations are generally

required. The latter are often based on uni-axial and constant amplitude (fully reversed cycles) tests, $R = \sigma_{min}/\sigma_{max} = -1$, imposed on a specimen of the studied material, see figure 2.1. Different load configurations could be considered but they give results that are more specific, which can be costly if experiments have to be repeated for multiple configurations. Uni-axial test results can generally be used to handle more complex loads, *e.g.* multi-axial, through certain characterisation methods and appropriate criteria that will not be described here, see *e.g.* [Pitoiset, 2001].

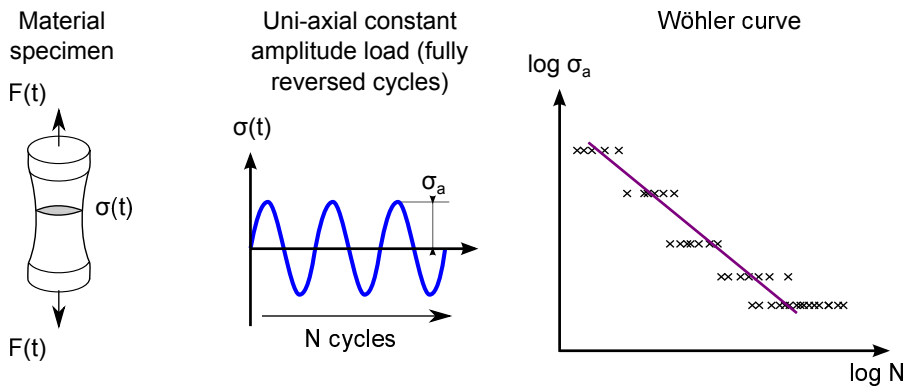

Figure 2.1: Experimental set-up: the stress $\sigma(t)$ is controlled (left). The applied load is composed of constant amplitude fully reversed cycles (center). Wöhler curve (S-N curve) obtained from the tested specimens (right).

Since the micro-structure of the material is seldom identical between several specimens, however carefully the specimens might be prepared, a significant scatter is generally observed in the experimental test results. Through the repetition of numerous fatigue tests, S-N curves or Wöhler curves can be drawn, see *e.g.* [Lalanne, 2010, AFNOR, 1991]. The latter link, on average, the constant amplitude of the imposed stress cycles σ_a to the number of cycles needed to reach failure N, as displayed in figure 2.1.

For most linear elastic materials, *e.g.* metals, it is often assumed that the load frequency has no effect on test results (within reasonable limits), see [Lalanne, 2010].

Different domains are generally identified to describe the fatigue phenomenon. Low-cycle fatigue corresponds to stress cycles that exceed the elastic limit and may generate plastic deformations. In such case, the number of cycles to failure is often low (*e.g.* $N < 1000$). On the other hand, high-cycle fatigue corresponds to stress cycles which amplitude is inferior to the elastic stress of the material. The material is damaged progressively and can endure a large number of cycles before failing, typically a few thousands to several million cycles. Eventually, for some materials, under a certain amplitude, labelled endurance limit σ_D, the cycles do not generate a permanent damage and the material will not experience failure. Here, the interest of the study is centred in the **high-cycle fatigue** domain.

In the high-cycle domain, multiple models can be identified, depending on the material

concerned and in view of the experimental results. The most simple and widely used model, for characterisation made with a load of constant amplitude σ_a, is the Basquin's relation [Basquin, 1910]:

$$N = K\sigma_a^{-\beta} \tag{2.1}$$

where $\beta > 0$ is the Basquin's exponent and K is a constant. N is the fatigue life of the specimen, *i.e.* the number of cycles that the latter is able to withstand before failure occurs. Both β and K are material parameters that have to be identified experimentally. This relation is deterministic and does not account for the scatter that is observed in practice. It is thus an **average description of the fatigue life** of the tested material. Models that include a probabilistic description of the observed scatter can be considered, such as the ESOPE model, see *e.g.* [AFNOR, 1991, Echard, 2012], which considers that for a given fatigue life value N, the associated amplitude σ_a is distributed normally.

The use of S-N curves remains a very empirical but yet widely applied approach. It does not involve a detailed analysis of the phenomena that may occur at the micro-scale. Even if it does not provide an understanding of micro-mechanical phenomena, this characterisation method is quite useful for a large number of practical applications.

Furthermore, if the load with a constant amplitude σ_a has a non-null mean σ_m, it is possible to account for the effect on fatigue strength. A possible (empirical) approach based on the use of the Goodman line, see [Lalanne, 2010], is to correct the amplitude of the load to σ_{aeq}, according to:

$$\sigma_{aeq} = \left(1 - \frac{\sigma_m}{R_m}\right)\sigma_a \tag{2.2}$$

where R_m is the ultimate tensile strength of the material.

2.1.2 Fatigue life assessment under variable amplitude loads

While fatigue strength characterisation often implies constant amplitude loads, most structures are subjected to variable amplitude loads. Thus, the assessment of the fatigue life of these structures requires a specific approach. The most simple and commonly used approach consists in **interpreting a variable amplitude load as a sequence of stress cycles**, which contributions (to the degradation of the structure) can be analysed individually and latter summed.

More precisely, the following assumptions are made. First, the load frequency has no influence on the fatigue phenomenon. Second, the contribution of cycles of different amplitudes can be studied individually and depends only on the amplitude (or corrected amplitude σ_{aeq}) of the cycles. Third, the order of the cycles in the sequence has no influence on the fatigue phenomenon.

The concept of **damage value** D is introduced, where $D = n/N$, n is the number of constant amplitude cycles and N is the fatigue life of the material, *i.e.* the number of cycles needed to provoke the failure of the material with such a constant amplitude load. Thus, if $D \geq 1$ the failure occurs. The approach known as the Palmgren-Miner rule [Miner, 1945], or linear accumulation rule, consists in **adding the contributions of the cycles of different amplitudes**:

$$D = \sum_{i=1}^{p} d_i = \sum_{i=1}^{p} \frac{n_i}{N_i} \tag{2.3}$$

where the load is composed of p different stress cycles of amplitude σ_i, which are repeated n_i times. For each stress amplitude, it would require N_i cycles to provoke the failure of the material and consequently the contribution of the n_i cycles only account for a fraction of the damage, namely $d_i = n_i/N_i$. Although the linear accumulation rule does not describe perfectly all material behaviours, it can be easily applied and gives good results for many applications (especially with metals and high-cycle fatigue), while alternative methods are generally more complex and application-specific, see [Lalanne, 2010] for a comprehensive study of available approaches.

In order to apply this rule, it is necessary to possess a strategy to transform variable amplitude loads into a sequence of cycles, or groups of cycles, of constant amplitude. The Rainflow counting procedure [Matsuishi and Endo, 1968, AFNOR, 1993] is the most commonly used approach to perform this decomposition of a variable amplitude load. It is used throughout this manuscript. First, the original load signal is transformed into a sequence of turning points (local extrema). Then, the application of the Rainflow counting algorithm yields a set of cycles defined by their min-max values, *i.e.* pairs of values $(\sigma_{min}, \sigma_{max})$. They can be sorted within classes of different stress levels and stored in so-called Rainflow matrices. Here, they are transformed into mean-amplitude pairs (σ_m, σ_a). The damage value D associated to a given load of variable amplitude, may then be calculated using equations (2.1), (2.2) and (2.3).

2.1.3 Damage equivalent load for analysis and testing

External loads and internal stress state

So far, fatigue theory has been described in relation with the stress state that exists within a given material, since the fatigue strength of such material has been characterised with respect to stress cycles. In practice, it may not be easy to calculate, measure or control the stress state inside a complex structure. However, this stress state depends on the external mechanical actions, which may be denoted as '**external loads**', that are applied on the structure. The latter are easier to measure or to calculate. Consequently, it is much more convenient to study load variability through the analysis of 'external loads'. Also, in a testing environment it is generally simpler to control the actions applied on

the structure rather than its internal stress state. The trade-off is that, when focusing on 'external loads', it is not directly possible to make a prediction regarding the fatigue life of the structure, other than through calculations of the internal stress field (*e.g.* using finite-elements analysis) or through very costly and specific fatigue testing at the level of the structure.

Under certain hypotheses, it is possible to use the different concepts of fatigue theory, while focusing only on the external mechanical actions imposed on a given structure or component rather than on its internal stress state. If the considered structure has a linear elastic behaviour, then there exists a linear relation between the external load and the stress state inside the material, see *e.g.* [Genet, 2006, Johannesson and Speckert, 2013]:

$$\sigma(t, M) = c(M)F(t) \tag{2.4}$$

where M is a point within the structure where the uni-axial stress $\sigma(t)$ is measured, and $c(M)$ is a constant that depends on the material and on the geometry of the structure. In this case, any cycle described by the external load corresponds to a cycle in the stress state of the material. Consequently there is a simple proportionality relation between the damage value that is calculated with the stress signal $\sigma(t)$ and the damage value that can be calculated using the external load $F(t)$.

Damage equivalent load

The concept of damage equivalent load may be defined, see *e.g.* [Thomas et al., 1999, Genet, 2006, Echard, 2012, Johannesson and Speckert, 2013]. When Palmgren-Miner's rule can be applied, it is convenient, either for testing or analysis, to convert a variable amplitude load into a simple constant amplitude load that generates the same damage, from the standpoint of the material. If those two loads are associated to the same damage value, the following equation may be written, using equations (2.1) and (2.3):

$$\frac{n_{eq}}{K\sigma_{eq}^{-\beta}} = \sum_{i=1}^{p} \frac{n_i}{K\sigma_i^{-\beta}} = D \tag{2.5}$$

where n_{eq} is the number of cycles of the load of constant amplitude (null mean) σ_{eq}, D is the result of the damage evaluation associated to the variable amplitude load and β and K are material parameters. If stress cycles σ_i (with null mean or corrected amplitude, see equation (2.2)) can be related to cycles of the external load using (2.4), then (2.5) may be transformed into:

$$F_{eq} = \left(\frac{1}{n_{eq}} \sum_{i=1}^{p} n_i F_i^{\beta} \right)^{\frac{1}{\beta}} \tag{2.6}$$

where F_i are the load cycles extracted through the application of Rainflow counting on the load signal $F(t)$. The value F_{eq}, which will be subsequently labelled **damage equivalent amplitude** (DEA), **is the amplitude of a fully reversed** ($F_{min} = -F_{max}$) **external load made of** n_{eq} **cycles that, if applied to the structure, would generate the same amount of damage as the variable amplitude load** $F(t)$.

One should note that, while dynamic effects, *i.e.* the frequency of the signal containing cycles, may reasonably be disregarded when considering the influence of stress cycles on the deterioration of the material, it is not so evident with external loads. If the frequency of the load is susceptible to provoke a dynamic response of the structure, *e.g.* amplification effects, care is advised when using the notion of damage equivalent external loads. Hence, this approach is only applicable when dealing with 'stiff' components, see [Johannesson and Speckert, 2013]. With the latter, within reasonable boundaries for the frequency of the equivalent load (n_{eq}, F_{eq}), **it can be considered that cycles of the external load are related to stress cycles inside the material in a 'quasi-static' manner**. This is generally true if the highest frequency in the load is notably lower that the first eigenfrequency of the structure.

Use of damage equivalent amplitude (DEA) and pseudo-damage

It can be seen that K and $c(M)$ conveniently disappear from equation (2.6). This is very interesting for several reasons. First, $c(M)$ can only be evaluated through a detailed analysis of the structure and/or finite-element calculations, which may be complex and/or costly. Second, while β is generally compiled in tables for multiple materials, K is often harder to estimate. Eventually and especially, during the design process, the structure can be iteratively modified and it is desirable, when analysing a variable loading environment, to do so in a manner that is as independent from the specifics of the structure as possible. Using equation (2.6), the comparison between two loads acting on the same component, in terms of the effect they have on its degradation, is only dependent on the Basquin's coefficient β.

From the standpoint of load variability analysis, this is a conceptual point that is quite noteworthy. Indeed, the main objective of this research work is to **characterise load variability and the effect it has on vehicle components**. Here, it is seen that the comparison between multiple loads inevitably depends on the component on which such loads are applied. If the notion of **load severity** is introduced and if **a load is said to be more 'severe' when its leads to a higher damage accumulation in the material (*i.e.* brings the component closer to failure)**, then the difference in severity between two loads depends on β.

From the standpoint of testing, the damage equivalent amplitude F_{eq} is directly the value that needs to be set into the test-rig, provided all the previous hypotheses regarding the damage equivalence of external loads are applicable. In this framework, the constant amplitude testing is supposed to produce the same damage on the component as a variable amplitude load, which may have been acquired for example through measurements in

operating conditions (*i.e.* in the actual loading environment).

The damage equivalent amplitude F_{eq} (DEA) is a very convenient tool to compare loading environments. It is an objective measure of the severity of different loads, as well as an easily interpretable value, since it shares the same unit as the external load. Also, as will be done throughout this manuscript, it is possible to **extend the notion of 'load' to any quantity that is proportional to a mechanical effort**, *e.g.* a displacement through $F = k\delta$ or an acceleration through $F = m\gamma$. This enables us to express a variable amplitude signal, which is deemed relevant for the study of load variability, as a simple scalar value, while somehow accounting for the fatigue phenomenon. This is **very convenient for statistical analysis** (*e.g.* of vehicle responses), where the manipulation of signals, power spectral densities (PSD), cycle histograms, etc., may be much more complex.

In what follows, if damage values are calculated on external loads described through effort signals or other type of quantities, the term '**pseudo-damage**' value will be preferred. It must not be forgotten that the severity of different loads has to be analysed in relation with a given component. In this framework, the parameter K of the fatigue strength model, see equation (2.1), generally cannot be determined simply, nor will this be attempted.

The relation $D > 1$, that is tested using (2.3), is no longer a criterion for the failure of the component if K is fixed to any desired value. Nonetheless, the pseudo-damage may still be used for comparison purposes. Here $K = 1$ is defined and the comparison between loads only depends on the Basquin's exponent β. This latter parameter β has to be selected in order to be representative of the studied component. The **pseudo-damage** value is calculated according to:

$$d = \sum_{i=1}^{p} n_i (\Delta y_i)^{\beta} \tag{2.7}$$

where Δy_i are the amplitudes of the cycles extracted (through Rainflow counting) from a given response signal y_i.

Practical testing with complex systems and loads

Arguably, the use of equivalent external loads represents a simplification of the fatigue problem and consequently it involves approximations. This approach may not be sufficient to assess the fatigue life or carry out appropriate testing of components when realistic and complex loads (*e.g.* multi-axial) and structures (*e.g.* non-linear or non-stiff) are involved. Palmgren-Miner's rule may not be applicable if the order of the cycles within sequences cannot be ignored. It is then possible to use alternative methods for experimental testing or fatigue life calculations based on simulation:

- Reconstruct variable amplitude random load sequences from Rainflow matrices, see

e.g. [Dreßler et al., 1997].

- Use scaled versions of a given load sequence or load spectra (number of cycles per stress level or stress classes), see *e.g.* [Heuler and Klätschke, 2005].
- Use repetitions of ordered sequences of load cycles or realistic blocks of load signals, see *e.g.* [Heuler and Klätschke, 2005].

More thorough discussions on the matter may be found in [Heuler and Klätschke, 2005, Johannesson and Speckert, 2013]. When non-stiff, non-linear complex structures and/or mutli-axial loads are studied, it may not necessarily be possible or relevant to simplify the load. It is generally advised to carry out testing with realistic loads, where the order of cycles, frequency of the signal and main loading directions are representative of actual operating conditions.

In some of the previous approaches, simple damage calculations can still be used, for example, in order to assess the contribution of different blocks of realistic load signal that are repeated on test rigs. Hence, **regardless of the aforementioned difficulties, the use of pseudo-damage values (in the sense of equation** (2.7)**) and equivalent load representations (DEA), constitutes a powerful tool to work with load variability and in the practical framework of vehicle design.** The latter context is described in the following section.

2.2 Design of vehicle components and reliability requirements

2.2.1 Vehicle development process

Reliability requirements and reliability targets

The development of a vehicle is essentially an optimisation problem, with multiple objectives involved. As in any product development context, the central goal is to maximize profitability, which traduces to maximizing sales volume while minimizing both design and production costs. More pragmatically, a product, *e.g.* a vehicle, is likely to maximise sales if it meets **customer requirements**. Reliability is one of these requirements. It is defined as 'the ability of a system to accomplish a required function in given conditions and during a given period of time', see *e.g.* [Lemaire, 2013].

Reliability requirements generally derive from the analysis of the gravity of potential failures. The consequences of failures may range from concerns for the safety of vehicle occupants to the dissatisfaction experienced by a customer who is not able to use its vehicle, in normal conditions or at all, or has to pay for repairs. Also, the car marker is generally willing to minimize the cost of the failures that it has to support through the warranty. Reliability targets are defined for the different components of the vehicle through

the study of such considerations. These targets may be expressed as failure probabilities or equivalently as the acceptable number of failed individuals within a population of vehicles.

Design and validation against reliability requirements

The definition of reliability targets is the first step in the process of design against reliability (see figure 2.2 below). The analysis of potential failures and the gravity of their consequences must be carried out at different levels, namely vehicle level, sub-system level and component level. For example, the failure of a sub-system may be due to the failure of one or several of its constituting components. In this case, the reliability target defined for a given sub-system impacts the definition of the reliability target set for its different constituents. This is not the focus of the present study.

Essentially, **reliability evaluation relates to the statistical analysis of the expected number of failed individuals within a population of components, given that they may be subjected to different loads and that their capacity to support such loads without failing is scattered**. Hence, to evaluate the reliability of a component it is imperative to have a quantitative description of the external loads to which the latter may be subjected when it is used. **The objective of the design process is then to make sure that the component possesses the required strength to support the loads to which it may be subjected, and thus meets the prescribed reliability target.**

This can be achieved either through an adaptation of the strength of the component, *e.g.* increasing thickness, modifying the geometry, choosing a material with a higher strength limit, diminishing fabrication scatter (*e.g.* welding precision, material quality, etc.) or through a modification of the external loads to which this component is subjected, *e.g.* modifying the load path spanning from the road to the component, changing boundary conditions (assembly, joints). Indeed, the loads applied on a particular component of the vehicle are often dependent on the characteristics of other components of the vehicle (*e.g.* tyre stiffness, suspension damping, etc.).

Since reliability is not the only requirement that constrains the design of a component of the vehicle, it is desirable that the strength of such component is neither inferior nor superior to what is actually needed, given the environment in which it is going to be used (and the mechanical characteristics of the vehicle). For example, cost and weight are requirements that are generally antagonistic to reliability and simultaneously very important in the automotive industry. Components should neither be oversized nor undersized.

The development of the vehicle is performed according to the process illustrated in figure 2.2. Generally the design stage is an iterative process and **it may be necessary to perform multiple reliability evaluations for different candidate designs of a given component, or different modifications in the load path**. During the validation stage, the load path extending from the road to the studied component no longer varies and a reliability assessment can be performed either through simulation,

physical testing or a combination of both. When validating complete sub-systems or dealing with complex loads or structures, physical testing is generally involved at some point.

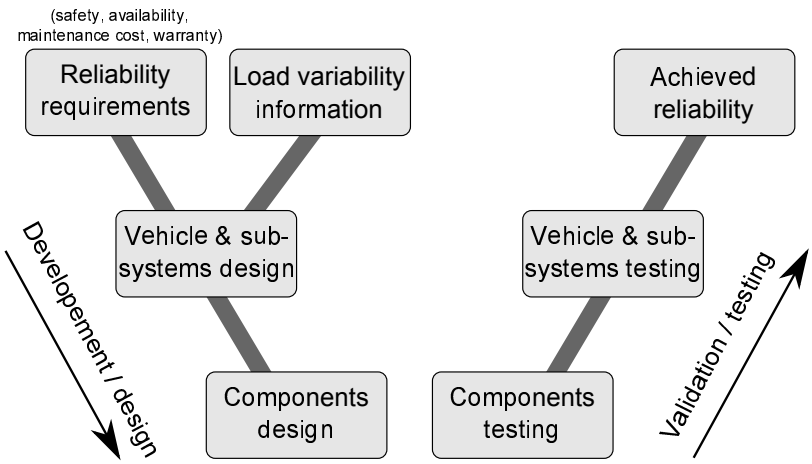

Figure 2.2: Vehicle development process. Design against reliability.

Let us strongly emphasize that it is imperative to possess a representative and quantitative description of load variability from the standpoint of each of individual component before any trustworthy evaluation can be made regarding their reliability, either during design or validation stages. **Acquiring relevant information on the variability of the external loads acting on a component is the central focus of the present manuscript and is discussed in the following subsection**.

2.2.2 characterisation of load variability

Strong diversity of the loads acting on vehicles

The diversity of loads imposed on vehicle components is arguably very strong, and its characterisation (or quantification) constitutes the main objective of this research work. This diversity may originate from:

- The multiple usages that can be made of the vehicle by different customers, *i.e.* the fractions of the distance covered within different 'situations', *e.g.* city routes, highway routes and so on. This is arguably extremely diverse.
- The multiple road surfaces that exist within a given region or country.
- The multiple driving behaviours of customers.
- The multiple level of cargo that can be loaded into the vehicle.

- The multiple vehicle designs which impact the external loads that are imposed on a particular component, through the modification of the load path (spanning from the road to the considered component).

Acquiring informations on load variability necessarily implies **collecting samples of load histories**, either through measurements or simulations. It is desirable to construct a quantitative (mathematical) description of this observed diversity.

Quantitative description of load variability

Load histories are complex entities, namely continuous signals, and their diversity is thus quite difficult to describe in a simple and objective manner. Nonetheless, in the subsetion 2.1.3 it has been shown that under certain (simplifying) assumptions, it is possible to transform load histories into scalar values more convenient for statistical analysis, namely pseudo-damage values or damage equivalent amplitudes (DEA). From the standpoint of load variability analysis, pseudo-damage values simply represent tools that render the issue more tractable.

Let d be the pseudo-damage value, calculated through (2.7), associated to a dynamic response signal of the vehicle that is directly related (*e.g.* linearly) to the external load applied on a studied component. If this value is calculated from different load histories acquired on different vehicles of the population (or on a given instrumented vehicle and with different drivers), then a sample of d values is obtained and a distribution can be identified. An example is displayed in figure 2.3.

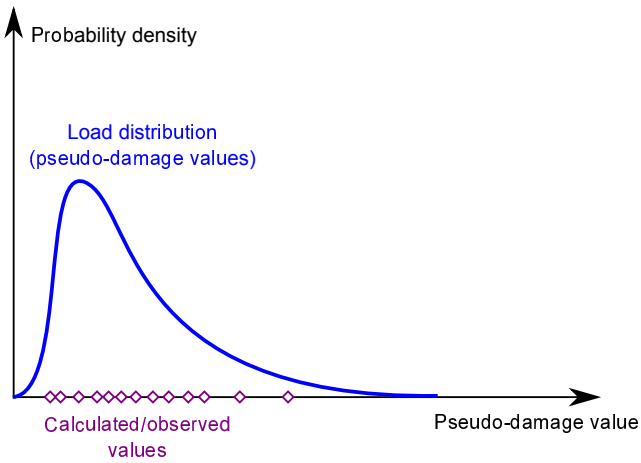

Figure 2.3: Distribution representing load variability.

The sample of pseudo-damage values represents a quantitative (and simplified) description of the variability associated to the external load acting on a given component, on a vehicle with a given set of characteristics and within the population of customers (drivers).

A similar distribution may be identified for all relevant response signals of the vehicle. The obtained and processed dataset is essentially a matrix of values (d_{ij}), where i is the number of performed measurements (or simulations) and j is the number of considered response signals (*e.g.* sensors on the instrumented vehicle).

Data acquisition process

Today for most car-markers such as Renault, the acquisition of information about load variability is based on the use of so-called **load measurement campaigns**, see *e.g.* [Thomas et al., 1999], [Heuler and Klätschke, 2005] or [Johannesson and Speckert, 2013], wherein load histories are recorded using an instrumented vehicle. Such campaigns can be performed according to different sampling strategies, more thoroughly described in subsection 5.2.2:

- **Random sampling campaigns**, wherein randomly selected drivers are provided with an instrumented vehicle which they can use as they desire.

- **Stratified sampling campaigns**, wherein certain circuits are selected for different 'life situations'. Drivers perform measurements on the latter with an instrumented vehicle. The obtained values are combined according to information that has been previously gathered through surveys, where customers are asked the fraction of the time that they attribute to different life situations.

The constitution and analysis of sufficiently large datasets based on such campaigns represent the core of the load characterisation issue. As the obtained dataset is the result of a sampling from the set of all possible load histories, it is obviously dependant on the chosen/observed load histories (*e.g.* circuits, drivers). Furthermore, since load measurement campaigns tend to be long and costly, **the size of this dataset is often naturally limited**.

In this manuscript a methodology is proposed and described in chapter 5 in order to **acquire information on load variability using simulation and stochastic modelling of the road excitation rather than measurements on a instrumented vehicles**.

The proposed methodology is a interesting approach to address the following issue. How is load variability affected, for the different components, when the loading environment is significantly modified, *e.g.* for a different country (with different road networks), for a population of drivers (customers) with different usage and behaviours or for a new vehicle (with different characteristics)? This issue is an important aspect of the vehicle development process. Yet, **answering such a question can be a long, difficult and costly task when using measurement**.

Practical difficulties, simulation, measurements and load variability

Before closing this subsection let us describe different difficulties that may be encountered when studying load variability within the framework of the development process illustrated in figure 2.2. They are listed in what follows.

One of the main difficulty of dealing with a complex system is that it is often difficult to separate load characterisation from design choices. Indeed, the loads that act on the different components are both dependant on the external environment of the vehicle (road and vehicle speed) and on the characteristics of the vehicle, *e.g.* the vertical roughness of the tyre, damping in the suspension system or mass of the different bodies. **The load path that spans from the road, through the wheels, and toward the studied components is influenced by the specificities of the design of the vehicle.** In early design stages, it is not always possible to carry out measurements on a vehicle that possesses the characteristics of the new vehicle being designed, since **no prototype has been built yet**.

Additionally, since **the vehicle development process is generally iterative**, different load characterisations may have to be carried out for different evolutions of the characteristics of the vehicle. Also in practice, components are designed individually and a modification of one of the components may influence its surrounding neighbours, in terms of the load path that originates from the road. This iterative process is often necessary to achieve a compromise between different and sometimes antagonistic requirements for the vehicle, *e.g.* reliability, acoustics, comfort, handling, passive safety, etc. If load variability is studied purely through measurements, the cost of iterative characterisations may become prohibitive.

Eventually, certain responses of the vehicle or loads applied to components **cannot be easily measured**. The knowledge of the external loads applied on such components is nonetheless needed to carry out simulations, fatigue calculations or submit components to individual testing. To obtain information about load histories that are difficult to measure, it is often preferable to use simulation whenever possible (*e.g.* in terms of precision).

It is desired that the design and validation processes are as short, efficient (yield components that are neither oversized nor undersized) and cost-effective as possible. **Consequently, such processes are generally composed of a combination of measurement-based and simulation-based methods**:

- The first and most direct but somehow risky approach is to make use of the loads measured on a vehicle which characteristics are reasonably close to the new vehicle being designed.
- A second approach is to make use of deterministic road excitation profiles, generally based on an arrangement of road sections from a company-specific proving ground. The relationship between these deterministic profiles and the load distribution representing the population of customers is assumed to be known in advance (based

on previous measurement campaigns). Such profiles may subsequently be used to derive load histories for any vehicle through simulation. This approach is detailed in the following subsection.

- A third approach is to derive loads from stochastic simulations (random simulations of different customers). In this case it is possible to use a vehicle model which corresponds to the new vehicle being designed. However, this approach is only relevant if the vehicle model can be fed with realistic realisations of road excitations. This is an objective of the methodology proposed within this manuscript.

2.2.3 Design, testing and assessment of reliability in practice

Exploitation of the information on load variability

The use of pseudo-damage values is an interesting approach to quantify the variability of load histories within a population of vehicles (customers). Yet, pseudo-damage values are seldom directly exploitable for design and testing purposes. Thus, **it is often necessary to rely on deterministic (and realistic) road excitation profiles in order for the load distribution to be exploited in practice**.

Let us note that, throughout this manuscript load histories are transformed into scalar values, namely pseudo-damage, so as to simplify the study of load variability. If the implied simplification is not applicable for certain components or systems, then the statistical analysis of load histories has to be handled differently. However, since the direct objective of the methodology proposed in this manuscript is to generate load histories through simulation, this does not represent an issue. Indeed the generated histories may be processes according to any approach desired.

Use of deterministic road excitation profiles

In the practical industrial context, deterministic road excitation profiles or 'testing profiles', can be used for various reasons. On the one hand, the load distribution acquired on a vehicle with particular characteristics may not be sufficiently representative of the load distribution that would be experienced by a component mounted on a newly designed vehicle. It is then necessary to find a way to somehow 'transpose' the load distribution for a vehicle with different characteristics (*i.e.* a different load path to the component). On the other hand, the use of a constant amplitude load (based on DEA) may sometimes not be sufficient to carry out relevant fatigue tests. This is especially true when testing sub-systems, components with complex fatigue behaviours or components subjected to multi-axial loads.

Through the use of deterministic road excitation profiles, realistic load histories may be derived, either from simulation (multi-body simulation (MBS), see subsection 2.3.2) or

from measurements (latter in the vehicle development process), for any given component and for a vehicle with any given characteristics.

Such testing profiles are generally composed of an arrangement of different driving operations realised on a company-specific proving ground. Multiple road surfaces, *e.g.* smooth asphalt, concrete tracks, rough cobblestone pavements, and transient obstacles such as speed bump, pot-holes, manhole covers, etc., are covered at specific speeds by the vehicle, thus constituting a specific testing schedule. The loads applied on the vehicle components by each section of those testing profiles can be repeated multiple time (by blocks) and the arrangement of sections can be specifically chosen with the objective to accumulate a target amount of pseudo-damage for various components on the measuring vehicle.

Generally, the instrumented vehicle used to acquire information on load variability (measurement campaign) is also employed to perform measurements associated to a given testing schedule on the company-specific proving ground. The relationship between the testing profile and a given quantile (generally high) of the load distribution obtained from the load measurement campaign may then be established. This is displayed in figure 2.4.

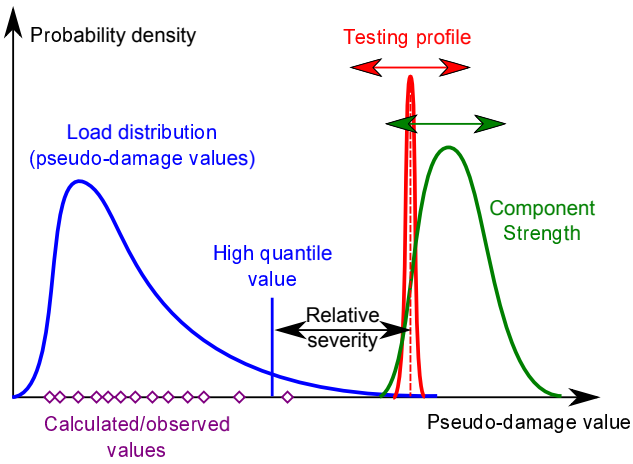

Figure 2.4: Use of the information on load variability. The relationship (or relative severity) between the testing profile and a given quantile of the load distribution may be established.

Ratios of pseudo-damage values (relative severity) may be established, for the different response signals on the vehicle, when considering any particular testing profile. Let us insist on the fact that **it is necessary to use the same vehicle on the proving ground and for the load measurement campaign in order to assess this relationship (relative severity)**.

Through the adjustment of the number and types of sections repeated within the testing schedule, it is possible to obtain realistic load histories corresponding to any desired pseudo-damage target. In practice it is quite difficult to adapt the damage ratios

as precisely as desired for all the different response signals, as it constitutes a delicate optimisation problem, see *e.g.* [Johannesson and Speckert, 2013].

Nonetheless, in order to be able to make use of the load histories obtained from these testing profiles, regardless of the considered vehicle, the following hypothesis must be formulated. It is assumed that the relative severity (for a given component and obtained through a particular measurement campaign with an instrumented vehicle) between the testing profile and the load distribution is independent of the considered vehicle. This is arguably a strong assumption. Yet, there is no alternative to 'transposing' the load distribution from one vehicle to another.

Realistic load histories for design and validation

Deterministic road excitation profiles may be used throughout the vehicle development process (see figure 2.2) as a source of information (adapted to the newly designed vehicle) about the loads applied on different components and their variability (yet indirectly). In such a case, the vehicle development does not necessarily imply the realisation of a long and costly measurement campaign. Let us note that this approach relies on multiple hypotheses and constitutes a practical simplification of the load characterisation and testing problems, which may nonetheless be very useful in an industrial context, see *e.g.* [Johannesson and Speckert, 2013] for more thorough discussions.

In **design stages**, it is relevant to use a very precise model of the vehicle (see subsection 2.3.2) in order to simulate through MBS the loads that will be imposed on the components of a specific vehicle by the testing profile. To carry out this simulation it is necessary that the road surfaces of the proving ground have been measured, *e.g.* through laser scanning, so that they can be used as inputs for simulation.

Design choices can then be iteratively adapted using simulated load histories as inputs for precise fatigue life calculations based on finite-element analyses (FEA), or for individual testing of components (more costly).

In **validation stages**, in order to obtain a very precise information (*i.e.* free from excessive simulation errors) about the loads applied on specific components of the new vehicle, measurements can be carried out according to the testing schedule on the company-specific proving ground. The measured loads may be reproduced and repeated multiple time on test-rigs. Such an approach is widely applied by car-makers such as Renault, see *e.g.* [Johannesson and Speckert, 2013]. Indeed, **it is often more appropriate to use realistic loads (rather than constant amplitude loads) when testing components' strength** and especially when dealing with complex multi-axial loads or structures with complex fatigue behaviours. Such deterministic (or quasi-deterministic) testing profiles are commonly used for fatigue tests and to characterise the strength distribution.

Also, for multiple components, **deterministic testing profiles**, generally corresponding to high quantiles of the load distribution, may very well be **used in practice to define design targets**. In practice and without directly performing a reliability evaluation,

the criterion for accepting the design of a component may be that the latter is able to withstand the testing profile, say on average for deterministic FEA or for a few tested components, *e.g.* on test rigs.

Let us emphasize that, as useful as deterministic road excitation profiles may be in practice, **any assessment of the reliability of the vehicle components within the population of customers imperatively requires that the relationship between such profiles and the load distribution is precisely known for the different components**, see figure 2.4.

Reliability calculation using deterministic excitation profiles

Using the same simplification of the fatigue problem that is used for load histories, the strength of a component may be expressed as a scalar value, namely a pseudo-damage value. Simply put, **the strength of a component is defined through the load it is able to withstand**, itself expressed as a scalar value. In this (scalar) framework, quite appropriate to handle randomly varying quantities, the formalisation of the reliability problem may be described as follows.

The probability of failure of a given component is defined by the probability that the pseudo-damage value associated to the load (S) exceeds the strength value (R) of the component. The probability of failure of the component may then be calculated using:

$$P_f = \text{Prob}(R \leq S) = \iint_{r \leq s} f_{R,S}(r,s) dr ds \tag{2.8}$$

where S is a random variable associated to the load distribution, R is a random variable associated to strength distribution and $f_{R,S}(r,s)$ is the joint density function. It is assumed that both values are independent and so $f_{R,S}(r,s) = f_R(r) f_S(s)$. A practical illustration of the reliability problem may be seen in figure 2.4.

For the sake of the example, a closed-form solution may be derived if additional hypotheses are made regarding the S and R distributions. If the latter are described by log-normal distributions, then the probability of failure P_f may be calculated using:

$$P_f = \text{Prob}(ln(R) - ln(S) \leq 0) = \Phi\left(\frac{\mu_{lnR} - \mu_{lnS}}{\sqrt{\sigma_{lnR}^2 + \sigma_{lnS}^2}}\right) \tag{2.9}$$

where $S \sim LN(\mu_{lnS}, \sigma_{lnS})$ and $R \sim LN(\mu_{lnR}, \sigma_{lnR})$ or equivalently $ln(S) \sim N(\mu_{lnS}, \sigma_{lnS})$ and $ln(R) \sim N(\mu_{lnR}, \sigma_{lnR})$. Φ is the cumulative density function (CDF) of the normal distribution $N(0,1)$.

In order to perform such a calculation, it is necessary to express both the load and strength distributions in terms of comparable pseudo-damage values. This is clearly not

a standard approach since it has been seen that the strength distribution is generally obtained from specific constant amplitude fatigue tests on standardized material specimens.

In practice, the following method may be used to **characterise the strength of the component in terms of pseudo-damage value**. The testing profile, which corresponds to realistic load histories, may be used to test a sample of components using test rigs, and thus get an assessment of the strength distribution R (*e.g.* by recording the pseudo-damage values that led the specimens to failure). This yields values for μ_{lnR} and σ_{lnR}. The latter characterise the strength of the component through the (external) loads that it is able to withstand. This approach to the characterisation of the strength distribution of a component is clearly an experimental based approach but is is quite useful (and simple) in practice.

By comparison, it may be quite difficult to get an assessment of strength variability through simulation. Indeed, this would imply calculating the stress state of the component through precise FEA calculations, in the presence of complex loads and with a strong difficulty to take into account the scatter in dimensions, material properties or fabrication residual stresses and their impact on the calculated stress field. For validation purpose, it is often preferred to rely on physical testing.

While the relationship between the strength distribution and the testing profile can be known, *e.g.* through the testing of a few components using such profile, the relationship between the load distribution S and the testing profile is also known (from previous load characterisation campaigns), see figure 2.4. Hence, μ_{lnS} and σ_{lnS} are known from an *a priori* hypothesis about the previously establish damage ratio (relative severity see figure 2.4). Eventually an assessment of the probability of failure may be derived using equation (2.9). Here, **provided the information on the variability of loads is accurate and the relationship between the testing profile and the load distribution is well known**, it is conceivable to obtain a good estimate of the reliability of the component.

2.3 Simulation of the loads acting on vehicle components

2.3.1 Vehicle dynamics and vertical responses

The different components of a vehicle are submitted to multiple dynamic loads. When the vehicle travels at a given speed on a road surface with a varying elevation, this road surface represents a time-varying boundary constraint for the wheels of the vehicle. The displacements of the wheels then induce a dynamic response of the vehicle. From the standpoint of the vehicle, this varying boundary constraint represents a vertical excitation. The relative movements (or vibrations) of the different bodies composing the vehicle are associated with forces applied on those same bodies. The reliability of vehicle components is dependant on these time-varying forces and the damage they induce.

In this manuscript, the **attention is restricted to vertical dynamics and road-**

induced loads. It may be argued that for many components, the road-induced vertical loads represent a large fraction of the damage. Consequently, the study of vehicle responses will be limited here to the effect of the actions imposed by the variation in road surface elevation.

Let us point out that non-vertical actions are also applied on the vehicle's components due to steering, accelerations or braking commands imposed by the driver. Additionally, longitudinal and lateral forces are applied on the tyres through the contact patch, when the vehicle travels on a irregular road surface. Here, only vertical dynamics will be modelled and longitudinal and lateral dynamics will be disregarded. It must be noted that non-vertical actions can induce vertical responses, due to pitch or roll movements. These components of the vertical responses will not be described by the selected (quarter-car) vehicle model.

Eventually, non-mechanical actions such as the effect of temperature, humidity cycles, corrosion, etc., are disregarded. Even if these latter factors may have a significant influence on the reliability of some components of the vehicle, they extend beyond the scope of the present work.

2.3.2 Architecture of the vehicle and vertical dynamics modelling

The vehicle is a very complex non-linear multi-body system. Simply described, it is composed of a rigid chassis structure on which the front and rear suspension systems, the engine and power-train, as well as the car body, are mounted. The technical requirements guiding the design of the suspension systems are multiple and include for example handling (driveability), ride comfort or safety. The definition of the suspension system, *i.e.* architecture, angles, stiffness, damping, etc., has a strong influence on the loads that are applied on all components of the chassis and car body. The car body is equipped with doors, passenger seats, interior and exterior trims, etc., and the fixations of all those equipments are subjected to fatigue.

When it comes to describing vertical dynamics of the vehicle, the simplest approach is to define a model composed of two entities, namely the sprung mass and unsprung mass (possibly unsprung masses). A so-called **linear quarter-car model**, see *e.g.* [Howe et al., 2004], is displayed in figure 2.5. It describes one quarter of the vehicle and considers the movement of each wheel, independently from the others.

Such a model cannot account for pitch and roll movements of the car body. Nonetheless, it can give a good description of the vertical dynamics of a vehicle travelling at a given speed on a particular road surface. As stated in [Bogsjo et al., 2012]: "Such a simplification of a physical vehicle cannot be expected to predict load exactly, but it will highlight the most important road characteristics as far as fatigue damage accumulation is concerned". Hence, it may be considered **sufficient for the statistical analysis of vertical road-induced loads in a first approach**. For this model, the tyre is represented by a simple spring and the displacement of the contact point on the road surface constitutes the vertical

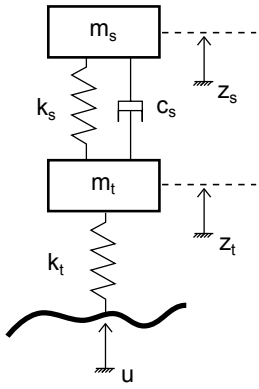

Figure 2.5: Quarter-car model of the vehicle.

excitation imposed to the model.

A more accurate representation of the typical architecture of the front and rear suspension systems is given in figure 2.6.

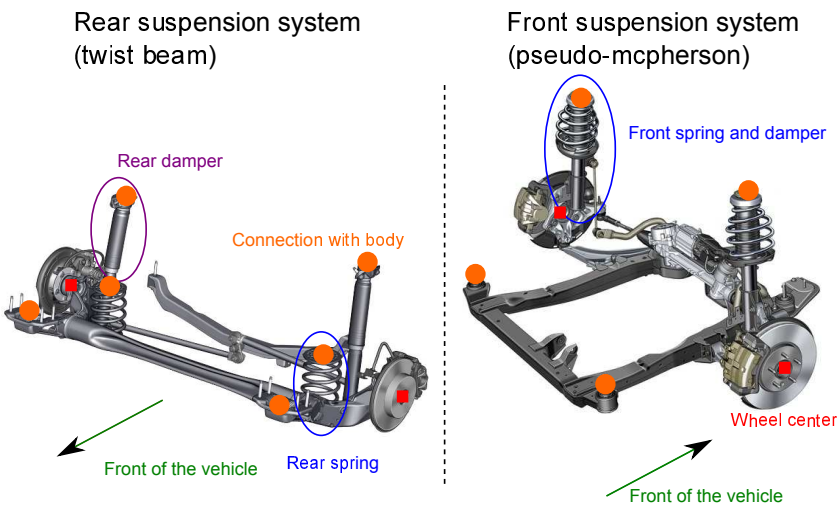

Figure 2.6: Typical architecture of front and rear suspension systems. Orange dots indicate connections with the chassis frame or car body.

In order to attribute values to the sprung mass m_s and unsprung mass m_t ('t' for tyre) it is necessary to determine which parts can be classified into those two sets. The sprung mass comprises by the chassis frame, car body and all equipments mounted on the car body (also the engine, sometimes considered as a third body for such simple models). The unsprung mass comprises the wheel hub, steering knuckle and brake disc and caliper. For some parts that connect both the sprung and unsprung mass, *e.g.* lower front arm, or spring, their mass has to be divided between the sprung and unsprung entities. This conversion of a multi-body problem into a two-body problem necessarily

implies simplifications and choices.

When the objective is to get an accurate description of the load path that extends from the road/tyre contact patch to individual components of the suspension system or chassis, it is necessary to rely on a more representative multi-body description of the vehicle. For example, in early design stages when no vehicle prototype is available, as described in subsection 2.2.3, it is interesting to simulate with high fidelity the responses to specific sections of a digitalized proving ground. In this case, a highly detailed multi-body model of the vehicle is used in combination with a representative tyre model, see *e.g.* [Johannesson and Speckert, 2013] for a discussion on tyre models. These simulations yield **realistic load histories** that can be used for finite-element (FE) fatigue calculations for different components (or even used on test-rigs). Such an example of a highly detailed model, in a state-of-the-art multi-body simulation (MBS) software is illustrated in figure 2.7.

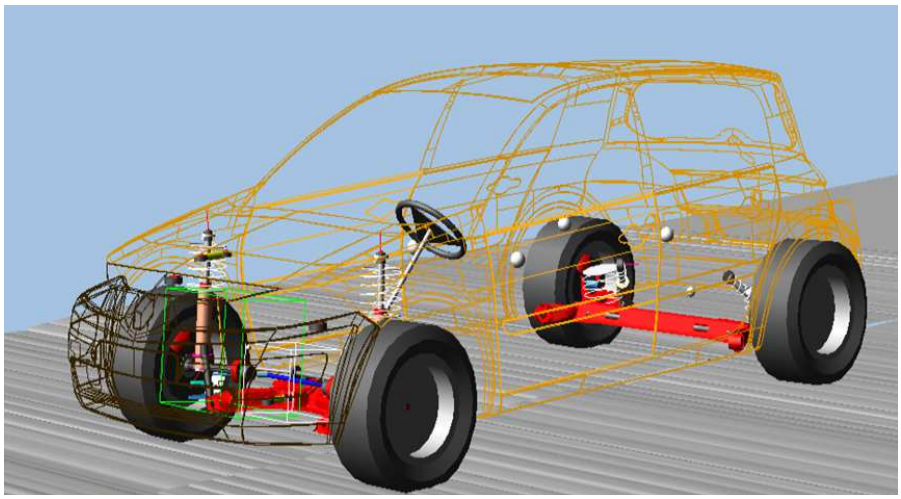

Figure 2.7: Highly detailed multi-body model in a multi-body simulation (MBS) software (for illustration purpose only). The vehicle travels on a digitalized road surface (obtained by scanning an actual proving ground).

2.3.3 Solving of the equations of vertical dynamics

The two degrees of freedom model (DoF) displayed in figure 2.5 is used here to discuss the resolution of the dynamics problem, which will be labelled throughout this manuscript as '**vehicle dynamics simulation**'. The two bodies define the following quantities that are extensively used in the following chapters, namely the suspension displacement $z_s - z_t$ (also noted $z_s z_t$), the sprung acceleration $\ddot{z}_s$ or a_s and the unsprung acceleration $\ddot{z}_t$ or a_t. The tyre is modelled by a simple spring whose extremity is driven by a time varying displacement u.

The quarter car model can be either purely linear or include non-linear elements of the real suspension system. The functioning of the damper is often very non-linear. Also, bump stops are mounted on the suspension system in order to limit the maximum clearance. When the suspension displacement is such that those stops are hit, the stiffness increases very significantly. Additional details are given in appendix B. The dynamics equation of the system may then be written:

$$\left\{ \begin{array}{c} \ddot{z}_s \\ \ddot{z}_t \\ \dot{z}_s \\ \dot{z}_t \end{array} \right\} = \left\{ \begin{array}{c} (1/m_s)\left(-F_c(\dot{z}_s, \dot{z}_t) - F_k(z_s, z_t)\right) \\ (1/m_t)\left(F_c(\dot{z}_s, \dot{z}_t) + F_k(z_s, z_t) + k_t u\right) \\ \dot{z}_s \\ \dot{z}_t \end{array} \right\} \tag{2.10}$$

where $F_c(\dot{z}_s, \dot{z}_t)$ is the force (potentially non-linear) applied by the sprung mass on the unsprung mass through the damper and $F_k(z_s, z_t)$ is the force (potentially non-linear) applied by the sprung mass on the unsprung mass through the spring (and bump stops). If non-linear aspects are accounted for, the system of Ordinary Differential Equations (ODE) in (2.10) has to be solved using a numerical integration scheme such as Runge-Kutta, see *e.g.* [Gear, 1971]. The formulation of the ODE, in an explicit form, may be re-written using state space representation:

$$\dot{\mathbf{x}}(t) = f(\mathbf{x}(t), t) \tag{2.11}$$

where the state vector is defined by $\mathbf{x} = [\dot{z}_s, \dot{z}_t, z_s, z_t]$. Upon completion of the numerical integration, the state vector $\mathbf{x}(t)$ may be used to calculate any desired output vector through $\mathbf{y}(t) = g(\mathbf{x}(t), u(t))$, where $g(.)$ is the output function which depends on the selected output vector.

In this manuscript, in order to deal with reasonable calculation times, non-linear aspect of the suspension system will be disregarded. The spring and damper connecting the sprung and unsprung masses are assumed to be linear. The model of the vehicle thus describes a linear time-invariant system and equation (2.10) may be written:

$$\begin{bmatrix} \ddot{z}_s \\ \ddot{z}_t \\ \dot{z}_s \\ \dot{z}_t \end{bmatrix} = \begin{bmatrix} -c_s/m_s & c_s/m_s & -k_s/m_s & k_s/m_s \\ c_s/m_t & -c_s/m_t & k_s/m_t & -(k_s+k_t)/m_t \\ 0 & 0 & 1 & 0 \\ 0 & 0 & 0 & 1 \end{bmatrix} \begin{bmatrix} \dot{z}_s \\ \dot{z}_t \\ z_s \\ z_t \end{bmatrix} + \begin{bmatrix} 0 \\ k_t/m_t \\ 0 \\ 0 \end{bmatrix} [u] \tag{2.12}$$

In matrix form and using space state representation, this yields:

$$\dot{\mathbf{x}}(t) = \mathbf{A}\mathbf{x}(t) + \mathbf{B}u(t) \tag{2.13}$$

where $\mathbf{A}$ is the state matrix and $\mathbf{B}$ is the input matrix. Also, the quantities of interest,

or output vector $\mathbf{y}(t)$, may not be directly available in the state vector. They are thus derived using:

$$\mathbf{y}(t) = \mathbf{C}\mathbf{x}(t) + \mathbf{D}u(t) \tag{2.14}$$

where $\mathbf{C}$ is the output matrix and $\mathbf{D}$ is the direct transmission matrix.

With a linear time-invariant system, the ODE is not necessarily solved using a numerical integration scheme and it is much more efficient to use Fourier transforms. Indeed, taking the Fourier transform of equations (2.13) and (2.14) and using simple algebra, see *e.g.* [Maybeck, 1979], leads to:

$$\mathrm{FT}(\mathbf{y}(t)) = \mathbf{y}(\omega) = \Big(\mathbf{C}(j\omega\mathbf{I} - \mathbf{A})^{-1}\mathbf{B} + \mathbf{D}\Big)\, u(\omega) = \mathbf{H}(\omega)u(\omega) \tag{2.15}$$

where $u(\omega) = \mathrm{FT}(u(t))$, $\mathrm{FT}(.)$ designates the Fourier transform and $\mathbf{H}(\omega)$ is the Frequency Response Function (FRF) of the system. The output vector $\mathbf{y}(t)$ can then be simply calculated from the knowledge of the excitation $u(t)$ by taking the inverse Fourier of equation (2.15). The calculation time associated to such an operation is very low as it only requires products of vectors of values. Throughout this manuscript, the 'simulation' of the vehicle's responses to a given road excitation $u(t)$ only involves the following calculation:

$$\mathbf{y}(t) = \mathrm{FT}^{-1}\left(\mathbf{H}(\omega)\mathrm{FT}(u(t))\right) \tag{2.16}$$

To remember

- The main objective of this research work is to provide an efficient solution to acquire a quantitative description of the load variability experienced by any given component within any given population of vehicles.
- This work is only concerned with road-induced vertical loads and failures due to high cycle fatigue.
- Simple statistical analyses can be carried out if the (time-varying) external loads acting on components are converted into (scalar) pseudo-damage values.
- The variability of road-induced loads is extremely significant within a population of vehicles (customers) due to the different road surfaces that may be selected and driver behaviours that may be applied.
- Reliability analysis is the study of the expected number of failed individuals within a population of components subjected to variable loads and possessing variable strengths.
- The loads acting on different components are dependent on the load path that extends from the road through the wheels to the said components, and are thus dependent on the mechanical characteristics of the vehicle.
- Acquiring samples of load histories through measurements is long and costly and requires a vehicle which cannot exactly share the characteristics of a new vehicle in early design stages.
- In practice, during design and testing stages, deterministic (and realistic) road excitation profiles, *e.g.* based on specific testing schedules on a company-specific proving ground, are used. Their relationship with the load distribution (pseudo-damage) representing the population of vehicles must be established before any reliability assessment can be made.
- A linear quarter-car model is adopted here, since it is extremely fast (using FFT and FRFs) and thus very appropriate for stochastic simulations.

Chapter 3

Estimation of road profiles from a vehicle's dynamic responses

Contents

3.1 Introduction **33**
3.2 Extracting road-related information from a vehicle's responses . . . **34**
3.2.1 Overview on road roughness characterisation 34
3.2.2 Road profiles and vehicle dynamics 36
3.2.3 Existing methods for the processing of vehicle's responses 37
3.2.4 Selected algorithm for the estimation of road profiles 38
3.3 Estimation of the excitation acting on a system: an inverse problem **39**
3.3.1 Inverse problems and related mathematical difficulties 39
3.3.2 Regularisation of inverse problems 42
3.3.3 Illustration on an example 43
3.4 An excitation estimation algorithm based on Kalman filtering theory **44**
3.4.1 The linear Kalman filter 44
3.4.2 A state augmented Kalman filter for excitation estimation 48
3.4.3 Regularisation through the Kalman filtering framework 50
3.5 Implementation of the algorithm for the estimation of road profiles **52**
3.5.1 Choice of a vehicle model for the estimation algorithm 53
3.5.2 Semi-empirical tuning of the estimation algorithm 56
3.6 Testing of the road estimation algorithm **61**
3.6.1 Testing framework and objective scalar criteria 61
3.6.2 Numerical testing of the road estimation algorithm 63
3.6.3 Physical testing of the road estimation algorithm 69
3.6.4 Sensitivity and limits of the algorithm 72
3.6.5 Discussion on the applicability of the algorithm 77
3.7 Synthesis and conclusion **80**

"The only source of knowledge is experience."
Albert Einstein

3.1 Introduction

The time evolution of the vertical loads acting on the different components of a vehicle is strongly related to the geometry of the road surface that is being covered by the vehicle. Any attempt to perform a quantitative assessment of the statistical variability of these loads, throughout the life of the vehicle, should therefore raise attention on the question of the variability of the road surfaces encountered by the said vehicle. As mentioned in introduction in chapter 1, the key concept underlying the complete research work exposed in the present manuscript is to focus statistical analysis efforts on the variability of the factors which determine the value of the loads experienced by the different components of the vehicle. They have been labelled as 'influential factors'. The variations in the geometry of the road surface, which is often and will subsequently be denoted as 'road roughness', is an influential factor that requires extensive attention.

The core objective of this chapter is to **select an adequate approach in view of collecting extensive statistical information on road roughness**. The method that is proposed here, seeks to **extract information from the dynamic responses that are generated on a vehicle by the road surface.** Indeed, when a vehicle covers a road surface at a given speed, this surface represents a time-varying boundary constraint on the wheels of the vehicle, which in turn produces a dynamic response on the vehicle. Thus, information about the road surface covered by the vehicle lies within its measurable responses and could in principle be extracted. Conceptually, this constitutes an inverse problem, which has to be handled with careful mathematical attention.

From a practical perspective, the selection of such an approach is motivated by its ability to permit large scale road characterisation, **with little instrumentation involved and no need for specific and expensive road measuring equipment**. It also offers the opportunity to extract valuable information on road roughness, **from existing datasets acquired during load characterisation campaigns**. The latter are carried out by most car manufacturers and represent large quantities of data that could be exploited. In the context of the present work, the existing datasets gather by Renault constitute an extensive source of information. In chapter 4, this information will be used to study road roughness variability and identify stochastic processes suited to describe the evolution of the latter.

The outline of the present chapter is as follows. The issue of road roughness characterisation is described in section 3.2. A study of the different approaches existing in literature is performed. Section 3.3 sets up the theoretical framework associated with the treatment of inverse problems. A concise examination of the mathematical difficulties that usually arise when dealing with such problems is carried out and opens the discussion on how to efficiently address those problems. In section 3.4, a particular estimation algorithm based on Kalman filtering theory is selected to address the considered inverse problem. Then, this algorithm is applied to the inversion of the vertical vehicle dynamics problem in section 3.5. The practical implementation of the filter is detailed. In section 3.6, experimental results based both on simulations and measurements are presented to

illustrate the validity of the proposed algorithm, give a quantitative appreciation of its efficiency and point to its limits. Eventually, a brief summary of the important points of the chapter is laid out in section 3.7 and an overall conclusion on the applicability of the selected method is provided.

3.2 Extracting road-related information from a vehicle's responses

3.2.1 Overview on road roughness characterisation

According to [Sayers et al., 1986], road roughness is "the variation in surface elevation that induces vibrations in traversing vehicles". A more thorough discussion on road roughness is given in chapter 4. Nonetheless, in the context of the present work, it clearly represents a factor that influences the dynamic response of a vehicle.

Obtaining information on road roughness can be achieved through two different approaches. The first and most straightforward method, is to carry out a 'direct' measurement of the road geometry. Here, the term 'direct' has to be understood in the large sense, as the so-called 'direct' measurement may involve the response of a specific measuring equipment (e.g. an instrumented trailer). The second type of approach is to gather information based solely on the dynamic responses induced on the vehicle by the road surface.

Direct road measurements, or measurement set-ups that involve specific measuring equipments, are not the focus of the present work. Extensive literature exists on the topic, see *e.g.* [Sayers et al., 1986, Gillespie et al., 1980] for discussions about the use of specific devices and the standardisation of the information they provide. A quite extensive description of the topic of road roughness characterisation may be found in [Sayers and Karamihas, 1998]. Nowadays, the two most common practices regarding road roughness characterisation are the following. The first one uses the response of a trailer linked to the vehicle, which consists in a pendulum ended by a wheel that closely follows the road surface and whose frequency response function (FRF) is well characterised. An estimate of the road geometry is obtained through inverse linear filtering, using the said FRF. The trailer is labelled APL (in French), for Longitudinal Profile Analyser, see [LCPC, 2000]. The other and most commonly employed approach generally includes laser sensors and a very accurate accelerometer. The double integration of the acceleration signal provides an inertial absolute reference and the distance between the latter and the road surface is measured by laser. With both information, the longitudinal profiles in the tracks of the lasers can be reconstructed. This method is often called inertial profile measurement, see [Prem, 1988]. Both techniques are illustrated in figure 3.1.

Conversely, 'indirect' methods are based on the processing of the responses measured on the vehicle into information about road roughness. In such case no specific measuring equipment is involved. The interest of such approaches is twofold.

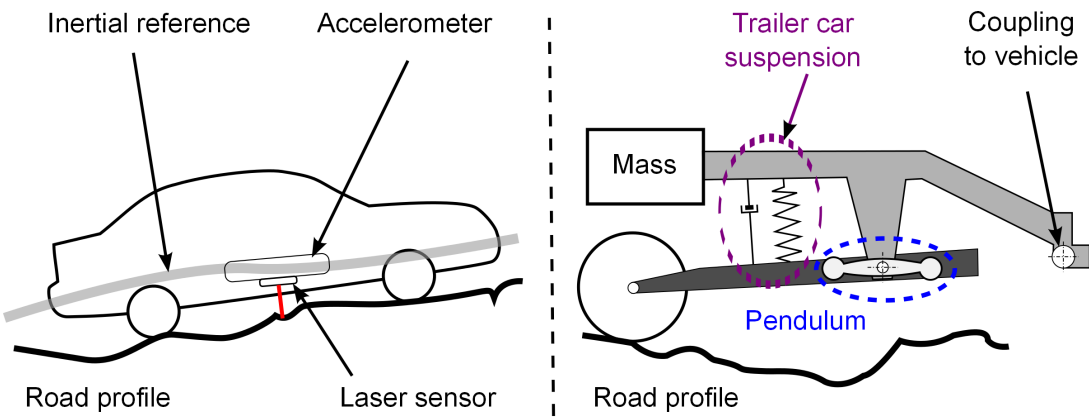

Figure 3.1: 'Direct' road measurement methods. Laser-based inertial profile measurement (left). Longitudinal Profile Analyser (right).

First, specific measuring devices can be expensive, visible and difficult to maintain, *e.g.* in severe environments. The approaches of interest here, only rely on cheap and commonly used sensors such as displacement and acceleration sensors. The vehicle from which data is extracted can cover hundreds to thousands of kilometres with little or no intervention on the measurement chain, thus enabling large scale characterisation campaigns to be carried out at a low cost. In principle, even if this is not considered in the present manuscript, it could be alimented by the on-board sensors that are being increasingly installed on commercial vehicles, *e.g.* using active suspension systems, and thus provide very large volumes of customer-related data with no need for a particular instrumented vehicle.

Secondly, these approaches can be used to extract information from existing datasets acquired through load characterisation campaigns, provided the required displacement and acceleration sensors were available. Such campaigns are performed by most car manufacturers. For these campaigns, the objective was not to acquire data on road roughness. However, they indirectly contain this information through the intermediary of the measured responses of the vehicle. This valuable information is not readily available and can only be accessed through a specific processing of the vehicle's responses, namely **the resolution of an inverse problem**.

In the present framework, the **existing datasets gathered by Renault constitute an extensive source of information on road roughness variability** and such an indirect approach is thus of particular interest as it can be used to process these datasets. Also, vehicle responses measurements are the only extensive source of data available in the context of this manuscript.

Let us point out that while an indirect method is presented here, it does not mean that direct measurements have to be disregarded as a potential source of information. The study of road roughness variability and the selection of an adequate stochastic model, which are detailed in chapter 4, are completely independent of the method that is chosen

to acquire data on road roughness; putting aside the issue regarding the quality of the data. Extracting information from a vehicle's dynamic responses is one potential but not exclusive way to proceed.

3.2.2 Road profiles and vehicle dynamics

When a vehicle covers a road surface at a given speed, this surface represents a time-varying boundary constraint on the wheels of the vehicle. So far, road roughness has mostly been associated with the notion of an irregularly shaped surface. For practical considerations, it is assumed that a full description of the road surface is not necessary and the focus of the study is restrained to longitudinal (*i.e.* along the driving direction) sections of the road surface subsequently denoted as road profiles, see subsection 4.3.1. Obviously, the use of the road estimation method proposed within this chapter can only provide information on the road profiles in the track of the wheels, as the rest of the road surface has not produced any response on the vehicle.

Although the moving contact between the tyre and the road is a surface contact in practice, it is assumed that the time-varying boundary constraint imposed on the system, can be represented by one, or several, unidimensional time-dependant quantities $(u_i(t))_{i=1..4}$. The latter will often be referred to as '**road excitations**' within this manuscript. Precisions about the tyre/road contact and tyre modelling are given in appendix C.

The direct purpose of the estimation algorithm introduced in this chapter is to **estimate the time-dependant road excitations imposed on the vehicle**. Subsequently, the acquisition of a road profile is a very simple matter when the speed of the vehicle $v(t)$ is known. It only consists in matching each time instance to its longitudinal position $x(t) = \int_0^t v(\tau)d\tau$ and associating it to its related value $u_i(x(t))$.

It is important to note that vertical road excitations are not the only mechanical actions imposed on the vehicle. Indeed, longitudinal and lateral forces also exert influence on the measured dynamic responses of the vehicle. Longitudinal actions comprise inertial forces that originate from acceleration or braking, as well as friction or percussive forces on the tyre. Lateral actions comprise inertial forces due to steering as well as friction forces on the tyre.

Here, a model describing only the vertical dynamics of the vehicle will be used and it cannot account for the influence of longitudinal and lateral actions on the measured vertical responses. Consequently, when solving the inverse problem, one should be aware that the contributions to the vehicle's responses that are due to non-vertical actions will be undistinguishable from the contribution due to the vertical road excitations. Since the estimate $u_i(t)$ obtained from the resolution of an inverse problem represents the excitation that 'best explains' the observed responses on the vehicle, it is inevitably going to be affected by these non-vertical actions.

This is arguably a strong simplification of the issue but taking into account non-vertical actions would render the problem much more complex. It may however be noted that since

the information on road profiles is eventually going to be used to quantify the variability of loads, the ability to further separate between vertical and non-vertical (yet assumed less influential) actions, might not be a serious impediment.

3.2.3 Existing methods for the processing of vehicle's responses

Multiple methods have been proposed in order to extract information on road profiles from the mechanical responses acquired on a vehicle and using only commonly available sensors. They have been developed for different applications which may include the real time control of suspension systems or the assessment of the need for maintenance on road networks. Here, the purpose is to analyse the variability of road-induced loads for reliability analysis.

In [Gonzalez et al., 2008], a frequency response function (FRF) directly written in the spatial domain and assuming constant speed is identified using a known input/output set of data. This FRF is then employed to extract the power spectral density (PSD) of the road profile from the PSD of a measured acceleration, using inverse linear filtering. In this case, PSDs are used in place of the Fourier transforms of the signals. Thus, the road geometry is not directly estimated and the focus is rather on its statistical characteristics, for the purpose of road roughness classification. Another technique is proposed in [Hugo et al., 2008] and involves the measurement of accelerations and of the force in the suspension. The approach solves a least-squares problem involving a simple force-displacement linear relation as a model for the tyre. Such methods do not represent an easy framework to combine the information that may originate from different sensors.

The building of *ad hoc* surrogate models for the resolution of the inverse problem has been considered, see *e.g.* [Ngwangwa et al., 2010, Yousefzadeh et al., 2010]. An artificial neural-network is trained on a known input/output set of data, in order to relate measured dynamic responses of the vehicle to the input road geometry. The choice of the network structure and its training can be delicate problems. Its potential domain of validity is also hard to evaluate.

The methods that have received specific interest in the context of the present work are techniques that traditionally belong to the domain of optimal control of systems. Indeed, the inverse problem may be viewed as a particular example of a control application if one realises that, searching for the input to apply to a system, in order to guarantee that the latter will achieve a desired response, is a control problem. In the present case, the desired response originates from measurements from which one wants to extract information.

The use of the method of control constraints has been proposed by [Burger, 2014]. It consists in the resolution of a system of differential-algebraic equations (DAE), where an algebraic constraint equation (3.2) is added to the ordinary differential equation (ODE) of the system (3.1). This imposes that the response of the system matches the measurement data that has been previously acquired. The DAE system may be written:

$$\dot{\mathbf{x}}(t) = f(\mathbf{x}(t), \mathbf{u}(t), t) \tag{3.1}$$

$$0 = \mathbf{y}_{data}(t) - h(\mathbf{x}(t), \mathbf{u}(t), t) \tag{3.2}$$

where $f(.,.,.)$ is the state function describing the dynamics of the system and $h(.,.,.)$ the observation function relating the state vector to the outputs, both potentially non-linear mappings. $\mathbf{y}_{data}(t)$ is the measured response of the system from which information on the excitation $\mathbf{u}(t)$ is extracted. The resolution of a DAE system represents a numerical challenge when the latter presents a high index, see [Burger, 2014], and it may be difficult to control the quality of the estimate. In this latter work, force tensors at the centres of the wheels are used as the input data and a six degrees of freedom virtual road profile is estimated.

A method, based on the theory of sliding mode control has been proposed to estimate road roughness in [Imine et al., 2006]. It produces an estimate of the excitation acting on the system through a discrete-time filtering based on the use of appropriate gain matrices, which operate a correction based on the difference between the predicted and the desired response of the system. Another matrix-based processing algorithm can be obtained through so-called Yule-Kucera parametrization or Q-parametrization, see [Doumiati et al., 2014, Tudon-Martinez et al., 2015]. As far as their practical functioning is concerned, such approaches are relatively similar to the use of the so-called Kalman filter that is discussed in the following subsection. They are data processing algorithms based both on discrete-time linear filtering. Nonetheless, the Kalman filtering framework is more convenient to make use of *a priori* knowledge on potential perturbations and errors while conserving a physical interpretation of the latter.

3.2.4 Selected algorithm for the estimation of road profiles

In the context of this research work, **a so-called augmented linear Kalman filter has been selected to estimate road profiles from a vehicle's responses**. This use of Kalman filtering theory in relation with the resolution of inverse problems has been proposed by [Lourens et al., 2012] and is summarized in this chapter in subsection 3.4.2. Here, it is applied to the issue of road roughness estimation, as proposed by [Jeong et al., 1990, Doumiati et al., 2011, Yu et al., 2013]. In these latter works, the main concern is the real time control of active suspension systems, whereas the purpose here is to carry out an analysis of road roughness variability, see [Fauriat et al., 2016], and ultimately, of the variability of road-induced loads. The formulation of the equations proposed in those references may vary depending on the model selected for the vehicle and on the *a priori* model selected for the excitation to estimate. This is further discussed when introducing the augmented Kalman filter in subsection 3.4.2. The practical implementation of the algorithm proposed in this research work is described in section 3.5 and has been published in [Fauriat et al., 2016].

The selected estimation algorithm, namely a augmented Kalman filter, possesses interesting features, particularly well adapted to the issue at hand. Its recursive structure and the fact that the matrices involved in the calculation are of very small size, which renders algebraic operations and matrix inversions relatively inexpensive, make it a fast algorithm. Also, its construction in a stochastic framework may be exploited to easily and efficiently combine all available *a priori* information in order to account for modelling imprecisions and perturbations. Additionally, the space state representation associated with Kalman filtering constitutes a flexible setting for the combination of the data originating from different sensors. Further details are given in section 3.4.

Essentially, the choice of this estimation algorithm is motivated by the need to balance contradictory requirements. A trade-off has to be found between the quality of the estimate and the ability to process large volumes of data, corresponding to thousands of kilometres, in order to collect extensive data on road roughness variability. **The augmented linear Kalman filter offers an interesting and controllable compromise in terms of the complexity of the vehicle model and computer intensiveness against the quality of the estimate.**

In order to introduce the particular implementation selected here for the Kalman filter, it is first necessary to discuss the mathematical difficulties related to the practical resolution of inverse problems. The stochastic framework associated to Kalman filtering theory is particularly helpful to address this type of problems.

3.3 Estimation of the excitation acting on a system: an inverse problem

3.3.1 Inverse problems and related mathematical difficulties

Inverse problems

In many practical situations, the information on a physical quantity of interest may not be readily available, either because its measurement is infeasible, costly or subjected to discrepancies introduced by the measuring equipment. In this context, it is relevant to look for more easily observable physical quantities, which are related to those of interest through a known relationship, *e.g.* a given law of physics. While the prediction of the response of a physical system to a given excitation constitutes a direct problem, it is sometimes interesting to consider 'inverting' the relationship in order to estimate the excitation that provoked an observed response of the system. The latter problem is labelled as an inverse problem.

Inverse problem theory covers a wide range of practical physical applications. It can be approached either from a rigorous mathematical standpoint or adopting a more application-oriented attitude and seeking *ad hoc* resolution techniques. An overview of the different difficulties that can be considered when dealing with inverse problems may

be found for example in [Idier, 2013]. In this reference it is said that "unlike direct problems, [inverse problems] have a nasty tendency to be 'naturally unstable' [...] and 'naive' inversion methods are not robust". Therefore, inverse problems have to be addressed with caution.

Mathematical treatment of inverse problems

More formally, let us consider $u \in \mathcal{U}$ and $y \in \mathcal{Y}$ two elements in two function spaces, *e.g.* $L^2(\mathbb{R})$ the space of square-integrable real-valued functions. For the sake of simplicity, let us remain in a linear framework and consider the linear operator between these function spaces $A : \mathcal{U} \mapsto \mathcal{Y}$. The direct problem is described by equation (3.3).

$$y = Au \tag{3.3}$$

From a physical standpoint, y is the response of the system to the excitation u and the objective is generally to calculate such response using numerical simulation methods. The operator A encompasses the information on the system's behaviour. Conversely, the inverse problem consists in the search for the solution $u \in \mathcal{U}$, when it exists, that satisfies equation (3.3) for a given (known) $y \in \mathcal{Y}$.

According to [Hadamard, 1923], an inverse problem is said to be well-posed (otherwise it is ill-posed) if:

- For each $y \in \mathcal{Y}$, there exists $u \in \mathcal{U}$ such that equation (3.3) is verified.
- The solution $u \in \mathcal{U}$ is unique.
- The solution u continuously depends on y, *i.e.* if a perturbation on the solution δy tends towards zero then δu tends towards zero.

While the study of the conditions under which existence and uniqueness of the solution are guaranteed is a complex mathematical issue, for practical physical applications it is always possible to slightly modify the formulation of the problem in order to obtain a unique solution.

First, for practical applications the response y is always a discrete set of values and it could be shown that in that (linear) case it is always possible to consider a well-posed problem, see [Idier, 2013]. Second and more importantly, it is always possible to search for solutions in the least squares sense.

$$u^\dagger = \arg\min_{u \in \mathcal{U}} \|y - Au\|_{\mathcal{Y}} \tag{3.4}$$

where $\|.\|_{\mathcal{Y}}$ is a chosen norm in the function space $\mathcal{Y}$. The solution $u^\dagger$ may not exactly satisfy equation (3.3), *i.e.* the estimated excitation $u^\dagger$ may not exactly reproduce the

known response y through the system characterised by A, yet an approximate solution can always be found according to equation (3.4). When the direct problem is non-linear and $\mathcal{F} : \mathcal{U} \mapsto \mathcal{Y}$ is a non-linear mapping such that $y = \mathcal{F}(u)$, approximate solutions of a least squares problem can also be sought.

On the other hand, the solution of the numerical minimization in equation (3.4) is generally unique, and if it is not, one particular solution can be selected according to any desired criterion (*e.g.* minimum norm in $\mathcal{X}$).

Instability of inverse problems in practice

Searching a solution by minimizing the difference between the measured response y and the predicted response of the system characterised by A to a given excitation u, namely $y_{pred} = Au$, according to (3.4), always provides a solution. However, this solution may not be acceptable since it can likely be quite different from the 'real' excitation (unknown) that has produced the response y. Also, a small modification of the measured response data y can have a very strong influence on the estimated excitation u.

Let us illustrate this latter difficulty by considering the response $y(t)$ of a linear (time-invariant) mechanical system, subjected to an excitation $u(t)$. In this case, the solution of the inverse problem may be expressed very simply and in a closed-form using Fourier Transforms (FT) and the so-called Frequency Response Function (FRF) of the system:

$$\widehat{u}(f) = \frac{\widehat{y}(f)}{\Gamma(f)} \tag{3.5}$$

where $\widehat{u}(f)$ and $\widehat{y}(f)$ are the FTs of $u(t)$ and $y(t)$ and $\Gamma(f)$ is the FRF of the system.

In practical cases, $y(t)$ is discretized on a regular time grid with sampling time dt, and thus $\widehat{y}(f) = FT(y(t))$ is discretized on a regular frequency grid $f \in [-f_s/2, f_s/2] = [-1/2dt, 1/2dt]$, generally using Fast Fourier Transform (FFT). Here, the instability of the solution and its sensitivity to perturbations of the measured response y can be easily perceived. Indeed, for frequency values f_i where $\Gamma(f_i)$ is small, the term $1/\Gamma(f_i)$ represents a strong amplification factor. In the associated frequency ranges the contribution of the components of the data $\widehat{y}(f_i)$ to the solution $\widehat{u}(f_i)$, according to equation (3.5), may be very important. From a different standpoint, it can be seen that components $\widehat{u}(f_i)$ in these frequency ranges can be added to the solution, and potentially strongly modify its content, with little impact on the response, $\Gamma(f_i)\widehat{u}(f_i) \approx 0$.

In practice, in certain frequency ranges, typically high frequencies for mechanical systems, the content of the response y should have been filtered out by the system ($\Gamma(f_i) \approx 0$). If the data y nonetheless possesses significant content within theses ranges, which can be due to external perturbations such as noises in the measuring equipment, the only possibility to get a fit to the data y, according to equation (3.5), is to consider a solution u with a strong content within such frequency ranges. In a sense, the solution u is no

longer physically 'acceptable', *i.e.* is no longer a representative image of the real excitation acting on the system, even if it satisfies equation (3.5) for an observed, potentially noisy, response.

Hence, the solution u of an inverse problem may be highly sensitive to small variations in the data y and in this context, a straightforward inversion of the direct problem such as that of equation (3.5) or a strict resolution of the minimization problem in equation (3.4) may not be a suitable approach. The technique usually adopted to circumvent this difficulty is called the regularisation of the inverse problem, see [Tikhonov, 1963].

3.3.2 Regularisation of inverse problems

There are several different approaches that may be classified as regularisation techniques, see *e.g.* [Idier, 2013], but they all share the same following principle. It is not appropriate to search for a solution u that guarantees an overly accurate fit to the data y through the system described by A. A regularised solution $u \in \mathcal{U}$ has to be selected as a trade-off: it must provide an acceptable fit to the data y and simultaneously be sufficiently representative of the 'real' excitation.

Arguably, the previous definition of a regularised solution is quite vague, but its justification is readily understandable. In practice the data y will be imperfect due to measurement errors and noises. Moreover, the operator A in equation (3.3), is an idealized representation of the system's behaviour. Consequently, **obtaining a solution u that very accurately fits the imperfect data y through the direct and idealized problem, may come at the cost of that solution being highly unstable and no longer physically representative.**

Regularisation can roughly be thought of as a loosening of the constraint of fit the data, as the latter constraint is not in itself a guarantee of an acceptable solution. There are two types of regularisation methods. The first type consists in minimizing a composite criterion $\mathcal{I}$, which assures that the aforementioned trade-off is reached:

$$\mathcal{I}(x) = \|y - Au\|_{\mathcal{Y}} + \alpha\mathcal{C}(u) \tag{3.6}$$

where $\alpha \in \mathbb{R}_+$ is called the **regularisation coefficient** and $\mathcal{C}$ is an operator that can be freely selected in order to penalize solutions that depart from *a priori* knowledge one may possess on the solution. The regularisation coefficient α controls the trade-off between the fidelity to the data and to the knowledge on the solution. An alternative approach that does not explicitly involve a regularisation coefficient, but behaves similarly, consists in minimizing the term $\|y - Au\|_{\mathcal{Y}}$ using an iterative method with a restriction on the number of iterations, often determined empirically. Indeed, an overly strong fitting can make the solution unstable. More details about efficient algorithms for the resolution of the minimization problem can be found in [Idier, 2013] and [Tarantola, 2005]. The Kalman filter method, that is presented in section 3.4, also pursues a compromise between *a priori*

knowledge on the solution and fidelity to the data y, even if it is not formally written in the form of equation (3.6).

The second type of regularisation methods consists in searching the solution on a suitably chosen subspace $\mathcal{U}' \subset \mathcal{U}$ of reduced dimension. The most straightforward approach is to employ a truncated single value decomposition of operator A. Components of u that are mapped onto y through small singular values of A are ignored. For the example of subsection 3.3.1, this is practically implemented by filtering out before solving the inverse problem, the frequency components in y where the signal to noise ratio is too low, *i.e.* $\Gamma(f_i)$ is small. One possible implementation of this idea is described as Wiener filtering, see [Idier, 2013]. Another technique is to use a parsimonious parametrization of the solution being searched, *e.g.* on a wavelet basis.

3.3.3 Illustration on an example

In order to illustrate the theoretical discussion laid out in this section, let us consider the following example. The road excitation shown in figure 3.2 (in red on the left-hand side) is used to simulate the response of a linear quarter-car model, see subsection 2.3.1, on $t \in [0, 10s]$ with $dt = 0.001s$. The road excitation, *i.e.* the displacement of the contact point between the road and the tyre in the time domain, is obtained from a known road profile and assuming that a particular constant speed has been assigned to the vehicle.

The simulated suspension displacement signal $y(t)$, is then perturbed manually to emulate phenomena that are likely to occur when real measured data are used as input for the estimation (inverse) problem. For such purpose, a saturation effect that may represent the hitting of a bump stop component in the suspension system, is applied. A small noise component (of 0.2% of the root mean square (RMS) value of the signal), is also added on the sinusoidal section of the profile in order to emulate measurement noise. Both perturbations can be visualized in figure 3.2 thanks to the close-ups displayed on the right-hand side.

Two estimations are realised. For the first estimation the perturbed data is used directly and the problem is not regularised. For the second estimation, the data is low-pass filtered with a cut-off frequency of 50Hz, thus providing a regularisation of the problem, as mentioned in the previous subsection. In both cases, the inverse problem is solved using the FRF associated to the suspension displacement response and using equation (3.5). The result is back transformed into the time domain through an inverse Fourier transform (IFFT) and gives a solution $u(t)$, which will be labelled as an estimate of the road profile. Both estimates are displayed in figure 3.2 on the left-hand side.

On the right-hand side of figure 3.2, the suspension displacement response corresponding to both estimates are shown. At first sight, both estimates seem like acceptable candidates for the solution of the inverse problem as they reproduce response data that accurately fits the perturbed input data. However as seen on the left-hand side of figure 3.2, the unregularised estimate is obviously not an acceptable solution, as it deviates too

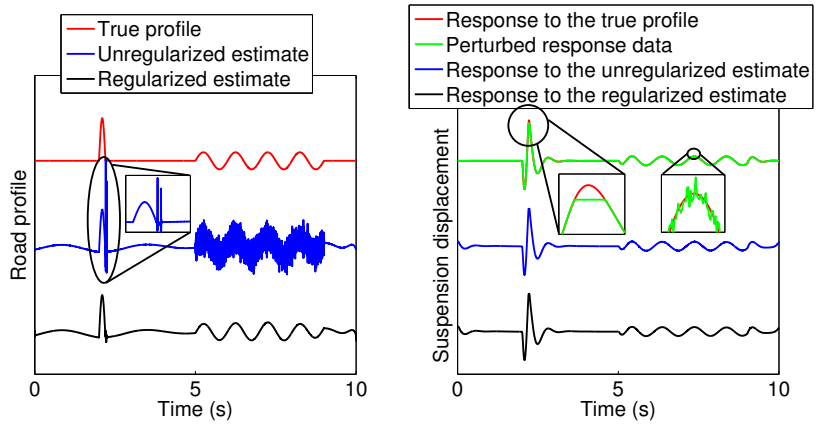

Figure 3.2: Comparison between the regularised and unregularised solutions to the inverse problem. The measurement data is obtained through a linear simulation. The perturbation of the measurement data consists in adding a saturation and noise.

much from the 'true' road excitation. To be more precise, sharp peaks are observed due to the saturation effect introduced in the data. Indeed, the linear model cannot 'explain' such an irregular response other than by assuming a visibly unrealistic excitation. Also, the noise in the sinusoidal section is strongly amplified.

Essentially, the constraint of fit to the data must not be overly enforced and a trade-off has to be reached between fidelity to the data and reasonable characteristics of the solution, known *a priori*. Although the regularised estimate does not provide as good a fit (yet the difference is hardly visible in the right-hand side of figure 3.2) to the perturbed data as the unregularised estimate does, it is much more realistic and 'close' to the actual excitation. The so-called augmented Kalman filter proposed in what follows is a interesting tool to regularise the inverse problem as well as combine the information that originates from different sensors.

3.4 An excitation estimation algorithm based on Kalman filtering theory

3.4.1 The linear Kalman filter

The theory of the Kalman filtering was introduced in a seminal paper [Kalman, 1960]. Kalman filters are now used in many domains of physics, engineering, communications, etc., and for multiple data processing treatments. In the present subsection, the main theoretical principles of Kalman filtering are laid out. The objective is to illustrate the processing of information that such a filter implies. Then, in the context of the estimation of road profiles from a vehicle's dynamic responses, the interesting features of this approach can be readily understood. Complete mathematical demonstrations are not presented here

and the reader may refer to [Maybeck, 1979], from which the descriptions given in what follows are extracted, for more details.

In [Maybeck, 1979] a straightforward description of the Kalman filter is given. "A Kalman filter is simply an optimal recursive data processing algorithm. [...] it incorporates all information that can be provided to it, [...] regardless of their precision, to estimate the current value of the variables of interest". The algorithm is built using both:

- The knowledge of the dynamic behaviour of the system and measuring devices
- The probabilistic description of the perturbations and noises that may act on the system and on measurement devices

Let us consider a linear, continuous, time-invariant system, described by a so-called state space representation, associated with discrete time measuring:

$$\dot{\mathbf{x}}(t) = \mathbf{A}\mathbf{x}(t) + \mathbf{B}\mathbf{u}(t) + \mathbf{w}(t) \tag{3.7}$$

$$\mathbf{y}(t_i) = \mathbf{C}\mathbf{x}(t_i) + \mathbf{v}(t_i) \tag{3.8}$$

where $\mathbf{x}(t)$ is the state vector, $\mathbf{u}$(t) is the excitation vector, $\mathbf{y}(t_i)$ is the output or measurement vector, $\mathbf{A}$ the state matrix describing the dynamics of the system, $\mathbf{B}$ the input matrix and $\mathbf{C}$ the output matrix. $\mathbf{w}(t)$ and $\mathbf{v}(t_i)$ which in simplified notation are rewritten $\mathbf{w}_t$ and $\mathbf{v}_i$ are respectively, a vector of zero-mean continuous Gaussian white noise processes and a vector of zero-mean discrete Gaussian white noise processes, with auto-covariance matrices $\mathbf{Q}(t)$ and $\mathbf{R}$ such that:

$$E\left[\mathbf{w}_t\mathbf{w}_{t'}^T\right] = \mathbf{Q}(t)\delta(t-t') \tag{3.9}$$

$$E\left[\mathbf{v}_k\mathbf{v}_l^T\right] = \mathbf{R}\delta_{k,l} \tag{3.10}$$

where $\delta(t-t') = 0$ if $t \neq t'$ and $\delta_{k,l} = 0$ if $k \neq l$, *i.e.* both $\mathbf{Q}(t)$ and $\mathbf{R}$ are diagonal. Although it is not a requirement for Kalman filtering to be applied, all noise processes are here considered to be stationary. It is further assumed that both vectors of processes are mutually uncorrelated. $\mathbf{w}_t$ is the state noise and $\mathbf{v}_i$ the measurement noise.

Conceptually, the Kalman filter works according to a recursive prediction-correction scheme. It makes use of the information available at time t_{i-1}, combined with the knowledge on the dynamics of the system and on the different perturbations, to predict the state of the system at time t_i (prediction step). It then extracts information from the new measurement taken at time t_i, when it becomes available, in order to correct the previous prediction of the state of the system (correction step). It also **operates in a stochastic framework, which is a convenient setting to account for imprecisions in the**

model of the system or perturbations of the measurement data. The iterative principle associated with Kalman filtering is illustrated in figure 3.3 and further described in what follows.

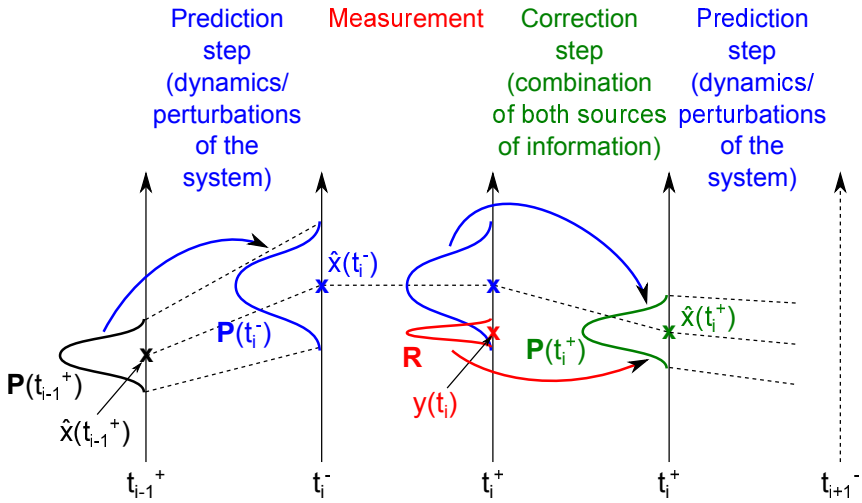

Figure 3.3: Principle of the Kalman filter: prediction-correction scheme. For the sake of simplicity, it is assumed that the state of a system is described by a single degree of freedom (displayed on a vertical axis). The mean value is marked by an 'x' symbol and the covariances are illustrated by a distribution.

Formally, the Kalman filter propagates the conditional expectation $\hat{\mathbf{x}}(t_i)$ and the conditional covariance $\mathbf{P}(t_i)$ of the state vector, from time t_{i-1} to time t_i. The latter are conditioned on all the measurement history, from time t_0 up to time t_i. Let us define the following notations:

$$\hat{\mathbf{x}}(t_i^+) = E\left[\mathbf{x}(t_i) | \left[\mathbf{y}(t_0) = \mathbf{y}_0, ..., \mathbf{y}(t_i) = \mathbf{y}_{t_i}\right]\right] \tag{3.11}$$

$$\mathbf{P}(t_i^+) = E\left[\left[\mathbf{x}(t_i) - \hat{\mathbf{x}}(t_i^+)\right]\left[\mathbf{x}(t_i) - \hat{\mathbf{x}}(t_i^+)\right]^T | \left[\mathbf{y}(t_0) = \mathbf{y}_0, ..., \mathbf{y}(t_i) = \mathbf{y}_{t_i}\right]\right] \tag{3.12}$$

where t_i^+ denotes that the measurement is available at time t_i. By contrast, at time t_i^-, the said measurement is not yet available.

Solving the linear stochastic differential equation (SDE) (3.7), assuming (for the sake of simplicity) that the excitation remains constant between two successive time instances, *i.e.* $\mathbf{u}(t) = \mathbf{u}(t_{i-1})$ for $t \in [t_{i-1}, t_i[$, and specializing the result for time t_i , yields, see technical details in [Maybeck, 1979]:

$$\mathbf{x}(t_i) = \mathbf{\Phi}(t_i, t_{i-1})\mathbf{x}(t_{i-1}) + \left[\int_{t_{i-1}}^{t_i} \mathbf{\Phi}(t_i, \tau)\mathbf{B}d\tau\right]\mathbf{u}(t_{i-1}) + \left[\int_{t_{i-1}}^{t_i} \mathbf{\Phi}(t_i, \tau)d\boldsymbol{\beta}(\tau)\right] \tag{3.13}$$

where $\mathbf{\Phi}(t, t_0)$ is the state transition matrix, which verifies:

$$d\left[\mathbf{\Phi}(t, t_0)\right]/dt = \mathbf{A}(t)\mathbf{\Phi}(t, t_0) \tag{3.14}$$

$$\mathbf{\Phi}(t_0, t_0) = \mathbf{I} \tag{3.15}$$

which in the time-invariant case becomes $\mathbf{\Phi}(t, t_0) = e^{\mathbf{A}(t-t_0)}$ and $d\boldsymbol{\beta}(\tau)$ is a vector of Brownian motion processes from which the vector of white noises $\mathbf{w}(t)$ derive, *i.e.* $\mathbf{w}(t) = d\boldsymbol{\beta}(t)/dt$.

Finally, taking the expectation and covariance of equation (3.13) conditioned on the history of measurements, yields the prediction equations:

$$\hat{\mathbf{x}}(t_i^-) = \mathbf{\Phi}(t_i, t_{i-1})\hat{\mathbf{x}}(t_{i-1}^+) + \left[\int_{t_{i-1}}^{t_i} \mathbf{\Phi}(t_i, \tau)\mathbf{B}d\tau\right]\mathbf{u}(t_{i-1}) \tag{3.16}$$

$$\mathbf{P}(t_i^-) = \mathbf{\Phi}(t_i, t_{i-1})\mathbf{P}(t_{i-1}^+)\mathbf{\Phi}^T(t_i, t_{i-1}) + \int_{t_{i-1}}^{t_i} \mathbf{\Phi}(t_i, \tau)\mathbf{Q}(\tau)\mathbf{\Phi}^T(t_i, \tau)d\tau \tag{3.17}$$

It should be noted that equations (3.16) and (3.17) take this form only if the state noise $\mathbf{w}(t)$ has zero-mean, and is perfectly uncorrelated, *i.e.* white. This is a necessary requirement to apply standard Kalman filtering theory and in particular to benefit from its features, namely that the estimates it provides is unbiased and of minimum variance. Before considering the rest of the algorithm let us fully discretize the **prediction equations** (3.16) and (3.17), for the time-invariant case:

$$\hat{\mathbf{x}}(t_i^-) = \mathbf{A}_d\hat{\mathbf{x}}(t_{i-1}^+) + \mathbf{B}_d\mathbf{u}(t_{i-1}) \tag{3.18}$$

$$\mathbf{P}(t_i^-) = \mathbf{A}_d\mathbf{P}(t_{i-1}^+)\mathbf{A}_d^T + \mathbf{Q}_d \tag{3.19}$$

where $\mathbf{A}_d = e^{\mathbf{A}dt}$, $\mathbf{B}_d = [(e^{\mathbf{A}dt}) - \mathbf{I}]\mathbf{A}^{-1}\mathbf{B}$ and $\mathbf{Q}_d = \int_{t_{i-1}}^{t_i} \mathbf{\Phi}(t_i, \tau)\mathbf{Q}(\tau)\mathbf{\Phi}^T(t_i, \tau)d\tau$ or more directly $\mathbf{Q}_d\delta_{k,l} = E[\mathbf{w}_k\mathbf{w}_l^T]$ if $\{\mathbf{w}_i\}$ is defined as a discrete noise process deriving from the continuous representation $\{\mathbf{w}_t\}$.

The equations of the correction step, derive from specific requirements regarding the performances of the Kalman filter, namely, one wants the estimate provided by the filter to be unbiased, *i.e.* $E[\mathbf{x}(t) - \hat{\mathbf{x}}(t)] = 0$ and of minimum variance. The derivation of these equations involves quite long matrix algebra and is not crucial to the understanding, thus the reader may refer to [Maybeck, 1979] for details. The **correction equations** are directly given here, in their time-invariant form:

$$\mathbf{K}(t_i) = \mathbf{P}(t_i^-)\mathbf{C}^T \left[\mathbf{C}\mathbf{P}(t_i^-)\mathbf{C}^T + \mathbf{R}\right]^{-1} \tag{3.20}$$

$$\hat{\mathbf{x}}(t_i^+) = \hat{\mathbf{x}}(t_i^-) + \mathbf{K}(t_i)\left[\mathbf{y}(t_i) - \mathbf{C}\hat{\mathbf{x}}(t_i^-)\right] \tag{3.21}$$

$$\mathbf{P}(t_i^+) = \mathbf{P}(t_i^-) - \mathbf{K}(t_i)\mathbf{C}\mathbf{P}(t_i^-) \tag{3.22}$$

The gain of the filter $\mathbf{K}(t_i)$ is calculated using equation (3.20). The state prediction is corrected with the information obtained from the measurement that becomes available at time t_i, using equation (3.21). Such correction depends on the difference between the measured vector $\mathbf{y}(t_i)$ and its predicted value before the measurement is available $\mathbf{C}\hat{\mathbf{x}}(t_i^-)$. This difference is often called the innovation. Let us purposely point out that, locally, this difference term strongly resembles the quantity that has to be minimized, see equation (3.4), in the framework of inverse problems. Hence, heuristically, the weight attributed to this term via **the gain of the filter determines how strongly the constraint of fit to the measurement data is enforced.** Lastly, the covariance is updated using (3.22).

To summarize, the discrete linear Kalman filter is the recursive algorithm constituted by equations (3.18) through (3.22). It must be initialized at time t_0 with *a priori* estimates of the initial state mean and covariance:

$$\hat{\mathbf{x}}_0 = E\left[\mathbf{x}(t_0)\right] \tag{3.23}$$

$$\mathbf{P}_0 = E\left[\left[\mathbf{x}(t_0) - \hat{\mathbf{x}}_0\right]\left[\mathbf{x}(t_0) - \hat{\mathbf{x}}_0\right]^T\right] \tag{3.24}$$

If no information exists on the initial state $\mathbf{x}(t_0)$, then $\mathbf{P}_0$ may be chosen arbitrarily large.

In many situations when using Kalman filtering, the input $\mathbf{u}(t)$ to the system is known. In the context of the present work, it is not known and the objective is to estimate it. This leads to a different implementation scheme for the Kalman filter, namely a state augmented filter.

3.4.2 A state augmented Kalman filter for excitation estimation

The Kalman filter presented in the previous subsection enables us to extract information on the state of the system from measurements. The connection with the inverse problem issue appears clearly if one considers the excitation to be estimated $\mathbf{u}(t)$ as being a part of the state of the system. This is the underlying principle of the approach that is proposed in what follows. In the subsequent description of the algorithm, a purely discrete framework is considered, *i.e.* $\mathbf{x}(t_k) = \mathbf{x}_k$. This may imply a discretisation of the dynamics of the continuous system being studied, such as the operation that uses equation (3.16) to get its discrete counterpart (3.18).

The idea of including the excitation into the state vector, thereby creating a so-called augmented Kalman filter is described in details in [Lourens et al., 2012]. Let us consider

the excitation vector $\mathbf{u}_k$ as being part of the state of the system and define a new augmented state vector:

$$\mathbf{x}_k^a = [\mathbf{x}_k, \mathbf{u}_k]^T \tag{3.25}$$

In this case, **the excitation $\mathbf{u}_k$ can be estimated by the Kalman algorithm along with the state of the system $\mathbf{x}_k$.** Let us further assume that the excitation being estimated is a correlated process of the form:

$$\mathbf{u}_{k+1} = \mathbf{u}_k + \boldsymbol{\eta}_k \tag{3.26}$$

where $\boldsymbol{\eta}_k$ is a vector of zero-mean Gaussian white noise processes, mutually uncorrelated with the state noise $\mathbf{w}_k$ and measurement noise $\mathbf{v}_k$. This is a crucial requirement, in order to remain in the domain of standard Kalman filtering theory. Its (diagonal) auto-covariance matrix $\mathbf{S}$ is :

$$E\left[\boldsymbol{\eta}_k \boldsymbol{\eta}_l^T\right] = \mathbf{S}\delta_{k,l} \tag{3.27}$$

The matrix $\mathbf{S}$ is of particular importance since it plays the role of the regularisation term, as does the α coefficient in equation (3.6). Indeed, according to equation (3.26), small values of $\mathbf{S}$ imply that the 'distance' between $\mathbf{u}_{k+1}$ and $\mathbf{u}_k$ is small on average, thus introducing a smoothing of the estimate. Conversely, with large values of $\mathbf{S}$, this distance can be large and no restriction (no regularisation) is imposed on the estimate. Therefore $\mathbf{S}$ represents *a priori* information on the excitation that is being estimated. In this context, one can prevent the solution of the inverse problem from becoming unrealistic.

The discrete augmented space state representation of the system may be written:

$$\begin{bmatrix} \mathbf{x}_{k+1} \\ \mathbf{u}_{k+1} \end{bmatrix} = \begin{bmatrix} \mathbf{A}_d & \mathbf{B}_d \\ 0 & \mathbf{I} \end{bmatrix} \begin{bmatrix} \mathbf{x}_k \\ \mathbf{u}_k \end{bmatrix} + \begin{bmatrix} \mathbf{w}_k \\ \boldsymbol{\eta}_k \end{bmatrix} \tag{3.28}$$

$$\mathbf{y}_k = [\mathbf{C} \;\; \mathbf{D}] \begin{bmatrix} \mathbf{x}_k \\ \mathbf{u}_k \end{bmatrix} + \mathbf{v}_k \tag{3.29}$$

where, contrary to the equations derived in subsection 3.4.1, a direct transmission matrix $\mathbf{D}$ is taken into account for the sake of comprehensiveness. As in subsection 3.4.1, the discrete system matrices are $\mathbf{A}_d = e^{\mathbf{A}dt}$ and $\mathbf{B}_d = [(e^{\mathbf{A}dt}) - \mathbf{I}]\mathbf{A}^{-1}\mathbf{B}$. Using the augmented state vector $\mathbf{x}^a$ and the augmented matrices $\mathbf{A}_a$ and $\mathbf{C}_a$, equations (3.28) and (3.29) become:

$$\mathbf{x}_{k+1}^a = \mathbf{A}_a \mathbf{x}_k^a + \boldsymbol{\zeta}_k \tag{3.30}$$

$$\mathbf{y}_k = \mathbf{C}_a \mathbf{x}_k^a + \mathbf{v}_k \tag{3.31}$$

where $\boldsymbol{\zeta}_k = [\mathbf{w}_k, \boldsymbol{\eta}_k]^T$. Applying the linear Kalman filter algorithm to this discrete system yields the following prediction equations:

$$\hat{\mathbf{x}}_k^{a-} = \mathbf{A}_a \hat{\mathbf{x}}_{k-1}^{a+} \tag{3.32}$$

$$\mathbf{P}_k^- = \mathbf{A}_a \mathbf{P}_{k-1}^+ \mathbf{A}_a^T + \mathbf{Q_a} \tag{3.33}$$

and correction equations:

$$\mathbf{K}_k = \mathbf{P}_k^- \mathbf{C}_a^T \left[\mathbf{C}_a \mathbf{P}_k^- \mathbf{C}_a^T + \mathbf{R} \right]^{-1} \tag{3.34}$$

$$\hat{\mathbf{x}}_k^{a+} = \hat{\mathbf{x}}_k^{a-} + \mathbf{K}_k \left[\mathbf{y}_k - \mathbf{C}_a \hat{\mathbf{x}}_k^{a-} \right] \tag{3.35}$$

$$\mathbf{P}_k^+ = \mathbf{P}_k^- - \mathbf{K}_k \mathbf{C}_a \mathbf{P}_k^- \tag{3.36}$$

where 'minus' exponents are used for time instances when the measurement is not available and 'plus' exponents when it becomes available.

Using the algorithm described in equation (3.32) through (3.36), an estimate $(\mathbf{u}_k)_{k=0..N}$ of the excitation acting on the system, *i.e.* a so-called regularised solution of the inverse problem, is obtained simultaneously with the estimate of the state of the system $\hat{\mathbf{x}}$. The algorithm is run from the initial time t_0, when the initial state is assumed to be $(\hat{\mathbf{x}}_0^a, \mathbf{P}_0)$, to final time t_N, using the data provided by the measurements $(\mathbf{y}_k)_{k=0..N}$. All the random processes involved, namely $\mathbf{w}_k$, $\mathbf{v}_k$, $\boldsymbol{\eta}_k$, are assumed to be stationary, Gaussian and white, to have zero-mean and to be mutually uncorrelated. Let us remind here, the corresponding covariance matrices:

$$\mathbf{Q}_a \delta_{k,l} = \begin{bmatrix} \mathbf{Q}_a \delta_{k,l} & 0 \\ 0 & \mathbf{S}\delta_{k,l} \end{bmatrix} = E\left[\boldsymbol{\zeta}_k \boldsymbol{\zeta}_l^T\right] = E\left[\begin{bmatrix} \mathbf{w}_k \\ \boldsymbol{\eta}_k \end{bmatrix} \begin{bmatrix} \mathbf{w}_l \\ \boldsymbol{\eta}_l \end{bmatrix}^T\right] \tag{3.37}$$

$$\mathbf{R}\delta_{k,l} = E\left[\mathbf{v}_k \mathbf{v}_l\right] \tag{3.38}$$

The choice of these covariance matrices is of great importance. This is where *a priori* knowledge on the system model, potential errors and perturbations, but also and especially *a priori* information on the excitation, which is to be estimated, comes into consideration. **The regularisation of the inverse problem, and the related quality of the solution, is determined through these matrices**.

3.4.3 Regularisation through the Kalman filtering framework

As described in subsection 3.3.2, searching for a solution that reproduces the imperfect measured data very accurately through an idealized model of the real system is not

in itself a guarantee for the quality of the estimated excitation. Kalman filtering is a particularly convenient framework to introduce *a priori* information on the excitation or on the imperfectness of the model or of the measurement data, as a efficient approach to regularise the inverse problem. Such information possibly comprises:

- Known imperfections in the modelling of the system dynamics (through the matrix $\mathbf{Q}_d$)
- Known noises introduced by the measuring equipment (through the matrix $\mathbf{R}$)
- Known imperfections of the relation (modelling) between the measurement and state vector (through the matrix $\mathbf{R}$)
- Known stochastic characteristics of the excitation being estimated (through the matrix $\mathbf{S}$)

First, let us remind here that the value of **the covariance matrix S of the excitation noise process**, see equation (3.26) and subsection 3.4.2, **plays the same role as the regularisation coefficient** α in equation (3.6). Indeed, the magnitude of the average 'distance' between $\mathbf{u}_{k+1}$ and $\mathbf{u}_k$ controls the smoothness that will be imposed on the solution through the algorithm.

Second, another component of the regularisation of the problem is directly linked to the confidence one attributes to the model of the dynamic system (through $\mathbf{Q}_d$) and of the excitation (through $\mathbf{S}$), relative to the confidence in the data and the ability of the model to exploit it (through $\mathbf{R}$). All information provided to the filter through the matrices $\mathbf{Q}_d$, $\mathbf{S}$ and $\mathbf{R}$, will be compiled within the Kalman gain $\mathbf{K}_k$ through equation (3.34), which is recalled here in its completely expended form:

$$\mathbf{K}_k = (\mathbf{A}_a\mathbf{P}^+_{k-1}\mathbf{A}_a^T + \mathbf{Q}_a)\mathbf{C}_a^T\left[\mathbf{C}_a(\mathbf{A}_a\mathbf{P}^+_{k-1}\mathbf{A}_a^T + \mathbf{Q}_a)\mathbf{C}_a^T + \mathbf{R}\right]^{-1} \tag{3.39}$$

Heuristically, the larger the covariance $\mathbf{Q}_a$ with respect to the covariance $\mathbf{R}$, the fewer the algorithm will 'trust' the model dynamics of the dynamics of the system and excitation and the more it will 'trust' the information it extracts from measurement data $(\mathbf{y}_k)_{k=0..N}$, and vice versa. The Kalman gain manages this compromise according to equation:

$$\hat{\mathbf{x}}_k^{a+} = \mathbf{A}_a\hat{\mathbf{x}}_{k-1}^{a+} + \mathbf{K}_k\left[\mathbf{y}_k - \mathbf{C}_a\hat{\mathbf{x}}_k^{a-}\right] \tag{3.40}$$

where a high gain $\mathbf{K}_k$ increases the fit to the measured data (yet using the model through $\mathbf{C}_a$) and a low gain favours the dynamic prediction (through $\mathbf{A}_a$). **This feature of the augmented Kalman filter algorithm makes it a particularly suitable choice for a controlled resolution of the inverse problem, in the context of imperfect models and data.**

The use of all available information on modelling errors is attractive in principle. Noise amplitudes can be regarded as uncertainty ranges on different components of the state or measurement vectors. In the framework of inverse problem theory, it may be seen as a controlled 'loosening' of the constraint of fit to the measured data, see equation (3.4). Yet one easily notices that the rigorous mathematical framework of Kalman filtering theory may not be strictly respected in this case. Indeed, modelling errors are not random quantities and it is very unlikely that those errors are uncorrelated. In principle, standard Kalman filtering theory only applies if the perturbations acting on the state and measurement equations (3.7) and (3.8) are purely uncorrelated, *i.e.* 'white noises'. If these requirements are not met, or cannot be met using a suitable transformation (*e.g.* decoloration of noises using shaping filters, see [Maybeck, 1979]), the prediction and correction equations (3.18) through (3.22) are not valid.

If the algorithm is applied in this practical setting, properties of the resulting estimate such as the fact that it is unbiased, of minimum variance or distributed normally (at each time instance) may be lost. Nevertheless, even if the conditions required to apply Kalman filtering theory are not perfectly gathered, the proposed algorithm is a very attractive way to combine the information that originates from all the different sensors (through the observation matrix $\mathbf{C}_a$ defined in the space state framework), as well as all available *a priori* information. In this context the selection of the matrices $\mathbf{Q}_d$, $\mathbf{S}$ and $\mathbf{R}$ is not straightforward. This is further detailed when discussing the so-called 'tuning' of the Kalman filter in subsection 3.5.2.

3.5 Implementation of the algorithm for the estimation of road profiles

In subsection 3.4.2, the equations of the augmented linear Kalman algorithm have been presented without specifying a particular system. In order to apply this algorithm for the estimation of road profiles using the measured responses of a vehicle it is both necessary to propose:

- A model for the vehicle and the associated measurement set-up (sensors), through the matrices $\mathbf{A}, \mathbf{B}, \mathbf{C}$ and $\mathbf{D}$

- Models for the description of the perturbations (including the excitation to be estimated) acting on the system and measurement set-up, through a selection of values for the matrices $\mathbf{Q}, \mathbf{S}$ and $\mathbf{R}$.

3.5.1 Choice of a vehicle model for the estimation algorithm

Estimation using a quarter-car model

For the sake of simplicity, the derivation of the different equations is proposed here for a quarter-car model of the vehicle, see subsection 2.3.2. The latter is displayed in figure 3.4.

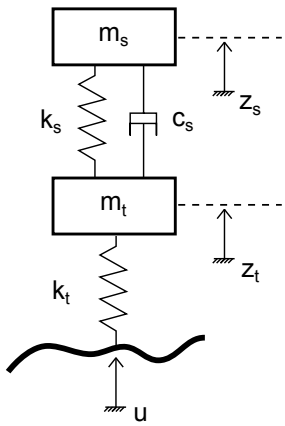

Figure 3.4: Quarter-car model of the vehicle, constituted by a 2 degrees-of-freedom model (2-DOF).

The state representation of the time-invariant vehicle model is given by the following Ordinary Differential Equation (ODE) :

$$\begin{bmatrix} \ddot{z}_s \\ \ddot{z}_t \\ \dot{z}_s \\ \dot{z}_t \end{bmatrix} = \begin{bmatrix} -c_s/m_s & c_s/m_s & -k_s/m_s & k_s/m_s \\ c_s/m_t & -c_s/m_t & k_s/m_t & -(k_s+k_t)/m_t \\ 0 & 0 & 1 & 0 \\ 0 & 0 & 0 & 1 \end{bmatrix} \begin{bmatrix} \dot{z}_s \\ \dot{z}_t \\ z_s \\ z_t \end{bmatrix} + \begin{bmatrix} 0 \\ k_t/m_t \\ 0 \\ 0 \end{bmatrix} [u] \tag{3.41}$$

The state vector is defined by $\mathbf{x}(t) = [\dot{z}_s, \dot{z}_t, z_s, z_t]$ which gives, in state space notations, and writing explicitly the time dependency:

$$\dot{\mathbf{x}}(t) = \mathbf{A}\mathbf{x}(t) + \mathbf{B}u(t) \tag{3.42}$$

As detailed in subsection 3.4.2, the ODE is discretized with sample time dt and an *a priori* model is selected for the excitation according to equation 3.26. The discrete augmented space state representation of the system may be written:

$$\begin{bmatrix} \mathbf{x}_{k+1} \\ u_{k+1} \end{bmatrix} = \begin{bmatrix} e^{\mathbf{A}dt} & [e^{\mathbf{A}dt} - \mathbf{I}]\mathbf{A}^{-1}\mathbf{B} \\ \mathbf{0}_{1\times 4} & 1 \end{bmatrix} \begin{bmatrix} \mathbf{x}_k \\ u_k \end{bmatrix} + \begin{bmatrix} \mathbf{w}_k \\ \eta_k \end{bmatrix} \tag{3.43}$$

or equivalently, using the augmented notations introduced in subsection 3.4.2:

$$\mathbf{x}_{k+1}^a = \mathbf{A}_a \mathbf{x}_k^a + \boldsymbol{\zeta}_k \tag{3.44}$$

Measurement set-up and choice of the processed responses

For the measurement equation, four output quantities (*i.e.* measured responses to be processed) are here selected in order to feed the estimation algorithm. They originate from three sensors on the vehicle, namely:

- $\ddot{z}_s$: from an acceleration sensor on the body of the vehicle (sprung mass m_s), generally close to the suspension mount, on the front (left or right) side of the body
- $\ddot{z}_t$: from an acceleration sensor on the steering knuckle (unsprung mass m_t), on the front (left of right) side
- $z_s - z_t$: from a displacement sensor that measures the suspension displacement, on the front (left of right) side

The forth output quantity z_s comes from the double integration of the body acceleration $\ddot{z}_s$. The mentioned sensors are generally mounted on the measuring vehicle for any load characterisation campaign. The (augmented) measurement equation is then:

$$\begin{bmatrix} z_s - z_t \\ z_s \\ \ddot{z}_s \\ \ddot{z}_t \end{bmatrix} = \begin{bmatrix} 0 & 0 & 1 & -1 & 0 \\ 0 & 0 & 1 & 0 & 0 \\ -c_s/m_s & c_s/m_s & -k_s/m_s & k_s/m_s & 0 \\ c_s/m_t & -c_s/m_t & k_s/m_t & -(k_s+k_t)/m_t & k_t/m_t \end{bmatrix} \begin{bmatrix} \dot{z}_s \\ \dot{z}_t \\ z_s \\ z_t \\ u \end{bmatrix} \tag{3.45}$$

Using the notations introduced in subsection 3.4.2, the discrete measurement equation becomes:

$$\mathbf{y}_k = \mathbf{C}_a \mathbf{x}_k^a + \mathbf{v}_k \tag{3.46}$$

In order to be able to estimate the actual value of the (augmented) state vector from given measurement data, the choice of the output matrix $\mathbf{C}_a$ cannot be arbitrary. In the terms of control theory, the space state representation must be observable. A necessary and sufficient condition for the system to be observable is that the observability matrix $\mathcal{O}$

has full rank, see [Maybeck, 1979]:

$$\mathcal{O} = \begin{bmatrix} \mathbf{C}_a \\ \mathbf{C}_a\mathbf{A}_a \\ \mathbf{C}_a\mathbf{A}_a^2 \\ \dots \\ \mathbf{C}_a\mathbf{A}_a^{n-1} \end{bmatrix} \tag{3.47}$$

where n is the order of the state representation. Here $n = 5$. Through simple algebra it can be shown that the proposed couple $(\mathbf{A}_a, \mathbf{C}_a)$, defined through equations (3.41), (3.43), and (3.45), does verify such a condition and is thus observable. The sprung mass displacement z_s has been added to the output vector in order to guarantee that the system is observable. In practice the latter cannot be measured and is obtained from the double integration the sprung acceleration. This operation may produce a drift phenomenon. This is further discussed in subsection 3.6.2.

Heuristically, a system is observable when the state of system can be estimated thanks to sufficient information coming from the chosen outputs in $\mathbf{y}$. This is especially important in the present case, as the excitation can only be estimated is there is sufficient information on the dynamic responses of the system. It should be noted that the more complex the model of the vehicle is, *i.e.* in terms of degrees of freedom, the larger the output vector (number of sensors) must be for the system to remain observable.

Other choices of output vectors $\mathbf{y}$ and related matrix $\mathbf{C}_a$ can be considered if one of the acceleration sensors is not available, namely, $\mathbf{y} = (z_s - z_t, z_s, \ddot{z}_s)$, and $\mathbf{y} = (z_s - z_t, z_t, \ddot{z}_t)$. It could be shown that these choices of output vectors lead to observable systems.

Discussion on the choice of the vehicle model

It is quite straightforward that a linear quarter-car model is a very strong simplification of the real and non-linear behaviour of the vehicle, see subsection 2.3.2. Hence the quality of the estimate may be far from optimal. Nonetheless the selection of this simple model is thought to be appropriate here due to the following reasons:

First, considering a non-linear model would compromise the fast nature of the linear Kalman filter. Indeed, applying the same approach for a non-linear system, *e.g.* using Extending Kalman Filtering (EKF), would very strongly increase the calculation time, which is a serious issue when processing large sets of data. Second, it could be argued that each of the four wheels of the vehicle are 'relatively independent' and considering a complete model of the vehicle may not represent a very strong gain in terms of precision. Third, a more complex model would involve more parameters to characterise, such as body inertia, which can be difficult to measure accurately or quite varying depending on vehicle cargo. Fourth, whereas the dynamics of the front of the vehicle may be considered as 'almost purely vertical', this is not so evident with the rear axle of the vehicle and the modelling may become much more complex.

There is evidently a compromise to be found between the complexity of the algorithm and the quality of the estimation. The comparison between results based on different models has been carried out and analysed, see 3.6.4.

Summary of the estimation algorithm

The proposed algorithm, or augmented Kalman filter, is described by equations (3.32) through (3.36), where the system is described by of equations (3.44) and (3.46). It allows to extract information on the road profile from the measured output vector $\mathbf{y} = (z_s - z_t, z_s, \ddot{z}_s, \ddot{z}_t)$.

In order to be able to apply such algorithm, values have to be defined for the covariance matrices $\mathbf{Q}_d$, $\mathbf{R}$ and for $S = E\left[\eta_k \eta_l\right] \delta_{k,l}$. Using the vocabulary of signal processing theory, this operation may be described as tuning the algorithm.

3.5.2 Semi-empirical tuning of the estimation algorithm

Principle of tuning

The issue of tuning of the filter is complex and is approached here with an empirical attitude. In the end, the objective of the tuning is to provide a tool that yields the best possible estimate of the road profile. In subsection 3.4.3, it has been said that the values selected for $\mathbf{Q}_d$, $\mathbf{R}$ and S determine the confidence that the algorithm attributes to the measurement data and to the capacity of the model to exploit it.

The vehicle model selected above is a simplified and idealized version of the actual mechanical system. In principle, the algorithm can somehow 'account' for modelling deficiencies. However, it has been said in subsection 3.4.3 that the hypotheses that are required to apply Kalman filtering are no longer respected since modelling errors are not necessarily 'white noises'. In consequence, **it is unlikely that values may be derived for the matrices $\mathbf{Q}_d$, $\mathbf{R}$ and for S based on rigorous mathematical considerations and there is necessarily an empirical aspect to the tuning of the filter.** To the best of the author's knowledge there is no example of a solution to such issue in literature and the latter is seldom discussed. Nonetheless, the reader may refer to [Maybeck, 1979] for more general details on the tuning of Kalman filters, as well as elaborate engineering-oriented discussions on the use of such filters.

A semi-empirical method is proposed here as a solution for the tuning of the algorithm. It is labelled 'semi-empirical' in order to highlight the fact that it combines both empirical data from experimentation and physics-based reasoning when it comes to the interpretation of error signals as noises. The principal question relative to tuning is then: how can one gather quantified *a priori* information on modelling errors or perturbations and how to feed it into the algorithm?

Semi-empirical tuning: study of error signals

First, the empirical part of the tuning operation consists in obtaining data, representative of potential error signals, and subsequently asses their magnitude, rather labelled 'strength' in what follows. This operation has been carried out in the following manner. A given pair of road profiles has been used to simulate the response of a highly detailed multi-body vehicle model, see subsection 2.3.2 for details on such a model. The latter serves has a reference to obtain the so-called 'true' responses that could have been measured on a real vehicle. The associated state and output vectors are calculated. Then, the second part of the tuning operation, is to derive the so-called 'error signals' that will be interpreted as noises in the framework of Kalman filtering. This second part is based on physical insight rather than purely on rigorous mathematical considerations.

The dynamic prediction error (associated with the state noise), is defined as the difference between the 'true' state of the system $\mathbf{x}_{k+1}^{true}$ at time t_{k+1}, and the predicted state at time t_{k+1}, given the 'true' state vector $\mathbf{x}_k^{true}$ and excitation u_k^{true}, at time t_k, as shown in equation (3.43), re-written differently here:

$$\mathbf{w}_k = \mathbf{x}_{k+1}^{true} - \left[e^{\mathbf{A}dt}\mathbf{x}_k^{true} + [e^{\mathbf{A}dt} - \mathbf{I}]\mathbf{A}^{-1}\mathbf{B}u_k^{true}\right] \tag{3.48}$$

In this case, the 'true' state $\mathbf{x}_k^{true}$ is known through the highly detailed simulation. The results are displayed in figure 3.5, for each component of the vector equation (3.48). The error signal or dynamic prediction error $\mathbf{w}_k$ is shown in red. The true state of the system, in blue is sometimes hardly distinguishable from the point-wise predicted state, in black. This figure gives a good idea of the magnitude of the modelling errors related to the state equation. Heuristically, the dynamic prediction error is the error affecting the point-wise prediction performed using the state equation (3.43) when the state vector is perfectly known at time instance t_k.

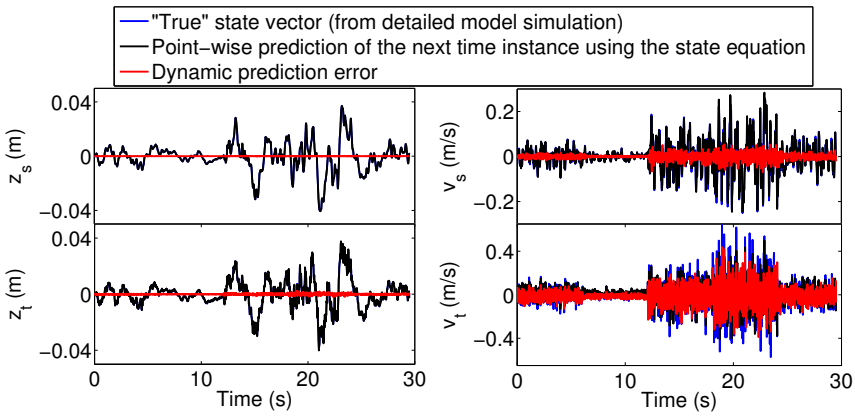

Figure 3.5: Empirical estimation of the state noise's strength. Visualization of the dynamic prediction error signals using an experimental simulation.

On the other hand, the output calculation error (associated with the measurement noise), is defined as the difference between the 'true' measurement vector $\mathbf{y}_k^{true}$ and the output vector calculated using the simple linear model (through $\mathbf{C}_a$) and the 'true' state vector $\mathbf{x}_k^{a,true}$, as displayed in equation (3.46), re-written differently here:

$$\mathbf{v}_k = \mathbf{y}_k^{true} - \mathbf{C}_a \mathbf{x}_k^{a,true} \tag{3.49}$$

In this case, the true state $\mathbf{x}_k^{a,true}$ and the true output $\mathbf{y}_k^{true}$ are known through the simulation involving the detailed model. The results are shown in figure 3.6, for each component of the vector equation (3.49). The error signal or output calculation error $\mathbf{v}_k$ is shown in red. The true output of the system, in blue is sometimes hardly distinguishable from the linearly calculated output. This figure gives a good idea of the magnitude of modelling errors related to the measurement equation. Heuristically, the output calculation error is the error affecting the measurement equation (3.46), used to calculate the output vector from the state vector when the latter is perfectly known.

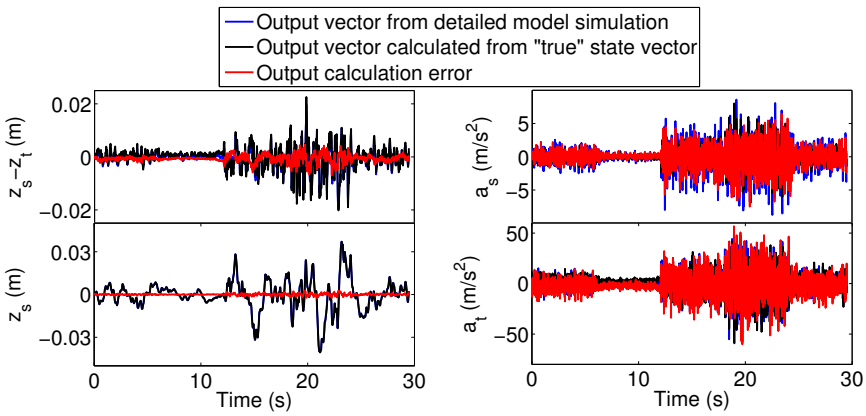

Figure 3.6: Empirical estimation of the measurement noise's strength. Visualization of output calculation error signals using an experimental simulation.

Both figures 3.5 and 3.6 illustrate quite clearly that modelling errors can be large. Consequently, it may not be appropriate to seek an exaggerated goodness of fit to the measured data. The linear model used to invert the physics of the problem visibly lacks precision. Nevertheless, **it is still possible to extract valuable information from the measurement data using this simple model**, as will be shown in the following section.

Semi-empirical tuning: identification of tuning values

Based on the strength of calculated error signals, a rough estimate may be obtained for the magnitude of the values of $\mathbf{Q}_d$ and $\mathbf{R}$. The latter must not be taken as an inflexible

Affected state component	Approx strength (% of RMS value of the component) of the error signal	Typical signal magnitude	Magnitude of covariance matrix $\mathbf{Q}_d$ (rounded)
$\dot{z}_s$	20%	0.05m/s	10^{-4}
$\dot{z}_t$	80%	0.2m/s	10^{-2}
z_s	1%	0.01m	10^{-8}
z_t	5%	0.01m	10^{-7}

Table 3.1: Semi-empirical assessment of the magnitude of the dynamic prediction error: strength of the state noises. Magnitudes of $\mathbf{Q}_d$ correspond to the variance of the different error signals ($\mathbf{w}_k$).

Affected measurement component	Approx strength (% of RMS value of the component) of the error signal	Typical signal magnitude	Magnitude of covariance matrix $\mathbf{R}$ (rounded)
$z_s - z_t$	15%	0.01m	10^{-6}
z_s	10%	0.01m	10^{-6}
$\ddot{z}_s$	60%	$1m/s^2$	1
$\ddot{z}_t$	100%	$10m/s^2$	100

Table 3.2: Semi-empirical assessment of the magnitude of the output calculation error: strength of the measurement noises. Magnitudes of $\mathbf{R}$ correspond to the variance of the different error signals ($\mathbf{v}_k$).

and exact calibration of the algorithm. Yet these values constitute a robust first guess that yields acceptable results (see following section) and do not vary very significantly for one road profile to another or from one vehicle to another. They are given in tables 3.1 and 3.2. The magnitude of each diagonal element of the covariance matrices $\mathbf{Q}_d$ and $\mathbf{R}$ corresponds to the variance of the related error signals $\mathbf{w}_k$ and $\mathbf{v}_k$, for each component of the state and measurement equations.

From this (starting) point, a finer tuning may be considered through more elaborate, purely empirical means. The most straightforward technique consists in setting up a calibration case. If an estimation is made in the case where both the true response of the vehicle and the true road profile are known, then the tuning can be iteratively adjusted in order to obtain the best possible estimation of the road profile. The optimisation of the tuning can be carried out either manually or using an optimisation scheme associated with suitable numerical criteria to judge the 'quality' of the estimate. Results presented in section 3.6 do not involve additional tuning. To sum up, the covariance matrices of the

state noise and measurement noise are:

$$\mathbf{Q}_d = \begin{bmatrix} 10^{-4} & 0 & 0 & 0 \\ 0 & 10^{-2} & 0 & 0 \\ 0 & 0 & 10^{-8} & 0 \\ 0 & 0 & 0 & 10^{-7} \end{bmatrix} \quad \text{and} \quad \mathbf{R} = \begin{bmatrix} 10^{-6} & 0 & 0 & 0 \\ 0 & 10^{-6} & 0 & 0 \\ 0 & 0 & 1 & 0 \\ 0 & 0 & 0 & 100 \end{bmatrix} \tag{3.50}$$

On the other hand, the choice of the S parameter (regularisation parameter) that is related to the *a priori* knowledge on the excitation noise process η_k, see equation (3.26), is also a complicated issue. A physical approach is to study the properties of the excitations that may be applied to the vehicle, and set up S in such a way that the modelled excitation process is representative of the excitation that is being estimated. Such an approach may be tricky as one generally does not know in advance the characteristics of the excitation that is to be estimated. In this study it is rather proposed to select S manually using a calibration setting, where both the true response and the true road profile are known simultaneously. The regularisation parameter S is thus kept as the only coefficient that may be manually adjusted to improve the 'quality' of the estimation in a purely empirical manner.

Influence of the sample time on the tuning

It must be pointed out that the strength of the state and excitation noises is dependant on the selected sample time dt. This may be seen in equation (3.48). Also for a given road excitation, the noise $\eta_k = u_{k+1} - u_k$ is clearly affected by the 'distance' between t_{k+1} and t_k. Essentially, the characteristics of the error signals and excitation noise will be different on different time frames. This reasoning indicates that the tuning of the filter has to be realised in accordance with the particular sample time that is used to process the measurement data (generally it is directly linked to the sampling frequency of the measurement data) or modified if the sample time changes. In this subsection all calculations have been conducted at $dt = 0.01s$ or 100Hz.

It has been noted that the different components of $\mathbf{Q}_d$ and $\mathbf{R}$ do not vary significantly with respect to one another when the sample time is modified. It is generally sufficient to modify the S parameter to account for a modification in the sample time. The starting value used here is generally $S = 10^{-7}$ for $dt = 0.001s$ and $S = 10^{-5}$ for $dt = 0.01s$. It is obtained by roughly studying the characteristics of a 'median' excitation process, which relates to the excitation noise $\eta_k = u_{k+1} - u_k$. The influence of the S parameter is further discussed using practical examples in the following section.

The practical implementation of the augmented Kalman filter for the estimation of road profiles, *i.e.* the selected vehicle model and tuning ap-

proach, is an original contribution of this research work, and has been published in [Fauriat et al., 2016]. It is tested in the following section.

3.6 Testing of the road estimation algorithm

3.6.1 Testing framework and objective scalar criteria

In the present section, the proposed road estimation algorithm is tested using various data sets $(\mathbf{y}_k)_{k=0..N}$, originating either from simulations or from real measurements. In order to be able to test the estimation algorithm and evaluate its performances, it is necessary that the exact geometry of the road profile, or so-called 'true' road profile, is known beforehand. It has to be known simultaneously with the associated responses on the vehicle, either simulated or measured.

In practice, road profiles are discretised sets of values. The choice of an appropriate measure for the difference between those two entities is not a trivial matter. This issue cannot be approached purely from a mathematical standpoint. To formulate a valuable judgement regarding the 'quality' of the estimation algorithm, it is necessary to consider the purpose served by the data produced by the algorithm. In the context of this manuscript, the road profile data is collected in view of gaining an understanding on the variability of road roughness so as to be able to propose a mathematical representation in the form of a stochastic process, see chapter 4. Subsequently, this understanding of the variability of road roughness is used to derive through simulation a quantified description of the variability of road-induced loads, see chapter 5. It is thus necessary to define **appropriate criteria** in order to objectively determine if the estimation algorithm is indeed adapted for such purposes.

Visual comparisons of signals or of their frequency content (PSD) can be useful but do not constitute a very objective approach. A more objective and systematic approach is considered in the following study. Two families of scalar criteria labelled as direct and indirect criteria are defined and used to carry out the comparison between the real road profile and its estimate produced by the algorithm.

Direct scalar criteria

First, direct criteria are focused on a direct comparison of the true and estimated road profiles. More precisely, it is proposed here to compare their spatial frequency content. Three spatial frequency bands are delimited, namely a low band 0.05 - 0.2 m^{-1}, a medium band 0.2 - 1 m^{-1} and a high band 1 - 5 m^{-1}. One can equivalently consider long wavelengths 5 - 20m, medium wavelengths 1 - 5m and short wavelengths 0.2 - 1m. The comparison of the content within these frequency bands is based on the use of a roughness coefficient. The latter is introduced in more details in chapter 4. At this point let us consider the power spectral density (PSD) $S_u(n)$ of the road profile $u(x)$ and further

assume that a one-parameter model is fitted on that PSD such that:

$$S(n) = S_0 \left(\frac{n}{n_0}\right)^{-w} \tag{3.51}$$

where S_0 is the said roughness coefficient, n is the spatial frequency (in m^{-1}), $n_0 = 0.1m^{-1}$ and w is a parameter related to the form of the modelled PSD, labelled waviness, which will be set to $w = 2$. On each frequency band j, a least squares regression is used to identify the coefficient S_{0j} giving the best fit between the calculated PSD $S_u(n)$, restrained to the said frequency band j, and the analytical form in equation (3.51). The comparison of the roughness coefficients corresponding to both the true and estimated profiles yields the scalar criterion (in percent) :

$$\delta S_{0j,estim} = \frac{S_{0j}^{estim} - S_{0j}^{true}}{S_{0j}^{true}} \times 100 \tag{3.52}$$

where 'true' refers to the real profile (which is known for the purpose of testing) and 'estim' refers to the profile that is obtained from the estimation algorithm. These scalar criteria may be used to **determine the domain (frequency-wise) of validity of the algorithm**. In relation with the next chapter, they also constitute an indication on the capacity of the estimation algorithm to provide data suited for the identification of a frequency-based stochastic model for road profiles.

Indirect scalar criteria

Secondly, indirect criteria involve the study of the mechanical responses of a given vehicle model to a given road profile. Here a linear quarter-car model is employed. In order to carry out an exploitable comparison, it is important to run both the simulation linked to the real and estimated road profiles, using the same direct model. This allows us to somehow set aside the issue of modelling errors. Such an approach **introduces physical insight into the evaluation of the quality of the estimation algorithm**. Indeed, potential discrepancies between both road profiles can be analysed in regards of the effect they have on the different predicted responses of the vehicle. This is of great significance if the estimated road profile are subsequently used to study the variability of road-induced load.

The damage equivalent amplitude (DEA), see subsection 2.1.3, is calculated from each considered response using the following relation and used as a scalar criterion:

$$y_{eq} = \left(\frac{\sum_{i=1}^{p} \Delta y_i^{\beta}}{n_{eq}}\right)^{1/\beta} \tag{3.53}$$

where $(\Delta y_i)_{i=1..p}$ are the amplitudes of the Rainflow ranges extracted from a given signal

y. In this subsection, a number of cycles of $n_{eq} = 200000$ cycles is selected and a Basquin's coefficient of $\beta = 5.6$ is used. The comparison between the response to the true profile y^{true} and to the estimated profile y^{estim}, using a linear model, yields the following indirect criterion (in percent):

$$\delta y_{estim} = \frac{y_{eq}^{estim} - y_{eq}^{true}}{y_{eq}^{true}} \times 100 \tag{3.54}$$

It must be remembered that all the comparisons based on such indirect criteria are dependent on the choice of the direct model.

Experimental setting and results

Simulation-based experiments as well as measurements on a real vehicle are presented in the following subsection. On the one hand, it is more convenient to use data from simulation as it allows us to test numerous scenarios, *e.g.* road profiles, vehicle speeds. However this introduces modelling imprecisions and therefore cannot formally guarantee that the method will be as efficient in the context of a real measurement. On the other hand, data obtained from measurements is not affected by modelling errors but in such case the true road profile may not always be known or may be difficult to know precisely, for instance when the trajectory of the vehicle on the road surface cannot be exactly controlled.

Let us insist on the fact that, except for the experiments wherein the contrary is explicitly mentioned, the road estimation algorithm is always based on a linear quarter-car model, no matter if the data has been generated with a different model. For all experimental cases, the measurement data is fed into the road estimation algorithm defined according to the implementation proposed in section 3.5.

For the sake of practicality, all scalar criteria are compiled in tables and given either directly in this chapter or in appendix D. Various time-based (or spatial) plots, PSD plots and level-cross (LC) plots, are also given in appendix D.

3.6.2 Numerical testing of the road estimation algorithm

Data obtained from a 2-DOF non-linear quarter car model

The first data set is obtained from the response of a two degrees-of-freedom (2-DOF) non-linear quarter-car model, see appendix B.1. The simulated response corresponds to a randomly generated road profile (see section 4.3) covered at $60km/h$.

The standard tuning ($\mathbf{Q}_d$ and $\mathbf{R}$) defined in equation (3.50) is employed. The S parameter is selected rather crudely at $S = 10^{-6}$. The simulation is carried out with a sampling frequency of 1000Hz.

The estimation algorithm gives the results displayed in the spatial plot D.1 and PSD plot D.2. The values reported on PSD plots are those of the roughness coefficients S_{0j}^{estim} and S_{0j}^{true}, identified through a least squares regression on each frequency band.

It is interesting to use this example as an illustration on the issue of the pre-processing of the data. In practice, the absolute body displacement is obtained from a double integration of the body acceleration and this may induce a drift phenomenon. The drift can be eliminated through high-pass filtering. The low-frequency content that is thus removed has little influence on vehicle responses and is of no particular interest within the estimate. In this example the measurement vector is high-pass filtered with a selected cut-off frequency of 0.5Hz. For all other experiments in this section a 0.2Hz high-pass filtering is applied on the measurement vector to remove drifts and offsets. As a comparison, figures D.3 and D.4 correspond to a setting where the body displacement is directly simulated and no filtering is thus needed. They can be compared with figures D.1 and D.2 to visualise the effect of this necessary pre-processing operation.

Comparison of the responses of a linear quarter-car model to both the estimated profile and the true profile are displayed on figures D.5, D.6 and D.7. The measurement data used as an input in the estimation algorithm is also shown on the same figures (in red). Zooms are operated on shorter sections in order to better visualise the differences between responses. These differences are more readily apparent on PSD or level-cross (LC) plots. The latter are given in figures D.8, D.9 and D.10. The indirect criterion δy_{estim} characterising the difference between the DEA associated to the real (in black) and estimated (in blue) profiles, is displayed on LC plots.

All the figures presented in appendix D, namely figures D.1 through D.10, can be used to visually assess the quality of the estimation algorithm. Nonetheless, the scalar criteria introduced in subsection 3.6.1 allow us to make this assessement more objectively. They are gathered in table 3.3.

Criterion (direct and indirect)	Value for the true profile	Value for the estimated profile	Relative error
Road roughness	(power in m^3) $\times 10^{-6}$		
Low band ($0.05m^{-1}$-$0.2m^{-1}$)	244.09	242.29	-0.8%
Medium band ($0.2m^{-1}$-$1m^{-1}$)	316.22	261.03	-17.4%
High band ($1m^{-1}$-$5m^{-1}$)	224.88	52.46	-76.7%
Damage equivalent amplitude	(use of linear quarter-car model)		
Suspension displacement (m)	0.0053	0.0052	-1.5%
Sprung mass acceleration (m/s^2)	1.58	1.44	-9.0%
Unsprung mass acceleration (m/s^2)	15.73	11.61	-26.2%

Table 3.3: Result of the estimation for the data set involving a 2-DOF non linear quarter-car model, in terms of scalar criteria. The S parameter is fixed at $S = 10^{-6}$.

When the data is obtained from an arguably 'simple' non-linear model (see figure B.1),

it has been noted that regularisation, in the form of the S parameter, is not really needed. With a high value for S, say $S = 1$, *i.e.* a very weak regularisation, the estimate converges almost perfectly to the true profile. This is illustrated in figure D.11. The convergence is displayed for the unsprung mass acceleration in figure D.12 and it appears clearly that **the fit with the non-linear data cannot be achieved**. However, this has **no particular consequence on the quality of the obtained estimate**.

To validate the estimation algorithm, this experimental case is therefore not sufficiently robust since the non-linearity of the model used to create the measurement data is very limited in comparison with what may be experienced on the actual vehicle. Testing the inversion of a physical problem with data synthesized from a direct model that too closely resembles the model used to invert the problem is sometimes referred to as the 'inverse crime', see [Idier, 2013]. Results for a weak regularisation, more precisely $S = 1$, are nonetheless given in table D.1.

Data obtained from a detailed multi-body vehicle model

Let us now consider data obtained from a highly detailed non-linear multi-body model of the vehicle associated with a complex tyre model, see details in subsection 2.3.2. A visualisation of a vehicle model in a multi-body simulation (MBS) software is displayed in figure 2.7. The sampling frequency of the simulation is fixed at 1000Hz. The standard tuning ($\mathbf{Q}_d$ and $\mathbf{R}$) defined in equation (3.50) is employed for the estimation algorithm.

Spatial descriptions of different pairs of road profiles are provided to the MBS solver. First, a pair of randomly generated road profiles (see section 4.3) is considered and covered with a speed target of $60km/h$. Secondly, a (symmetrical) pair of road profiles made of randomly synthesized transient patterns (see section 4.3) is covered with a speed target of $30km/h$. Eventually, a pair of road profiles corresponding to a real rough pavement track used for validation purposes at Renault, is covered with a speed target of $60km/h$. For the first two experiments, only the left road profile is estimated. The road estimation algorithm is always based on a quarter-car model.

The S parameter is adapted empirically in order for the estimation to yield a good compromised between all scalar criteria in table 3.4. Eventually, $S = 10^{-7}$ is selected.

Data obtained from a detailed multi-body vehicle model: first dataset

For the first pair of randomly generated profiles, the resulting estimate (left profile) is displayed in figure D.13 and D.14 and the scalar criteria are compiled in table 3.4.

Criterion (direct and indirect)	Value for the true profile	Value for the estimated profile	Relative error
Road roughness	(power in m^3) $\times 10^{-6}$		
Low band ($0.05m^{-1}$-$0.2m^{-1}$)	83.45	57.45	-31.2%
Medium band ($0.2m^{-1}$-$1m^{-1}$)	94.41	106.85	13.2%
High band ($1m^{-1}$-$5m^{-1}$)	89.32	16.55	-81.5%
Damage equivalent amplitude	(use of linear quarter-car model)		
Suspension displacement (m)	0.0028	0.0026	-8.9%
Sprung mass acceleration (m/s^2)	0.84	0.93	10.8%
Unsprung mass acceleration (m/s^2)	8.13	8.33	2.6%

Table 3.4: Result of the estimation for the data set 1 involving a detailed (MBS) model, in terms of scalar criteria. The considered road profile is randomly generated. The S parameter is fixed at $S = 10^{-7}$.

As previously mentioned, the low frequency discrepancy between the signals due to the pre-processing of data, is of minor importance. The quality of the estimate is fairly reasonable. The shape of the PSD of the estimate is noticeably distinct from the one of the true profile but the estimation of the roughness values remains acceptable, apart for the high frequency band. When observing the scalar indirect criteria, it appears that the estimated profile produces responses that are relatively similar, namely in a $\pm 15\%$ interval in terms of DEA, to the responses produced by the true profile.

Data obtained from a detailed multi-body vehicle model: second dataset

For the second pair of transient-laden road profiles, the estimate (left profile) is displayed on figure D.15. Suspension displacement responses are also compared on figure D.16. One clearly sees that in the case of transient patterns, the detailed model, which includes a sophisticated tyre model, gives a response (in red) that is strongly different from that of a linear model (in blue and black). This shows that the proposed road estimation algorithm may yield less precise results when dealing with strongly non-linear responses. Nonetheless, the form and position of the different obstacles is correctly identified, even if their amplitude can be affected significantly. The comparison of scalar criteria is given in table 3.5.

Criterion (direct and indirect)	Value for the true (filtered) profile	Value for the estimated profile	Relative error
Road roughness	(power in m^3) $\times 10^{-6}$		
Low band ($0.05m^{-1}$-$0.2m^{-1}$)	54.02	41.45	-23.3%
Medium band ($0.2m^{-1}$-$1m^{-1}$)	14.97	8.12	-45.7%
High band ($1m^{-1}$-$5m^{-1}$)	0.98	0.23	-76.9%
Equivalent damage amplitude	(use of linear quarter-car model)		
Suspension displacement (m)	0.0035	0.0027	-24.2%
Sprung mass acceleration (m/s^2)	0.52	0.40	-23.7%
Unsprung mass acceleration (m/s^2)	5.87	2.48	-57.8%

Table 3.5: Result of the estimation for the data set 2, involving a detailed (MBS) model, in terms of scalar criteria. The considered road profile is laden with transient obstacles. A 'geometric filter' has been applied on true road profile before carrying out the comparison, see appendix C. The S parameter is fixed to $S = 10^{-7}$.

In table 3.5 the estimate is compared with a true profile that has been filtered in order to make it more representative of the displacement of a point on the lower end of the tyre. The reason for this filtering is described in what follows and illustrated in appendix C.

The 'true' road geometry provided to the MBS solver which comprises a detailed tyre model, is essentially the description of the local altitude of the road surface. It may never be an admissible trajectory of the contact point between the road and the tyre. For instance, when the vehicle crosses a pot-hole, it is not likely that the tyre will follow exactly the shape of the pot-hole. With such rapidly varying profiles, it is not appropriate to equate the exact road geometry with the vertical excitation imposed on the linear model, as the latter cannot account for the uni-directional and non-permanent surface contact that actually occurs between the tyre and the road. This demonstrates that **the comparison between the input 'road geometry' and the 'estimated road excitation' is a delicate matter**.

Here, the measurement data obtained through the detailed vehicle and tyre models, has been impacted by a 'realistic' vertical excitation and not directly by a geometric constraint following the exact vertical evolution of the road profile. An additional discussion on this issue is given in appendix C. Let us simplify here by saying that with rapidly varying profiles the comparison between the true geometry of the road profile and the evolution of the estimate must not be analysed with an overly rigid attitude (raw comparison of criteria). Indeed, in this case, both sets of values may actually represent different physical quantities. The comparison between the so-called (geometric) filtered and unfiltered road profiles is given in table C.2.

Data obtained from a detailed multi-body vehicle model: third dataset

Lastly, for a pair of road profiles corresponding to a real rough pavement, the resulting estimates (for both the left and right wheel of the vehicle) are displayed in figures D.17 and D.18. Scalar criteria are given in table 3.6.

Wheel (L or R)	Criterion (direct and indirect)	Value for the true profile	Value for the estimated profile	Relative error
Road roughness		(power in m^3) $\times 10^{-6}$		
L	Low band ($0.05m^{-1}$-$0.2m^{-1}$)	405.82	337.81	-16.8%
	Medium band ($0.2m^{-1}$-$1m^{-1}$)	2668.6	2207	-17.3%
	High band ($1m^{-1}$-$5m^{-1}$)	794.71	477.6	-39.9%
R	Low band ($0.05m^{-1}$-$0.2m^{-1}$)	462.81	279.27	-39.7%
	Medium band ($0.2m^{-1}$-$1m^{-1}$)	4646.9	3155.4	-32.1%
	High band ($1m^{-1}$-$5m^{-1}$)	888.62	360.74	-59.4%
Equivalent damage amplitude		(use of linear quarter-car model)		
L	Suspension displacement	0.0064	0.0061	-5.0%
	Sprung mass acceleration	3.28	2.94	-10.5%
	Unsprung mass acceleration	27.13	25.16	-7.3%
R	Suspension displacement	0.0080	0.0074	-8.0%
	Sprung mass acceleration	4.12	3.49	-15.3%
	Unsprung mass acceleration	30.64	28.08	-8.34%

Table 3.6: Result of the estimation for the data set 3, involving a detailed (MBS) model, in terms of scalar criteria. The considered road profile corresponds to a real rough pavement track. The S parameter is fixed to $S = 10^{-7}$.

The description of the low and medium spatial frequency content of the profile is not very good. Again, since these road profiles are very severe and tend to engage the vehicle in the strongly non-linear domain in terms of its responses, the road estimation based on a linear model yields poorer results in this case. **The high frequency content is lost, both because of the regularisation and of the natural filtering of the tyre**. This is apparent in figure D.18 when considering the frequency peak occurring at approximately $6m^{-1}$, which relates to the characteristic length of a paving stone (appx $15cm$). This high frequency content is filtered out by the geometry of the tyre (see figure C.2) and therefore cannot correspond to the vertical position of the contact patch, nor being estimated through vehicle responses. The adequacy in terms of damage potential is quite good (within a $\pm 15\%$ interval), according to the values of the indirect criteria in table 3.6.

3.6.3 Physical testing of the road estimation algorithm

Data obtained from a measurement on a vertical test-rig

A real measurement has been carried out with the aim of testing the method without introducing modelling imprecisions within the data. The vehicle is mounted on a test rig constituted of four vertical actuators, or 'four-posts rig'. The rig is shown in figure 3.7 in a simulation environment only for visualisation purposes. A selected pair of vertical excitations representing road profiles, *i.e.* vertical positions target for each actuator (delayed by the length of the vehicle for the rear signals), are imposed on the vehicle by the test rig. The time position of each of the actuators is recorded simultaneously with the vehicle's responses.

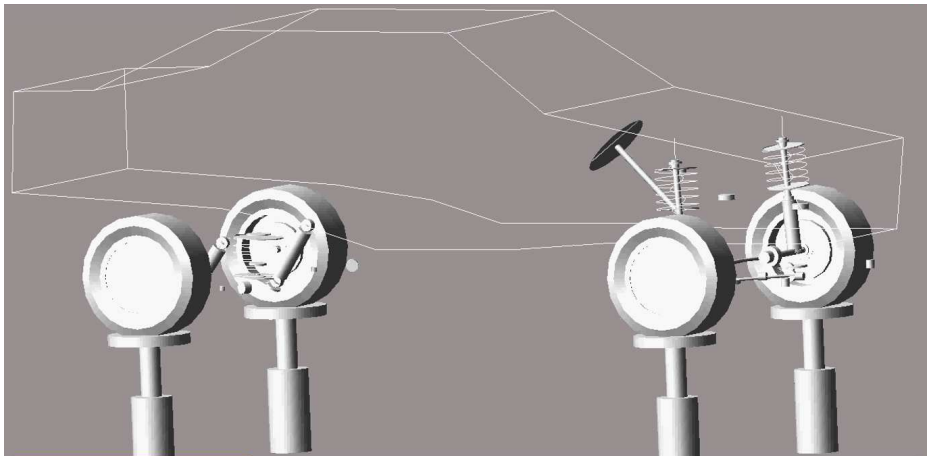

Figure 3.7: Illustration of the four-post vertical test rig. The rig is shown in a simulation environment for the sake of simplicity of visualisation.

The measured vehicle responses are then fed into the estimation algorithm. An estimate of the (front left) road profile is obtained and latter compared to the excitation imposed by the test rig. The standard tuning ($\mathbf{Q}$ and $\mathbf{R}$) defined in equation (3.50) is employed. A good compromise between the different scalar criteria is sought, and the regularisation coefficient $S = 10^{-7.6}$ is selected empirically after different tries. The sampling frequency used for the measurement and the estimation is 1024Hz. Two different experimental cases are considered, namely a pair of randomly generated road profiles (see section 4.3) and a pair of realistic profiles (see below).

In this experimental setting the real non-linearity of the vehicle dynamics affects the measurement data. Yet, here the wheel is not rotating, which modifies the physics of the road/tyre surface contact. An analysis of the effect of this simplification is discussed in appendix C. Let us just point out here that it does not modify much the low and medium frequency content of the excitation.

Data obtained from a measurement on a vertical test-rig: first dataset

The results corresponding to the first case are displayed in figures D.19 and D.20. The numerical results associated with the estimation are given in table 3.7.

Criterion (direct and indirect)	Value for the true profile	Value for the estimated profile	Relative error
Road roughness	(power in m^3) $\times 10^{-6}$		
Low band ($0.05m^{-1}$-$0.2m^{-1}$)	101.66	87.50	-13.9%
Medium band ($0.2m^{-1}$-$1m^{-1}$)	104.68	88.01	-15.9%
High band ($1m^{-1}$-$5m^{-1}$)	5.56	11.22	101.9%
Damage equivalent amplitude	(use of linear quarter-car model)		
Suspension displacement (m)	0.0046	0.0042	-9.2%
Sprung mass acceleration (m/s^2)	1.31	1.25	-4.7%
Unsprung mass acceleration (m/s^2)	11.27	11.85	5.2%

Table 3.7: Result of the estimation for the data set 1, involving a measurement on a vertical test-rig, in terms of scalar criteria. The considered road profiles are randomly generated. The S parameter is fixed to $S = 10^{-7.6}$.

The estimation method yields a very good description of the evolution of the vertical excitation. The estimation on the first two frequency bands is relatively good. One may notice in figure D.20 that the frequency content drops after approximately $3m^{-1}$, which is due to the dynamic capabilities of the rig (approximatively 50Hz, reached for an assumed vehicle speed of 60km/h and $f = vn = (60/3.6) * 3 \approx 50$). The comparison of both the true and estimated profiles, in terms of DEA of the responses they generate, also yields very good results.

To further illustrate the effect and necessity of regularisation, a comparison between the responses to the true profile and to the estimated profile in terms of unsprung mass acceleration, calculated using the same simple linear model, is shown on figures D.21 and D.22. In the first figure, a regularisation has been enforced ($S = 10^{-7.6}$), whereas in the second it has not ($S = 1$). One can see that the difference between the data (in red) and the response to the estimated profile (in blue), increases with the regularisation. The regularisation has an analogous effect to loosening the constraint of fit to the data. In return, when using the same model, the response to the estimate becomes more representative when regularisation is applied, of the response to the true profile (in black). The difference between the red and black curves on both the PSD and LC plots clearly illustrates the modelling deficiency of the linear model, with respect to the true dynamics of the vehicle. The impact of regularisation can also be analysed by comparing the numerical values in table 3.7 to those of table 3.8.

Criterion (direct and indirect)	Value for the true profile	Value for the estimated profile	Relative error
Road roughness	(power in m^3) $\times 10^{-6}$		
Low band ($0.05m^{-1}$-$0.2m^{-1}$)	101.66	94.30	-7.2%
Medium band ($0.2m^{-1}$-$1m^{-1}$)	104.68	184.10	75.9%
High band ($1m^{-1}$-$5m^{-1}$)	5.56	279.00	4917.7%
Equivalent damage amplitude	(use of linear quarter-car model)		
Suspension displacement (m)	0.0046	0.0048	4.4%
Sprung mass acceleration (m/s^2)	1.31	2.23	70.3%
Unsprung mass acceleration (m/s^2)	11.27	27.72	146.0%

Table 3.8: Result of the estimation for the data set 1, involving a measurement on a vertical test-rig, in terms of scalar criteria. The considered road profile is randomly generated. No significant regularisation is applied, $S = 10^0 = 1$.

It is visibly not appropriate to search for an excitation that maximizes the fit to the measurement data through the linear model, as this excitation will no longer be representative of the true road profile. Indeed, it is important that the estimated road profile induces responses which accurately represent the responses to the true profile, no matter what model is selected.

In logical terms, the 'damage equivalence' observed between both responses when the same linear model is used, is a necessary condition for the estimate to be acceptable (not exactly sufficient as this would require testing the method using vehicle models with an higher fidelity). **Regularisation is clearly needed, as the estimate obtained through the unregularised algorithm does not satisfy this necessary condition (*i.e.* damage equivalence between true and estimated profiles through the linear quarter-car model).**

The effect of the sampling frequency of the data can be studied with this example. It has previously been said on subsection 3.5.2 that the tuning of the filter (only the dynamic part, *i.e.* $\mathbf{Q}$ and S) has to be adapted in order to account for the variation, with sample time dt, in the magnitude of the errors signals and of the random component of the excitation (according to equation (3.26)).

The result of an estimation carried out with different sampling frequencies (using a simple re-sampling from 1024Hz to 204.8Hz) for the measurement data, is given in figure D.23. In one case, the regularisation coefficient has been empirically adapted to the value $S = 10^{-6.2}$ for the sampling frequency of 204.8Hz, instead of $S = 10^{-7.6}$ for 1024Hz. In another case it has not been adapted. It clearly appears that S must be adapted. Once again this operation is done empirically. It represents a tuning step for the algorithm, when the sampling frequency of the input data is given. When the estimation algorithm will be applied in the following chapters, the value 200Hz will be the maximum frequency available for the measurement data. It has been noted that it seems sufficient to adapt the value for S, even if the value for $\mathbf{Q}$ should theoretically be modified also.

Data obtained from a measurement on a vertical test-rig: second dataset

The second experimental case is based on the use of realistic road profiles which correspond to six 300-meter long rough pavement tracks. More precisely, the profile injected by the test rig is not the exact road geometry but a rig-specific signal, obtained through an iterative attempt to recreate the responses of the vehicle that have been measured on the actual tracks. This method called iterative learning control, see [De Cuyper et al., 2003] for example, is frequently applied on validation test rigs so as to find a testing signal which can be easily repeated. This avoids validating vehicles by driving then on thousands of kilometres. In principle this operation also constitutes an inverse problem, but in practice this way of solving the problem can only be applied for relatively short sections, as it is necessary to iterate with a real physical vehicle on the rig, to progressively converge to an acceptable signal. This latter method is not the main concern here and suffices it to say that the injected vertical excitations correspond to relatively realistic excitations.

The vehicle responses are fed into the algorithm and the result of the comparison with the true profile is shown in figures D.24 and D.25. Numerical results for this second measurement-based case are displayed in table 3.9. The results are acceptable, yet it seems that as the high-frequency content within the injected excitation has been smoothed by the iteration procedure, the regularisation carried over from the preceding example, namely $S = 10^{-7.6}$, may be overly strong.

Criterion (direct and indirect)	Value for the true profile	Value for the estimated profile	Relative error
Road roughness	(power in m^3) $\times 10^{-6}$		
Low band ($0.05m^{-1}$-$0.2m^{-1}$)	225.34	166.17	-26.3%
Medium band ($0.2m^{-1}$-$1m^{-1}$)	1013.70	793.39	-21.7%
High band ($1m^{-1}$-$5m^{-1}$)	6.86	18.12	163.2%
Equivalent damage amplitude	(use of linear quarter-car model)		
Suspension displacement (m)	0.0096	0.0075	-21.3%
Sprung mass acceleration (m/s^2)	4.05	3.15	-22.1%
Unsprung mass acceleration (m/s^2)	29.29	24.1	-17.9%

Table 3.9: Result of the estimation for the data set 2, involving a measurement on a vertical test-rig, in terms of scalar criteria. The considered road profile corresponds to a realistic rough paved track. The S parameter is fixed to $S = 10^{-7.6}$.

3.6.4 Sensitivity and limits of the algorithm

Sensitivity of the algorithm to its 'design' parameters

In the previous subsection, results have been proposed for a given design of the estimation algorithm, namely a set of values for tuning parameters and mechanical characteristics. Several experiments are now proposed in order to quantify the sensitivity of the

algorithm to such factors. The objective here is not to carry out an extensive analysis of all possible configurations but rather to identify the main factors impacting the quality of the estimation and to get insights into their potential effects when the method is applied in a practical context. General trends and behaviours are identified and explanations are proposed accordingly.

The majority of the experiments proposed here is performed with measurement data obtained from a linear quarter-car model. Even if this may not be an optimal choice, there is no computer efficient alternative if one considers that the sensitivity that is observed would be fairly similar with a slightly more complicated 2-DOF non-linear model, see appendix B.1.

Randomly generated road profiles (based on a given stochastic model with fixed parameters, see section 4.3) are used to simulate the responses of a 2-DOF linear model. The mechanical characteristics selected for the simulation step (direct problem) do not vary across the whole design of experiments (see reference in table D.3). Conversely, for each estimation of the road profile from given responses (inverse problem), a particular arrangement of values is selected for the mechanical characteristics, namely mass, stiffness and damping, as well as for the tuning parameters, namely $\mathbf{Q}$, $\mathbf{R}$ and S, that are provided to the estimation algorithm. In order to acquire a robust information on this sensitivity, the process is repeated on 30 randomly generated profiles for each arrangement of the tuning parameters and mechanical characteristics.

Sensitivity of the algorithm to its 'design' parameters: tuning factors

First, the different values of the tuning parameters are sequentially modified according to table D.2. For each arrangement (30 estimations), only one parameter is modified at a time, apart from the regularisation coefficient S which takes two values. Interaction effects are not taken into account. In figures D.26, D.27 and D.28, the influence of the tuning on the direct criteria is studied. The tuning parameters are modified sequentially, as indicated in these figures, where sets of 30 estimations are scattered vertically. The arrangement used as a reference is shown in the first position (in red) and described in table D.2. It corresponds to the result of the semi-empirical tuning described in equation (3.50).

The effect of regularisation is studied and its influence on both direct and indirect criteria is shown in figure D.29. As the model used is very simple, the estimate convergences to the real solution when the regularisation diminishes. This has already been noticed in the subsection 3.6.2. Therefore, this analysis of the sensitivity to regularisation is not exploitable for high values of S (low regularisation), as the direct model is identical to the model used for the inversion of the problem. Figure D.29 is rather presented here to analyse the effect of a strong regularisation, involving low values of S.

To sum up, it is seen that the estimation is relatively insensitive to the tuning parameters in $\mathbf{Q}$. In fact this may only be true if their relative values with respect to one

another do not depart significantly. However the estimation is much more sensitive to the parameters in **R** as they directly relate to the confidence in the measurement data and to the capacity of the model to extract relevant information from the latter data. Without much surprise, **the high-frequency component of the excitation is very sensitive to the value of the regularisation parameter** S. Conversely, the low frequency band and the medium frequency band (at least within a reasonable variation range for S) are much less impacted by the choice of S.

Sensitivity of the algorithm to its 'design' parameters: mechanical characteristics

Secondly, the different values of the vehicle's mechanical characteristics are sequentially modified (only for the estimation and not for simulation) according to table D.3. As before, only one parameter is modified at a time, apart from the regularisation coefficient S, and interaction effects are not taken into account. The objective is to emulate a situation where the characteristics of the vehicle are not precisely known, in order to asses the effect that this lack of precision has on the estimate. For the reference arrangement (in red, 30 estimations), the mechanical characteristics provided to the estimation algorithm are the exact characteristics that are used for all simulations. The resulting sensitivity is illustrated on figures D.30, D.31 and D.32, for the different arrangements.

The influence of a deficiency in the knowledge of vehicle characteristics is also illustrated using data generated through the detailed MBS on figure D.33, for both the direct and indirect criteria. In this latter case, only one simulation has been carried out and there is no information on the scatter.

To sum up, the most influential characteristics are the mass of the body (m_s) and the stiffness of the tyre (k_s). The former seems to have more influence on the low and medium frequency content of the estimation. The latter has a large influence on the high frequency content, but also a significant influence across the whole frequency spectrum. The influence of the damping coefficient (c_s) is also significant. The analysis of the sensitivity to the mechanical characteristics is in fact a rather obvious issue if it is viewed from the following standpoint. **Any characteristic that strongly influences the value of the responses of the vehicle is a characteristic that will have a strong impact on the inversion of the problem**, *i.e.* on the obtained estimate of the excitation. Such a parameter has to be as precisely known as possible, in order to get an accurate estimate of the excitation.

Sensitivity to the speed of the vehicle

Let us recall that, the end objective of the proposed algorithm is to identify the road profiles from the measured responses of the vehicle. However, the direct product of the resolution of the inverse problem is the time history of the altitude of the contact point between the road and the tyre or **'road excitation'**. In order to get a spatial description

of the road profile, *i.e.* $u(x)$, it is necessary to match each time instance to its relative longitudinal position x, using the measured speed of the vehicle $v(t)$. Even if this operation is relatively simple and does not represent an issue here, the influence of the vehicle's speed on the quality of the obtained estimate is not insignificant. Indeed, it has a powerful effect on the frequency content of the time excitation $u(t)$ imposed by the road on the vehicle.

For a given spatial frequency content of the road profile $u(x)$, the effect of the vehicle's speed is to modulate the frequency content of the time excitation $u(t)$. The spatial frequency content (in m^{-1}) is mapped on a particular time frequency band (in Hz) depending on the vehicle's speed. For a few speed values, the correspondence between the spatial frequency of the road profile and the time frequency of the induced excitation is given in table 3.10. If one assumes that the frequency band wherein the vehicle shows significant responses roughly lies between 0.2 and 30Hz, then it seems difficult to estimate from these vehicle responses, the content of the road excitation that provokes responses outside of this interval. Indeed, the latter has been filtered out of the responses by the mechanical system. In the previous table, frequency bands that appear fully (in red) or partially (in magenta) out of reach for the estimation, are displayed.

Spatial frequency (m^{-1})	Very low band 0.01 - 0.05	Low band 0.05 - 0.2	Medium band 0.2 - 1	High band 1 - 5	Very high band 5 - 10
Speed (km/h)	Corresponding temporal frequency band in Hz				
10	0.03 - 0.14	0.14 - 0.56	0.56 - 2.78	2.78 - 13.9	13.9 - 27.8
30	0.08 - 0.42	0.42 - 1.67	1.67 - 8.33	8.33 - 41.7	41.7 - 83.3
60	0.17 - 0.83	0.83 - 3.33	3.33 - 16.7	16.7 - 83.3	83.3 - 167
90	0.25 - 1.25	1.25 - 5	5 - 25	25 - 125	125 - 250
110	0.31 - 1.53	1.53 - 6.11	6.11 - 30.6	30.6 - 152	152 - 306
130	0.36 - 1.81	1.81 - 7.22	7.22 - 36.11	36.11 - 181	181 - 361

Table 3.10: Correspondence between the spatial frequency of the road profile and the time frequency of the excitation, for several vehicle's speeds.

To further illustrate this issue, a given road profile is covered at different speeds through simulation (linear quarter-car model), thereby generating different sets of measurement data. Estimations of the road profile are carried out using each dataset and the comparison of the resulting estimates is displayed in figure D.34 and in terms of scalar criteria in table D.4.

Moreover, 30 repeated calculations for each speed value and for different randomly generated road profiles are carried out to get a more robust information on the influence of speed. The results of these estimations are plotted in figure D.35. Once again the analysis of this last figure has to be done carefully as the estimate converges to the true solution when no regularisation is imposed. The reality seemingly lies between the two extremes involving either no regularisation ($S = 1$) or a regularisation ($S = 10^{-6}$).

It clearly appears that depending on the speed of the vehicle a part of the spatial frequency content may be lost or at least underestimated. Indeed, some significant spatial frequency content of the road profile $u(x)$ may be mapped on either a very low time frequency band (say below 0.2Hz) or a very high time frequency band (say above 30Hz) within the excitation $u(t)$. As the latter does not produce significant responses on the vehicle, this induces a loss of information. Such information can never be extracted from the said responses. Consequently, **both ends of the spatial frequency spectrum of the road profile $u(x)$ can be underestimated if the speed of the vehicle is either too low or too high**. The spatial frequency content perceived in the estimate is thus quite strongly dependent on the speed that the vehicle had when crossing over the road profile.

Extension to more complex and/or non-linear models

The use of more complex models has been considered. It is presented here in view of discussing their relevance. The complexity of the model can be thought either in terms of number of degrees of freedom or in terms of non-linear phenomena and behaviours within the vehicle model.

First, the estimation algorithm has been implemented for a bicycle and a full vehicle model, see details in appendix B. One may logically assume, that if the dynamics of the vehicle body, *e.g.* roll and pitch movements, is better understood, then the estimation can yield better results. A calculation has been carried out with data originating from the four-post test rig measurement set-up considered in the previous subsection, and where the responses have been measured everywhere on the vehicle. The results of the comparisons (for the front left profile) between the estimates obtained using the linear quarter-car, bicycle and full-car model is shown in figure D.36 and scalar criteria are given in table D.5.

It is not easy to detect a significant improvement of the quality of the estimation when a more complex linear model is used. The difficulty that arises when a more complicated model is considered is that, the latter implies more characterisations of the vehicle characteristics, *e.g.* the inertia of the body, as well as the selection of new tuning parameters. It also implies that, the more degrees of freedom in the state vector, the more information has to be acquired through sensors in order for the system to remain observable. Even if the quality of the estimate can be improved in theory, the consideration of a more complex model for the estimation of the road profile is not attempted in the rest of this manuscript.

Secondly, the data obtained through the detailed MBS in subsection 3.6.2 has been used to test a non-linear algorithm. The latter is based on the theory of Extended Kalman Filtering (EKF), where the propagation equation of the state conditional expectation is a non-linear ordinary differential equation (ODE), and the propagation of the covariance as well as the correcting step are based on locally linearised (around the current state) propagation and observation matrices. More details can be found in [Maybeck, 1979]. The results are exposed in figure D.37 and in table D.6.

It appears that the influence on the estimate, through the different criteria, is noticeable but yet quite limited. In contrast the computation time increases dramatically from less than one second for the linear Kalman filter to more than $3000s$ for the stepwise linearised filtering (EKF) and for a road profile of $500m$ in the present example.

Here the non linear algorithm does not seem to be of great use based on the presented calculation. Yet this should not be overly generalized since the non-linear model proposed to invert the direct problem here, only takes into account the non-linearity of the suspension system. The interpretation on the attractiveness of EKF could possibly be different if a more representative non-linear model was considered, especially improving the knowledge on the tyre dynamics. Nonetheless with such a non-linear algorithm, the computation time is a serious drawback when the objective is to process large volumes of measurement data.

3.6.5 Discussion on the applicability of the algorithm

Numerical results in the form of the selected direct and indirect criteria, as well as different plots, have been presented in subsection 3.6.2 and 3.6.3 and in appendix D, with the aim of formulating a judgement on the quality of the estimation algorithm. Multiple issues have been discussed, ranging from the pre-processing of the data to the limits of the experimental validation framework. In view of all the experimental results, **it appears difficult to rule on the quality of the method as a whole since different degrees of precision can be noticed, either when the origin of the measurement data changes or when comparing one criterion to another.** This is clearly an engineering problem more than a theoretical problem.

In this context, let us summarize general trends, highlight important remarks and points to eventual limits of the method, while adopting an engineering standpoint. Let us also keep in mind the framework in which the method is to be applied and how its outputs are to be used, as previously discussed when introducing the testing criteria in subsection 3.6.1.

Validity of the method

For a start, let us recall that the experiment involving a 2-DOF non-linear model is useful to study trends and sensitivities but may not be very representative as a validating case. The experiments based either on the detailed multi-body simulation (MBS) or on the measurements on a vertical test-rig offer a much more robust ground for the validation of the estimation algorithm.

Overall, both for randomly generated profiles or realistic ones, the estimation method provides a good description of the spatial evolution of the road profile from only a few response signals on the vehicle. Based on visual comparisons, it is clearly possible to identify the main characteristics of the road profile, namely distinguish between sections

with different roughness levels or identify transient patterns' locations and shapes. The analysis of direct criteria shows that the method provides an acceptable assessment of both the low and medium (the upper bound of the medium band may have to be somewhat lowered) spatial frequency content of the sought road profile.

The high spatial frequency content is generally unattainable because of the action of different phenomena, among which the regularisation of the inverse problem is a strong contributor. The influence of vehicle speed, the natural tendency of the tyre to filter out high spatial frequencies or the possible non-permanent contact between the tyre and the road may also explain some of the loss in the high spatial frequency band. Eventually, when a simple 2-DOF linear model is selected, **the comparison of the responses to both the true and estimated profiles indicates that those responses correspond to relatively similar damage equivalent amplitudes (DEA). This is a necessary condition for the method to be valid**, however, conceptually it is not a sufficient condition, as the comparison could be poorer with a finer modelling of the vehicle dynamics.

Essentially, it is proved that **the proposed road estimation method is a valuable tool for the statistical analysis of road roughness variability** (ultimately, as a building block for the statistical analysis of road-induced fatigue loads). **It yields a good description of the road profile and can processes several kilometres of data through a simple model in a matter of a few seconds.**

The experimental results shown in the present chapter show that the road estimation algorithm yields estimates that are representative of real road profiles and that this algorithm can be applied in the next chapters (4 and 5). A certain attention is nonetheless given to its identified limitations such as the loss in high spatial frequency content or the influence of speed for example. Further precisions are given in the next chapter, when the estimation method is applied on extensive datasets. In this latter case, the defined tuning is the same as in equation (3.50) and the S parameter is fixed to $S = 10^{-6}$ for a sampling frequency of $200Hz$.

Limitations and conceptual difficulties

While the estimation is fast, inexpensive and a valuable tool for statistical analysis, it nevertheless presents some limitations that have to be pointed out.

On the one hand, the issue of tuning somewhat specific to the selected algorithm, should not be seen as a difficulty. It rather represents an opportunity to obtain valuable (and realistic) results from a simple model of the vehicle. It should not be forgotten that the interesting feature of the Kalman-based algorithm is its ability to balance the contradictory requirements of modelling complexity and subsequent quality of the estimate versus fast computation, as mentioned in section 3.2.4.

Once a model is selected and a measurement set-up is defined, an adequate tuning can be identified. Additionally, there is no reason for the tuning to vary significantly from one

measurement vehicle to another if the measurement set-up is similar. Nonetheless, **the impact of the tuning on the results is very strong and the tuning operation should therefore be handled carefully.**

On the other hand, as the estimation is based on the resolution of an inverse problem, the method is affected by the following conceptual limitations. **Any alternative technique or improvement on the proposed algorithm would be identically affected by such limitations.**

First, **the obtained estimate will be dependent on the knowledge of the dynamics of the mechanical system that has provoked the measured responses**. Any mechanical characteristic that strongly affects the response of the system will also have a strong influence on the estimation. The issues of the selection of a model and of the identification of its mechanical characteristics are coupled in relation to this remark. There is a **compromise to be found between the model complexity and the quality of the obtained estimate**. Indeed, a more complex model will require additional characterisations (such as roll or pitch related inertias), which generate additional sources of errors and make the issue of tuning more complex. It will also require information from more sensors in order for the system to remain observable. In the context of this work, the selection of a linear quarter-car model is deemed sufficient. While they theoretically offer an opportunity to increase the fidelity of the method, complex models also involve a higher investment in the characterisation and instrumentation of the vehicle employed for the measurement. As a rule it is more beneficial to first improve the knowledge on high-impact mechanical characteristic (tyre stiffness for example) than to consider very complex models. This also means that if certain characteristics are difficult to estimate precisely, it may be a waste of effort to look for unnecessarily complex models.

Moreover, as the method is based on measured responses, the content of such responses is inherited and does not necessarily represent the best available information for the identification of the road profile covered by the vehicle. The influence of the speed of the vehicle is a clear example of this remark. It is a serious impediment on the method for which there is no countermeasure to be applied. Indeed, if the speed of the vehicle is such that a significant part of the spatial frequency content of the road profile is mapped on a time frequency band of the excitation that does not generate a significant response on the vehicle, then **regardless of the treatment applied on the data, the resolution of the inverse problem is not likely to extract information on such spatial frequency band**. This is a clear limitation to the characterisation of road profiles from a vehicle's responses. Indeed, there needs to be a significant response of the vehicle for the estimation to be carried out and within certain spatial frequency ranges, this is conditioned on the speed of the vehicle.

Finally, let us recall that, the estimation method proposed in the present chapter is designed as an inexpensive data processing algorithm to convert measurement data on vehicle responses into valuable information on road profiles. It is by no means the most straightforward method to characterise road profiles (they could be directly measured), as it suffers from the aforementioned limitations. This is why it may seem inappropriate

to build a complex model of a mechanical system which is clearly not primarily made for road measuring.

3.7 Synthesis and conclusion

A short overview on the different approaches to the characterisation of road roughness has been given. Here, a so-called indirect method is selected as it can be used to extract road related information from existing (large) data sets. The latter have been acquired through load characterisation campaigns that did not include specific instrumentation, other than acceleration and displacement sensors. The proposed method seeks to estimate the road profiles covered by a given vehicle from the dynamic responses that those profiles caused on the vehicle.

Searching for the excitation acting on the vehicle given its dynamic responses constitutes an inverse problem. With such problems it has been noted that seeking the best solution in the least squares sense is generally not an appropriate way to obtain a good candidate for the estimated excitation. Indeed, because of imprecise knowledge on the data or on the mechanical behaviour of the system, inverse problems have a tendency to behave chaotically and yield results that may no longer be physically representative. A so-called regularisation of the problem is often operated through the input of some additional *a priori* knowledge either on the excitation to be estimated or on the errors related to the model describing the dynamics of the vehicle. The strength of the proposed estimation method based on linear Kalman filtering theory lies in the transition from the deterministic functional analysis framework to a stochastic based framework, where such *a priori* knowledge can be efficiently introduced. The selected method is well adapted for the solving of the considered inverse problem.

The Kalman-based estimation algorithm constitutes a fast and a very convenient data processing algorithm when it comes to combining the information that originates from different measurement sources while considering *a priori* knowledge on their precision or on the ability of the chosen model to exploit them. In the present case of input estimation, the searched excitation is added to the state vector of the system and estimated simultaneously, thus making the algorithm an augmented Kalman filter. The method provides an interesting compromise when the objective is to **rapidly process large volumes of data through a relatively simple model, in view of extracting extensive statistical information on road roughness, while compensating for modelling deficiencies and thus retain an acceptable precision in an operational context.**

Practically, the estimation algorithm is here based on a linear 2-degrees of freedom (DOF) model (or quarter-car model) and it processes the measured **suspension displacement** as well as the **unsprung and sprung mass accelerations**. It yields an estimate of the time-varying boundary constraint applied on the base of the related tyre. The recorded speed of the vehicle is then used to match each time instance with its longitudinal position, thereby providing a spatial description of the road profile. A semi-empirical

approach, based on the study of the potential errors between the 2-DOF model and a detailed multi-body model (also embedding a detailed tyre model), has been proposed as a means to operate the tuning of the algorithm and account for modelling errors. The regularisation parameter, which essentially controls the anticipated smoothness of the solution, is kept as a purely empirical parameter that can be adjusted using a calibration case in order to get the best possible estimate, for a given association constituted of a selected model and measurement set-up.

The results of the different experimentations performed within this chapter show that **the estimation method provides a good description of the spatial evolution of the road profile, rapidly and from only a few response signals on the vehicle**. It is able to identify the main characteristics of the road profile, namely distinguish between sections with different roughness levels or identify transient patterns' locations and shapes. The experimentations show that the method provides an acceptable and objective assessment of both the low and medium spatial frequency content of the sought road profile. The high spatial frequency content is generally unattainable, either because of the necessary regularisation of the problem, of the excessive speed of the vehicle or because the tyre has a tendency to filter out the high spatial frequency content. Furthermore, the comparison of the responses to both the true and estimated profile through the same linear model, indicates that those responses correspond to relatively similar loads, in terms of damage equivalence (DEA). The estimates obtained from the algorithm are thus fairly representative images of the true road profiles.

It is important to note that the proposed tuning of the filter leads to acceptable results. The tuning operation is of great significance as it very strongly impacts the results. Nonetheless, it does not represent a serious difficulty for the use of the proposed method as it can be fixed once and for all, *i.e.* for a given model/measurement set-up, using an appropriate calibration case.

On the other hand, as an indirect approach, the estimation method is **unavoidably bound to some limitations**. First, the obtained estimate will always **depend on the knowledge one possesses on the dynamics of the vehicle**. Any mechanical characteristic that strongly impacts the responses of the vehicle will obviously represent a parameter to which the estimation is highly sensitive. The mass of the body, dampness in the suspension and the stiffness of the tyre are good examples of impacting factors. A compromise should be reached in terms of complexity and fidelity of the model against the quality of the estimate. Indeed, complicated models may improve the estimation but they are also likely to require more characterisations (and related sources of errors) and necessarily require information from more sensors if the system is to remain observable, thus increasing the cost of the method. All potential improvements of the method will necessarily be related to this compromise.

Secondly, **the method is quite sensitive to the speed of the vehicle**. Indeed, with different vehicle speeds, the processing of the responses corresponding to the same road surface may yield significantly different results. Depending on vehicle speed, a significant content of the road profile within a given spatial frequency band may induce a time

excitation which no longer produces significant responses on the vehicle due to the natural filtering of the mechanical system. It is then impossible to estimate the content of such a spatial frequency band from the responses of the vehicle. It will potentially lead to underestimate either the low part or the high part of the spatial spectrum, depending on the speed of the vehicle. As vehicle speed is inherited from the measurements, there is no possibility for the proposed data processing algorithm to circumvent this issue. One appropriate approach to handle the problem is to focus the analysis on the bandwidth of the estimation which is not susceptible to an underestimation of the content.

To sum up, it is proved that the proposed estimation method is **a valuable tool to extract accurate and quantitative road-related statistical information** from vehicle responses, even if the model used for the dynamics of the vehicle is quite simplistic and if the method itself is necessarily affected by some limitations, due to its indirect nature. Additionally, it is fast and inexpensive and thus **demonstrates great exploratory potential in the statistical sense**.

In the framework of the current research work, the estimation method allows us to extract valuable information on road roughness at no cost from existing data sets gathered by Renault through load measurement campaigns. Here, it is the only available source of extensive statistical information on road roughness. The data processing algorithm is practically applied in the following chapter.

In terms of opportunity, the proposed method paves the way for considering cheap and extensive road characterisation campaigns on thousands of kilometres, requiring only very little and not specific instrumentation. Also, multiple sensors are becoming increasingly present on commercial vehicles, for example due to active suspension systems. This allows us to consider a very extensive source of statistical and highly customer-related information if large volumes of data can be collected on commercial vehicles. In this latter context, the proposed estimation method represents an inexpensive and efficient data processing algorithm able to add value to mass collection of response-based data.

To remember

- The presented road estimation algorithm seeks the most likely road excitation, given the responses that have been observed on the vehicle and given the knowledge of its dynamic behaviour.
- The augmented Kalman filter is a fast algorithm which efficiently combines the information originating from different sensors while accounting for the capacity of the model to exploit them.
- The suspension displacement, sprung acceleration, unsprung acceleration and vehicle speed are used to obtain an estimate of the road profile.
- A simple linear quarter-car model is used for the estimation. Non-linear models would strongly increase the cost of the estimation.
- The proposed road estimation algorithm provides a good description of the spatial evolution of the road profile, *e.g.* smooth sections, rough sections, positions and forms of transient patterns such as speed bumps or pot-holes, etc.
- It can extract valuable information rapidly and at no cost from existing large datasets acquired through load measurement campaigns.
- Even if there are clear limitations in terms of the attainable precision, the estimation algorithm demonstrates great exploratory potential, in the statistical sense.
- It paves the way for extensive analyses of road roughness variability, with no need for expensive measuring equipment.
- The quality of the results depends on three items namely, the tuning of the filter, the knowledge of the vehicle's characteristics and the speed on the road section. Contrary to the first two items, the influence of speed cannot be diminished with better knowledge or a more precise calibration.

Chapter 4

Stochastic modelling of road and speed profiles

Contents

4.1 Introduction **85**
4.2 Principal elements of stochastic process theory **86**
4.2.1 Randomness, random variables and stochastic processes 86
4.2.2 Spectral representation of stochastic processes 88
4.2.3 Identification of a stationary process and generation of trajectories . . . 90
4.3 Stochastic modelling of road profiles **92**
4.3.1 Road roughness, road profiles and vertical excitations 92
4.3.2 Stochastic models for road profiles in literature 93
4.3.3 Proposed candidate model structures and parameter identification . . . 97
4.4 Stochastic modelling of speed profiles **104**
4.4.1 Speed of the vehicle and its evolution 104
4.4.2 Stochastic models for speed profiles 106
4.4.3 Proposed candidate model structures and parameter identification . . . 107
4.5 Exploitation of available data: testing of the considered models . . **113**
4.5.1 Example of data acquisition from load measurement campaigns 114
4.5.2 Statistical characteristics of the estimated road profiles 117
4.5.3 Selection of representative stochastic models for road and speed 120
4.6 Synthesis and conclusion **126**

The word 'chance' then expresses only our ignorance of the causes of the phenomena that we observe to occur and to succeed one another in no apparent order. Probability is relative in part to this ignorance, and in part to our knowledge.

Pierre-Simon de Laplace

4.1 Introduction

The time history of the fatigue loads acting on many components of a vehicle, throughout the life of the latter, is largely determined by the influence of two factors, namely road roughness and vehicle speed. Since both factors are continuously varying random quantities, they have to be described using stochastic processes. Identifying and selecting a tractable mathematical representation, or stochastic model, for the continuous evolution of those factors, serve two purposes. First, it allows us to compare and classify road or speed profiles with different 'characteristics', thus providing an objective tool to perform statistical analyses. Secondly, and more importantly in the context of the present research work, a stochastic model can be used to **generate random realisations of road and speed profiles**, in view of carrying out vehicle dynamic simulations and subsequently work on the variability of road-induced fatigue loads.

This chapter proposes a thorough study of the evolution, or statistical variability, of road roughness and vehicle speed, both previously denoted as influential factors. Different stochastic models are considered and the selection of a particular model for both factors is performed according to relevant criteria. First, the selected model should be statistically representative, in the sense that a sample of realisations generated from the model should posses the same 'characteristics' that could have been measured on real profiles. Also and since the end purpose is to study road-induced loads, the proposed models should produce responses on the vehicle that are representative of the responses provoked by real profiles. **The selection and validation of adequate models for road roughness and vehicle speed is the core objective of this chapter**.

The road estimation algorithm presented in the previous chapter is used to process the data acquired through load measurement campaigns into statistical information about the variability of the road excitation. Conversely, speed profiles are directly measured. Based on the analysis of existing literature on the subject and on the available data on road and speed profiles, several candidate model structures are proposed. Statistical criteria, as well as criteria linked to the responses on the vehicle, are defined and employed to **test the validity of the candidate models against the data provided by the measurement campaigns**. The study highlights the various difficulties related to the selection of a statistically representative model.

The outline of the present chapter is as follows. Section 4.2, briefly reminds theoretical basics of stochastic process representation. The mathematical tools which permit a quantified description of the previously mentioned 'characteristics' of a continuously varying random quantity are also introduced. Road roughness is precisely defined in section 4.3 and the estimation algorithm presented in the previous chapter is applied on existing data sets (from load measurement campaigns) in order to constitute a database of road profiles. Then, stochastic road models existing in literature are discussed in the context of the present application and several candidate model structures are introduced. Subsequently, the evolution of vehicle speed is studied in section 4.4 and candidate models are also proposed. An extensive study based on the collected database of profiles is carried out

in section 4.5. The different statistical and response-based criteria are used to compare real profiles and randomly generated profiles, thus assessing the capacity of the different model candidates to be a representative description of the statistical variability of road and speed factors. A concise summary and emphasize on the key points presented in the chapter are given in section 4.6.

4.2 Principal elements of stochastic process theory

Let us open this chapter by introducing some notions from the domain of stochastic process theory and briefly describing the associated mathematical framework. The objective of this section is not to provide a comprehensive description in terms of probability theory, such may be found for example in [Parzen, 1962, Papoulis, 1991], but rather to give an outlook on the mathematical tools that are used throughout the present manuscript.

4.2.1 Randomness, random variables and stochastic processes

Randomness is a complex concept which can be associated to multiple interpretations, see *e.g.* [Papoulis, 1991]. Throughout this manuscript, randomness is viewed as the inability, despite the best knowledge at disposal, to predict the exact outcome of an experiment. In a nutshell, probability theory may be seen as a set of tools defined in a consistent mathematical framework whose practical purpose is to get a quantitative description of the scatter that can be expected, when the experiment is repeated a large number of times.

Random variables

Let us consider the sample set Ω, as the set of all possible outcomes of an experiment. Formally, a random variable X is a function that assigns a value to each outcome $\omega \in \Omega$, $X : \omega \mapsto X(\omega)$, which for physical quantities is generally a real value ($X(\omega) \in \mathbb{R}$). A quantitative description of the expected variability (or scatter) of the considered quantity is embodied by the so-called distribution of the associated random variable. The distribution function $F_X(x)$, or Cumulative Density Function (CDF), of the random variable X is defined through the probability that a particular realisation (outcome) of this random variable will not exceed a given threshold x:

$$\text{Prob}(X \leq x) = F_X(x) = \int_{-\infty}^{x} f_X(u)du \tag{4.1}$$

where $f_X : x \in \mathbb{R} \mapsto f_X(x) \in \mathbb{R}$ is the Probability Density Function (PDF), such that $p(x \leq X \leq x + dx) = f_X(x)dx$. Hence, **the randomness of a given physical quantity is perfectly 'characterised' if its PDF is known**.

The concept of density functions may be extended to sets of random variables. The joint density function f_{XY} of two random variables X and Y is defined through:

$$\text{Prob}(x \leq X \leq x + dx \cap y \leq Y \leq y + dy) = f_{XY}(x, y)dxdy \tag{4.2}$$

From an engineering standpoint, these density functions provide a measure of the probability that a physical quantity of interest (or a set of quantities) will assume values (or a set of values) in a given interval.

Random processes

When the quantity to study is not a scalar value in $\mathbb{R}$ or a set of values in $\mathbb{R}^d$ but a continuously varying parameter, for example an electrical tension varying in time, the concept of random variables has to be extended to the domain of stochastic processes. According to [Parzen, 1962], a stochastic process is a family of random variables $\{X(t)\}$ indexed by a parameter t varying in an index set T. If T is a continuous set, such as $\mathbb{R}$, the stochastic process $\{X(t)\}$ is constituted by an infinite and non-numerable set of random variables. A stochastic process may also be seen as a set of random functions $\{X(t, \omega)\}$ such that:

$$X : (t, \omega) \mapsto X(t, \omega) \text{ with } \omega \in \Omega, t \in T \tag{4.3}$$

With such a definition, for a given $\omega_0 \in \Omega$, $X(t, \omega_0)$ is a continuous function of t, which is a realisation of the process also called trajectory. For a fixed $t_0 \in T$, $X(t_0, \omega)$, generally noted X_{t_0}, is a random variable for which $X_{t_0}(\omega_0)$ is a realisation (here scalar).

According to [Papoulis, 1991], $\{X(t)\}$ is fully characterised, in the probabilistic sense, if for all subset $\{X_{t_1}, ...X_{t_n}\}$, and for all $n \in \mathbb{N}$, the joint CDF (or equivalently the joint PDF):

$$F_{X_{t_1}...X_{t_n}}(x_1, ..., x_n) = \text{Prob}(X_{t_1} \leq x_1 \cap ... \cap X_{t_n} \leq x_n) \tag{4.4}$$

is known. This description of such a complex function, for all subsets $\{X_{t_1}, ...X_{t_n}\}$, is seldom available, except in specific cases. Often, it is very difficult to make a practical use of the tools of stochastic process theory if the considered stochastic process does not exhibit additional features. For example, if the process is stationary, *i.e.* if its statistical properties do not change along the index set (usually time), then the issue of the characterisation of the process can be greatly simplified.

Stationary processes

A stochastic process $\{X(t)\}$ is said to be strictly stationary if any translation along the index set T leaves the joint distributions unchanged, which may be translated into the

following proposition. For any $k \in \mathbb{R}$ and any $n \in \mathbb{N}$:

$$f_{X_{t_1}...X_{t_n}}(x_1, ..., x_n) = f_{X_{t_1+k}...X_{t_n+k}}(x_1, ..., x_n) \tag{4.5}$$

Strict stationarity is quite restrictive and it is often sufficient to consider processes that are stationary up to the order 2. A stochastic process $\{X(t)\}$ is said to be stationary up to the order 2, or wide-sense stationary, if its statistical moments up to the order 2, are insensitive to a translation along the index set T. This may be written as follows:

$$E[X_{t_1}^p X_{t_2}^q] = E[X_{t_1+k}^p X_{t_2+k}^q] \tag{4.6}$$

for any $k \in \mathbb{R}$, any $(t_1, t_2) \in T^2$ and any $(p, q) \in \mathbb{N}^2$ such that $p + q \leq 2$. Using simple algebra and equation (4.6), it can be shown that in this case, the covariance between any two random variable X_t and X_s only depends on the distance between the latter, namely $|t - s|$.

In this case, it seems much easier to build a mathematical description of a stationary process through the analysis of what may be thought of as its 'correlation structure' (*i.e.* the correlation between any two points) rather than directly proposing a model for the joint density function in equation (4.4), which is impractical.

4.2.2 Spectral representation of stochastic processes

Fourier analysis of deterministic functions can be adapted for the study of stationary stochastic processes. Indeed, if a stochastic process $\{X(t)\}$ is seen as a family of functions, according to the definition (4.3), then Fourier analysis can be applied on each trajectory of the process.

Fourier-based representation of deterministic functions

Let x be an element of the Hilbert space of square integrable functions on a given interval $[-T, T] \subset \mathbb{R}$, denoted $L^2([-T, T])$ and x_T a restriction of x to the interval $[-T, T]$ (*i.e.* $x(t)$ is null outside of the interval $[-T, T]$). The function $x_T : t \mapsto x_T(t)$ can be expressed on a frequency-based basis, *i.e.* as the sum (infinite and non-numerable) of harmonic components, using the so-called Fourier Transform (FT):

$$x_T(t) = \int_{-\infty}^{\infty} \hat{x}_T(f) e^{2j\pi ft} df \tag{4.7}$$

where $\hat{x}_T(f)$ is the FT of $x_T(t)$. In particular for discrete signals, the time signal $x(t)$ and its FT $\hat{x}(f)$, generally obtained through a Fast Fourier Transform algorithm (FFT),

contain rigorously the same information. If one defines the Power Spectral Density (PSD), see *e.g.* [Priestley, 1981] for the rigorous mathematical framework, as:

$$h(f) = \lim_{T\to\infty} \left(\frac{|\hat{x}_T(f)|^2}{2T} \right) \tag{4.8}$$

The quantity $h(f)df$ may be interpreted as the contribution (a 'density' of power) of the frequency components between f and $f + df$ to the overall power of the signal, here deterministic.

Spectral representation of stationary processes

In a stochastic framework, if $x(t)$ represents one trajectory of the stochastic process $\{X(t)\}$, then $h(f)$ is also a random function. The interest of spectral analysis of stationary stochastic processes becomes apparent when the PSD $h(f)$ is averaged over all realisations. Let us then denote $S(f)$, the PSD of the stochastic process:

$$S(f) = \lim_{T\to\infty} E\left[\frac{|\hat{X}_T(f)|^2}{2T} \right] \tag{4.9}$$

The so-called 'frequency content' of the stochastic process is intimately tied to what may be thought of as its 'correlation structure'. In fact it may be shown, see [Priestley, 1981, Parzen, 1962], that according to the Wiener-Khintchine theorem, the Power Spectral Density (PSD) of a stationary stochastic process $\{X(t)\}$ is the Fourier transform of its autocovariance function:

$$S(f) = \int_{-\infty}^{\infty} R(\tau) e^{-2j\pi f\tau} d\tau \tag{4.10}$$

where $R(\tau) = E[X(t)X(t+\tau)]$ is the autocovariance function of $\{X(t)\}$, noting that, for the sake of simplicity, the process has generally a null mean (or is transformed accordingly with no loss of generality). $S(f)df$ represents the average contribution from the frequencies comprised between f and $f + df$ to the overall power of the signal. Heuristically, if the correlation between two close points ($\tau = |t - s|$ small) is strong, then realisations $x(t)$ of the process will, on average, appear quite smooth, which is equivalent to say that the content of $x(t)$ is rather concentrated on the low frequency part of the spectrum. Conversely, with a weak correlation between close points, $x(t)$ is visibly more 'irregular', and the high frequency part of the spectrum is stronger. This is a very simplistic, yet very illustrative, view of the relationship between the spectral content and the correlation structure of the process.

From the engineering standpoint, whereas observed realisations $x(t)$ may seem very different from one another, the physics of the phenomena studied in practice is likely

to lead to different PSD realisations $h(f)$ that share similar features. Simply put, it is much more interesting to carry out a statistical analysis in the frequency domain than in the time (or spatial) domain. **In a sense, the PSD of a stationary stochastic process $S(f)$ "embodies a statistical description of the correlation structure of such a process".** In fact, it may be shown that for certain types of stationary process, namely Gaussian processes, the knowledge of the autocovariance function or equivalently its Fourier transform, namely the PSD $S(f)$, completely 'characterises' the stochastic process. Hence, for such processes, the characterisation resumes to an estimation problem, wherein the PSD is the main quantity of interest.

Spectral representations for non-stationary processes

For the sake of simplicity spectral representations have been introduced here with the particular example of Fourier bases. Let us point out that even if the expansion of the correlation structure on a basis made of harmonic (stationary by nature) components implies that such a correlation structure is stationary, so-called spectral decompositions are not strictly limited to Fourier basis and stationary processes.

Indeed, the autocovariance function $R(t,s) = E[X(t)X(s)]$ may be decomposed using non-stationary bases, through a different orthogonal expansion, see *e.g.* [Priestley, 1981, Ghanem and Spanos, 2003]. Karhunen-Loeve Decomposition (KLD) is a particular example of such expansions, see [Ghanem and Spanos, 2003] for details, where the basis of the expansion is directly composed of the eigenvectors of the autocovariance function $R(t,s)$. The coordinates on this latter basis are random. Wavelet bases can also be considered.

4.2.3 Identification of a stationary process and generation of trajectories

Spectral estimation

Let us consider here Gaussian processes. A stochastic process $\{X(t)\}$ is said to be Gaussian if any set $\{X_{t_1}, ...X_{t_n}\}$ has a joint distribution equal to a multi-normal distribution. **A stationary Gaussian process is completely determined if its statistical moments are known up to the order two**, see equation (4.6). For lack of better information on higher-order moments, the choice of the Gaussian process is generally the most reasonable and the most generic, see *e.g.* [Parzen, 1962, Priestley, 1981] for discussions on this point. Consequently in that framework, identifying a model for the process is equivalent to obtaining an estimate of its PSD (second-order moment).

There exists various method to obtain a spectral estimate (PSD) from a given trajectory. The most straightforward method makes use of the so-called periodogram I, which

for discrete signals in practical cases may be written:

$$I(f) = \frac{dt}{N} \left| \sum_{k=0}^{N-1} x_k e^{-2j\pi kf} \right|^2 \tag{4.11}$$

where $(x_k)_{k=0,\ldots,N-1}$ is the discrete trajectory with sample time dt and $f \in [-1/2dt, 1/2dt]$. In practice it is calculated through an FFT algorithm. This estimator is seldom used as such since it suffers from issues such as spectral leakage or non-consistency (its variance increases as N increases). To attenuate the former, a windowing is applied. To limit the non-consistency, the signal is generally sectioned and the average over different and potentially overlapping sections is calculated. This latter approach is known as Welch's estimation and as been applied to all spectral estimations within this manuscript, along with Hanning windowing. Detailed discussions about spectral estimation may be found in [Priestley, 1981].

Generation of random realisations from a stationary Gaussian process

The use of a frequency-based description represents a convenient framework for the generation of realisations (trajectories) from a given stationary Gaussian process. In [Shinozuka and Jan, 1972], trajectories are generated through a discrete series of cosine functions, using an equation of the following form:

$$x(t) = \lambda \sum_{i=1}^{N} \sqrt{S(f_i)} \cos(f_i t + \phi_i) \tag{4.12}$$

where $\lambda \in \mathbb{R}$, $(S(f_i))_{i=1,\ldots,N}$ are read from the target PSD at discrete instances and $(\phi_i)_{i=1,\ldots,N} \in [0, 2\pi]^N$ is a set of random phases angles drawn from a uniform distribution.

Another technique for the generation of trajectories is to view the considered process as the output of a linear filter in which a perfectly uncorrelated signal (white noise) is injected. This technique is often described, see *e.g.* [Priestley, 1981, Papoulis, 1991, Maybeck, 1979], as a generation based on 'shaping filters'. The linear filtering relation is:

$$x(t) = \int_{-\infty}^{\infty} \nu(t-\tau) g(\tau) d\tau \tag{4.13}$$

where $\nu(\tau)$ is an input signal for the filter, $g(\tau)$ is the impulse response of the filter and τ is a dummy variable. Using the linearity of equation (4.13) and of the Fourier transform, the following relation between the PSD of the input and output signals may be derived:

$$h_x(f) = |\Gamma(f)|^2 h_\nu(f) \tag{4.14}$$

where $h_x(f)$ is the PSD of $x(t)$, $h_\nu(f)$ is the PSD of $\nu(t)$ and $\Gamma(f)$ is the Frequency Response Function (FRF) of the filter, *i.e.* the Fourier transform of $g(\tau)$. If one takes ν as a perfectly uncorrelated signal (white noise), *i.e.* $E[\nu_t \nu_s] = \sigma_\nu^2 \delta_{t,s}$, $\forall (t,s) \in \mathbb{R}^2$, where $\sigma_\nu \in \mathbb{R}$ is a constant, then $h_\nu(f)$ does not depend on the frequency, *i.e.* $h_\nu(f) = \lambda \in \mathbb{R}$. The FRF can then be chosen in order for the filter to produce the target PSD, namely $S(f)$, which is equivalent to verify:

$$|\Gamma(f)|^2 = \frac{S(f)}{\lambda} \tag{4.15}$$

The filter, through its FRF, imprints the desired correlation structure on the input white noise. This last generation technique is used throughout the manuscript. Also it is possible to use an input white noise with non-stationary properties, *e.g.* a non-constant variance, thus generating a piecewise-stationary process with no discontinuities. This last feature will be used to create piecewise-stationary processes within this chapter.

4.3 Stochastic modelling of road profiles

4.3.1 Road roughness, road profiles and vertical excitations

The following definition of road roughness is given by [Sayers et al., 1986]. Road roughness is "the variation in [road] surface elevation that induces vibration in traversing vehicles". The same reference adds that "by causing vehicle vibrations, [road] roughness has a direct influence on vehicle wear, ride comfort and safety". Consequently, the issue of the characterisation of road roughness appears in various domains, *e.g.*, maintenance of road networks, reduction of safety risks, design of suspension systems adapted to comfort requirements, and so on.

In the present context, the variation in the geometry of road surfaces, or road roughness, indeed constitutes an 'influential factor' (as defined in the introduction chapter 1) with respect to the vertical excitations imposed on the vehicle. Let us point out that, even if road roughness may also influence the longitudinal and lateral efforts applied on the tyres, the present study is exclusively focused on vertical excitations, see 2.3.1. There is an obvious link between the variability of road surfaces, which according to [Robson and Dodds, 1976], "are necessarily irregular, however carefully they are prepared", and the fatigue and reliability of vehicle components.

Different quantitative descriptions may be proposed for road roughness. For comparative or statistical analyses, criteria such as the International Roughness Index (IRI) [Sayers et al., 1986] or the ISO roughness coefficient [ISO8608, 1995] are interesting scalar tools. However, in order to carry out vehicle dynamics simulations, a full description of the road geometry must be available.

In practice, the boundary constraint at the interface between the tyre and the road is

a surface contact, see the discussion in appendix C. The dynamic response of the vehicle is dependant on this surface contact, which seems to indicate that the variability of a two-dimensional entity, namely a surface, should be studied. However, proposing a model for the complete road surface constitutes a complicated mathematical task. Additionally it may not be strictly needed since the main focus here is vertical excitations. It is much more relevant, and simple, to consider longitudinal sections of the road surface, namely road profiles, see [Sayers and Karamihas, 1998]. Two profiles, symmetrical with respect to the median longitudinal axis of the vehicle (near-side wheels / off-side wheels) may be considered, see [Kamash and Robson, 1978]. The use of two road profiles is generally sufficient to carry out vehicle dynamics simulations with good accuracy, no matter the considered tyre model.

In such a context, **proposing a probabilistic model to describe the variability of road roughness may be traduced into proposing a probabilistic model for road profiles**. Subsequently, random road profiles can be generated using such a model. Stochastic process theory discussed in section 4.2 can be applied to describe a continuously varying quantity, namely the altitude of the road profile varying along the longitudinal axis defined by the moving direction of the vehicle. If a single road profile is considered, a uni-dimensional stochastic process is adapted, however if two profiles (near-side / off-side) are required for the simulation, then a bi-dimensional, or vector process, must be used, see [Kamash and Robson, 1978, Bogsjö, 2007]. For the sake of clarity, throughout this manuscript only one-dimensional processes are considered, but any development proposed here identically applies to more complex road models.

4.3.2 Stochastic models for road profiles in literature

General remarks on road modelling using stochastic process theory

In a seminal paper, [Dodds and Robson, 1973] considered the use of stochastic process theory to model road profiles, stating that "road surfaces appear amenable to representation as realisations of random processes". Obviously, road profiles are complex entities exhibiting a continuous and random variation that seems difficult to characterise. Nonetheless, according to [Robson and Dodds, 1976], it may be expected that "roads of a given class do show essentially similar irregularities", thus motivating the search for a tractable representation, *i.e.* a model in the form of a stochastic process with a specific structure and a set of identifiable parameters.

The selection of an appropriate model in the form of a stochastic process generally involves some level of simplification or approximation. This has been pointed out by [Kamash and Robson, 1978]: "The evident need for a description to be representative rather than individual, considerably affects the precision to which it can aspire. If it must apply approximately to all roads of the class, then it cannot meticulously describe each one of them. It can only be an approximation."

It is often assumed that road profiles can be represented by a stationary Gaussian

process. This assertion does not derive so much from observational evidence but rather from the fact that, as noted by [Robson and Dodds, 1976]: "if a process does not have these characteristics, both description and analysis are in general so inordinately complex as to discourage analytical treatment".

Road profiles as realisations of stationary Gaussian processes

As mentioned in subsection 4.2.3, a stationary Gaussian process is completely characterised if its Power Spectral Density (PSD) is known. Different PSD models have been proposed in literature, generally based on extensive analysis of numerous road profiles acquired through specific measuring equipment, as discussed in subsection 3.2.1. A comprehensive description of the multiple existing models is offered by [Andren, 2006].

From a general perspective, a rough analysis of the different PSD calculated on a large variety of roads shows that the spectral content is, for most roads, distributed in a similar fashion across the spatial frequency spectrum and that roads vary from one another mainly in terms of overall roughness, which can be interpreted in terms of the root-mean square value (RMS value) of the profile's geometry. Hence, the simplest model is the ISO model, see [ISO8608, 1995]:

$$S(n) = S_0 \left(\frac{n}{n_0} \right)^{-w} \tag{4.16}$$

where $S(n)$ is the PSD of the stationary process, n is the spatial frequency (in m^{-1}) with $n_0 = 0.1m^{-1}$. S_0 is the so-called **'roughness coefficient'** that alone distinguishes road profiles from one another. The waviness w controls the distribution of content across the frequency spectrum and is generally set to $w = 2$ for the ISO model (often with the objective to compare roads according to a single scalar value). S_0 is a scalar criterion and as such it is very amenable to statistical analysis.

Two different road profiles, generated according to the one parameter ($w = 2$ is imposed) PSD model in equation (4.16) and using the random generation technique presented in subsection 4.2.3 are displayed in figure 4.1, along with their PSD estimate (obtained by Welch's algorithm) and the original PSD target.

This model is generally considered as acceptable in a given spatial frequency interval, namely $n \in [0.01m^{-1}, 10m^{-1}]$, see [ISO8608, 1995]. It can be noted that, outside of this interval (one also has to take into account vehicle speed), the road profile is likely to produce very weak or no response at all on the vehicle.

A slightly more involved model consists in splitting the one-line PSD in equation (4.16) into a two-lines PSD, as proposed by [Dodds and Robson, 1973]. The two-lines

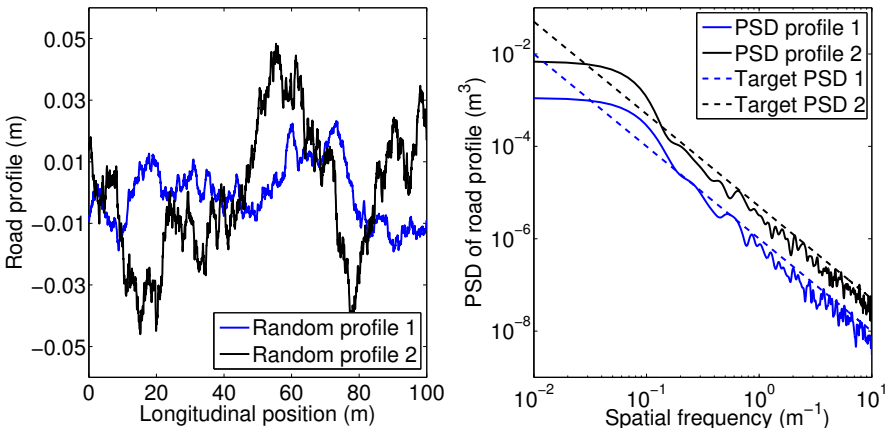

Figure 4.1: Example of two $100m$-long randomly generated profiles (left) using the ISO PSD model and their PSD estimate (right). The blue profile has $S_0 = 100.10^{-6}m^3$ and the black profile has $S_0 = 500.10^{-6}m^3$.

model considered here may be written:

$$S(n) = \begin{cases} S_1 \left(\frac{n}{n_0}\right)^{-w_1} & \text{if } n \leq n_c \\ S_2 \left(\frac{n}{n_0}\right)^{-w_2} & \text{if } n > n_c \end{cases} \tag{4.17}$$

where S_1 and w_1 are coefficients corresponding to the low frequency part of the spatial spectrum, while S_2 and w_2 correspond to the high frequency part. The spatial frequency spectrum is split at frequency n_c.

A $1km$-long section of a measured road profile is displayed on figure 4.2, along with its calculated PSD. The parameters S_1, S_2, w_1 and w_2 are identified according to the methods presented in the following subsection 4.3.3 and the two-lines analytical model based on equation (4.17), is displayed in the PSD plot of figure 4.2 (black lines). It is clear that in that case, a one-line model may be too different from the observed PSD of the real profile.

The one-line and two-lines models presented here constitute quite generic descriptions. Other and more specific formulations for the PSD model that are not described here may be found in [Andren, 2006].

Non-stationary and non-Gaussian character of real roads

Unfortunately a stochastic model based on a stationary Gaussian process may not be sufficiently representative of real road profiles. As pointed out by [Bruscella et al., 1999], "road surface [generation] **cannot be based on spectral characteristics alone for vehicle simulation, [due to] their inherent non-Gaussian and non-stationary**

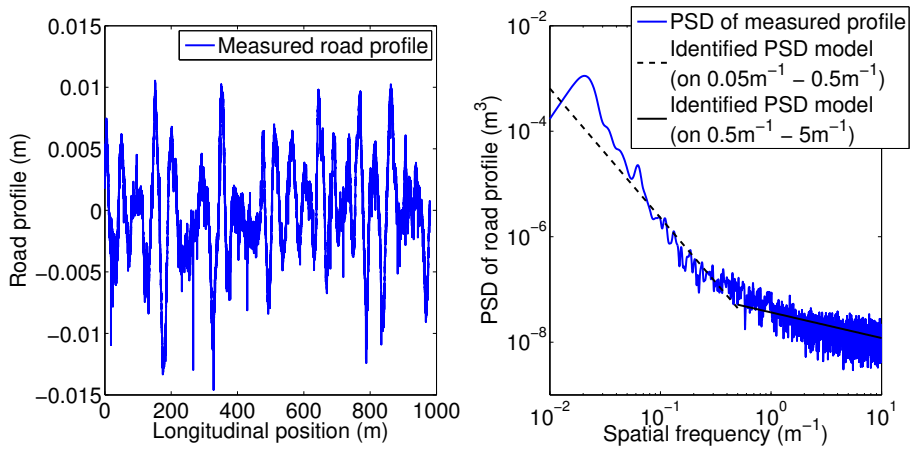

Figure 4.2: Measured road profile (left). PSD estimate of the measured road profile (right). A two-lines PSD model is fitted on the PSD estimate.

properties".

The non-stationary character of real roads has been discussed by many authors, see *e.g.* [Charles, 1993, Bruscella et al., 1999, Rouillard, 2009] and is particularly apparent when long road profiles are considered, while the stationary hypothesis may be more appropriate for shorter road sections.

Also, in [Dodds and Robson, 1973] it is stated that roads can only be considered as realisations of a stationary process "provided that the effect of such occasional large irregularities as pothole are removed from the analysis and treated separately". In what follows, these irregularities are referred to as **'transients'**, in opposition to a stationary road surface (or sections). Transients play a role in increasing the kurtosis value of observed profile data, thus making such data apparently also non-Gaussian, see *e.g.* [Bruscella et al., 1999, Rouillard et al., 2001]. More importantly in the present context where load and reliability analysis is the end purpose driving the building of a road model, transients are expected to be a strong contributor to the accumulation of fatigue damage on vehicle's components, see [Oijer and Edlund, 2004, Bogsjö, 2006, Bogsjö and Rychlik, 2009]. Therefore, they must be taken into account. This is not possible if random profiles are generated from a purely stationary and Gaussian process.

On the use of a frequency-based representation

To sum up, a (spatial) frequency-based analysis of road profiles generally provides an interesting **basis for the generation of random realisations** but when the study of road-induced damage accumulation is the end purpose of these realisations, **this type of representation alone may be insufficient**. Indeed, the non-stationary nature of real roads and the occasional presence of transient patterns such as bumps or potholes, may

have a significant impact on damage accumulation and should therefore be accounted for.

From a mathematical standpoint, various solutions can be proposed as representative models, given the observed features of real road profiles. Several candidate model structures can be found for example in [Bogsjo et al., 2012] and the structures of particular interest for the present manuscript are described in the following subsection 4.3.3. Let us insist on the fact that here for the description of road roughness variability, any considered model should constitute a compromise. Indeed, it cannot be simultaneously representative of a diverse set of roads (of a given 'class' or 'type') and provide a precise description of every single road profile within that set. This makes the selection but also and especially the validation of a model, a complex issue.

For the sake of completeness let us point out that other spectral descriptions of the correlation structure, not necessarily frequency-based, can be envisioned but will not be considered in this manuscript. Such descriptions have been considered when analysing road profiles and may include wavelet basis, see *e.g.* [Steinwolf et al., 2002] or specific mode-based decompositions of the signals, see *e.g.* [Gagarin et al., 2004]. Examples of optimal mode-based decompositions, namely Karhunen-Loeve decompositions, have not been found in the literature related to road modelling. These descriptions generally share the same limitation, namely that it is difficult to propose an *a priori* basis (other than harmonic function) for the generation of random realisations. On the other hand, Markov chains models (not a spectral formulation, strictly speaking) are also considered for road modelling, see [Ferris, 2004].

4.3.3 Proposed candidate model structures and parameter identification

Different candidate model structures are proposed in the present subsection. Each candidate is tested against real profile data (obtained from the methodology presented in chapter 3) in section 4.5 and the selection of a particular model, suitable for the analysis of road-induced loads, is carried out accordingly. Additionally, practical methods allowing us to identify the parameters associated to each model, are detailed here. The different models that are considered:

- Rely on a frequency-based description
- Are either stationary or make use of a particular strategy to handle non-stationarity
- Either include synthesized transient patterns or not

Frequency-based description of the 'correlation structure'

All the models considered here involve a frequency-based description of the correlation structure, through a given analytical form for the PSD. Two analytical

forms are here studied, namely the one-line PSD model described by equation (4.16) and the two-lines PSD model in equation (4.17).

The identification of parameters is based on the calculation of the PSD of a measured (or estimated) road profile. The PSD is calculated using Welch's algorithm, as described in subsection 4.2.3. When a PSD estimate is available, a least squares regression is used to determine either S_0, see equation (4.16) or S_1,w_1, w_2 and S_2, see equation (4.17). The result of this identification is illustrated on the right-hand side of figure 4.2. The split frequency n_c is selected by experience at $0.5m$, see also [Andren, 2006]. The S_2 parameter can be deduced from the three other parameters if a connection is imposed between the two lines of the PSD.

Stationarity of real and generated random road profiles

Here, **a particular strategy to generate non-stationary realisations is chosen based on the work from** [Bogsjo et al., 2012]. It consists in dividing the generated trajectory into M sections of identical lengths and in modulating the variance, directly linked to the 'overall roughness level' on those sections, so that the variance of the whole profile σ^2 remains unchanged. The considered stochastic process is thus piecewise-stationary. This may be written as follows:

$$\frac{1}{M}\sum_{j=1}^{M}\sigma_j^2 = \sigma^2 \tag{4.18}$$

where $(\sigma_j^2)_{j=1,\dots,M}$ are the variances on the M sections of length L so that $L_{tot} = ML$ is the total length of the profile and σ^2 is its variance. For this model, the PSD target retains the same shape for all the different sections; it is only modulated and the PSD evaluated across the whole profile (now non-stationary) remains almost unchanged, see figure 4.5. Here $L = 200m$ is selected from experience and as advised in [Johannesson and Rychlik, 2014]. Let us introduce normalized variances $r_j = \sigma_j^2/\sigma^2$ and study their possible evolution based on an actual example.

In figure 4.3, the normalized variance on 200m-long sections is calculated from a measured road (with a laser-based road measuring device) and clearly testifies of the non-stationary character of real roads.

In [Bogsjo et al., 2012], it is proposed to choose a Gamma distribution to model the evolution of normalized variances. Non-stationary realisations can then be generated by randomly drawing a set of normalized variances $(r_j)_{j=1,\dots,M}$ from the Gamma distribution and using it to modulate the profile being generated. The PDF of the Gamma distribution is:

$$f_R(r|a,b) = \frac{1}{b^a\Gamma(a)}r^{a-1}e^{-r/b} \tag{4.19}$$

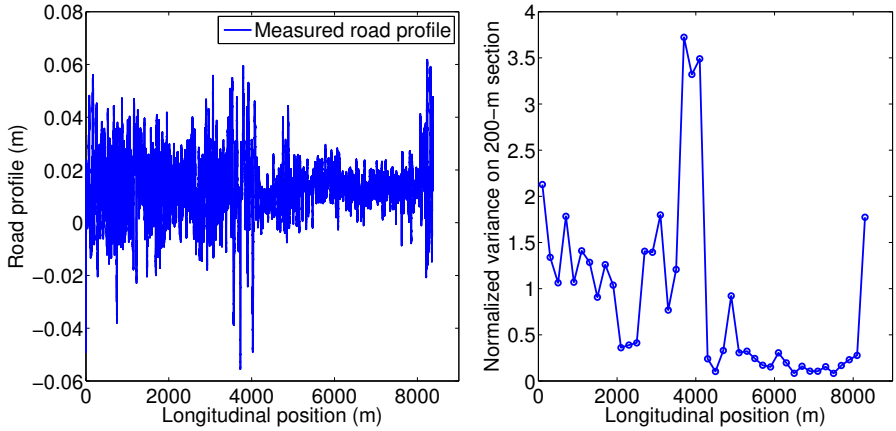

Figure 4.3: Non-stationary character of a real road. Normalized variance $(r_j)_{j=1,\ldots,M}$ are calculated on sections of length $L = 200m$.

where $\Gamma(.)$ is the Gamma function and a and b are the two parameters of the distribution. The mean of a Gamma distributed random variable R is $E[R] = ab$. In the present case, the mean of the normalized variances $(r_j)_{j=1,\ldots,M}$ is necessarily unitary, so that equation (4.18) is satisfied. With this condition, generating realisations for $(r_j)_{j=1,\ldots,M}$ through a Gamma distribution only requires one parameter γ. It may thus be written that $R \sim \Gamma(1/\gamma, \gamma)$ and $E[R] = 1$.

The identification of the model parameter γ is quite straightforward. The normalized variances can be calculated for any desired measured (or estimated) road profile, as displayed in figure 4.3. The latter should nevertheless be sufficiently long; $10km$ is a good target, see [Johannesson and Rychlik, 2014]. The γ parameter is then estimated using this sample of normalized variances, through a simple Maximum Likelihood Estimation (MLE) procedure, see *e.g.* [Priestley, 1981]. In figure 4.4, the comparison between a fitted Gamma CDF and the empirical CDF constructed from the normalized variances $(r_j)_{j=1,\ldots,M}$ calculated on the measured road profile, is displayed for illustration purposes.

With this approach, the non-stationary character of the road profiles is described by a single parameter and random realisations can be generated rather easily. To be more specific, it is possible to generate a set of normalized variances $(r_j)_{j=1,\ldots,M}$ according to the Gamma distribution of parameter γ and use it to modulate the variance of the white noise injected in the 'shaping filter' described in subsection 4.2.3. This is described precisely in [Bogsjo et al., 2012, Johannesson and Rychlik, 2014]. One obtains a non-stationary realisation with smooth transitions between stationary sections of identical lengths L. The example of a randomly generated non-stationary road profile is displayed in figure 4.5.

Other methods have been proposed to deal with the non-stationary character of real roads, see *e.g.* [Charles, 1993, Rouillard et al., 2001]. They are generally based on the same principle as the method introduced above and proposed by [Bogsjo et al., 2012].

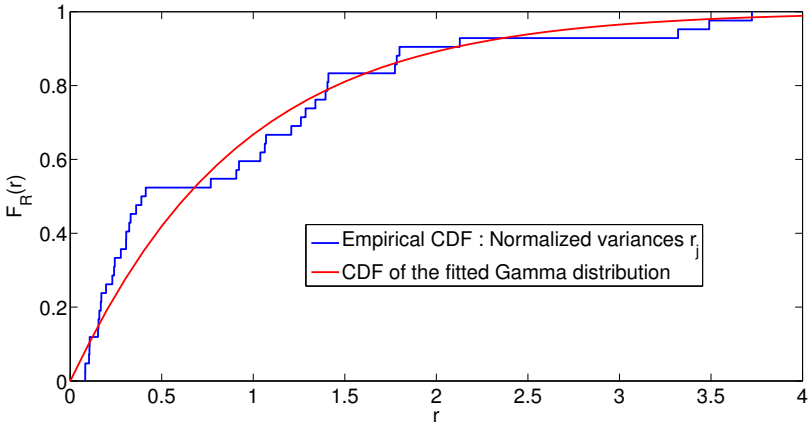

Figure 4.4: Comparison between the empirical CDF associated to the normalized variances $(r_j)_{j=1,\ldots,M}$ calculated on the measured road profile and a fitted Gamma CDF.

The generated trajectory is decomposed into stationary sections with a given variance and length, while the underlying spectral characteristics (the PSD) are left unchanged, *i.e.* as evaluated across the complete trajectory. These other methods thus **only differ on how to propose values for the evolution of the lengths and variances of the different 'stationary sections'**. They may be more suited to achieve a precise description of a given profile but they do not appear as convenient as the method chosen here, when it comes to proposing a model for a diverse set of roads while limiting the number of parameters involved, namely a single parameter γ for the selected approach. Here a fixed length may not be the most representative choice when comparing profiles, however it may be sufficient as far as damage accumulation is concerned, see [Johannesson and Rychlik, 2014] for additional information.

Modelling and synthesis of transient patterns in road profiles

Real road profiles often contain occasional transient patterns such as potholes, speed bumps, and so on. They should be accounted for as they can have a strong influence on the damage accumulation imposed on vehicle components, as discussed for example by [Oijer and Edlund, 2004, Bogsjö and Rychlik, 2009]. The literature is not very dense on the subject of transients and the issue is quite difficult to address as road profiles can be very different from one another in that regard.

Here an original model is proposed in order to synthesize transients. It is inspired by the work in [Rouillard et al., 2000, Oijer and Edlund, 2004]. It relies on the analysis of the distribution of transients across road profiles, in terms of the number of occurrences per kilometre and of the distribution of their amplitude. As far as the generation of road profiles is concerned, transient patterns of a predefined mathematical form

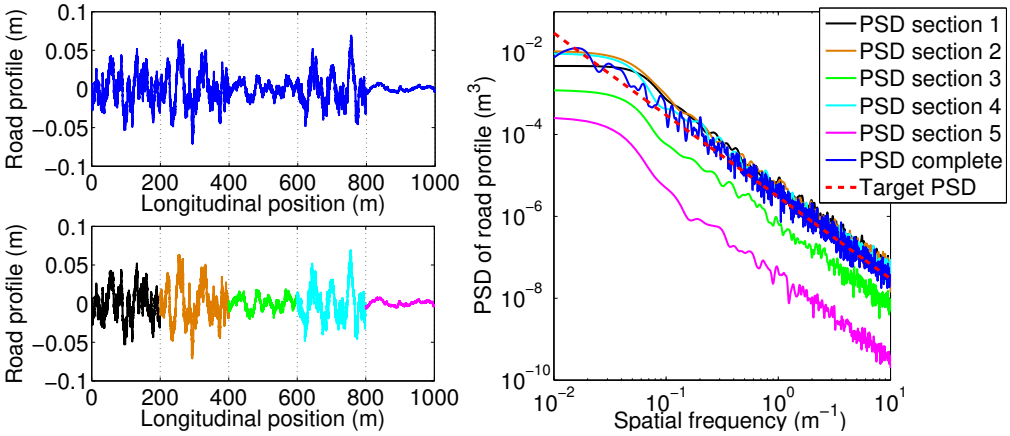

Figure 4.5: Random realisation of a non-stationary profile. The complete profile (top left) is made of stationary sections (different colors, bottom left), connected with smooth transitions. The PSD estimate on the whole profile is compared to its target PSD and to the PSD estimates on each sections (right).

are occasionally added to a previously generated trajectory (based on a frequency-based description). An example of trajectory generated according to this modelling strategy is given in figure 4.6.

More precisely, transient patterns of the form $x \mapsto e^{-x^2}$ are synthesized here. Their length is chosen as a constant and fixed to $2m$, based on experience and on the visual analysis of numerous road profiles. The distance between two transients is randomly drawn from an exponential distribution, where the parameter of the distribution λ (in m) is directly deduced from the average number of transients per kilometre. The amplitude of the transients is randomly drawn from an exponential (and translated) distribution of parameter ϕ (in m). The identification of both the frequency parameter λ and the amplitude parameter ϕ implies the identification and counting of transients as well as the assessment of their amplitudes.

First, transients have to be identified (*i.e.* localized) and counted within a given road profile. Different identification criteria may be considered, see *e.g.* [Rouillard et al., 2000, Steinwolf et al., 2002, Bogsjö, 2006]. The automatic detection and counting of transients may not be so straightforward when considering directly the road profile. Conversely, a detection criterion based on the response of the vehicle is much more convenient and the following response-based criterion is thus proposed. The considered road profile is used to simulate the response of a linear quarter-car model (see subsection 2.3.2) travelling at a selected speed of $30km/h$. **The unsprung acceleration is calculated and any peak above a selected threshold, here $50m/s^2$, is considered as an indicator of the presence of a transient within the road profile.**

This is arguably a very empirical and questionable approach but it is also simple.

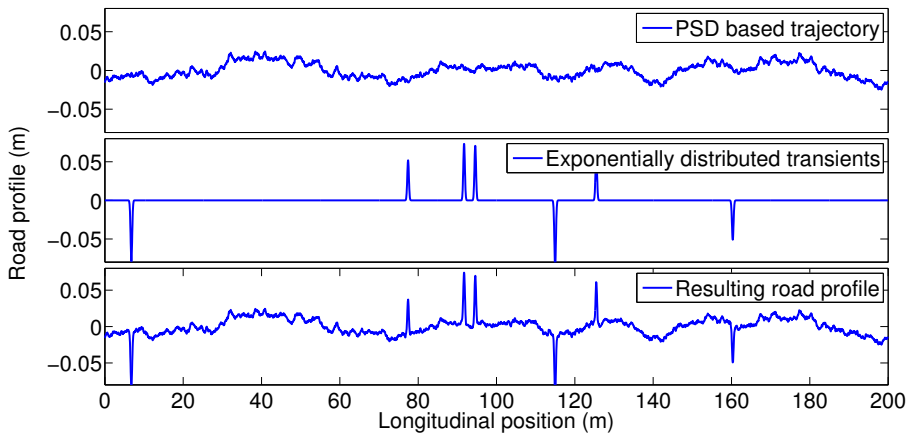

Figure 4.6: Example of a generated road profile to which transients patterns, of the form $x \mapsto e^{-x^2}$, have been added using two exponential distributions, namely for the distance between one another and for their amplitude.

The threshold and speed values have been selected empirically and have provided good detection capabilities when tested visually with different road profiles (see figure 4.14 in subsection 4.4.3). Using this approach, transients can be counted and the λ parameter can be identified based on the available data on road profiles.

Secondly, as a particular form and length has been selected for the transients to be synthesized, it would not be appropriate to directly read the amplitude of multiple transients of potentially different forms, when they are identified within the road profile. Here, it is proposed to synthesize transients that seek to 'provoke the same response on the vehicle' than the ones that have been identified. Hence a calibration case is considered. Transients of the selected specific form ($x \mapsto e^{-x^2}$) and of increasing amplitudes are fed into the same linear quarter-car model and latter matched to the unsprung acceleration they provoke. This calibration case is shown in figure 4.7.

It is then possible to identify transitively, *i.e.* through the value of the response criterion (unsprung acceleration), the amplitude of the synthetic transient pattern ($x \mapsto e^{-x^2}$) that can be added to the generated road profile in order to provoke a response that is relatively similar with the associated transient originally present in the studied road profile. Hence this simplification allows us to consider a single parameter, namely the height (or amplitude), to handle transients that could be of various forms, lengths and heights.

Once again, this is an empirical approach and it is proposed here as a **relatively simple solution to model complex and diversified transient patterns that can occur in road profiles**. The parameter of the amplitude distribution ϕ can be identified through the latter.

An example of the result of such an identification is given in figure 4.8. The data

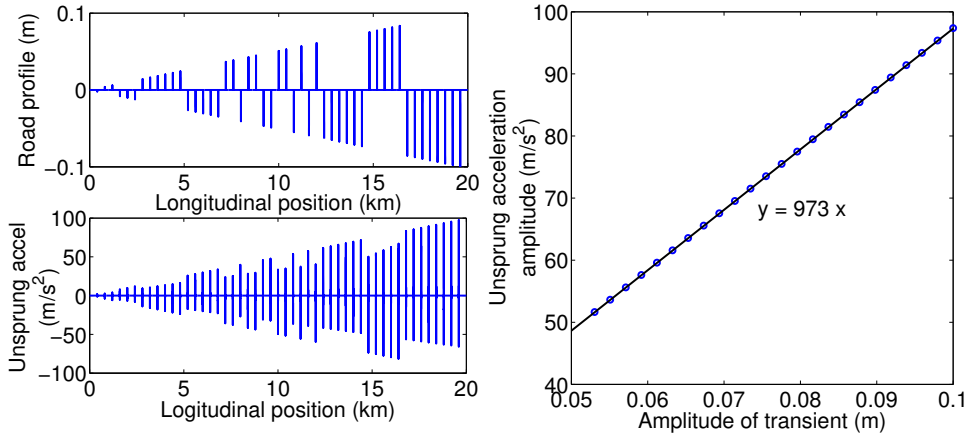

Figure 4.7: Calibration, through a simple quarter-car model travelling at $30km/h$, of the relation (right) between the unsprung acceleration peaks (bottom left) and the amplitude of transient patterns (upper left) of the form $x \mapsto e^{-x^2}$.

used for identification of both distributions is composed of $200km$ of estimated road profiles (see subsection 4.5.1). Transients are counted and their amplitude is assessed using the procedure above. The two parameters λ and ϕ are subsequently identified from the obtained sample through MLE, and displayed on figure 4.8.

Summary of the candidate model structures

The different candidate model structures considered in this manuscript, which are tested against real profiles data in section 4.5, are summarized in table 4.1. The number and notations of the parameters that are necessary to completely characterise the different models are also given.

Model candidate	Correlation structure	Non-stationary strategy	Transients modelling	Constituting parameters
R#1	One-line PSD	Piecewise-stat.	No transients	S_0, $w = 2$, γ
R#2	Two-line PSD	Stationary	No transients	S_1, w_1, w_2
R#3	Two-line PSD	Piecewise-stat.	No transients	S_1, w_1, w_2, γ
R#4	Exact PSD	Piecewise-stat.	No transients	Full PSD, γ
R#5	Two-line PSD	Piecewise-stat.	Exp.distributed	S_1, w_1, w_2, γ, λ, ϕ

Table 4.1: Different candidate stochastic road models. All modelling options are tested against real data in section 4.5.

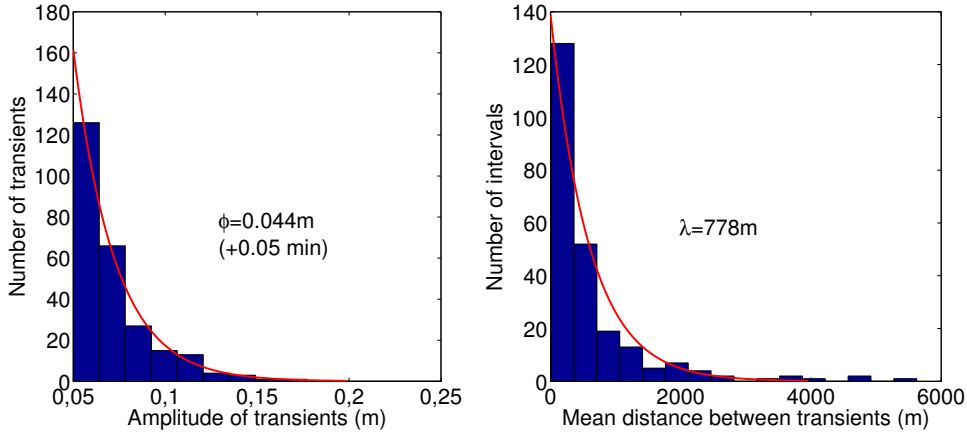

Figure 4.8: Distribution of the amplitude of transients (left) and of the distance between transients (right). The distribution of amplitude is a translated ($+0.05m$, being the minimum level to detect a transient) exponential distribution. The source of information is constituted by $200km$ of estimated road profile.

4.4 Stochastic modelling of speed profiles

4.4.1 Speed of the vehicle and its evolution

The speed at which a vehicle covers a given road profile determines the vertical excitation, or more formally, the time evolution of the boundary constraint imposed on such vehicle. If $u(x)$ is the expression of the road profile as a function of the spatial coordinate x, and $v(t)$ is the time evolution of the vehicle's speed, then the time evolution of the boundary constraint imposed on the vehicle, namely $u(t)$, derives from those two entities. Practically, in order to proceed to vehicle dynamics simulations, one has to match time instances, generally spaced regularly at sample time dt, with their longitudinal position, according to:

$$x(t_0) = \int_{t=0}^{t=t_0} v(t)dt \tag{4.20}$$

The corresponding altitude of the excitation at that time instance $u(t_0)$ can be read, or interpolated if need be, from the road profile at that longitudinal position $u(x(t_0))$.

In consequence, the dynamic characteristics of the vertical excitation are highly dependant on the speed of the vehicle. The latter has a direct influence on the loads acting on the vehicle's components and can thus be referred to as an 'influential factor' (as described in the introduction chapter 1). Its evolution should be studied in the statistical sense, if one seeks to acquire a description of the variability of road-induced fatigue loads.

As previously mentioned, the present work is focused only on vertical excitations, see

subsection 2.3.1. Longitudinal dynamics of the vehicle, *i.e.* inertial actions resulting from braking or acceleration inputs of the driver, even if they may also induce vertical responses through pitch movements, are disregarded.

In such a context, **the speed of the vehicle** $v(t)$ **should simply be seen as a 'moving cursor' that reads the road profile** $u(x)$ **and transforms it** (a sort of dilation of the longitudinal axis) **into a time-varying excitation** $u(t)$. Conceptually, it is even interesting to view the vehicle as motionless, while the road profile is 'scrolling' below the wheels of the vehicle. An example of two readings of the same road profile, at different speeds, is shown in figure 4.9. Let us note that, in the context of a purely vertical excitation, sharp discontinuities in vehicle's speed do not imply discontinuities in the vertical excitation, *i.e.* the 'moving cursor' can read the road profile $u(x)$ in a jerky manner without making the excitation $u(t)$ jerky, as seen in figure 4.9.

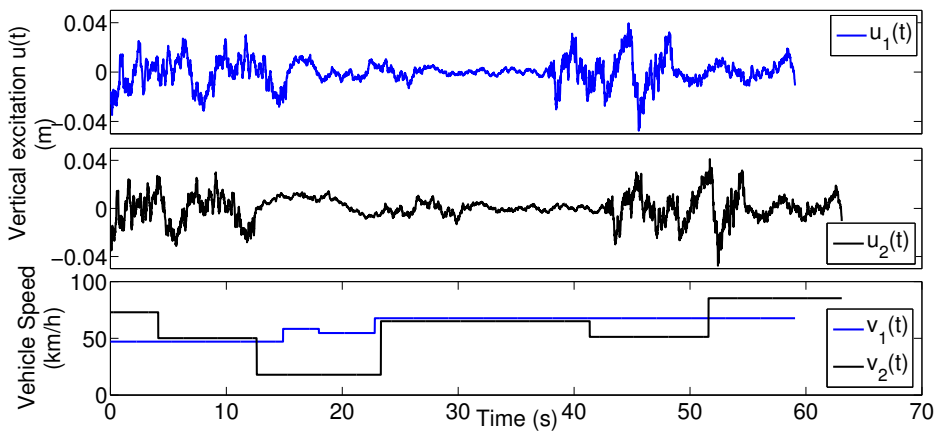

Figure 4.9: Vertical excitations $u_1(t)$ and $u_2(t)$, corresponding to the same road profile $u(x)$, for two different speed signals $v_1(t)$ and $v_2(t)$.

Before considering the mathematical characteristics of speed profiles, it is relevant to analyse the factors that may affect the evolution of vehicle speed. Ultimately, **the speed profile is determined by the input of the driver**, and thus influenced by the driver's behaviour, itself deriving from multiple considerations such as comfort, driving sensations, safety, trip duration, fuel consumption or care for the vehicle longevity. However, **there are also external factors from the driver's standpoint**, such as the topology of the route (curviness, hilliness), traffic flow, traffic regulations (traffic lights, stops), speed limitations or weather conditions, to which the driver has to adapt through the modulation of vehicle speed. This makes the definition of a stochastic model a highly complicated issue and calls for simplification at some point.

4.4.2 Stochastic models for speed profiles

Any simplification of the problem of vehicle's speed modelling needs to be conceived in close relation with the purpose that the model is build to serve. In the present context, it may not be relevant to build a model with an excessive level of sophistication and complexity, especially since the variety of external factors that may influence the speed profiles can be vast and extremely hard to grasp.

Some references propose to address the issue of vehicle speed in relation with the effect it has on the mechanical response of the vehicle. They study the influence of vehicle speed on the statistical characteristics, *e.g.* spectral characteristics, of the vertical excitation imposed on the vehicle, see *e.g.* [Virchis and Robson, 1971, Sobczyk et al., 1977]. However, the discussions proposed in those references are rather focused on the consequences of a varying speed on the vertical excitation and not on the evolution of the speed itself nor on the causes that provoke such an evolution. Therefore these results are not particularly helpful when it comes to building a stochastic description for the overall evolution of vehicle speed. In the framework of damage accumulation analysis, the complete history of vehicle speed needs to be known as it impacts the complete history of the vertical excitation and loads.

In order to encounter research work discussing the evolution of vehicle speed over long periods, it is necessary to turn to domains that can be quite remote from load variability analysis, which tackle problems like the minimization of travelling duration, the minimization of fuel consumption, both being cumulative quantities, or the analysis or regulation of traffic flow, see *e.g.* [Kharoufeh and Gautam, 2004]. It readily appears that speed profiles cannot be considered as stationary.

In the present context **a specific approach is proposed**. It considers that the speed profile is randomly evolving between different 'states' for which the evolution of speed is dependant both on external and behavioural factors.

To illustrate that a stochastic model randomly switching between states is a relevant choice, it is interesting to examine different speed recordings that correspond to the same route. This is displayed in figure 4.10, where three drivers with different driving behaviours (willingly exacerbated for visualization purposes), namely increasing driving aggressiveness, have imposed different speed profiles when covering the same route. One clearly notices the non-stationary character of speed profiles. Also, it is seen that external factors causing the variation of the vehicle speed along the route (topology of the route, speed regulations, etc.) adopt a similar evolution for the different drivers. Consequently, even if the precise causes that produced the switching between different states are unknown from the sole observation of the speed profile, the statistics of the length and speed values associated to the different states can be studied. A stochastic model is proposed here to describe such statistics.

Let us insist on the fact that here it is important to **study the evolution of vehicle speed in the spatial domain**, *i.e.* work on a description for $v(x)$, **as the objective is**

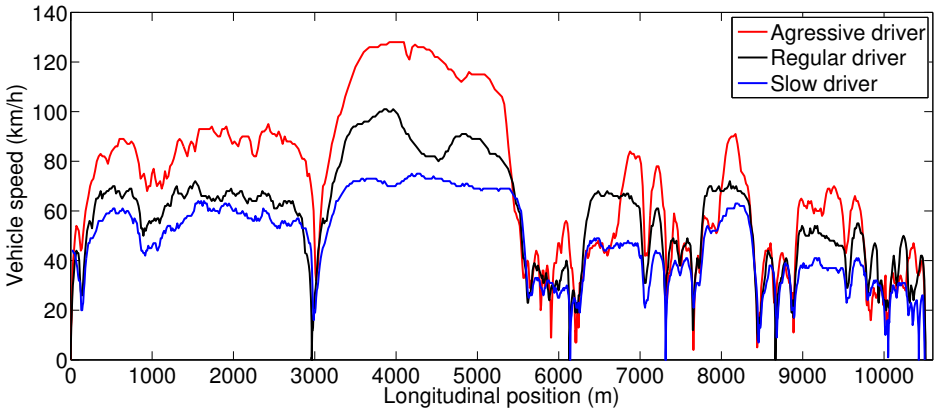

Figure 4.10: Comparison of several drivers on the same route. Different driving behaviours have been adopted by the drivers, namely increasing aggressiveness.

to analyse the accumulation of damage. This is relatively obvious if one examines the situation where the vehicle is not moving at all. Indeed, even if such a situation lasts for a long period of time, no damage accumulation is occurring. Hence, the quantity of interest here is not the time evolution of the speed value but rather the speed value that the vehicle assumes on any covered (spatial) section of the road profile. This in turn influences the vertical excitation that this section will generate on the vehicle. With a given sample time dt, a random trajectory for $v(x)$ can be easily transformed back to the time domain, namely $v(t)$, in order to subsequently define the time-varying vertical excitation $u(t)$ and carry out vehicle dynamics simulation.

The literature on the statistical analysis of vehicle speed and its relation to load variability is, to the best knowledge of the author, very sparse to non-existent. **The stochastic models proposed in this work are both relatively simple since they willingly disregard external causes such as traffic or topology and specific to the issue of load variability.**

4.4.3 Proposed candidate model structures and parameter identification

Constant speed profiles

The simplest way of defining a speed profile for the vehicle is to assume that the latter is constant when the vehicle covers a given road profile, *i.e.* $\forall x, v(x) = v_c$. The most natural approach to identify a speed value v_c is to equate it with the spatial mean of the given speed recording of interest:

$$v_c = \frac{1}{L} \int_{x=0}^{x=L} v(x) dx \tag{4.21}$$

where L is the total length associated with the covered distance corresponding to the speed history on $[0, t_{max}]$:

$$L = \int_{t=0}^{t=t_{max}} v(t)dt \tag{4.22}$$

The use of a constant speed value is generally the approach taken in literature when considering road-induced loads, see *e.g.* [Sun, 2001, Howe et al., 2004, Bogsjo et al., 2012]. A scalar quantity v_c is very amenable to study the diversity of the speed of vehicles among a population of drivers, which may cover different road profiles and different route types (Highway, city road, etc.). Here, the speed process is a degenerate stochastic process, namely a constant process, and stochastic process theory is of no particular use.

Proposed piecewise-constant stochastic model

A more realistic model can be constructed if one assumes that the speed of the vehicle evolves between different states, wherein it holds a constant value. The 'switching between states' depends on unknown external parameters, *e.g.* topology, speed limitations or traffic flow.

A speed profile measured on a $10km$-long route is displayed in figure 4.11 and a particular treatment is applied in order to identify segments where the speed profile is almost constant (see appendix E for details). It appears that a succession of constant speed segments can be a good approximation of the speed profile, noticeably more representative than a strictly constant speed v_c, while being a simple enough mathematical representation of a complex process. As previously stated, discontinuities in the speed profile are not a concern if only the vertical dynamics is studied.

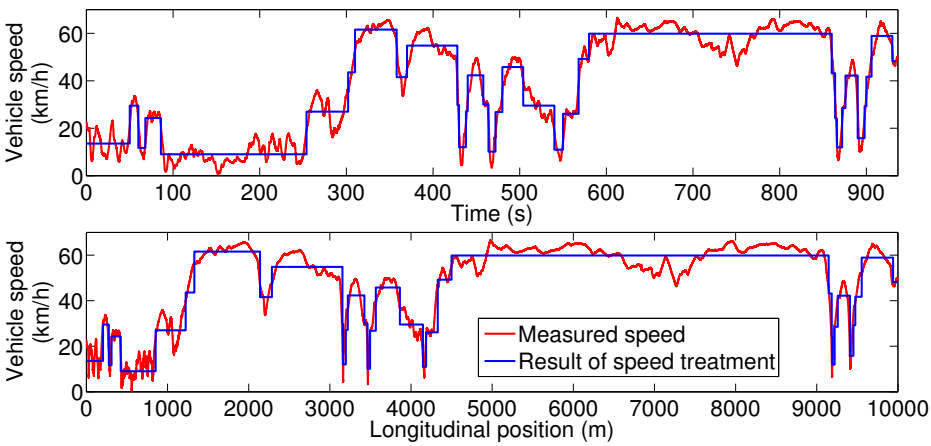

Figure 4.11: Measured vehicle speed and division in constant speed sections. The speed profile is expressed both in the time domain (top) and spatial domain (bottom).

Based on the previous analysis, the following piecewise-constant model is proposed. It is constructed by juxtaposing segments, whose length is a random value, for which the speed of the vehicle is constant and a random value. Hence, to completely specify this model, it is necessary to identify two distributions.

A particular example is studied here as a way of getting insigh into these distributions. The data used is composed of $200km$ worth of recorded speed signals (see subsection 4.5.1). The speed signals are all processed according to the treatment already illustrated in figure 4.11 and detailed in appendix E. A set of segments with a given length and associated speed value is thus identified. The result of this collection of segments is given in figure 4.12. It readily appears that the length of the segments could be represented by an exponential distribution, while the speed on those segments is well described by a Gaussian distribution. The histograms corresponding to both variables are displayed in the bottom and left part of figure 4.12.

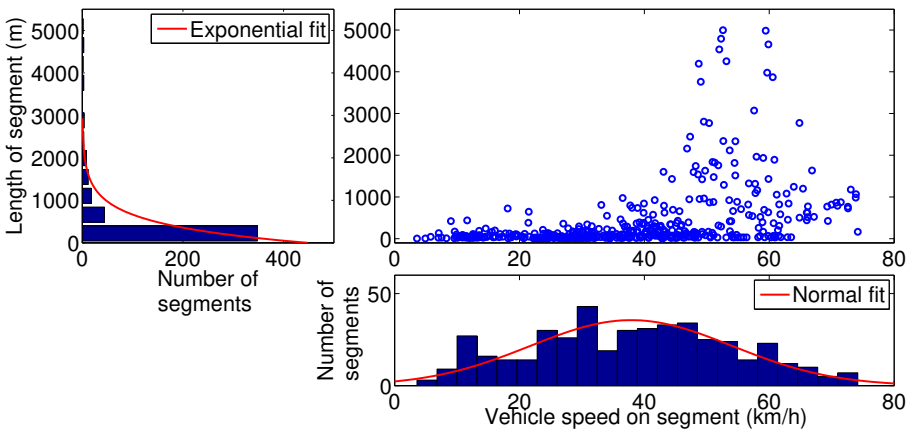

Figure 4.12: Distributions of the length and speed value of the different segments (center). The marginal distributions are also displayed (left and bottom).

Additionally, those two variables exhibit a correlation in figure 4.12. Indeed, at higher speeds, the distance covered is likely to be more important. The correlation between the segments' length and their associated speed value must be accounted for since segments corresponding to higher speeds may span on longer sections of the road profile while being generally synonymous with higher damage accumulation.

To sum up, the proposed stochastic model for vehicle speed requires the identification of four parameters:

- Two parameters v_m and σ_v are needed for the normal distribution representing the speed values on the different segments.
- One parameter θ is needed for the exponential distribution representing the lengths of the different segments.

- One parameter ρ_{ls} is necessary to characterise the correlation between the length and the speed value associated to a given segment.

Identification of the parameters of the speed model

The parameters of the marginal normal distribution v_m and σ_v and of the marginal exponential distribution θ are identified through MLE, see the fitted distributions in figure 4.12. The correlation coefficient is identified here through the use of a Gaussian copula, which is a relatively simple tool to subsequently generate correlated values. Couples made of speed/length values are sent to $[0,1]^2$ using the fitted parametric CDFs, then a bivariate Gaussian copula is fitted using MLE and the correlation coefficient ρ_{ls} is deduced, see [Bouyé et al., 2000] for technical details.

The fitted Gaussian copula combined with the use of the parametric distribution parameters is used for the generation of correlated speed/length realisations. An example of speed profile generated according to this stochastic model is given in figure 4.13.

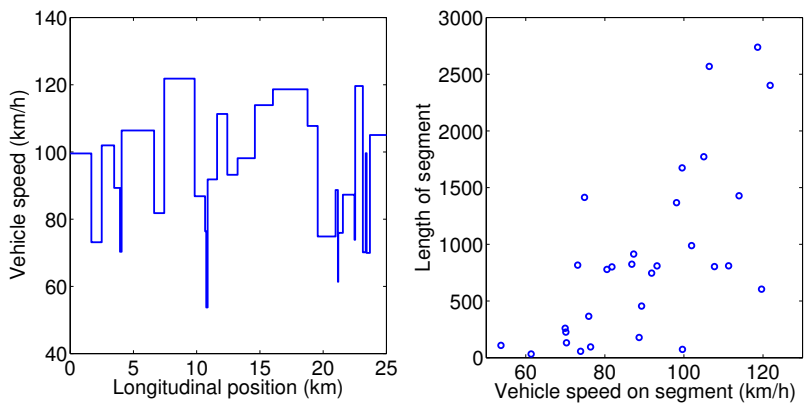

Figure 4.13: Example of a randomly generated speed profile, with parameters $v_m = 90km/h$, $s_v = 0.2v_m$, $\theta = 1000m$ and $\rho_{ls} = 0.7$.

Correlation between speed and road profiles

Let us point out that for the proposed model, the speed of the vehicle evolves between different states but the underlying reasons which cause the switching between states and the selection of a new speed value are completely disregarded by the model. However, in the present context of the study of road-induced vertical loads, the evolution of speed cannot be studied independently from all external factors. Indeed, there is an external factor of direct interest in the present framework and which may lead the speed of the vehicle to evolve, namely road roughness.

When observing simultaneously realistic speed profiles and road profiles (here obtained from measurements and the use of the road estimation method described in chapter 3), it is possible to observe an influence of the covered road profile on the variation in the speed of the vehicle. The most visible manifestation of this correlation occurs when transient patterns are contained within the road profile. **The driver naturally adapt its speed (most of the time) when he encounters and detects a transient pattern, in order to avoid either serious discomfort or important damage accumulation for the vehicle.**

This phenomenon can be seen in figure 4.14 where a road and associated speed profile (in blue) are compared in the spatial domain. Several transients are contained within the road profile and they can be identified using the approach presented in subsection 4.3.3. A notable drop in the recorded vehicle's speed is often observed in the vicinity of the transients.

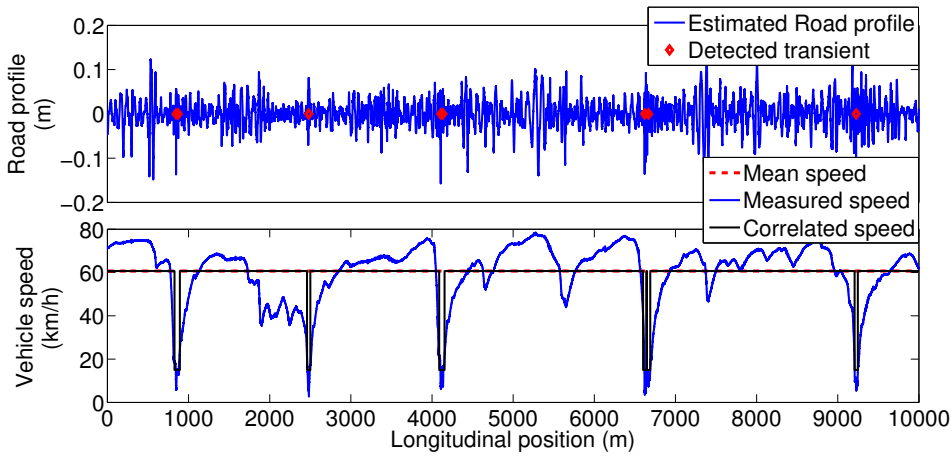

Figure 4.14: Observed correlation between measured speed profile and road profile (estimated). The transients are detected (based solely on the road profile) according to the method presented in subsection 4.3.3.

The following approach is proposed to take into account this relation between road and speed in the vicinity of transients. The positions of the transients contained within the road profile are identified using the response-based technique described in subsection 4.3.3. They are marked in the upper part of figure 4.14. In the vicinity of transients, the speed value associated to any generated random speed profile is lowered to a predefined 'transient crossing value' v_{tr}. A constant speed profile, with speed reductions in the vicinity of transients is displayed in the lower part of figure 4.14 (in black).

The correlation between road and speed in the vicinity of transient patterns has a critical influence on the damage accumulation. This may be demonstrated by considering a simple experiment. The road profile displayed in figure 4.14, which contains a handful of transient patterns, is covered with different speed profiles obtained

from the different modelling hypothesis, which either imply a strategy to account for the correlation or not. The variability of the damage accumulation is then studied. Three sets of generated speed profiles are considered:

- Constant speed profiles, where the target speed v_c is drawn from a normal distribution
- Random speed profiles (piecewise-constant) generated using the stochastic model proposed in this subsection, for which 4 parameters have to be defined. Here the target speed v_m is drawn from a normal distribution and the other parameters s_v, θ and ρ_{ls} are assigned fixed values for all the different realisations, namely $20km/h$, $1000m$ and 0.7.
- Constant speed profiles but with the addition of a correlation between road and speed. On a $40m$ window around the detected transient (on the road profile) the speed is lowered to $v_{tr} = 20km/h$.

A set of 20 random target speed values is drawn from a normal distribution and used to generate speed profiles from the different models above. The damage equivalent amplitudes (DEA) are calculated on the three response signals of a linear quarter-car model, namely suspension displacement, sprung acceleration and unsprung acceleration, and corresponding to the different speed profiles. They are plotted against the spatial mean of those speed profiles in figure 4.15.

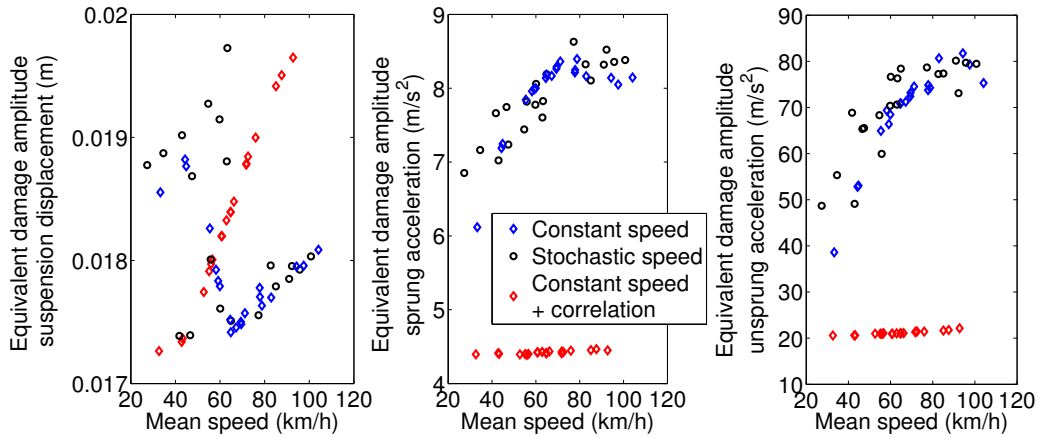

Figure 4.15: Influence of the speed stochastic model on damage accumulation. Role of the correlation between road and speed in the vicinity of transients.

It is obvious that **the effect of the correlation between the speed and road profiles is of major importance**. Indeed, the speed profiles involving a lowering of speed in the vicinity of transients exhibit very different damage values. Transients in the road profile generate high amplitude responses and consequently account for a large

fraction of the damage, as pointed out by [Bogsjö, 2006, Bogsjö and Rychlik, 2009]. The large majority of drivers will lower their speed when crossing a transient. If the speed is not adapted, unrealistic level of damage, with respect to real drivers, could be reached and the prediction of the road-induced damage is likely to be erroneous. Therefore this phenomenon should be taken into account if transient patterns are contained within the road profile.

In this manuscript the road/speed correlation is only studied in the vicinity of transients. It could reasonably be argued that a correlation also exists between the 'overall level of roughness' of the road profile and the evolution of the speed profile. This is further discussed when introducing life situations in the following chapter 5. More complex models for the road/speed correlation could theoretically be envisioned but will not be discussed here, mostly to avoid making the speed model too specific or too arbitrary and because it is likely that their contribution is less important than a strategy to handle transients, as demanded by the analysis of figure 4.15.

Summary of considered models

The different candidate model structures considered in this manuscript, which are tested against real profile data in section 4.5, are summarized in table 4.2. They include the original model structures proposed within this section. The number and notations of the parameters that are necessary to completely characterise the different models are also given.

Modelling option	Speed evolution	Correlation road/speed	Constituting parameters
S#1	Constant	No correlation	v_c
S#2	Constant	Speed reduct. for transients	v_c, v_{tr}
S#3	Piecewise-constant	No correlation	v_m, s_v, θ, ρ_{ls}
S#4	Piecewise-constant	Speed reduct. for transients	v_m, s_v, θ, ρ_{ls}, v_{tr}

Table 4.2: Different candidate stochastic speed models. All modelling options are tested against real data in section 4.5.

4.5 Exploitation of available data: testing of the considered models

In sections 4.3 and 4.4, candidate model structures have been proposed, respectively for the stochastic representations of road profiles and speed profiles. In order to validate the selection of an appropriate model, it is necessary to possess samples of data for both road and speed profiles.

In this manuscript it is proposed to collect data on road profiles from load measurement

campaigns and through the use of the road estimation algorithm described in the preceding chapter 3. Let us point out that all estimated road profiles may have been affected by the estimation method and that one should exercise care with the obtained data. As far as speed profiles are concerned, no estimation method is necessary since the latter are directly measured.

4.5.1 Example of data acquisition from load measurement campaigns

In this subsection, an example is given for the acquisition of road profile data through the application of the road estimation method on datasets corresponding to load measurement campaigns. Two configurations of load measurement campaigns are considered. In the first configuration, the routes are imposed in relation with predefined route types. In the second configuration, the driver may use its vehicle freely and thus is not forced to follow a particular route.

The recorded signals used for the application of the road estimation method include: the suspension displacement, the sprung acceleration and the body acceleration. The recorded speed of the vehicle is also needed. Let us note that in what follows, only one profile is estimated based on the use of the signals recorded on one of the front wheels (namely the left wheel).

First example: Processing of a route-imposed campaign

The considered campaign is composed of the following recordings. 5 route types are defined, namely city routes (V), country routes (R), highways (A), mountain routes (M) and off-road routes (P) and 7 circuits are defined within each of these categories, which totals to 35 different circuits. The majority of these circuits are approximatively $50km$ long. Each circuit is covered by 4 different drivers, who repeat the circuit with 3 different cargo, namely empty, half-full and full. Consequently, the campaign is composed of 420 recordings (7 circuits $\times$ 5 road types $\times$ 4 drivers $\times$ 3 cargo). Let us point out that a few of them may be unusable due to sensor failures.

The road estimation method is applied on all recordings and yields a large set of estimated road profiles, some of them being different estimations of the road profile corresponding to the same circuit (35 in total). The PSD of all estimates is calculated and the roughness coefficient S_0 defined in equation (4.16), with $w = 2$, is identified for each estimate through a least squares regression on the spatial frequency band $0.05-0.5m^{-1}$. This restrained spatial band is considered as a domain where the validity of the estimation method is acceptable and not excessively subjected to an underestimation of the road profile content due to vehicle speed, as discussed in subsection 3.6.4. The results are displayed and sorted by route type and by circuit in figure 4.16. The use of the scalar value S_0 is quite convenient for visualisation purpose or statistical analysis, even if it may not be sufficient to fully characterise road profiles.

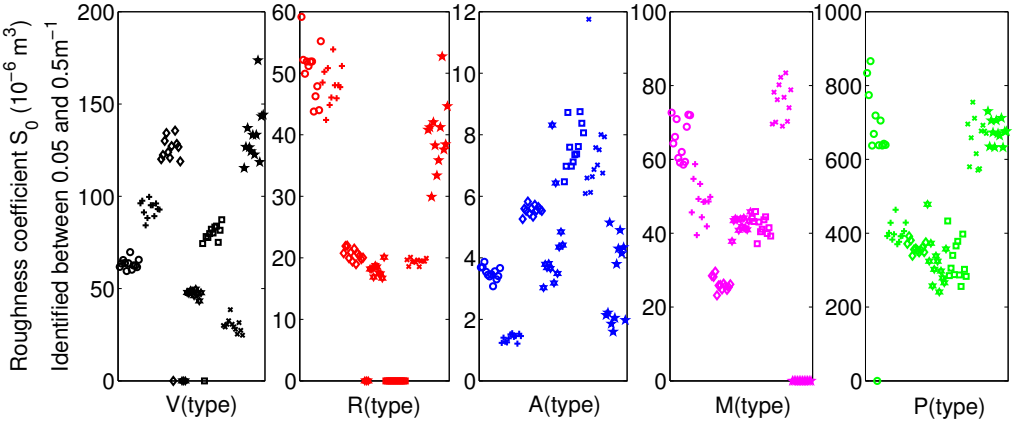

Figure 4.16: Results of the processing of the route imposed campaign, sorted by route type. The different marker symbols correspond to different circuits (7 for each road type). Note that vertical axes are not scaled identically as it would be less convenient for visualisation. Unusable recordings are associated to null roughness values.

Expectedly and reassuringly, results cluster around a similar S_0 value for the same circuit. However, the different S_0 estimates corresponding to the same circuit can exhibit a significant spread due to various reasons. First, even if the imposed route is identical, it is very unlikely that the driver has covered rigorously the same trajectory across $50km$. Secondly, as discussed in the previous chapter, the estimation method is not immune to the influence of speed and it is likely that the speed profiles are different when considering two recordings on the same circuit. Thirdly, even if a change in cargo is taken into account through a modification of the sprung mass of the model involved in the road estimation method, the estimation can still be affected.

Overall the results of the campaign's processing testify to the quality and usefulness of the road estimation method for studying the statistical variability of road profiles, at a relatively low cost and with no specific road measuring equipment. **This is a strong argument for the use of this road estimation algorithm within the context of the methodology proposed in this manuscript in order to analyse the variability of road-induced fatigue loads. Indeed, statistical information on road variability is crucially needed in this case**. This has been pointed out in our publication [Fauriat et al., 2016].

Let us recall that here the results are presented through S_0 in a visualisation-friendly representation but the full description of the road profile, *i.e.* $u(x)$, is in fact the direct output of the road estimation algorithm.

Second example: Processing of a route-free campaign

The considered campaign is made of multiple recordings. A given vehicle is lent to several customers, who were allowed to use the vehicle to their liking and covered multiple profiles with different lengths. The different response signals and the speed of the vehicle are recorded automatically when the vehicle is in use. Here, only the recordings associated to covered distances exceeding $10km$ are considered. As for the route-imposed campaign, the road estimation method is applied to each recording and the roughness coefficient S_0 is identified from the resulting road estimate. The results of the processing of the campaign are displayed in figure 4.17

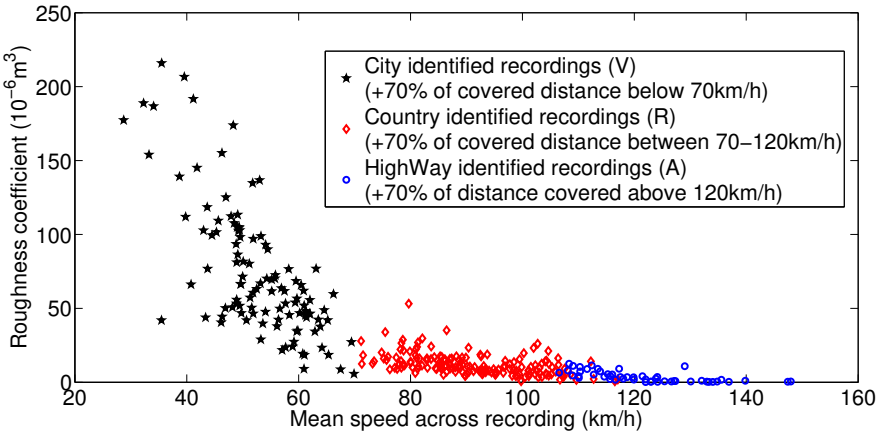

Figure 4.17: Results of the processing of the route free campaign. Each recording is at least $10km$-long. The identification of the route type is done *a posteriori*.

There is no particular route type associated to each recording since no particular information is provided by the driver who uses his vehicle normally. However it is interesting to proceed to an *a posteriori* classification of the recordings. The latter operation is here realised using a speed-based classification rule. Indeed, based on the observation of the speed profile, one can classify the different recordings, arguably in a somewhat subjective and rough manner, into a few categories. The rule is given and applied in figure 4.17. The recordings that did not meet any of the three classification criteria are not displayed. This approach is proposed here purely for visualisation purposes and is thus not discussed in more details here.

It readily appears that there exists a correlation between the road roughness and the speed of the vehicle, as discussed in subsection 4.4.3. Yet this correlation is visibly not linear and in this context it may be relevant to introduce different route categories. Within these different categories, the variation in the parameters of the road and speed stochastic models can be more easily related, in order to somehow account for this correlation. This will be further discussed in subsection 5.4.1.

The data provided by the route-free campaign is not put to further use within the boundaries of this chapter. It is nevertheless interesting in order to visualise the distribution of the roughness parameter S_0 across the different route categories. It has also been presented to illustrate (see figure 4.17) the correlation between road roughness and vehicle speed.

Dataset used for the selection of stochastic models for road and speed

In order to test the stochastic models proposed in this chapter against real (in fact estimated) profile data, a set of road profiles is extracted from the processed route-imposed campaign and used as a reference set for the multiple comparisons.

Three sets of twenty $10km$-long road profiles are manually selected from the different recordings in order to make sure that the latter correspond to different road profiles. Each of the three sets corresponds to a different route type, namely city roads (V), country roads (R) and highway (A), which totals to $200km$ worth of road and speed profiles for each of the different categories. The reference set is composed of a total of 60 (20×3) road and speed profiles.

4.5.2 Statistical characteristics of the estimated road profiles

Suitable criteria for comparison and analysis: 'constituting parameters'

The mathematical structures that have been introduced in this chapter as models for road profiles necessarily represent a simplification of a complex randomly varying quantity. A first approach to the validation of a selected stochastic model would be to make sure that randomly generated profiles and real profiles share the same 'statistical characteristics'. This is a tricky matter since the criteria for which a comparison can be realised are in part subjectively chosen, depending on the 'characteristics' that are considered relevant for the issue at hand. If a stochastic model is built to reproduce with fidelity these 'characteristics', then it can be seen as 'representative' of real profiles. Again, this is in part based on specific choices.

In this subsection, real (estimated) road profiles are displayed and the parameters of the different candidate structures proposed in subsection 4.3.3 are identified in relation with these profiles. The latter may somehow be considered as a description, based on a handful of scalar values, of the 'statistical characteristics' associated to a given road profile. They will be subsequently denoted as '**constituting parameters**' of the stochastic models, in the sense that they fully determine the road (and speed) model once a given model structure has been selected.

They are all displayed in figures 4.18, 4.19 and 4.20, respectively for three $10km$-long road profiles for which they are identified. These three profiles belong to three different route types (namely V, R and A). The one-line and two-line PSD models are compared

with the PSD estimate of the real (estimated) profile (left). The normalized variances are calculated on 200m-long sections of the profile (bottom right). Transients are identified using the approach proposed in subsection 4.3.3 and localized on the road profile (top right). All constituting parameters are displayed in the different figures.

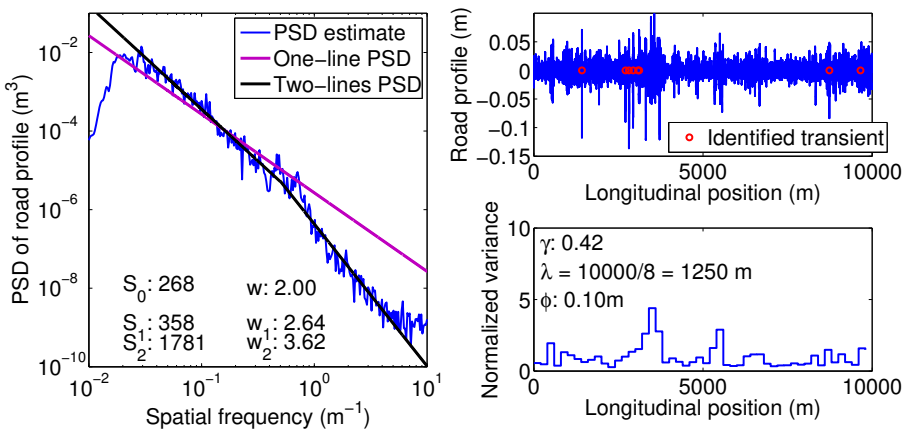

Figure 4.18: Statistical characteristics for a city road profile (V).

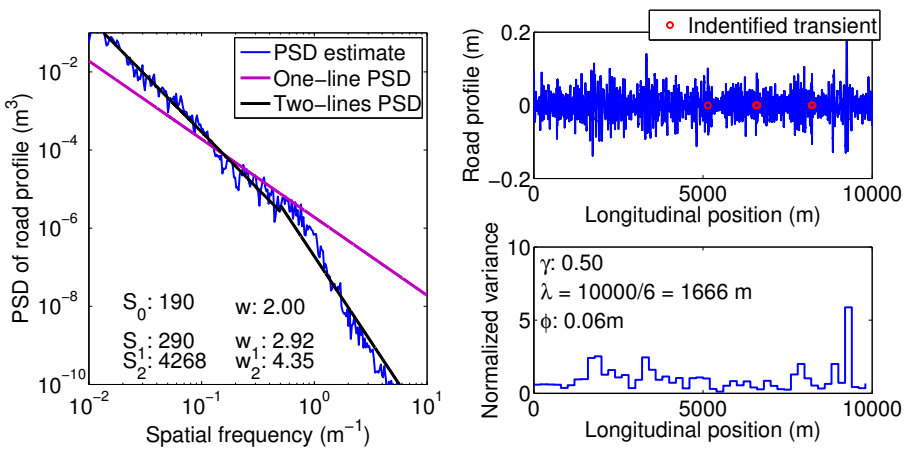

Figure 4.19: Statistical characteristics for a country road profile (R).

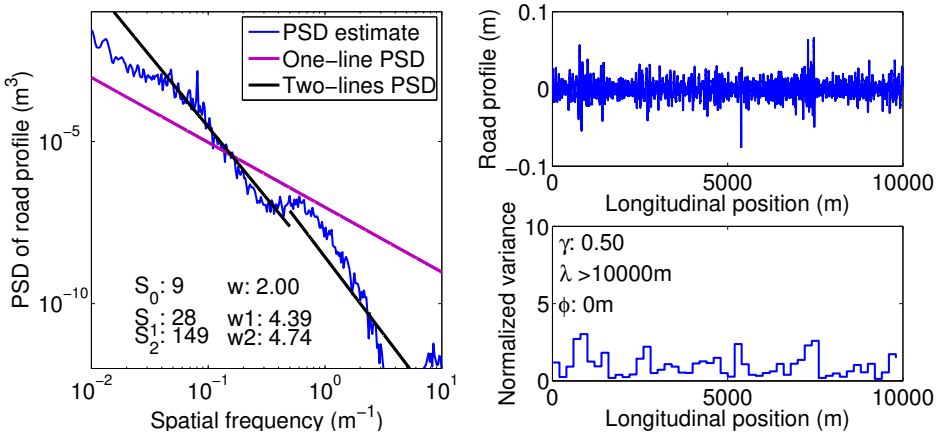

Figure 4.20: Statistical characteristics for a highway profile (A).

Let us point out that, for the one-line PSD model, $w = 2$ is willingly hold constant for all processed recordings, in order to allow one-dimensional comparisons such as those displayed in figures 4.16 or 4.17. However, w could easily be identified from each estimated profile in order to provide a better fit.

It is seen in figures 4.18, 4.19 and 4.20, that the PSD of the real road profiles can be significantly different from the one-line and two-lines models. It is also seen in these figures that real road profiles cannot really be described by a stationary process.

Variation in constituting parameters

The variation in the parameters of the fitted two-lines PSD model identified for each one of the 60 road profiles can be analysed. All values are displayed in figure 4.21. Let us recall that here the parameters are identified on $10km$-long profiles. It is seen that S_1, w_1 and w_2 span on quite large intervals and it could be shown that such a large variation in these parameters has an strong influence on the road-induced loads (see subsection 5.3.3). The significant variation of S_0 within each route category can also be observed in figures 4.16 or 4.17.

Owing to the strong observed variability of the constituting parameters within each route category, a set of difficult statistical questions can be laid out here:

- What is the appropriate profile length needed to identify each of the parameters of the model?
- Should one identify a unique set of parameters for each route category or consider that the constituting parameters (of the stochastic models) are themselves distributed? This is clearly observed when considering different realisations from a seemingly identical route category.

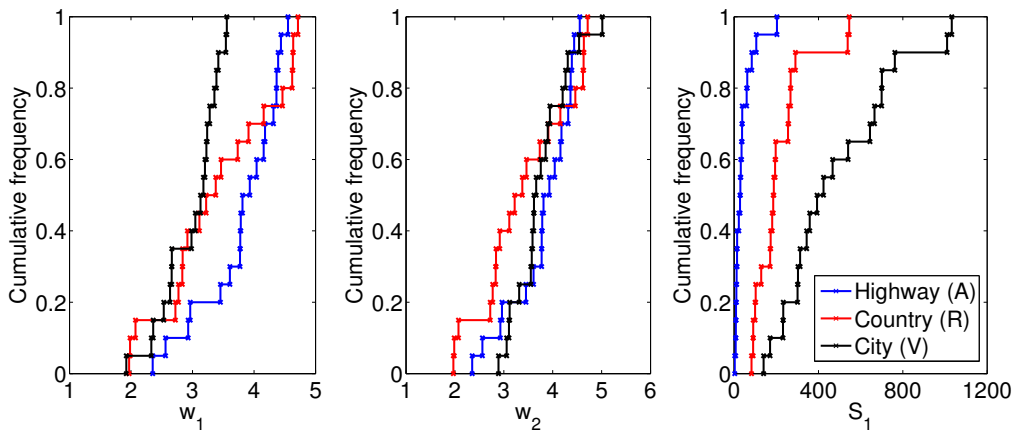

Figure 4.21: Variability of PSD parameters for 20 profiles of 3 route categories.

- Should certain parameters be considered as unique for a given route category while other are distributed? If so, how to decide which parameters are fixed and what is the appropriate length of profile needed to identify them?

There does not seem to exist perfect solution to this problem. It is necessary to chose a particular approach to handle this modelling issue that is relevant for the present context, while many approaches may be possible and reasonable. Indeed it can be expected that there is less variation in constituting parameters if they are identified over longer profiles. Yet the non-stationary character of the profile is likely to increase (the variation in road characteristics has to appear somewhere). In addition, simulations on very long profiles become more costly. Also in practice when acquiring road profile samples, it may be difficult to make sure that long profiles rightfully belong to an identified route category. Eventually, the different drivers of a population do not necessarily select the same routes, which may become a problem if the identification has provoked too much 'averaging'. These questions are discussed more thoroughly in subsection 5.4.1.

In what follows, all comparison are realised using $10km$-long road and speed profiles, for which constituting parameters are identified according to the methods described in subsections 4.3.3 and 4.4.3.

4.5.3 Selection of representative stochastic models for road and speed

Selection and validation framework

It is quite difficult to assert that a particular model leads to generate representative road profiles if this assertion is only rooted in the comparison of statistical characteristics such as the PSD, the variation in normalized variance or the average number of transients

contained within the profile. The use of a PSD-based representation, purely stationary or piecewise-stationary, and the use of a predefined transient form do constitute specific choices, which will unavoidably impose a particular structure on any generated realisation. Hence it is not guaranteed *a priori* that such realisations are representative of real profiles. To be convinced by this argument, suffices it to consider that very different road profiles may well possess a relatively similar PSD, as shown in figure 4.22. Consequently, **observing a match between a handful of selected statistical characteristics is necessary but not sufficient to declare that the model is appropriate**.

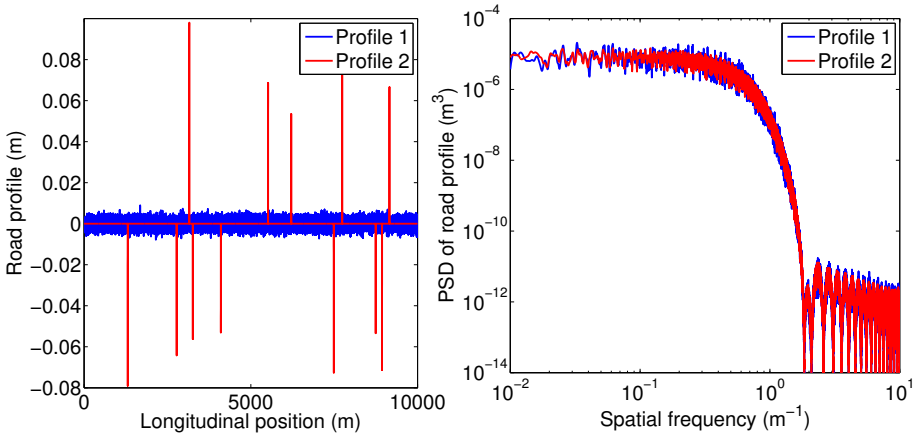

Figure 4.22: Illustrative example of the limits of the PSD-based description. An equivalence in terms of PSD, a so-called 'statistical characteristic', is not a guarantee that a PSD-based generated profile is a representative image of a real profile. Very different profiles may share a similar PSD estimate.

To better judge the quality of the profiles generated according to the proposed models, it is relevant to express the difference between randomly generated profiles and real profiles in terms of the effect they both have on the vehicle's responses, and subsequently on the damage accumulation. Damage-based criteria, which may be labelled as indirect criteria since they do not rely on the direct comparison of profiles, can provide a more exploitable information than a (direct) comparison of statistical characteristics. Such comparisons are also more appropriate to assess whether the proposed stochastic models are suited for the analysis of road-induced fatigue loads.

In view of proposing an objective and systematic approach for the selection of representative stochastic models, the following procedure is considered. For each one of the 60 road/speed profile pairs serving as references (20 for each route category), the constituting parameters of the tested stochastic model structures are identified, according to the inference techniques described in subsections 4.3.3 and 4.4.3 and as illustrated in figures 4.18, 4.19 and 4.20. Then, for each one of the 60 identified vectors of constituting parameters, 30 random realisations are generated from the considered stochastic models and fed into a linear quarter-car model to carry out 30 simulations. Each of the 60 real road/speed

profile pair (*i.e.* road excitation) is also fed into the same linear model to assess the corresponding damage-related values (in order to only compare simulated values and somehow limit the influence of simulation errors which are not the central focus here).

The damage equivalent amplitude (DEA), see subsection 2.1.3, is calculated from each considered response using the following relation and used as a scalar criterion:

$$y_{eq} = \left(\frac{\sum_{i=1}^{p} \Delta y_i^{\beta}}{n_{eq}} \right)^{1/\beta} \tag{4.23}$$

where $(\Delta y_i)_{i=1..p}$ are the amplitudes of the Rainflow ranges extracted from a given signal y. In this subsection, a number of cycles of $n_{eq} = 200000$ cycles is selected and a Basquin's coefficient of $\beta = 5.6$ is used. DEA are calculated for three response signals, namely the suspension displacement, the sprung acceleration and the unsprung acceleration.

Each set of 30 DEA calculated from randomly generated profiles is compared to the DEA corresponding to the associated 'real' road/speed profile pair. The operation is repeated for each of the 60 pairs (and thus for each associated vector of constituting parameters).

Application of the validation procedure

An example of the selection and validation procedure is given for a particular modelling hypothesis in figure 4.23, for the 20 city routes (V). The example relates to a piecewise-stationary road model based on a two-lines PSD, with no transients (R#3) and a piecewise-constant speed model (S#3).

The 20 city routes (V) are displayed sequentially on the x-axis (upper part of figure 4.23) and for each route, the DEA associated to the real road and speed profiles (in blue) is compared with the results of the 30 simulations (black diamonds spread vertically) based on randomly generated profiles and on a given vector of identified constituting parameters for the stochastic models.

Should the randomly generated profiles be a perfect representation of an observed road/speed pair, the average DEA calculated on the set of 30 simulations would be reasonably close with the damage corresponding to the real road/speed pair, and for all responses. This would mean that the selected stochastic models are an adequate representation of the profile pair used to identify their constituting parameters. Also, when considering the comparison of values across the complete set of 20 routes, the predicted DEA distribution based on the randomly generated realisations would be identical to the DEA distribution deduced from the exact 20 pairs of road/speed profiles (see lower part of figure 4.23).

The validation procedure and the selection of representative models is thus based on the comparison between both DEA distributions across the complete set of profiles

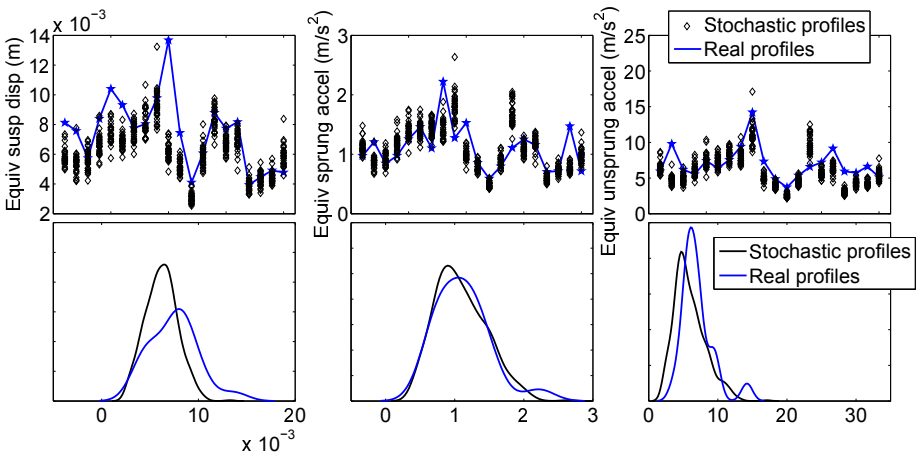

Figure 4.23: Illustration of the validation procedure for a given modelling hypothesis. The results correspond to the 20 city routes (V), displayed sequentially (upper part). Kernel density estimates (lower part) are used to visualise the empirical distribution of damage equivalent amplitudes for the complete set of 20 routes.

(3×20 profiles of $10km$). While a visual comparison is obviously fruitful, see figure 4.23, it is not easy to compare models in this manner. Hence, two criteria are introduced to allow a more quantified and objective comparison. Those criteria are respectively the empirical mean of the DEA distribution and its empirical 90% quantile (which is important for reliability analysis and gives a good idea of the scatter of values). All the different candidate stochastic models introduced in subsections 4.3.3 and subsections 4.4.3 are compared using these criteria.

An example of comparison is given in table 4.3 for the stochastic models considered in figure 4.23 and for all route types.

Road model	Speed model	Road type	Response signal	Real mean	Model mean	error %	Real q_{90}	Model q_{90}	error %
			$z_s z_t$	0.0075	0.0067	-10%	0.0098	0.0090	-8%
R#3	S#3	V	a_s	1.110	1.189	7%	1.472	1.718	17%
			a_t	6.998	6.529	-7%	9.396	9.954	6%
			$z_s z_t$	0.0078	0.0062	-21%	0.0113	0.0093	-17%
R#3	S#3	R	a_s	1.229	1.068	-13%	1.813	1.836	1%
			a_t	7.897	6.070	-23%	10.426	11.344	9%
			$z_s z_t$	0.0062	0.0053	-16%	0.0083	0.0093	12%
R#3	S#3	A	a_s	0.917	0.746	-19%	1.217	1.209	-1%
			a_t	5.804	3.854	-34%	6.728	6.056	-10%

Table 4.3: Example of the validation procedure for the candidate models R#3 and S#3. Comparison of mean and 90% quantile of the DEA distributions.

The simultaneous comparison of all candidate models and route types is displayed in figures 4.24 and 4.25 for the two different criteria.

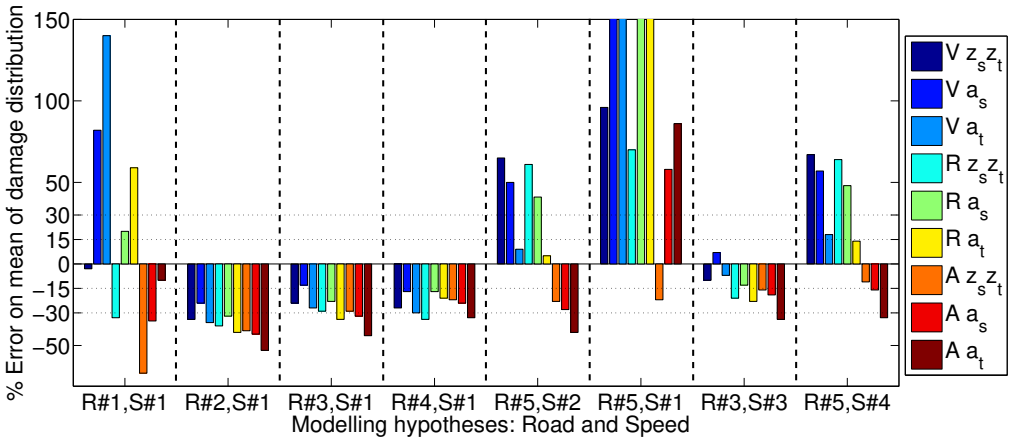

Figure 4.24: Comparison of candidate models: mean DEA criterion.

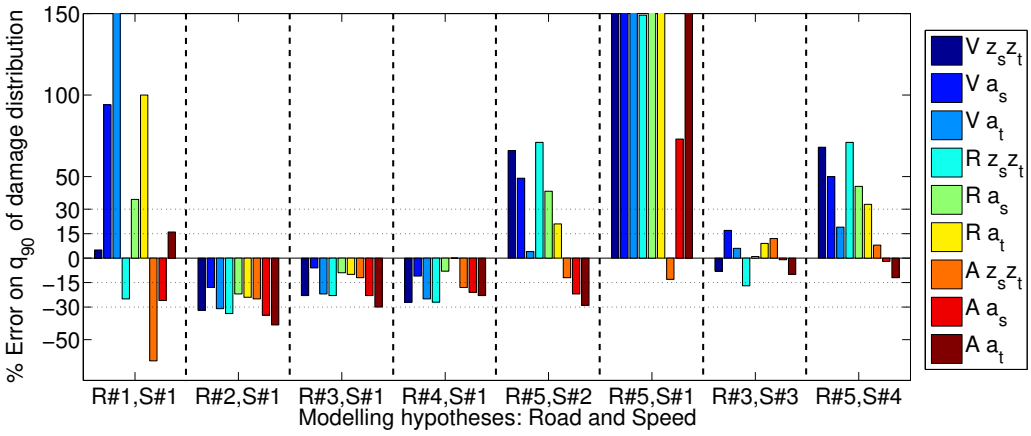

Figure 4.25: Comparison of candidate models: q_{90} DEA criterion.

Analysis of the results

The possible combinations of model candidates are not all displayed in figures 4.24 and 4.25 since the analyses are rather performed by comparing two model combinations (see below). The results of the comparisons seem to indicate that the more representative stochastic models for road and speed are:

- (R#3) A piecewise-stationary road model based on a two-lines PSD description, a gamma distribution of the normalized variances and no additional transients. It

involves 4 parameters, namely S_1, w_1, w_2, γ.

- (S#3) A piecewise-constant speed model, based on segments whose length is distributed exponentially and correlated to the speed on that segment. It involves 4 parameters, namely v_m, s_v, θ, ρ_{ls}.

For these models, the numerical results are displayed in table 4.3. For the high quantile value q_{90}, which is of great interest for durability analyses, most of the results are within a $\pm 15\%$ margin of error.

Several remarks can be made from the analysis of figures 4.24 and 4.25. First it appears quite clearly that a one-line PSD model (R#1) constitutes a too crude representation of the frequency content of the profile since it will sequentially underestimate or overestimate either the low or high frequency content and impact one or more response signals. Secondly, it appears that **a stationary model** (R#2) **systematically underestimates the damage due to unaccounted high variance sections**. Thirdly, the comparison between the two-lines PSD (R#3) and the generations obtained using the full PSD (this is no longer a model) of the observed profile (R#4), shows that the difference is quite small. This points to the conclusion that **the two-lines PSD is an acceptable simplification of the full PSD**, which introduces relatively little error.

Eventually, on the subject of transients, it is quite obvious that if such transients are added to the generated road profiles (R#5), a speed model with no account for the road/speed correlation (S#1 or S#3) is no longer a viable option. The results are much better when this correlation is handled by an appropriate speed model (S#2 or S#4). It is seen that transients can account for a significant part of the damage. Nonetheless, **the stochastic description proposed here for transients appears appears to be unsatisfactory**. **The correlation between road and speed in the vicinity of transients is particularly difficult to model and yet very influential**. It can easily be argued that the diversity of behaviours within a population of drivers is large. Also, using a single generic form, namely $x \mapsto e^{-x^2}$, as a model for all transients is a strong hypothesis.

The modelling of transients (and road/speed correlation in their vicinity) could possibly be improved. However, any improvement will likely be synonymous with a **higher complexity of the models and a need for more extensive information** about the diversity of behaviours within the population of drivers. Let us point out that the results in terms of damage seem highly sensitive to the constituting parameters linked to transients (in particular ϕ and v_{tr}) and consequently to the modelling hypotheses that are selected to describe the latter. When synthesizing transients, it is easy to unwillingly introduce very high levels of damage. This make the modelling of transients a difficult and sensitive issue.

Let us provide a partial justification for the preference of road and speed models disregarding transients. Even if real road profiles clearly contain transients and if disregarding them within the stochastic road model constitutes a notable discrepancy, the fact that

drivers adapt their speed in the vicinity of transients diminishes their influence on the vertical excitations. Also, if transients are not included in the road model it becomes unnecessary to adapt the speed model for them. Moreover, for the piecewise-stationary road model proposed by [Bogsjo et al., 2012], occasional high variance sections that can be generated through the gamma distribution may be seen as 'rough' sections, which could somehow be interpreted as a collection of transients (even if they are less severe than synthesized transients of the form $x \mapsto e^{-x^2}$).

4.6 Synthesis and conclusion

In this chapter, a precise definition of road roughness and vehicle speed, both considered as factors which determine the statistical variability of road-induced fatigue loads, has been given. It has been shown that such factors are continuously varying quantities and that their representation, or modelling, involves stochastic process theory. Here, the purpose of stochastic models is to be able to generate representative trajectories of those continuously varying quantities, *i.e.* trajectories that reasonably resemble the road or speed profiles that could have been measured in practice. The objective is also to construct a parsimonious representation, *i.e.* based on a handful of parameters, which nonetheless provides a quantitative and tractable description of the significant statistical variability that exists when studying such factors across the complete life of one or several vehicles.

Multiple stochastic model candidates have been either selected based on the study of existing literature or proposed based on empirical analysis of available road and speed profile data. Here, the available data originates mostly from existing load measurement campaigns. While the vehicle's speed is directly recorded, the road profile is not readily accessible and must be estimated using the road estimation algorithm proposed in the preceding chapter 3. Existing data from load measurement campaigns has been processed with such an algorithm in the present chapter.

The selection of an acceptable model and the validation of its 'representativeness' have been performed based on real profile data and based on two types of criteria. First, a few selected 'statistical characteristics' deemed relevant for the issue, are compared. Second and most significantly, response-based (DEA) criteria compared between real profiles and randomly generated profiles allow us to asses more objectively the effect of potential discrepancies between the profiles, in terms of the damage accumulation that they induce on the vehicle. **A testing and selection procedure has been presented here**, using a reference dataset which regroups 60 estimated road profiles ($10km$-long) and measured speed profiles within different route categories. This study offers an objective approach to judging the multiple candidate models and assessing their fidelity.

As far as road roughness is concerned, the selected stochastic model structure relies on a spatial frequency-based description, thus involving the use of power spectral density (PSD), for which an analytical model (3 parameters for a two-lines PSD where the

connection between the two lines is imposed) can be proposed, through the analysis of measured road profiles. However, as a realisation generated solely from a PSD description is naturally stationary, a given strategy has been proposed to handle the non-stationary character of real roads that is observed in practice. This strategy involves the application of a set of modulating coefficients drawn from a one-parameter Gamma distribution of unitary mean, which do not alter the PSD target identified on the (long) complete profile, while accounting for possibly 'rougher' sections. **The selected model is thus a piecewise-stationary Gaussian process based on 4 parameters denoted** S_1, w_1, w_2, γ.

As far as vehicle speed is concerned, **the selected stochastic model is made of a piecewise-constant process**, randomly switching between normally distributed speed values (2 paramters) at spatial positions distributed according to an exponential distribution (1 parameter). The length of a given section depends (1 correlation parameter) on the current speed on this constant speed section. The model is only concerned with reproducing the statistics of observed speed profiles, where the vehicle evolves between almost constant speed states, while it disregards the underlying causes for the speed value to switch. The latter include external causes such as the route topology, traffic regulation or traffic flow, and behavioural causes such as the driver's care for comfort, safety, trip duration, fuel saving, vehicle durability, and so on. The selected model is thus based on 4 parameters denoted v_m, s_v, θ, ρ_{ls}.

The correlation between roughness and speed that is observed in practice, especially in the vicinity of severe transient patterns, where the driver generally adapts its speed to avoid serious discomfort or damage, has been discussed. It has been seen that modelling both transients and the reduction of speed that they imply is a rather complicated issue since it can be very sensitive to the choice of model and parameters. Additionally, the effect of transients on the vertical excitation is naturally decreased by the correlation between road and speed profiles that occurs with real drivers. Consequently it has been decided not to artificially synthesize transients. Also, the different results indicate that the candidate model structure proposed in this chapter for transients is not satisfactory.

Furthermore, **a correlation between road and speed factors is naturally imposed by the division of their 'domain of variation' into several categories** (*e.g.* city route, country route, highway route, etc.). The use of different categories of routes, or types, is related to the notion of life situations, introduced in the following chapter. Through this operation it is easier to handle the variation of the constituting parameters of stochastic models. Methods for the identification of such constituting parameters, using available profiles in those categories, have been described in relation with the proposed models. Nonetheless, it has been seen that within the boundary of each of these categories, a strong scatter can be observed for the parameters identified on $10km$-long sections of road and speed profiles.

Let us close this chapter by discussing limitations. **It is difficult to 'rigorously validate' the selection of a stochastic model and the best that can be done is to compare randomly generated realisations with real profiles according to**

criteria that have been deemed relevant for the application at hand. Also the selection of a model is difficult in the context of complex and strongly varying phenomena and when few data is available. Consequently, the candidate structures proposed in the present manuscript may not be optimal solutions. Complex statistical questions have been raised, when discussing the variability of the identified and quite scattered **'constituting parameters'** of stochastic models as well as discussing the length of the samples to consider. The use of such parameters arguably represent a simplification, in the form of a parsimonious description, which can be useful to describe the variability of road and speed profiles across the complete history of different vehicles. Yet there does not seem to be a perfect or generic answer to such a complicated characterisation issue.

Overall the stochastic models (*i.e.* mathematical structures) eventually selected for road and speed are thought to be reasonable compromises (complexity versus representativeness) in view of the data at hand.

To remember

- Road and speed profiles are continuously varying quantities and can be modelled as realisations of stochastic processes.
- Multiple candidate model structures have been proposed, based on the analysis of literature and on the analysis of available road and speed profile data.
- Road and speed stochastic models have been selected based on a comparative study between randomly generated realisations and real profiles, according to both statistical and response-based (using a linear quarter-car model) criteria.
- The selected road model is a piecewise-stationary Gaussian process with a PSD model using power laws with negative exponents. It is described by 4 parameters.
- The selected speed model is a piecewise-constant process where a correlation is imposed between the length of constant speed sections and the speed on such sections. It is described by 4 parameters.
- No specific correlation model between road and speed profiles has been proposed.
- No satisfactory model has been found for transient patterns such as speed bumps or pot-holes. Their influence is naturally diminished since drivers adapt their speed to cover them. They are disregarded here.
- The parameters of stochastic models are labelled as 'constituting parameters'. They represent a parsimonious (8 parameters) description of complex continuously varying quantities. When identified on $10km$-long sections, a strong scatter is observed for such parameters.
- Different route categories may be defined and the variation of constituting parameters within each category is generally reduced.
- It is difficult to rigorously and objectively validate a stochastic model. The best that can be done is to compare randomly generated profiles to real profiles according to some chosen criteria.

Chapter 5

Stochastic simulation of road-induced fatigue loads

Contents

5.1 Introduction **131**
5.2 Proposed methodology for load characterisation **132**
5.2.1 Variability of loads and reliability concerns 132
5.2.2 On the characterisation of loads: diversity and life situations 132
5.2.3 Proposed methodology: stochastic simulation of road-induced loads . . 135
5.3 Testing of the proposed stochastic simulation methodology **140**
5.3.1 Available data for testing and statistics on input parameters 140
5.3.2 Comparison of predicted and observed (measured) load variability . . . 144
5.3.3 Comparison of predicted and observed load sensitivity 149
5.4 Prediction of the load life of vehicles **153**
5.4.1 Statistical analysis and extrapolation 154
5.4.2 Study of extrapolation hypotheses 160
5.4.3 Prediction of the life of a population of vehicles 163
5.5 Application of stochastic simulation for reliability analysis **167**
5.5.1 Design of reliable components and vehicle development process 167
5.5.2 Realisation of different stochastic simulation campaigns 168
5.5.3 Modifications of influential factors and reliability assessment 170
5.6 Synthesis and conclusion **172**

"As far as the laws of mathematics refer to reality, they are not certain, as far as they are certain, they do not refer to reality."
Albert Einstein

5.1 Introduction

In order to design vehicle components that meet specific reliability requirements, it is imperative to possess a precise description of the variability of the loads applied on such components. Among a population of vehicles associated to different customers, each defining a particular usage for his vehicle, the load histories experienced by different components are arguably extremely diverse. Attempting to either record or propose a descriptive model for the variation of multiple mechanical responses throughout the complete life histories of many vehicles, is a formidable task. Consequently, **the analysis of road-induced load histories necessarily implies both some form of simplification regarding the issue of load characterisation and the use of specific statistical methods**.

Generally, the acquisition of information about road-induced loads is based on **measurements of load histories** within the population of vehicles (customers). Essentially, this may be considered as an operation of sampling from the (theoretical) set of all possible loads. The selection of relevant samples and the processing of the information contained within these samples is a complicated issue, which is discussed here. It is nevertheless an unavoidable step in the pursuit of a quantitative description of the load history of vehicles. The **division of the life of vehicles into different 'life situations'** is an interesting approach to consider in this context.

The research work described in this manuscript is based on the core idea of concentrating the statistical analysis and probabilistic modelling efforts on the influential factors determining the evolution of road-induced loads, namely road and speed variations, rather than sampling from the set of possible loads directly. Stochastic models are used to generate random realisations of road and speed profiles and the latter are subsequently used to perform vehicle dynamics simulations. Through this approach, an arbitrarily large set of load histories can be generated rather inexpensively and for a vehicle with any given characteristics, using simulation. The proposed methodology essentially consists in **combining the use of dynamics simulation and the use of stochastic modelling** (of input factors). Statistical analysis methods can then be applied using this constructed set of load histories, as they would be applied if the data originated from measurements instead of simulations.

The outline of the present chapter is as follows. A presentation of different load sampling approaches is given in section 5.2 and the notion of life situations, composing the vehicle's history, is introduced. The stochastic simulation methodology proposed within this research work is then detailed in the same section. In section 5.3, stochastic simulations are carried out, exploiting statistical information on input parameters that is extracted from real measurement campaigns. The methodology is tested through the comparison of both the damage distributions obtained from simulations and from measured data. The comparison of both the predicted and observed sensitivities to influential factors is also carried out. In the following section 5.4, the simulated sets of loads are used to make predictions for the complete life of vehicles. The statistical hypotheses associated to such predictions as well as the quality that they can achieve, are discussed. Eventually,

in section 5.5, all the introduced methods are employed to address practical questions in the framework of reliability analysis, design and validation. All important concepts and remarks are summarized in section 5.6.

5.2 Proposed methodology for load characterisation

5.2.1 Variability of loads and reliability concerns

Let us first remind that the end purpose of the present work is to analyse the reliability of vehicle components and that the attention is centred here on vertical excitations and on potential failures due only to fatigue, see subsection 2.3.1.

The fatigue phenomenon described in section 2.1 is inherently a cumulative phenomenon and it is thus imperative to analyse complete load histories, up to the point when a reliability assessment is proposed. Also, in most practical cases, fatigue analysis is intimately linked with randomness since loads are seldom perfectly repeatable in a real environment and the strength of given materials is subject to scatter. Consequently, any analysis of the reliability of a population of vehicle components compels to work with statistics and probability theory and within a cumulative framework.

Many probabilistic-based approaches are commonly used in the context of fatigue theory, see *e.g.*, [Dirlik, 1985], [Pitoiset, 2001], [Benasciutti and Tovo, 2005]. However, in these latter references focused on fatigue life calculation methods, the load is assumed to be well known. Conversely in this manuscript, **the main purpose is to gain knowledge about the variability of loads, both across their complete history for a given vehicle and between different vehicles within a given population.**

Both a quantified description of the variability of the loads experienced by a given component and a quantified description of the scatter observed with respect to the strength of such a component, are absolutely necessary if any reliability prediction within a population of interest is to be made. While these two elements are required, only the first part of the problem, namely **load variability**, is tackled in this manuscript.

It is quite convenient to quantify load variability in terms of one or several scalar criteria since the latter are more adapted for statistical processing, analysis and interpretation. Generally, this may be done through the use of pseudo-damage values or damage equivalent amplitudes (DEA), see subsection 2.1.3, based on the combination of Rainflow cycle counting, Miner's rule and a Basquin's model for the material's fatigue life.

5.2.2 On the characterisation of loads: diversity and life situations

In order to acquire information about the load variability experienced by vehicle components, it is necessary to collect load histories within the population of vehicles (and related customers/drivers) that is studied. As the diversity of loads is expected to be

large and as vehicle lives represent extremely long load histories, it is important to choose wisely the load histories that are collected. **For practical reasons, such histories are necessarily of limited length and the life of the vehicle is necessarily divided in shorter segments**. Different approaches can be considered when it comes to selecting and collecting 'relevant samples' of load histories within the population.

Sampling strategies

The first and most straightforward method consists in recording loads for different customers of the population and for a sufficiently long fraction of the life of the vehicle. In practice, a particular vehicle is selected, equipped with multiple sensors and handed over (sequentially) to a sample of customers, which can use the vehicle as they desire. In statistical terms, **this can be viewed as an operation of random sampling from the theoretical set of all possible load histories**, *i.e.* vehicle lives. This approach is costly. Indeed, load histories are often extremely variable across time, as well as very diverse from one vehicle to another. This tends to increase the need to record long fractions of the life of vehicles and it implies that the size of the sample has to include numerous drivers in order to emulate the life of different vehicles.

Another approach to the issue of load characterisation can be considered. It is **based on the use of additional knowledge regarding vehicle lives and on the concept of life situations**. Such an approach is largely used, see for example [Thomas et al., 1999], [Heuler and Klätschke, 2005] [Johannesson and Speckert, 2013], either for cars or other mechanical structures, when life situations, phases or sequences can be clearly identified. As an example, for an air-plane it is quite obvious that the loads undergone during the take-off, in-flight and landing phases will be both very different and quite distinguishable. Yet, they should all be accounted for, as their cumulative effects inflict damage on the components. Similarly, vehicles' load history may be decomposed into an arrangement of identifiable situations.

On the one hand, the relative proportion of the different situations composing the life of a vehicle can be assessed, *e.g.* through surveys, without necessarily implying measurements. On the other hand, the variability of the loads within each life situation may be analysed independently. Generally, an instrumented vehicle is used to perform measurements within each life situation. Statistical information regarding the complete load history of vehicles is subsequently derived through the combination of both sources of knowledge. This approach may be seen as an application of the principle of **stratified sampling** [Neyman, 1934]. In this framework, life situations constitute the so-called 'strata' within the 'population of loads'.

The division of the life of vehicles (say a few hundred thousand kilometres) into shorter and measurable segments (say a few hundred kilometres at most), possibly corresponding to multiple life situations, is illustrated in figure 5.1. The variability in load history between one vehicle and another is partly related to the variability in the relative proportions of the different life situations.

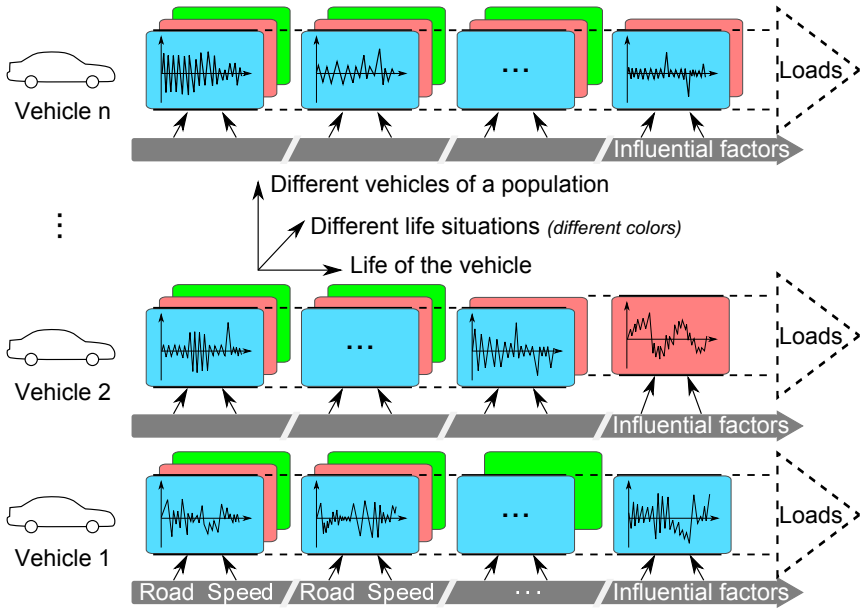

Figure 5.1: Division and characterisation of vehicles' load life.

Let us assume that the load associated with a given life situation can be express as a scalar value d_i, as discussed in section 5.2.1. Also, let us define α_i as the relative proportion of this life situation among the complete load history of the vehicle. The value characterising the load over the complete history of the vehicle d_{tot}, is then simply derived through the sum of the different contributions:

$$d_{tot} = \sum_{i=1}^{p} \alpha_i d_i \tag{5.1}$$

where p is the number of life situations and $\sum_{i=1}^{p} \alpha_i = 1$. For a given vehicle (customer), both $\mathbf{d} = (d_i)_{i=1,\ldots,p}$ and $\boldsymbol{\alpha} = (\alpha_i)_{i=1,\ldots,p}$ are vectors of random values. As an illustration, throughout this manuscript the following life situations are defined. Five route (travel) types are considered, namely city, country, highway, mountain and off-road travels. For each of these route types, three levels of cargo are selected, namely empty vehicle, half cargo and full cargo. This totals to 15 different life situations.

Interests and limitations of the stratified sampling approach

Statistical data on the relative proportions of different life situations $\boldsymbol{\alpha}$, for different customers of a population, represent **very valuable information about the lives of vehicles**. The former data is often available, through surveys, much more cheaply than measurements on an instrumented vehicle. It thus represents an opportunity to characterise more extensively the variability of vehicle lives within the population.

Life situations are in fact generally defined (and identified) through the specification of a domain of variation for influential factors (see figure 5.1), such as the type of road being covered or the type of speed profile (*e.g.* low speed in city traffic, high speed on a highway travel). **The information on the relative proportion of different life situations thus constitutes knowledge on the variability of influential factors, namely road and speed profiles, throughout the life of the different vehicles of the population**. Hence, stratified sampling and the concept of life situations are very interesting when they are combined with the analysis of the variability of influential factors. This is an important part of the methodology that is proposed in the following subsection, in association with stratified sampling.

It is relevant to note that the division of vehicles' load history and in consequence the definition of each life situation, is based on *a priori* choices and hypotheses. Indeed, the life of a vehicle is not necessarily a clear succession of distinct segments but a continuum. In practice it may not be easy to objectively define the boundaries of life situations or to assess unambiguously the relative proportion and load contributions corresponding to each life situation. Also the definition of life situations should be realised so that surveyed customers can clearly identify the different situations and asses their relative proportions.

Stratified sampling is particularly effective when customer usage variability, *i.e.* the variability in $\boldsymbol{\alpha}$ among a population of customer, is a strong contributor to the overall variability of load histories. If the load values d_i associated to each life situation correspond to significanlty distinct strata, then the overall load variability is almost entirely due to the variability in the proportions $\boldsymbol{\alpha}$, though equation (5.1). Conversely, if the distributions representing each d_i value are strongly overlapping (*i.e.* if life situations are not very distinct), then information about the relative proportion of each situation is of little use.

Indeed, it is not very helpful to identify the proportion of different situations if they contribute similarly to the load history of the vehicle. In such a case, stratified sampling has no particular advantage over random sampling. Two examples are given in figure 5.2. In the first case (left), the effectiveness of stratified sampling can be high and in the second case (right) it is likely quite poor.

Further discussions about the division of the lives of vehicles, the associated statistical hypotheses and the prediction of vehicles' load life (see figure 5.1) are proposed in subsections 5.3.1 and 5.4.1.

5.2.3 Proposed methodology: stochastic simulation of road-induced loads

The proposed methodology of stochastic simulation of road-induced loads is the backbone of the present manuscript and is described in this section. A synthetic representation of the methodology is shown in figure 5.3 where all the different and necessary elements for the application of the methodology are displayed.

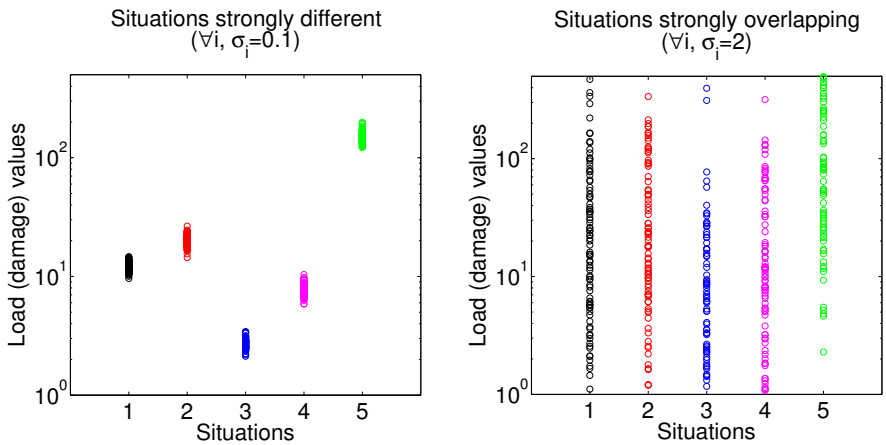

Figure 5.2: Illustration of the heterogeneity of strata. On the right-hand side there is no strong distinction between all strata and stratified sampling represents no particular advantage over random sampling.

Description of the proposed methodology

Putting aside difficult statistical questions, the principle of the methodology is quite straightforward. **Essentially, the methodology is based on the coupling of stochastic modelling of influential factors, namely the variation in road and speed profiles, with vehicle dynamics (multi-body) simulation.** It aims at characterising load variability through the use of simulation rather than measurements on an instrumented vehicle. Also, the methodology proposed here is applied in the framework of the stratified sampling approach described in section 5.2.2. Thus, the methodology may be thought of as an analogy to traditional load measurement campaigns based on stratified sampling, see *e.g.* [Thomas et al., 1999, Johannesson and Speckert, 2013], but in the domain of simulation. This simulation-based methodology has been presented in [Fauriat et al., 2015b].

In order to recreate, through simulation, a representative image of the loads that could have been measured in practice within a given life situation, it is imperative to possess both:

- **A representative description of the evolution of influential factors, namely road roughness and vehicle speed.**
- **A representative model of the dynamic behaviour of the vehicle (including knowledge of its cargo).**

For each life situation, **random realisations** (trajectories of the continuous stochastic processes) **are generated using the selected stochastic road and speed models** (see chapter 4). **The random road and speed profiles are then used to perform**

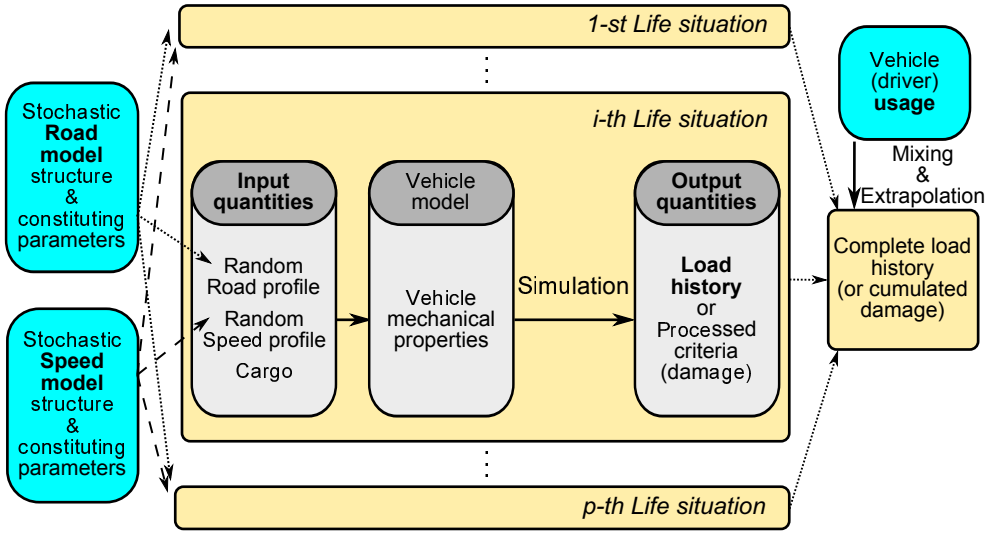

Figure 5.3: Synthetic representation of the proposed stochastic simulation methodology.

vehicle dynamic simulations. Mechanical responses (*i.e.* displacements, accelerations) on the vehicle can be evaluated for any degree of freedom (DoF) of the model. As discussed in subsection 2.1.3, mechanical responses may be considered as an information on the loads that are applied on certain components of the vehicle. The model selected here to describe the dynamics of the vehicle is a linear quarter-car model, described in subsection 2.3.2. Its mass characteristics are adapted depending on the value of the cargo. The complete process is illustrated in figure 5.3.

The combined use of stochastic modelling and simulation is discussed in several references, see *e.g.* [Cebon, 1999, Sun, 2001, Ferris, 2004, Bogsjo et al., 2012]. However, to best of the author's knowledge, there is no existing example of a comprehensive approach based on simulation, which purpose is to acquire a quantitative (statistical) description of load variability among a population of vehicles.

In order to obtain quantitative information about load variability through the use of the proposed methodology, **it is nevertheless imperative to possess a precise description of the variability of influential factors within the population of vehicles**. A **road estimation algorithm** has been proposed in chapter 3 in order to gather the statistical data that are needed to identify the constituting parameters of the stochastic road model and study their variation between (and potentially within) the different life situations.

Eventually, the combination of the load (statistical) information derived from simulations with the statistical data acquired on vehicle usage variability, *i.e.* the relative proportions $\boldsymbol{\alpha}$ of the different life situations and their distribution, as well as the extrapolation to a given target mileage (usually high, say $200000km$), are also displayed in figure 5.3 ('mixing and extrapolation') since they are a part of the methodology. Nevertheless,

such treatments are not necessarily specific to a simulation-based approach and also have to be carried out when the load information originates from measurements (in a stratified sampling framework). Thus, they are of no particular interest in the current section and are rather discussed along with the statistical hypotheses to which they are related, in subsection 5.4.1. Elements about the division of vehicles' life and statistical sampling have also been introduced in subsection 5.2.2 and are further discussed in subsection 5.3.1.

Simulation-based paradigm and interest of the methodology

The core conceptual idea underlying the proposed methodology as well as the complete work presented in this manuscript, and published in [Fauriat et al., 2015b], is the following. **The objective is to concentrate the statistical analysis and probabilistic modelling efforts on influential factors**, (input quantities from the standpoint of vehicle dynamics) **rather than sampling directly from observable load histories** (output quantities), traditionally acquired through measurements. Once values are defined for road roughness, vehicle speed and cargo, the mechanical loads (output quantities) are completely determined and their value can be accessed through simulation, provided the simulation tool is sufficiently representative. This simulation-based paradigm offers numerous interesting advantages and perspectives.

First, **road and speed profiles are vehicle-independents factors and consequently loads can be derived through simulation for any given vehicle** (and related component) with known mechanical characteristics. Conversely, with measurements, any acquired load history is dependant on the characteristics of the vehicle used for the measurements. Also, in early design phases, when a vehicle is not available, a simulation-based approach is the only conceivable solution to obtain load information that is adapted to a vehicle (and related component) of interest. Measured loads are of no particular value if one parameter of the vehicle dynamics is modified.

Second, since measurements are inevitably costly and time-consuming, the size of collected load samples is naturally limited to a 'reasonable number'. It is not the case with the proposed methodology where, provided sufficient information on input parameters is available, **an arbitrarily large set of load histories can be generated through simulation**. Concerns about computer time and cost are minor in comparison with the cost of measurements. As a consequence and again if the knowledge on input parameters is sufficient, a more extensive analysis of the 'population of loads' can be derived from simulation than from measurements.

Third, with simulation it is much easier to control input parameters than with measurements. **This allows us to willingly variate input parameters for sensibility analyses** or in view of carrying out comparisons between different life situations or between clearly defined loading environments, *e.g.* new markets or new populations of customers. By comparison, it would be both extremely costly and difficult to set up sensitivity analyses using measurements.

Fourth, it is possible to capitalize knowledge when considering influential factors, *i.e.* build databases or carry out statistical analysis, and **it is often more easy to propose a knowledge-based stochastic model for those factors**, rather than for loads. Indeed, the latter are the results of a complex combination of the previous factors and of the dynamic behaviour of a specific vehicle.

Fifth, it is not always possible or **it may be very costly to acquire certain response signals of the vehicle using sensors**. With simulation, if the model is accurate enough and sufficiently detailed, any response signal can be calculated regardless of such practical considerations.

To sum up, the major interests of the stochastic simulation methodology which couples simulation with statistics, are its ability to **extract valuable information about the loads acting on any vehicle, from the processing of large volumes of statistical information (if available) on the environment of such a vehicle (road roughness, drivers' behaviour), in a rapid, inexpensive and flexible manner**.

Possible difficulties and limitations

A simulation-based approach has multiple advantages over a traditional load measurement campaign, but it also presents some limitations and sources or error, which should be underlined.

First and most obviously, any result from the stochastic simulation methodology is depending on the quality and fidelity of the selected dynamic model for the vehicle. The choice of the model has to take into account both the need for representativeness of the model but also the computer intensiveness of the simulation. Indeed, as the objective is to carry out a large number of simulations (Monte-Carlo/Sampling-based approach), the calculation cost can be an important concern here, even if the cost of measurements is generally much higher. Additionally, the behaviour of the vehicle is in fact often strongly non-linear as it involves geometrical non-linearities (suspension geometry) and mechanical non-linearities (friction, non-permanent contacts due to 'stop' components, elasto-plastic components, etc.), see subsection 2.3.2. The behaviour of the tyres is also quite complex. Moreover the contact with the road is not necessarily permanent.

Second, as discussed in chapter 4, the selection of particular structures for both the road and speed stochastic models, as well as for the correlation between them, is a very involved issue. Any model necessarily involves simplifications (*i.e.* choices), in the search for mathematical tractability, with respect to the observed variability of real quantities. As the variability of road and speed profiles is particularly large, it is difficult to rigorously validate the choice of a given model.

There is a clear trade-off, when comparing simulation and measurement-based load characterisation. Measurements are more accurate and necessarily realistic as far as the variation of influential factors goes, but they are costly and quite restrictive as they depends on a selected measurement set-up (and vehicle). **Simulations are much more**

flexible, fast, cheap and allow us to process statistical information more extensively, but they may induce modelling issues, either stochastic or related to dynamic simulation.

5.3 Testing of the proposed stochastic simulation methodology

The methodology proposed in the present manuscript for the purpose of load variability analysis has been fully described in subsection 5.2.3 and is summarized in figure 5.3. The main objective of this section is to test and validate the ability of the methodology to make representative predictions in terms of load histories and subsequently, in terms of load variability. Additional details are given regarding its practical implementation and the calculations that are carried out. The methodology is tested against datasets acquired by Renault within the context of conventional load measurement campaigns, see *e.g.* [Thomas et al., 1999].

5.3.1 Available data for testing and statistics on input parameters

Two load measurement campaigns are **considered as a source of data for the testing of the methodology.** They are route-imposed campaigns (see 4.5.1) carried out by Renault in two different countries. In this framework, the type of the route associated to each recording is known *a priori*, since the circuit is purposefully selected to match a given category. The route types include city (V), country (R), highway (A), mountain (M) and off-road (P) circuits.

For the stochastic simulation methodology, such campaigns **'can' represent a source of statistical information on influential factors**. Speed-related information is readily available since vehicle's speed is directly recorded. On the other hand, road-related information is accessed through the application of the road estimation method (see chapter 3) on the different recordings. The latter include vertical accelerations sensors for the sprung and unsprung masses, as well as suspension displacement sensors. For recordings associated to different vehicle cargo (empty, half-full and full), the correct value is provided to the estimation algorithm.

In this section, the testing of the methodology is performed for five life situations, associated to the different route types. When performing stochastic simulations, the cargo of the vehicle is selected randomly among three values corresponding to three level of cargo, namely empty, half-full and full.

Processing of the recorded data

Each road/speed profile pair obtained from the different recordings is used to calculate the constituting parameters of the stochastic models selected in chapter 4, through the inference approaches proposed in relation with such models. To be more specific, for each recording, road/speed profile pairs corresponding to $10km$ are extracted (generally 4 or 5 profiles out of an approximately $40/50km$-long recording). A vector of constituting parameters is identified for each pair, namely $\{S_1, w_1, w_2, \gamma, v_m, s_v, \theta, \rho_{ls}\}$, see chapter 4.

The results of the processing of measurement recordings are partly illustrated in figures 5.4 and 5.5, in the (S_1, v_m) plane. Each point in these figures corresponds to a $10km$-long road/speed profile pair.

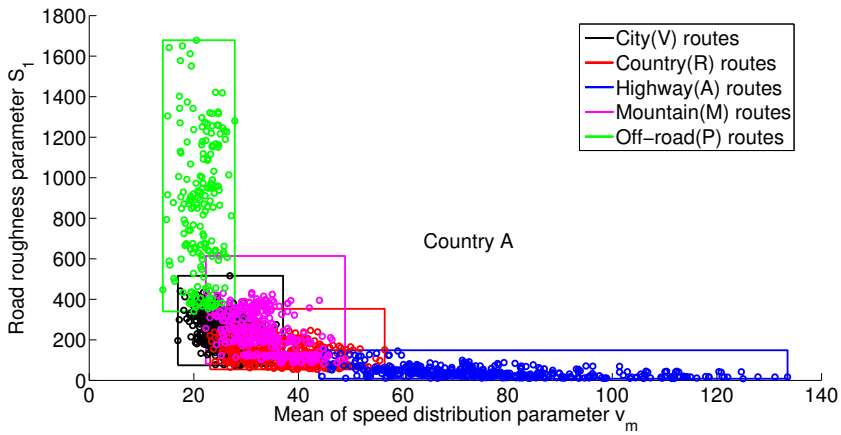

Figure 5.4: Variation of the road and speed stochastic model's constituting parameters across recordings: country A. Min-Max boxes are drawn to better visualize the spread of the different populations (strata).

Arguably, S_1 and v_m are the most distinctive embodiment of the characteristics of both the road and speed profiles and their influence on the load histories is dominant. As such, they represent appropriate quantities for a visual (rough) comparison of loading environments, *e.g.* two different countries. Let us note that, the sensitivity of the loads to such parameters is more thoroughly studied in subsection 5.3.3.

Additionally, S_1 and v_m, are interesting quantities in regards to the definition of life situations. Indeed, if usage variability is to be assessed through surveys, then life situations must necessarily be identifiable. The latter are often identified through considerations involving the 'overall level of road roughness', which can be associated with S_1 or the 'average speed', which can be associated to v_m. For example, roughly speaking, highways routes are generally composed of smooth roads covered at relatively high speeds. Conversely, off-road routes tend to include very rough surfaces, often covered at low speeds. In figures 5.4 and 5.5, **life situations may be somewhat assimilated to clusters of**

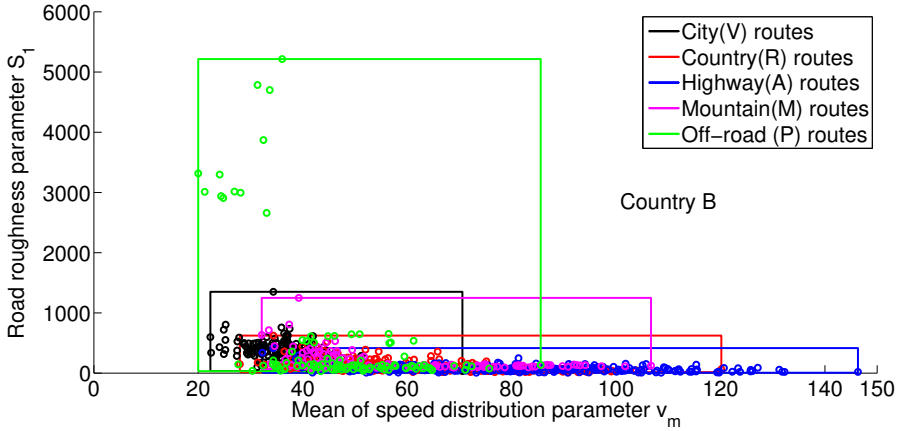

Figure 5.5: Variation of the road and speed stochastic model's constituting parameters across recordings: country B. Min-Max boxes are drawn to better visualize the spread of the different populations (strata).

points or strata, in terms of constituting parameters of the stochastic road and speed models.

Life situations and clustering of parameters

Here, circuits of different types have been selected manually on a map and classified based on subjective choices, prior to the measurements. The observed clustering in figures 5.4 and 5.5 is the natural consequence of this selection and classification. As pointed out in subsection 5.2.2, it may not be easy to objectively define the boundaries between different life situations. It is also difficult to unambiguously classify an actual circuit into a particular category. The split of the different clusters is not always evident and it clearly varies between the two campaigns (country A and B). Certain life situations are visibly overlapping in the (S_1, v_m) plane, in figures 5.4 and 5.5. Furthermore, when observing the obtained results along other dimensions of the vector of constituting parameters, the split of the strata may be very limited. This is illustrated in figure 5.6, where it is not easy to identify clearly distinct clusters.

This shows that the **definition of life situations should not necessarily be based on a rigid clustering for all parameters.** Some life situations may share similar/overlapping evolutions for certain constituting parameters. Let us insist again on the fact that in order to gather data on the relative proportion of the different life situations within the lives of vehicles, **the customer that is surveyed has to be able to identify** (it can only be subjectively) **the different situations.**

Based on the analysis of figures 5.4 and 5.5, it is quite apparent that the variation in constituting parameters is reduced within the boundaries of each defined life situation.

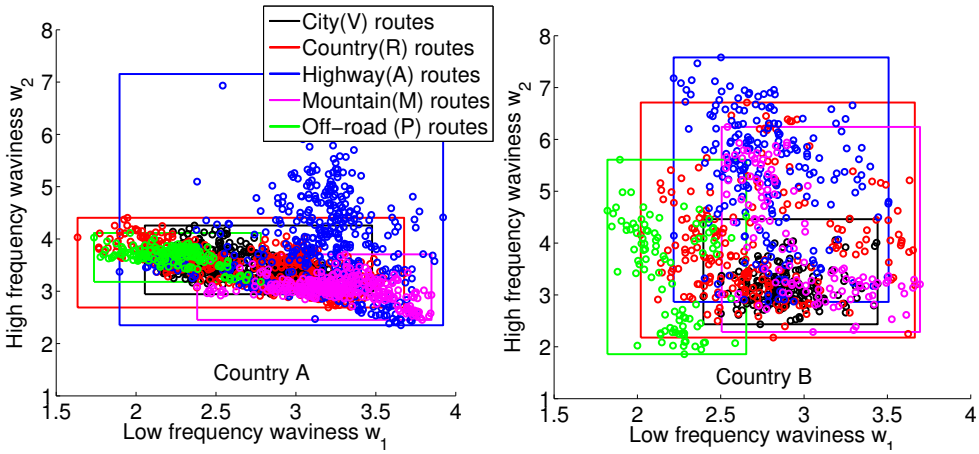

Figure 5.6: Variation of constituting parameters: waviness (w_1,w_2) of the road model. Min-Max boxes are drawn to better visualize the spread of the different populations (strata).

Hence, as mentioned in subsection 5.2.2, any information on the relative proportion of different life situations represents **knowledge on the variability of influential factors, namely road and speed profiles, throughout the life of the different vehicles of a population.**

Statistical information on influential factors and testing

As discussed in subsection 4.5.2, there does not seem to exist a perfect solution to the probabilistic modelling of the variability of influential factors across vehicle lives. In chapter 4, stochastic model structures have been selected. The aforementioned **constituting parameters** of these selected structures are here considered as a simplified description of the variability of road and speed profiles. **Heuristically, they represent a 'projection' of these continuously varying quantities on a vector of finite dimension** (here $n = 8$ dimensions). Through this simplification, the variability of influential factors may be studied somewhat more objectively and easily, *e.g.* through the analysis of the scatter-plots in figures 5.4, 5.5 and 5.6.

The different vectors of constituting parameters of the form $\{S_1, w_1, w_2, \gamma, v_m, s_v, \theta, \rho_{ls}\}$ have been identified here using $10km$-long profiles. It can be expected that the scatter of the constituting parameters would likely decrease if the latter were identified on longer profiles (trajectories), due to a natural averaging effect. However, the non-stationary character of the profile would likely increase (*e.g.* through the γ parameter). The choice of the length of trajectories, either for the identification of parameters or for the generation of random realisations, is further discussed in subsection 5.4.1.

In the present section, the objective is not to propose a model for the variability of

influential factors across the lives of a population of vehicles. The purpose is rather to test the stochastic simulation methodology against the available datasets, *i.e.* the two load measurement campaigns carried out by Renault in two different countries. **To perform an exploitable comparison, it is necessary to use the same information about the 'variability of influential factors' in both the simulation and measurement frameworks**.

Consequently and in order to avoid introducing errors that could be linked to statistical choices and hypotheses (*i.e.* on the modelling of the variability of influential factors), the performed stochastic simulations are based on **a random re-sampling from the collected set of vectors of constituting parameters**, see figures 5.4, 5.5 and 5.6. The resulting comparisons between the measured and predicted load variability are thus based on seemingly identical 'input statistics'. All comparisons are carried out for $10km$-long sections.

5.3.2 Comparison of predicted and observed (measured) load variability

Practical implementation of the stochastic simulation methodology

The stochastic models used to generate random realisations of road and speed profiles are the models selected in chapter 4. Vectors of values for their constituting parameters, namely $\{S_1, w_1, w_2, \gamma, v_m, s_v, \theta, \rho_{ls}\}$, are randomly sampled from the collected set of vectors described previously in subsection 5.3.1. For each randomly generated vector of constituting parameters a pair of road and speed profiles is generated. The resulting road excitation (road and speed) is fed to the vehicle model. All simulations are carried out using a linear quarter-car model (see subsection 2.3.2).

Stochastic simulations are performed for the five different life situations defined previously in subsection 5.3.1. Each life situation is associated with a distinct set of constituting parameters (see clusters in figures 5.4 and 5.5). The simulated load histories as well as the measured load histories are used for comparisons. More precisely, the calculated mechanical responses, namely the suspension displacement, the sprung mass acceleration and the unsprung mass acceleration, are converted into damage equivalent amplitudes (DEA), see subsection 2.1.3:

$$y_{eq} = \left(\frac{\sum_{i=1}^{p} \Delta y_i^{\beta}}{n_{eq}} \right)^{1/\beta} \tag{5.2}$$

where $(\Delta y_i)_{i=1..p}$ are the amplitudes of the Rainflow ranges extracted from a given signal y. In this subsection, a number of cycles of $n_{eq} = 200000$ cycles is selected and a Basquin's coefficient of $\beta = 5.6$ is used.

In this context, *i.e.* using a re-sampling strategy, the variation in influential factors within the simulation-based setting should match, in principle, the variation that is ob-

served within the measurement-based setting.

Experimental framework and possible comparisons

Three types of response signals are compared through their associated DEA:

- **Stochastic simulations**: responses obtained from the simulation of randomly generated road excitations (road and speed), where the latter are based on the collected sets of constituting parameters (re-sampling) described above and on the selected stochastic models for road and speed (see chapter 4)
- **Simulated from estimated excitations**: responses obtained from the simulation of the road excitations (road and speed) directly acquired from the road estimation method (*i.e.* 'real' profiles with no stochastic model involved).
- **Measured responses**: responses obtained directly from the sensors on the instrumented vehicle used to perform the load measurement campaign.

For each one of the five life situations, 500 DEA are considered for each of those three response types. First, 500 stochastic simulations are performed using random re-sampling. Second, 'real' road/speed profile pairs are randomly selected from the available dataset (obtained from the processing of the measurement campaign) and used to perform simulations. The random selection may include repetitions in order to get 500 DEA. Third, 500 DEA corresponding to measured responses on the vehicle are randomly selected (potentially with repetitions). For the first country, approximately 200 to 400 profiles of $10km$ are available depending on the life situation. For the second country, approximately 100 to 200 profiles of $10km$ are available depending on the life situation.

All of the three types of considered responses are illustrated in figure 5.7. For each set of damage equivalent amplitudes, the mean value and a high quantile value, namely the 95% quantile, are estimated and used for comparisons. The objective is to verify whether the predicted load variability is representative of the observed (measured) load variability.

The comparison between the results of stochastic simulations and the simulated responses of estimated road excitations, provides us with information on the representativeness of the selected stochastic models with respect to 'real' road and speed profiles. As the same dynamics model is used in both cases, the influence of simulation-related errors is expected to be limited. Simply put, this comparison allows us to **test whether the evolution of influential factors is 'well modelled' by the selected stochastic model structures** (*i.e.* test whether the randomly generated profiles are representative of real ones). Hence, it represents the most relevant criteria for the testing of the methodology.

On the other hand, the differences between the results of the simulation of 'real' excitation (*i.e.* no stochastic model involved) and the loads actually measured on a vehicle, may be affected by both simulation-related errors and the quality of the road estimation

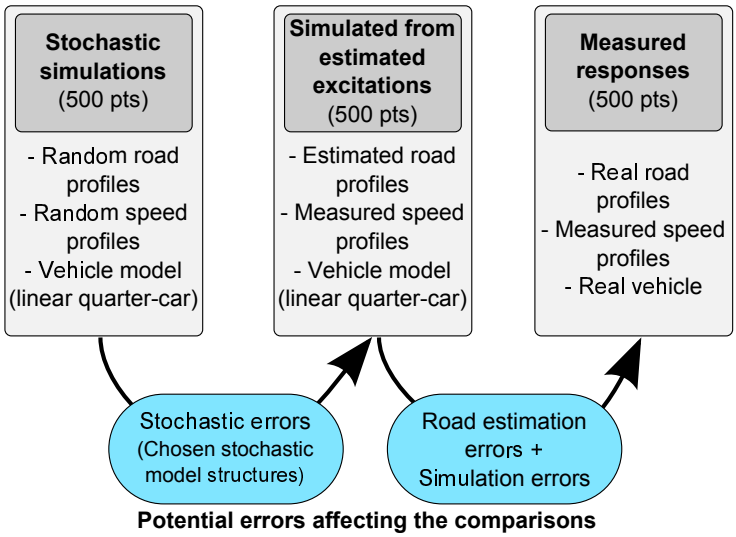

Figure 5.7: Validation of the methodology: compared loads.

algorithm (but no stochastic error). It has to be emphasized that, with a simple vehicle model, namely a linear quarter-car model, any comparison between measured and simulated values has to be analysed with caution since simulation-related errors could be significant.

Analysis of the results and comparisons of load variability

Only some of the figures are displayed in this section for simplicity and clarity. The complete set of figures related to the comparison of the predicted and observed (measured) load variability, is given in appendix F.1.

The three distributions corresponding to the different types of responses, namely results from stochastic simulations, from the simulation of estimated excitations and from measurements, are compared in figure 5.8 for the five life situations and for the suspension displacement response.

It appears that the quality of the stochastic simulation methodology is not similar for all situations. One can observe a relatively stable bias between the measured responses and the responses corresponding to the simulation of estimated excitations. It can be argued that this bias is largely due to the imprecisions associated to the simple vehicle model. The comparisons for the other mechanical responses, namely the sprung and unsprung mass accelerations, are given in figures F.2 and F.3.

A more objective comparison is realised through the use of scalar values, namely the mean value and 95% quantile of the different distributions, and summarized in tables 5.1 and 5.2 (also given in tables F.1 and F.2). The content of tables 5.1 and 5.2, is also illustrated in figures F.7 and F.8.

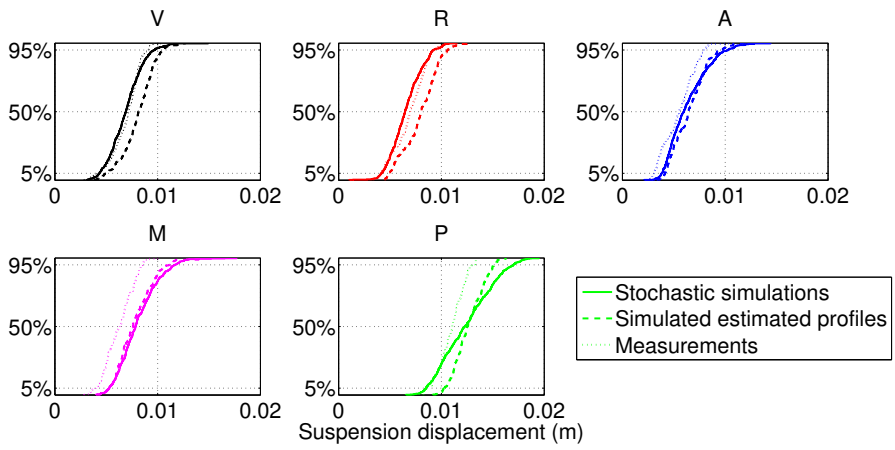

Figure 5.8: Comparisons of predicted and measured distributions: Suspension displacement. Country A.

Life situ.	Resp.	Stochastic simulations	Simulated est.profiles	Measured responses	% error col1/col2	% error col2/col3	% error col1/col3
V		0.0069	0.0080	0.0069	-13.8%	16.6%	0.5%
R		0.0066	0.0080	0.0069	-17.5%	15.1%	-5.0%
A	$z_s z_t$	0.0064	0.0065	0.0054	-1.7%	19.5%	17.5%
M		0.0081	0.0079	0.0062	2.7%	26.9%	30.3%
P		0.0124	0.0127	0.0110	-2.5%	15.3%	12.4%
V		1.15	1.65	1.25	-30.5%	32.4%	-8.0%
R		1.20	1.90	1.41	-36.9%	34.5%	-15.1%
A	a_s	1.01	1.33	1.01	-23.9%	31.4%	0.0%
M		1.20	1.84	1.25	-35.0%	47.3%	-4.2%
P		2.22	2.54	1.92	-12.4%	32.5%	16.1%
V		6.59	12.24	15.60	-46.5%	-21.6%	-57.7%
R		7.42	14.90	19.61	-50.2%	-24.0%	-62.2%
A	a_t	5.68	9.96	13.03	-43.0%	-23.5%	-56.4%
M		6.31	14.57	15.91	-56.7%	-8.4%	-60.3%
P		13.16	17.74	22.77	-25.8%	-22.1%	-42.2%

Table 5.1: Testing of the methodology: comparison of mean values, country A.

Life situ.	Resp.	Stochastic simulations	Simulated est.profiles	Measured responses	% error col1/col2	% error col2/col3	% error col1/col3
V		0.010	0.010	0.009	-7.7%	16.2%	7.3%
R		0.009	0.011	0.009	-15.6%	14.9%	-3.1%
A	$z_s z_t$	0.010	0.009	0.008	12.3%	16.5%	30.8%
M		0.012	0.012	0.009	0.7%	35.4%	36.2%
P		0.017	0.015	0.013	11.6%	14.6%	27.9%
V		1.68	2.16	1.68	-22.1%	28.1%	-0.2%
R		1.85	2.78	2.01	-33.3%	38.4%	-7.8%
A	a_s	1.64	2.14	1.55	-23.0%	38.1%	6.3%
M		1.83	3.08	1.86	-40.5%	66.0%	-1.3%
P		3.04	3.00	2.35	1.4%	27.5%	29.2%
V		10.52	16.62	21.79	-36.7%	-23.8%	-51.7%
R		12.45	21.59	30.55	-42.3%	-29.3%	-59.2%
A	a_t	10.90	15.81	21.99	-31.0%	-28.1%	-50.4%
M		10.50	24.67	26.13	-57.4%	-5.6%	-59.8%
P		18.55	21.83	29.10	-15.0%	-25.0%	-36.3%

Table 5.2: Testing of the methodology: comparison of 95% quantiles, country A.

For DEA values, a prediction within a ±15% interval is of acceptable quality. With a Basquin's coefficient of $\beta = 5$, a difference of 15% for DEA, traduces to a difference of $1.15^5 \approx 2$ in terms of pseudo-damage value (see subsection 2.1.3), which will be considered as acceptable here (see *e.g.* [Johannesson and Speckert, 2013]). In order to facilitate the visual comparison, a ±15% interval is displayed around the DEA of simulated responses to estimated excitations in figures F.4, F.5 and F.6. As mentioned above, comparing these latter responses with the results of stochastic simulation allows us to assess the validity of the methodology. Indeed, they represent the target that would be achieved if stochastic models were perfectly representative of 'real' profiles.

It appears that, for the suspension displacement, the predictions of stochastic simulations are almost entirely contained within a ±15% interval (col1/col2 in tables F.1 and F.2) around the results of the simulation of estimated excitations. As far as the other responses are concerned (see appendix F.1), the predictions are much poorer for sprung and unsprung accelerations. This may be due to the fact that those responses are expected to be more sensitive to the quality of the modelling of road and speed profiles.

The results of the comparisons for the second load measurement campaign (country B), see appendix F.1, figures F.9 and F.10 and tables F.3 and F.4, provide approximately the same conclusions. Results are even poorer for this second comparison.

In view of the results presented in this section, caution is advised when using stochastic simulations to predict load variability. **The practical implementation of the proposed methodology**; most significantly through the **selected stochastic models for road and speed**; seems to yield results that are of limited precision and may **not be**

sufficiently representative for precise load variability analyses. The different causes for the deficiencies in precision of the selected stochastic models are latter discussed in subsection 5.4.3. The applicability of the practical implementation of the methodology is also discussed.

Nonetheless, the methodology may yield relevant information (at a low cost and time) in the case where **extensive statistical data on the variation of influential factors is available within a given environment**, *e.g.* a country or a population of drivers, or when the mechanical characteristics of the vehicle are modified. **Essentially, the methodology may be used to study trends and make broad comparisons between different datasets on influential factors and/or different vehicles, even if the precision of the predictions can be limited.** Also, as a simulation based approach, it is very convenient for sensitivity analysis. This is illustrated and validated in the following subsection.

5.3.3 Comparison of predicted and observed load sensitivity

In order to verify whether the stochastic simulation methodology is a relevant approach for sensitivity analyses (and analyses of overall trends), it is tested against a set of load measurements, in this subsection. Here, all life situations are lumped together (including the different cargo). The sensitivity of loads to the constituting parameters of both the road model $\{S_1, w_1, w_2, \gamma\}$ and the speed model $\{v_m, s_v, L_m\}$ (ρ_{ls} is taken as a constant), is analysed. For this purpose, the following experiment is carried out.

On the one hand, multiple stochastic simulations are performed, with variations in the constituting parameters. The associated DEA $\mathbf{d}_s$ are calculated and the predicted sensitivity can be deduced. On the other hand, the different measured responses are also used to calculate DEA $\mathbf{d}_m$ and for each value, the associated road (estimated) and speed (measured) profiles are used to infer the corresponding vector of constituting parameters $\{S_1, w_1, w_2, \gamma, v_m, s_v, L_m\}$. From both these data, the observed sensitivity can be assessed.

Stochastic framework and sensitivity analysis

In subsection 5.3.1, it has been said that constituting parameters represent a simplified description of complex quantities, namely road and speed profiles, based on a handful of scalar values. The objective of the sensitivity analysis study proposed here is to make sure that if such parameters vary in practice, thus triggering a variation in the loads experienced by the vehicle, the same variation in loads can be predicted through the methodology.

Within the simulation framework, the variation of input values $\boldsymbol{\xi}$ can be precisely controlled and multiple points can be selected in order to study the sensitivity to such input values. Conversely, within the measurement framework, the number of points is limited and the values of inputs are inherited from the selected measurement records. The use of Monte-Carlo-based analysis with large populations or the use of local perturbation

methods is thus not considered here, see *e.g.* [Saltelli et al., 2006] for an overview.

In the present context, the use of response surfaces is very convenient. Here, for a given vector of input values $\boldsymbol{\xi}$, the value of the output DEA $\mathbf{d}$ is stochastic. Indeed, there is inherent randomness in the stochastic processes associated to the constituting parameters in $\boldsymbol{\xi}$ and the same input values may be matched on different output values. Thus there is an obvious limitation to any precise analysis as the identified response surface (deterministic) cannot be 'interpolating'. The objective is rather to study 'average' trends. For any DEA, either from a simulated or a measurement dataset, the following equations may be written:

$$d_s^{(k)} = \hat{d}_s^{(k)} + \epsilon_s \tag{5.3}$$

$$d_m^{(k)} = \hat{d}_m^{(k)} + \epsilon_m \tag{5.4}$$

where ϵ_s and ϵ_m are random values, potentially quite significant, and $\hat{d}_s^{(k)}$ and $\hat{d}_m^{(k)}$ are calculated from the equation of the response surface identified using respectively the simulation dataset and the measurement dataset. Since response surfaces are identified here using a least-square approach, they minimize ϵ_s and ϵ_m.

Regardless of the unavoidable variability, the response surfaces may thus be seen as a good description, on average, of the relationship between the output and input values. Simply put, the response surfaces yield a valuable image of the trends that can be observed from a set of data. This is arguably a rough approach, but it nonetheless yields interesting information.

Let us point out that in the simulation-based framework, response surfaces could be identified using quantiles of the DEA distribution (*i.e.* studies of the sensitivity of quantiles to input parameters) rather than individual values, thus diminishing the spread of the data ϵ_s. However, this is not possible for measurement data and the comparison could not be performed.

Construction of response surfaces

A response surface is constructed both for simulation ($\mathbf{d}_s$) and measurement based ($\mathbf{d}_m$) load-related (damage) values. With the selected approach, the information on the sensitivity of loads to influential factors is here readily obtained from the coefficients of the response surface. Let $\boldsymbol{\xi} = \{S_1, w_1, w_2, \gamma, v_m, s_v, L_m\} = \{\xi_1, \xi_2, ..., \xi_7\}$ be the (regression) parameters on which the response surface is built. The following formulation is selected for the response surface:

$$\hat{\tilde{d}}_s^{(k)} = \nu_{s,0}^{(k)} + \sum_{i=1}^{7} \nu_{s,i}^{(k)}\, \tilde{\xi}_i + \sum_{i=1,j=2}^{i=7,j=7,i>j} \nu_{s,ij}^{(k)}\, \tilde{\xi}_i \tilde{\xi}_j \tag{5.5}$$

$$\hat{\tilde{d}}_m^{(k)} = \nu_{m,0}^{(k)} + \sum_{i=1}^{7} \nu_{m,i}^{(k)}\, \tilde{\xi}_i + \sum_{i=1,j=2}^{i=7,j=7,i>j} \nu_{m,ij}^{(k)}\, \tilde{\xi}_i \tilde{\xi}_j \tag{5.6}$$

where k is the studied response (*e.g.* suspension displacement), $\boldsymbol{\nu}_s^{(k)} = (\nu_{s,i}^{(k)}, \nu_{s,ij}^{(k)})_{ij}$ are the coefficients of the response surface built on simulated loads, $\boldsymbol{\nu}_m^{(k)} = (\nu_{m,i}^{(k)}, \nu_{m,ij}^{(k)})_{ij}$ are the coefficients of the response surface built on measured loads and:

$$\tilde{\xi}_i = \frac{\xi_i - E[\xi_i]}{\sqrt{E\left[(\xi_i - E[\xi_i])^2\right]}} \text{ and } \tilde{d} = \frac{d - E[d]}{\sqrt{E\left[(d - E[d])^2\right]}} \tag{5.7}$$

are normalized variables. Higher order terms have not been considered here, since it has been noticed after a few tries that they do not provide more relevant information or a gain in precision.

Here a set of vectors of regression parameters Ξ_s of size $N = 1000$ is used to run stochastic simulations. This yields $(\mathbf{d}_{s,n})_{n=1,\ldots,N}$ values. In fact, the former vectors are selected (randomly) among the available vectors of constituting parameters that have been obtained from the processing of a load measurement campaign. This forces values of ξ_i to evolve within realistic intervals of variation (in the associated seventh-dimensional space). Another set of regression parameters Ξ_m of size N is built. The latter parameters are identified in accordance with the road and speed profiles associated with the different measurement-based DEA values $(\mathbf{d}_{m,n})_{n=1,\ldots,N}$. Here, there are a bit more than $N = 1000$ vectors in this dataset of $10km$-long profiles from different life situations.

For given sets of simulation-related $\{\Xi_s, \mathbf{d}_s\}$ and measurement-related data $\{\Xi_m, \mathbf{d}_m\}$, the coefficients of the response surfaces $\boldsymbol{\nu}_s$ and $\boldsymbol{\nu}_m$ may be identified by a simple least squares approach:

$$\boldsymbol{\nu}_s^{(k)} = (\mathbf{X}_s^T \mathbf{X}_s)^{-1} \mathbf{X}_s^T \mathbf{D}_s^{(k)} \tag{5.8}$$

$$\boldsymbol{\nu}_m^{(k)} = (\mathbf{X}_m^T \mathbf{X}_m)^{-1} \mathbf{X}_m^T \mathbf{D}_m^{(k)} \tag{5.9}$$

$\mathbf{X}_s$ and $\mathbf{X}_m$ are $(29 \times N)$ matrices where the parameters $\tilde{\xi}_i$ are taken from the sets Ξ_s and Ξ_m, sorted row-wise and arranged in their order of appearance in equations (5.5) and (5.6). $\mathbf{D}_s^{(k)}$ and $\mathbf{D}_m^{(k)}$ are vectors of equivalent damage amplitudes, for the k-th mechanical response, and are taken from the sets $\tilde{\mathbf{d}}_s$ and $\tilde{\mathbf{d}}_m$.

Analysis of the results and comparisons of load sensitivity

The identification of the response surface's coefficients yields the values illustrated in figure 5.9 for suspension displacement. The values for all responses are given in table 5.3. Figures F.11, F.12 and F.13, illustrating the coefficients for all responses are given in appendix F.2. Additionally, the response surfaces as well as the points used to construct them are represented, considering only two dimensions (S_1, v_m), in figure 5.10.

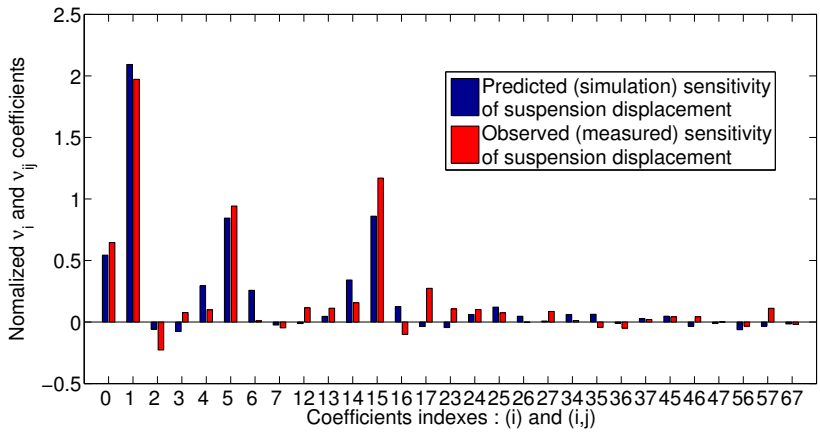

Figure 5.9: Coefficients of simulation and measurement-based response surfaces for suspension displacement.

From the analysis of the results in table 5.3, it is seen that the predicted sensitivity, derived from simulations, is quite representative of the observed sensitivity, derived from the measurements. In both cases, it appears that the most significant factors, with respect to the variation of damage, are the overall roughness S_1, the mean speed v_m and their interaction. For these factors the predicted and observed effects are relatively similar. One may notice that for the accelerations, and especially for the unsprung acceleration, w_1 and w_2 are also important contributors. The most significant difference concerns the scatter in speed s_v and may point to a limitation in the speed model (especially the use of a Gaussian copula to account for the correlation between v_m and s_v).

To conclude, this experiment seems to demonstrate a clear interest for the use of the methodology, since the sensitivity which is observed from measurements is rather well predicted through the use of simulation. **The proposed stochastic simulation methodology can be viewed as a powerful tool for sensitivity and trend analyses**. Indeed, it is much easier and cheaper to sample points through simulation than through measurements. This is a also very interesting tool when extensive statistical information on the variation of influential factors is available (or can be collected cheaply) within different environments, *e.g.* different countries. Such data may be processed rapidly and inexpensively into information on the difference between the latter environments in terms of load variability.

Coeff.		Simulations-based			Measurements-based		
index	Param.	$z_s z_t$	a_s	a_t	$z_s z_t$	a_s	a_t
0	/	0.65	0.62	0.57	0.51	0.56	0.68
1	S_1	2.27	2.04	1.77	1.78	1.59	1.56
2	w_1	-0.07	-0.50	-0.76	-0.20	-0.41	-0.51
3	w_2	-0.08	-0.18	-0.29	0.05	-0.38	-0.46
4	γ	0.29	0.23	0.19	0.13	0.11	0.07
5	v_m	0.97	1.01	0.99	0.75	1.00	1.25
6	s_v	0.29	0.36	0.40	0.00	-0.02	-0.06
7	L_m	-0.02	-0.06	-0.09	-0.01	0.05	0.05
1,2	S_1, w_1	-0.10	-0.25	-0.31	0.06	-0.11	-0.17
1,3	S_1, w_2	-0.01	-0.11	-0.18	0.01	-0.09	-0.06
1,4	S_1, γ	0.38	0.31	0.27	0.19	0.26	0.21
1,5	S_1, v_m	1.06	1.06	0.97	1.05	1.28	1.51
1,6	S_1, s_v	0.17	0.26	0.30	-0.15	-0.24	-0.23
1,7	S_1, L_m	0.01	0.00	0.00	0.26	0.07	0.09

Table 5.3: Coefficients of simulation and measurement-based response surfaces. Only the most significant coefficients are displayed.

Overall, the results present in this section allow us to be confident in the ability of the methodology to enable interesting comparisons, trend analyses and statistical data processing, regardless of biases and deficiencies in precision that may be involved when performing a single prediction of load variability.

5.4 Prediction of the load life of vehicles

In the previous section, the methodology of stochastic simulation has been tested using a random re-sampling of the constituting parameters identified from two measurement campaigns. The resulting comparisons between the predicted and observed (measured) load variability are thus based on the same statistical data on the variation of influential factors. Additionally, comparisons have been realised for each life situation and based on $10km$-long profiles.

As mentioned in subsection 5.2.2 and illustrated in figure 5.1, any attempt at characterising load variability (for a given mileage target, say $200000km$) necessarily implies a division of the life of the vehicle. In order to perform predictions for the complete load histories (load lives) of a population of vehicles and their related components, appropriate statistical hypotheses have to be used to process the information acquired for 'short' segments. Such hypotheses have to be considered both when using load histories acquired from simulation or from measurements.

The **extrapolation from short segments**, as well as the issue of the **variability**

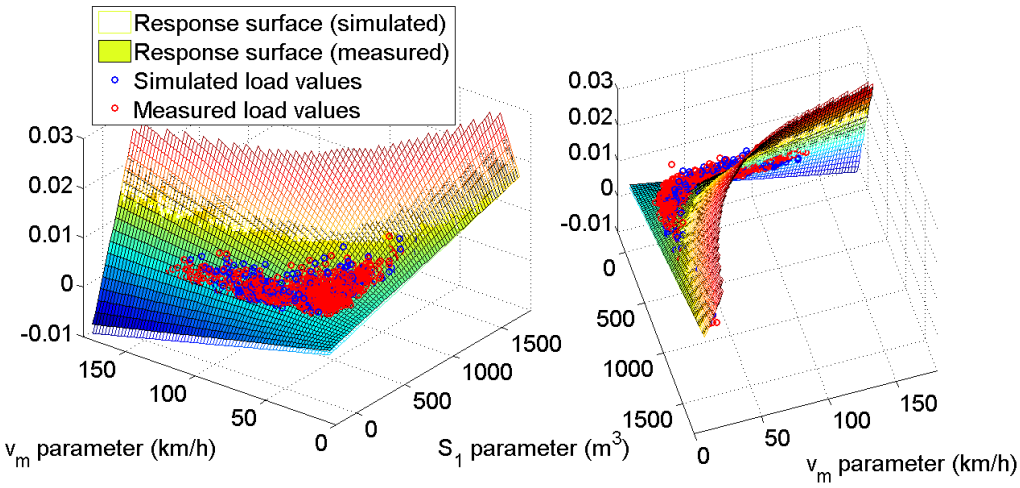

Figure 5.10: Simulation and measurement-based response surfaces. They both minimize the distance between each population of load-related (damage) values. Here, with only two dimensions involved, namely S_1 and v_m the response surface may be visualized on a three dimensional plot.

of influential factors across the life of different vehicles of a population, are discussed and analysed in subsections 5.4.1 and 5.4.2. A particular extrapolation rule is latter applied and used to compare simulation-based and measurement-based predictions in subsection 5.4.3. Again the same statistical data on the variability of influential factors is used in both cases.

5.4.1 Statistical analysis and extrapolation

Let the reader be advised that this subsection is quite conceptual. The following discussions are original contributions of the present research work. They aim at pointing out the difficulties that are inherent to any load prediction concerning the complete life of vehicles.

In the presence of limited information (this is the case here), it is sometimes only possible to rely on reasoning, expert judgement and hypotheses. Also, since road and speed profiles are extremely diverse and varying quantities, it is unlikely that they can be precisely described by simple and 'well-defined' stochastic models. The choice of a representative model for such quantities can hardly be rigorously justified and one should select a solution that is adapted to the issue at hand.

Both remarks highlight the fact that the issue here clearly belongs to the domain of statistics, namely the study of the scatter of a given quantity within a population of interest.

Analysis and modelling of the variability of influential factors

In subsection 5.3.1, it has been said that **constituting parameters** of the selected stochastic models can be used as a **simplified description of the variability of road and speed profiles**. Heuristically, they represent a 'projection' of these continuously varying quantities on a vector of finite dimension (here $n = 8$ dimensions) and for a given length, here $10km$. Through this simplification it is more easy to analyse the variability of influential factors than with continuously varying profiles.

In this manuscript, constituting parameters have been identified using $10km$-long trajectories of road and speed profiles. There is no theoretical objection to the selection of a smaller or larger value for the length of trajectories. However, **the value of** $10km$ **selected in this manuscript is considered as a good compromise** given the following remarks (non-necessarily an exhaustive list):

- It can be expected that if a stochastic process is selected as a model for longer profiles, the latter will exhibit a more variable and non-stationary character (which is observed in practice). Conversely, the scatter associated to its constituting parameters is likely to be reduced, due to a natural averaging effect.
- When measured long profiles are used as a source of information on constituting parameters, it may be difficult to associate a particular route category to the latter. Indeed, long profiles can contain different segments and it may become difficult to claim that the vehicle is on 'a given route' or on 'a given type of route'.
- It may be difficult to obtain an exploitable description of the diversity of roads if roads that are very different are lumped together when using long profiles.
- Also, the simulation of long profiles can be costly in terms of computation time.
- Conversely, with profiles that are very short, the scatter of the constituting parameters may become very important and difficult to describe and model.
- The simulation of profiles that are too short may yield very scattered damage distributions and this may be a problem when using such data for extrapolations (see below).
- Similarly, profiles that are very long can cause difficulties when performing extrapolations (see below). Indeed, the natural averaging effect may not account for the fact that, for example, different customers might select different (in statistical terms) roads or applied different speed profiles (see below).

For all the calculations carried out throughout this manuscript, the variation of constituting parameters is studied in association with a fixed length of $10km$. The same is true for their identification, for the study of recorded loads and for the generation of random trajectories (road/speed) to feed the simulation of load histories.

Ultimately, the variability of constituting parameters has to be studied in relation with the population of vehicles for which a load characterisation is sought. Let us recall that the main purpose of the stochastic models here is to generate random realisations '**that are statistically representative of the road excitations (road and speed) to which vehicles are actually subjected**'. This rises a difficult statistical question: **how are constituting parameters (influential factors) distributed across the life of different vehicles of a given population?** There is clearly no absolute answer to such questions. The answer likely depends on the population that is being studied and most significantly on the statistical information that is available.

Definition of life situations and distribution of parameters

As mentioned in subsection 5.2.2 and illustrated in figure 5.1, the information on the relative proportion of the different life situations (*e.g.* results of a survey) constitutes **valuable knowledge on the variability of influential factors throughout the life of the different vehicles of a given population**.

On $10km$ sections, a strong scatter is observed in terms of constituting parameters, see *e.g.* figure 5.4. If any realistic prediction of load variability within a given population is to be achieved, **a probabilistic description has to be proposed for this scatter**. Using appropriate distribution models, an arbitrarily large sample of load histories can be obtained through stochastic simulation.

It appears that it may be **easier to propose distribution models for constituting parameters and their correlation within the boundaries of each life situation**. First, the scatter is generally reduced. Second, the correlation between constituting parameters is partly accounted for, since distribution models (for road and speed) can be naturally associated to one another within the different strata (life situations). This appears in figure 5.11, where one can note that if all life situations are lumped together, the correlation between road roughness S_1 and speed v_m is visibly non-linear.

This is a very interesting feature of the proposed stochastic simulation methodology, namely the combination of stochastic modelling and stratified sampling.

Due to the limited amount of data, **no specific parametric distribution model is prescribed by the author here**. The selection of a model (*e.g.* a normal or gamma distribution) and the identification of its parameters should be done on a case by case basis, depending on the statistical information at hand. The diversity in terms of road profiles and speed profiles for a given population of vehicles is arguably very significant.

Also, **no model is proposed for the possible correlation between constituting parameters** (within each life situation) in this manuscript. Proposing models for the correlations between 'marginal' distributions can prove to be very difficult and imply a non desirable accumulation of mathematical hypotheses when too few data is available.

Let us recall here that, he different situations that the vehicle encounters represent a

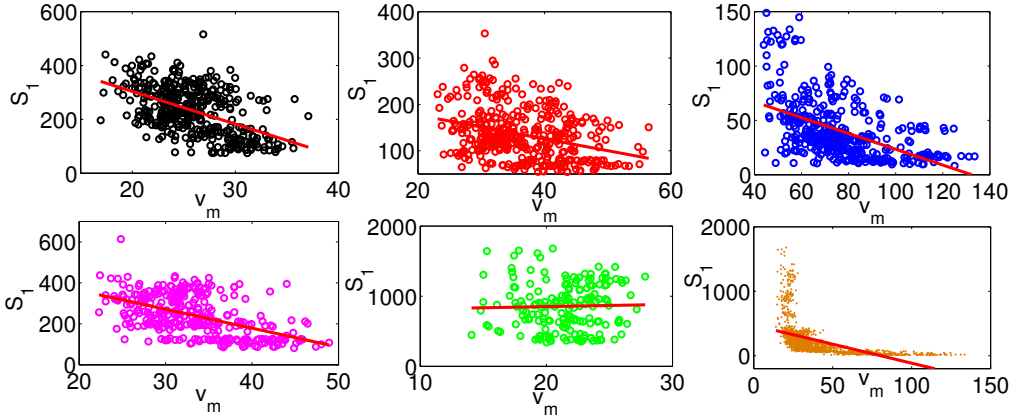

Figure 5.11: Visualisation of the correlation between S_1 and v_m. The correlation can be different for the different life situations. From top left to bottom right: city, country, highway, mountain, unpaved and full population. A first order linear regression is displayed on the figures (red solid line) to illustrate the correlation between both factors. On the bottom right figure, it appears that the correlation is clearly not linear when the complete population is considered.

continuum and not a succession of clearly defined 'life situations'. Hence, care is advise when defining the boundaries of life situations and identifying distribution models for the associated constituting parameters. Let us also insist on the fact that the issue of the definition of life situations is not specific to a simulation-based methodology but also has to be considered in the framework of a load measurement campaign based on a stratified sampling strategy, see *e.g.* [Thomas et al., 1999].

Extrapolation to a vehicle's complete load history

A **division of the life of the vehicle into short segments is generally operated for practical reasons.** Such division is illustrated in figure 5.1. When the complete life of a vehicle is studied, it is necessary to extrapolate from the information that has been acquired on short segments, in order to make predictions representing much longer segments, say $200000km$. Fatigue is a cumulative phenomenon, see subsection 5.2.1, and it is necessary to **cumulate the different contributions of each short segment**. In the context of limited information, this represents a particularly complex statistical problem.

A major difficulty appears as it can reasonably be argued that a **correlation exists between the different segments constituting the life of a particular vehicle**, see figure 5.1. This issue has been discussed by the authors in [Fauriat et al., 2015a]. Let us note that, this issue is quite easy to understand when considering the variation of constituting parameters (road and speed) across the life of different vehicles.

For example, the following questions can be considered:

- Does the driver present a rather constant driving behaviour, *e.g.* an aggressive behaviour. If so, there is an obvious correlation between different realisations (on short sections and for different life situations) of the constituting parameters of the speed model, for a given vehicle.
- Does the distribution of the constituting parameters of the road model is identical from the standpoint of all vehicles, or do some vehicles tend to cover only a limited number of roads? If so, there is a correlation between different realisations of the constituting parameters of the road model, for a given vehicle.

In figure 5.1, one could consider that the evolution of constituting parameters is distinct for different vehicle lives.

Essentially, so far, the load variability that has been characterised is the load variability corresponding to all the possible realisations (within each life situations) of $10km$-long segments for the considered population of vehicles (*e.g.* all drivers and roads lumped together). Any attempt to propose probabilistic models to account for the correlation between different realisations, throughout the life of a given vehicle, is obviously associated with much statistical complexity.

This issue is seldom discussed in literature. One piece of work on the topic may be found in [Dreßler et al., 2009]. Ultimately, the objective here is to select the approach which is the most representative of the lives of real vehicles.

Here, there is insufficient data to propose models describing these correlations based on the analysis of the variability of influential factors across vehicle lives. It is rather proposed to **study the correlation between DEA or pseudo-damage values and propose an extrapolation rule accordingly**. This is essentially the approach that is taken when load histories are acquired through measurements and latter used to extrapolate to the full life of the vehicle. Indeed, let us recall that the issue of extrapolation is not specific to a simulation-based approach, since measured loads are also of limited length for practical reasons. It is interesting to present the issue in terms of two limit (extreme) hypotheses, see [Dreßler et al., 2009].

In the first case, the damage value that is obtained for a $10km$-long segment is assumed to be representative of the average value for all $10km$-long segments, for the same life situation and across the life of the considered vehicle. Hence, **in this case, the extrapolation rule resumes to a simple proportionality rule**. If d is the observed damage value and L_{km} is the target mileage (in km), then the average damage value for the total life is $d_{tot} = d.L_{km}/10$. This extrapolation strategy corresponds to a **perfect correlation between the simulated/measured realisation and all the subsequent ones** (not simulated/measured). In this case the 'load severity' associated with a particular driver (vehicle life) is fully homogeneous. This is quite unlikely. It would mean that the

driver covers, on average, the same road surfaces with the same speed profiles (in terms of constituting parameters).

This hypothesis may be appropriate when the observed load value corresponds to a 'sufficiently' long segment, say at least a few thousand kilometres or more. In this case, the value is more likely to be an 'average' value. For a $10km$-long profile this extrapolation strategy might yield very severe (or soft) homogeneous drivers, *i.e.* which are severe (or soft) across the whole life of the vehicle (selected roads and speeds).

Conversely for the second (extreme) case, the life of the vehicle is assumed to be composed of realisations that are independent. Load values are randomly selected from the set corresponding to all $10km$-long simulated/measured realisations associated to the given population (roads and drivers lumped together). The random values independently taken from this set are then summed in order to obtain a damage value that corresponds to the target mileage. For example, if a given life situation represents $40000km$ out of the $200000km$ for which a prediction is sought, then for this situation, $40000/10 = 4000$ realisations are drawn from the simulated/measured set and summed. This extrapolation strategy corresponds to a **perfect independence between the simulated/measured realisation and all the subsequent ones** (not simulated/measured). In such case the 'load severity' of the driver is fully heterogeneous. This is also quite unlikely.

This second extrapolation strategy, by virtue of the central limit theorem, leads to a strongly restrained variability of the loads. Indeed, if $d_{tot} = d_1 + d_2 + ... + d_q$ is the sum of independent and identically distributed random variables, then for a sufficiently large number of realisations q, one has:

$$d \sim N(q\mu_d, \sqrt{q}\sigma_d) \tag{5.10}$$

where μ_d and σ_d are respectively the sample mean and standard deviation of the individual damage distribution d_i. Hence when q is large, which is very likely if the extrapolation is made from $10km$, then the predictions have a mean value of $q.\mu_d$, with a scatter that is relatively weak with respect to such value, namely $\sqrt{q}\sigma_d$. This is arguably not very representative of a realistic population of vehicles, where different drivers have different driving behaviours and select different roads.

The comparison between the extrapolation strategy based on a proportionality rule and the strategy based on the sum of independent samples is illustrated in figure 5.12. Here values are randomly drawn from a log-normal distribution (of parameters $\mu_{ln} = 2$ and $\sigma_{ln} = 1.5$). For 10 generated trajectories (in blue), *i.e.* load histories, 1000 realisations corresponding to $10km$ sections are randomly drawn from the log-normal distribution and summed. This represents load lives corresponding to $10000km$.

One readily notices that the second extrapolation strategy leads to a scatter that is very reduced when the total distance is important, *i.e.* when the number of independent realisations is high (by virtue of the central limit theorem).

It can be expected that a realistic extrapolation rule lies somewhere in between both

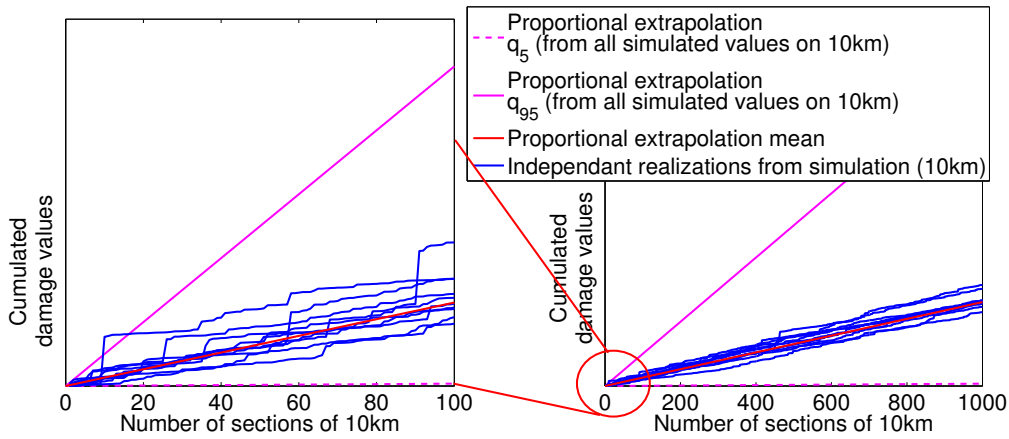

Figure 5.12: Extrapolation using independent realisations of damage values. Multiple cumulated damage trajectories are generated to illustrate the scatter. A zoom is operated on the first $1000km$ (left) out of $10000km$ (right). q_5 and q_{95} represent respectively the 5% and 95% quantiles of the set of available values (here a log-normal distribution).

these extreme cases. **The first rule is extremely severe and conservative (especially when the load information is extracted from short profiles). The second rule is very soft and it is possible that extreme (*e.g.* severe) drivers are not well represented.** It is easily seen in figure 5.12, that high quantile values that would be predicted at the target mileage would be very different for both extrapolation strategies.

5.4.2 Study of extrapolation hypotheses

There does not seem to be a generic answer to the issue of extrapolation. An appropriate answer most likely depends on the available statistical data about the evolution of influential factors across the life of a vehicle and between different vehicles. Here, some illustrations are given using the dataset at disposal, namely the results of both a route-imposed and a route-free measurement campaigns.

First, it appears that the scatter in damage values diminishes over longer segments. This is observed in figure 5.13 through the comparison of measured load histories acquired on segments of different lengths. Here the data originates from a route-imposed campaign and life situations are lumped together (the same phenomenon is observed for life situations taken independently). The displayed damage values are divided by a unit length of $10km$ in order to be able to make the comparison between segments of different lengths.

One may notice that the mean damage value per unit length (over all life situations), is relatively stable. Conversely, it clearly appears that the scatter of damage realisations is much stronger for shorter segments, as expected. Such scatter is illustrated using the ratio between a high quantile of the distribution, here 95%, and the median quantile.

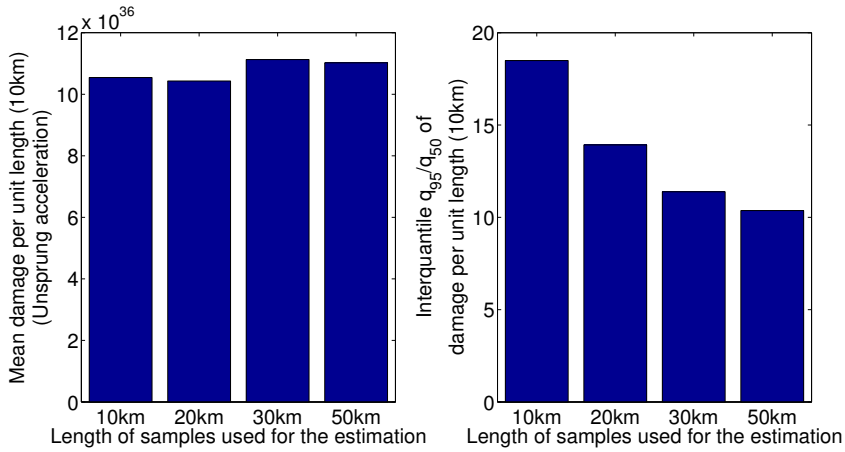

Figure 5.13: Evolution of the scatter in damage over increasingly longer segments. The smaller set of load histories, namely for $50km$, contains approximatively 300 realisations.

Additionally, it is relevant to analyse, with realistic data, the evolution of the load lives of vehicles over longer distances. In figure 5.14, different drivers and their associated load histories acquired within the framework of a route-free campaign are displayed. Here, no (*a priori*) distinctions are made between different life situations since the drivers continuously select their desired routes. The values of damage calculated on segments of unit length of $10km$ are cumulated.

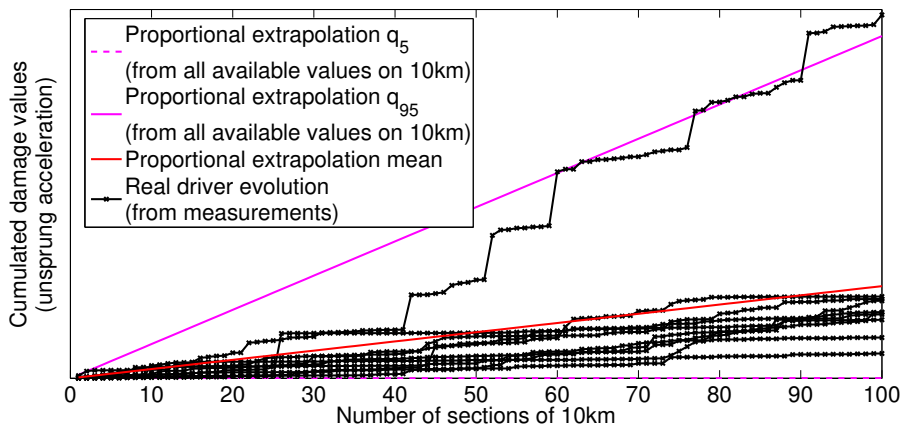

Figure 5.14: Evolution of cumulated damage over long segments. Illustration of the issue of extrapolation and comparison with 'real drivers'.

Also in figure 5.14, the comparison is made between 'real' load lives and the extrapolation scheme based on a proportionality rule. For this extrapolation rule, it is considered that the value observed on $10km$ is representative of the average value over all $10km$-long

segments encountered by the driver during the life of its vehicle. The mean value and the high and low quantiles of the set of available (measured) damage values for $10km$-long segments, are identified and extrapolated with the proportionality rule. Through the comparison, it is observed that one of the drivers tends to generate high damage values much more frequently. It is an example of a possible correlation between the realisations of damage values.

Lastly, let us illustrate the comparison between the two extrapolation strategies in terms of quantile values and for a significant number of trajectories, here 1000 repetitions. The said comparison is displayed in figure 5.15. Here the damage values are extracted from load histories that have been measured in the context of a route-imposed campaign. All life situations have been lumped together. Both the values on $10km$ and $50km$-long segments are randomly and independently sampled from the available set of data.

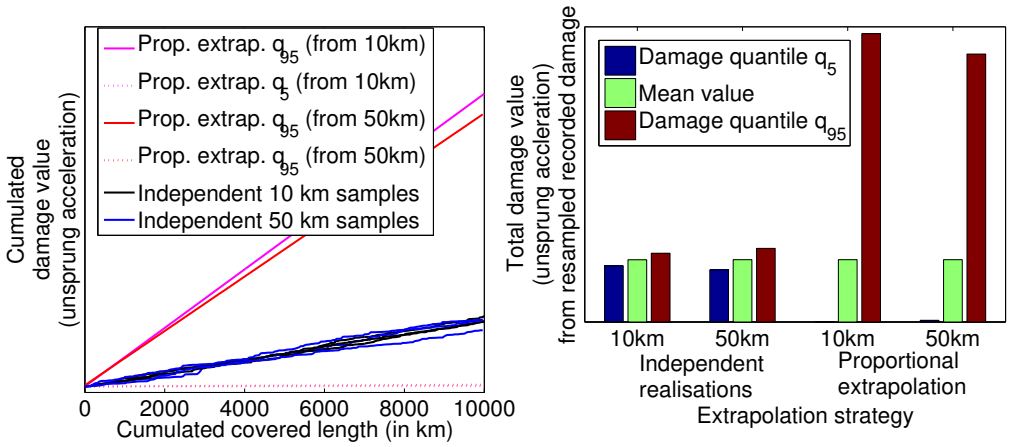

Figure 5.15: Comparison of the two limit extrapolation strategies using load histories with different lengths. On the left-hand side, only a few cumulated damage trajectories are displayed. On the right-hand side, for the extrapolation using independent realisations, 1000 trajectories are considered for the assessment of quantile values.

It is seen that the difference between the quantiles predicted from samples of different lengths is not so significant. On the other hand, the influence of the extrapolation strategy on the predicted variability of loads, for $10000km$, is extremely significant. The mean value is well estimated regardless of the extrapolation strategy. However, **the high and low quantile values, which characterise the spread of the population of loads, are very different**.

The choice of the extrapolation strategy is a serious issue since it is both extremely difficult to address and simultaneously extremely influential on the predicted load variability when the complete lives of a population of vehicles are studied. High quantiles, and the related tails of the distributions of load values (for a high target mileage), constitute the most important feature of load characterisation in

the framework of reliability analyses.

It is very important to lay out the question of the extrapolation strategy, in the context of this chapter, as it is a crucial part of the issue of reliability analysis of vehicle components. **Such issue is not necessarily specific to the simulation-based methodology, which elaboration and description is the central objective of this manuscript.** Nonetheless, a more thorough analysis of that question remains a perspective of the present work. **In what follows, the (conservative) hypothesis of proportional extrapolation will be applied**, as used in the framework of conventional load characterisation campaigns, see *e.g.* [Thomas et al., 1999, Johannesson and Speckert, 2013].

5.4.3 Prediction of the life of a population of vehicles

Testing framework: complete simulated campaigns

In this subsection, a complete simulated campaign based on the proposed stochastic simulation methodology is tested against the data originating form two route-imposed measurement campaigns already described in section 5.3. This comparison is based on the three types of responses discussed in subsection 5.3.2 and displayed in figure 5.7. As in subsection 5.3.2, the constituting parameters of the stochastic road and speed models are obtained using a random re-sampling from the sets of parameters identified from the two measurement campaigns. A linear quarter-car model is used, see 2.3.2.

Unlike the comparison in subsection 5.3.2, here the contributions of all elementary life situations are summed, based on available information on the relative proportion of these life situations (obtained from a survey), see figure 5.16. More precisely, multiple vectors (approximately 2000) of relative proportion $\boldsymbol{\alpha}$, see subsection 5.2.2 are associate to vectors of damage values d containing realisations for the different life situations. Then, an extrapolation is realised using the proportionality rule described in subsection 5.4.1, to a target mileage of $200000km$. All the considered load samples, either simulated or measured, represent segments of length $10km$.

The sum of the contributions of all life situations and the application of the extrapolation rule yields a prediction for the variability of the complete load lives of a population of vehicles. The comparison between the predicted distribution based on stochastic simulation, on the simulation of estimated road excitations and on measured loads is displayed in figure 5.17 for the suspension displacement DEA. All responses, namely suspension displacement and sprung and unsprung accelerations are also given in appendix F.3, in figures F.14, F.15 and F.16.

For a comprehensive comparison, the low quantile, high quantile and mean value of the DEA distribution are all gathered in tables 5.4 and 5.5, receptively for countries A and B. The values are given for three mechanical responses on the vehicle, namely suspension displacement $z_s z_t$, sprung acceleration a_s and unsprung acceleration a_t.

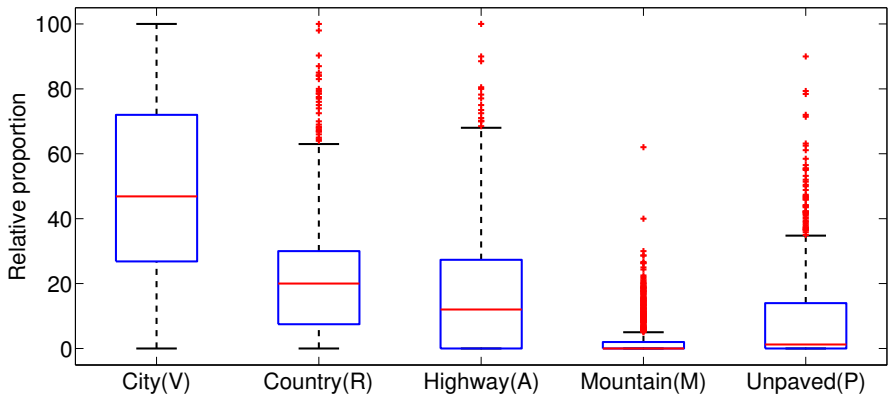

Figure 5.16: Relative proportion of different life situations. This data is the result of a survey carried out among approximatively 2000 customers. The boxes represent the 25%, median and 75% quantiles. Points above the 95% quantile are denoted by markers.

Value	Resp.	Stochastic simulations	Simulated est.profiles	Measured responses	% error col1/col2	% error col2/col3	% error col1/col3
q_5		0.031	0.038	0.032	-17.4%	18.0%	-2.5%
Mean	$z_s z_t$	0.055	0.056	0.048	-2.2%	16.5%	13.9%
q_{95}		0.070	0.068	0.058	3.1%	17.1%	20.7%
q_5		5.00	7.80	6.00	-35.8%	30.1%	-16.5%
Mean	a_s	9.70	12.5	9.01	-22.5%	38.9%	7.7%
q_{95}		12.4	14.3	10.9	-13.7%	31.7%	13.6%
q_5		26.7	57.7	73.5	-53.7%	-21.5%	-63.7%
Mean	a_t	59.4	93.8	118.0	-36.7%	-20.6%	-49.7%
q_{95}		75.7	107.8	144.2	-29.8%	-25.2%	-47.5%

Table 5.4: Comparison of predicted load lives. Country A. DEA values.

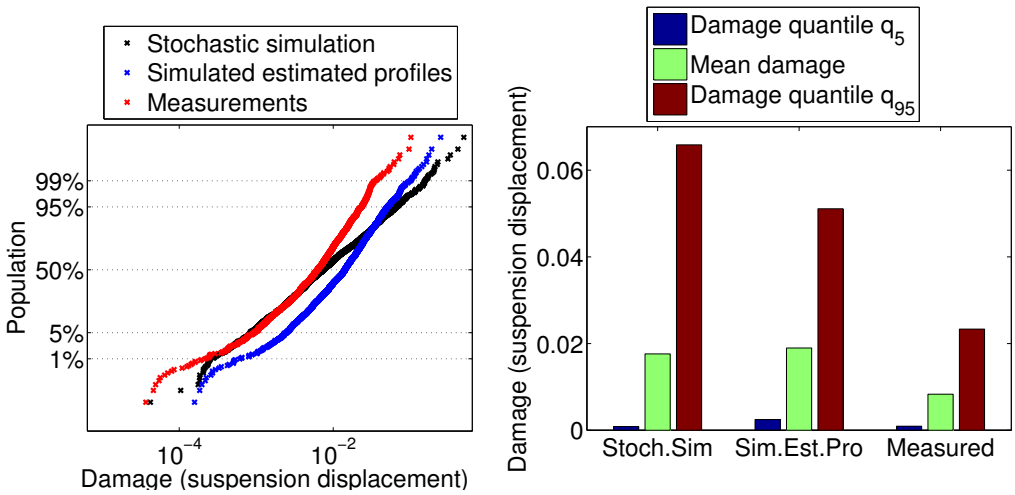

Figure 5.17: Predicted variability of the load lives of a population vehicles, for suspension displacement. The three types of responses in figure 5.7 are used as inputs to make the predictions and the comparison is displayed. Country A.

Value	Resp.	Stochastic simulations	Simulated est.profiles	Measured responses	% error col1/col2	% error col2/col3	% error col1/col3
q_5		0.036	0.034	0.030	7.9%	11.4%	20.2%
Mean	$z_s z_t$	0.080	0.053	0.047	50.7%	13.7%	71.4%
q_{95}		0.090	0.063	0.056	42.6%	14.0%	62.6%
q_5		6.17	7.48	5.52	-17.5%	35.4%	11.7%
Mean	a_s	14.9	12.9	9.5	15.0%	36.7%	57.2%
q_{95}		16.3	15.6	11.6	4.5%	34.2%	40.3%
q_5		35.0	50.2	66.0	-30.3%	-23.9%	-46.9%
Mean	a_t	89.3	102.5	126.6	-12.9%	-19.0%	-29.4%
q_{95}		110.4	124.5	158.5	-11.3%	-21.5%	-30.4%

Table 5.5: Comparison of predicted load lives. Country B. DEA values.

Analysis of the results

First, the comparison between the simulations of estimated excitations and measured responses can be affected by errors from the road estimation algorithm as well as errors due to the lack of fidelity of vehicle dynamics simulation. This first comparison, see tables 5.4 and 5.5 (col2/col3), shows that there is a relatively stable bias, different for each response, possibly due to the combination of road estimation and simulation errors. This is regrettable but it does not constitute a major impediment since predictions, *e.g.* for different countries, may still be **analysed in relative terms**. In this regard, the

perspectives for improvement are :

- An amelioration of the vehicle model used for simulation, *e.g.* a more representative tyre model, a non-linear description of the suspension system. This trade-off is a significant increase in calculation time.
- A finer tuning of the road estimation algorithm.
- A more precise description of the characteristics of the vehicle that carried out the measurements used by the road estimation algorithm.

On the other hand, as described in subsection 5.3.2, the comparison between the stochastic simulations and the simulations of estimated excitations is a better indicator of the quality of the stochastic simulation methodology introduced in this manuscript. With a re-sampling of the constituting parameters identified on the set of estimated road profiles and measured speed profiles, the potential for errors is limited here to the **errors due to the choice of the road and speed stochastic models.**

The results displayed by the comparison, in table 5.4 and 5.5 (col1/col2) show **significant discrepancies**. As a difference of 15% in damage equivalent amplitude corresponds to a factor 2 in terms of damage when $\beta = 5$, discrepancies that are significantly larger in amplitude can difficutly be considered as acceptable. The following reasons may be considered as an explanation to such results:

- Disregarding transient (potholes, speed bumps, etc.) in the stochastic road model may be an overly strong simplification. Yet, the selection of a model for transients and the identification of its parameters is a very sensitive issue that arguably has a significant influence in terms of predicted damage. In the context of this work no sufficiently precise and comprehensive answer to such issue has been found, nor does it exist in literature (to the best of the author's knowledge). Nonetheless, their influence is strongly emphasized, see [Oijer and Edlund, 2004, Bogsjö, 2006].
- Also, the strong correlation that has been observed between transients and vehicle speed around those transients, see figure 4.14, is obviously quite difficult to model. Indeed, drivers' behaviour may be very diverse within the population and it is unlikely that a simple and generic solution can be proposed for such a complex issue. It has been shown in figure 4.15 that the damage value is very sensitive to such phenomenon. Again, no answer can be found (to the best of the author's knowledge) in literature.
- More marginally, but not completely insignificantly, the use of a (non-stationary) PSD-based representation for road profiles may be too much of a constraint with respect to the actual evolution of real road profiles, see figure 4.22. Yet, it appears much more difficult to propose a model that is mathematically tractable if the latter is not based on such a simplification.

In view of these results, it appears that the practical implementation of the stochastic simulation methodology that is proposed here, *i.e.* the selected probabilistic descriptions for road and speed profiles, presents significant deficiencies in terms of precision. The analysis of the causes of errors seems to indicate that any increase in precision is likely to require the construction of more complex stochastic models. In turn, a more extensive statistical knowledge about the variability of road and speed profiles within the population, appears to be needed in order to select more elaborate models. Essentially, **the precision of the stochastic simulation methodology is naturally limited and a trade-off has to be reached between precision and complexity of the stochastic models involved.**

It can be argued that, if a very precise description of the load variability is sought, *e.g.* as a direct input to the elaboration of validation profiles, see subsection 2.2.3, it is potentially more appropriate to carry out a measurement campaign. However, **a measurement-based load characterisation is inevitably less convenient when studying trends (*e.g.* between different countries), sensitivities to influential factors, the loads acting on a vehicle with different characteristics or when carrying out more extensive (in terms of the volume of statistical information) analysis of load variability** (where the number of measurement samples will always be limited). It has been shown that the proposed methodology is rather well adapted for this latter purposes, see subsection 5.3.3, and to the processing of extensive statistical information, even if the precision of predictions can be limited. The practical application of the methodology is discussed next.

5.5 Application of stochastic simulation for reliability analysis

The methodology of stochastic simulation has been introduced in section 5.2. Its relevance for the study of load variability has been tested, discussed and analysed in both sections 5.3 and 5.4. Opportunities and limitations have been pointed out in view of the available results. In this section, application examples of the methodology are proposed in the specific framework in which it is destined to be used, namely the design of reliable vehicle components.

5.5.1 Design of reliable components and vehicle development process

The design and validation processes associated to the development of vehicles have been discussed in section 2.2. It has been pointed out that, the acquisition of information on the diversity of the loads imposed on the components of vehicles is based on load measurement campaigns.

Through measurements, it may be quite difficult to **anticipate the effect of the modification of influential factors make the decision to either adjust design targets and validation procedures accordingly or plan additional measurement campaigns** (if they are indeed required to obtain more precise information). In the context of vehicle development, such adjustments may be needed when designing a vehicle with quite different characteristics, destined to a different market (country) or to a different population of customers (usage). In such a case and if sufficient statistical information about the road and speed factors can be gathered, then the use of the stochastic simulation methodology can **yield valuable information rapidly and at a rather low cost and help making the appropriate decision**.

In what follows, an example is given for the use of the stochastic simulation methodology in this framework. A few illustrative modifications of the distribution of constituting parameters are performed. The objective is to emulate a country with roads of a poorer overall quality, a population with more aggressive driving behaviours or a vehicle with different characteristics. Subsequently, with the results of the simulated campaigns, the effect on the reliability of the components is illustrated. Also, the need to adapt design and validation targets is underlined using a simple stress-strength interference calculation, see *e.g* [Thomas et al., 1999, Johannesson and Speckert, 2013].

5.5.2 Realisation of different stochastic simulation campaigns

The methodology of stochastic simulation described in subsection 5.2.3 has been applied here. The extrapolation strategy (to $200000km$) and mixing information, see figure 5.16, described in subsection 5.4.3 is also used here. Different stochastic simulation campaigns are performed with different distributions of the constituting parameters of road and speed models (*i.e.* different statistical data on the variation of influential factors) and different vehicle characteristics.

Simulated campaigns

All the constituting parameters of the road and speed models, expect for the correlation parameter between road and speed ($\rho_{ls} = 0.8$), *i.e.* $\{S_1, w_1, w_2, \gamma, v_m, s_v, \theta\}$ are randomly drawn (for each road/speed realisation and each life situation) from a gamma distribution for which the mean and standard deviation, associated to the reference campaign, may be found in the following table 5.6.

Here, the objective is not to randomly re-sample from a dataset obtained from a measurement campaign. It is rather to assume that we posses statistical information on the variation of influential factors for a reference campaign (*e.g.* a given population) and study the effect of modifications of this statistical information.

The gamma distribution describes only positive values and has displayed a good fit with respect to the dataset presented in section 5.3.1. The parameters of the gamma

Constituting parameter	Mean value					Standard deviation				
	V	R	A	M	P	V	R	A	M	P
S_1	200	100	40	200	800	80	50	25	100	500
w_1	2.8	2.6	3	3	3.2	0.3	0.5	0.4	0.3	0.2
w_2	3.4	3.5	4	3	3.6	0.3	0.3	0.8	0.2	0.2
γ	0.5	0.5	1	0.7	0.2	0.2	0.2	0.4	0.2	0.1
v_m	25	40	80	35	20	4	6	20	5	3
s_v	10	15	20	10	10	2	3	8	3	2
θ	300	600	1000	500	500	100	500	800	300	400

Table 5.6: Mean and standard deviation of the gamma distributions of constituting parameters of both the road and speed models. Distribution parameters are different for each of the five life situations.

distribution $X \sim \Gamma(a, b)$, can be simply derived from their relation with the mean and standard deviation.

The reference characteristics of the linear quarter-car model used for the simulations, see subsection 2.3.2, are given in table 5.7.

Characteristics	m_s	c_s	k_s	m_t	k_t
	$420kg$	$1500N.s/m$	$30000N/m$	$46kg$	$250000N/m$

Table 5.7: Reference vehicle characteristics.

The following stochastic simulation campaigns are carried out, as an example of the application of the methodology. Only one modification is applied at a time, with respect to the reference campaign:

- #1 (Reference) Influential factors defined above in tables 5.6 and 5.7.
- #2 Mean values of the distributions of roughness parameter S_1 increased by 25%.
- #3 Mean values of the distributions of roughness parameter S_1 increased by 50%.
- #4 Mean values of the distributions of mean speed parameter v_m increased by 15%.
- #5 Sprung mass m_s increased by 10%.
- #6 Tyre roughness k_t increased by 15%.
- #7 Suspension damping c_s increased by 30%.

Many other modifications could be considered. Here, the objective is only to present an illustrative example through the modification of the most significant factors (see subsection 5.3.3) within ranges known by experience.

Comparisons of load variability and sensitivity to influential factors

For each one of the different campaigns, the medium and high quantiles (95%) are identified for each different response on the vehicle, namely the suspension displacement, sprung and unsprung accelerations. They are both divided by the value obtained for the reference campaign and displayed in figure 5.18.

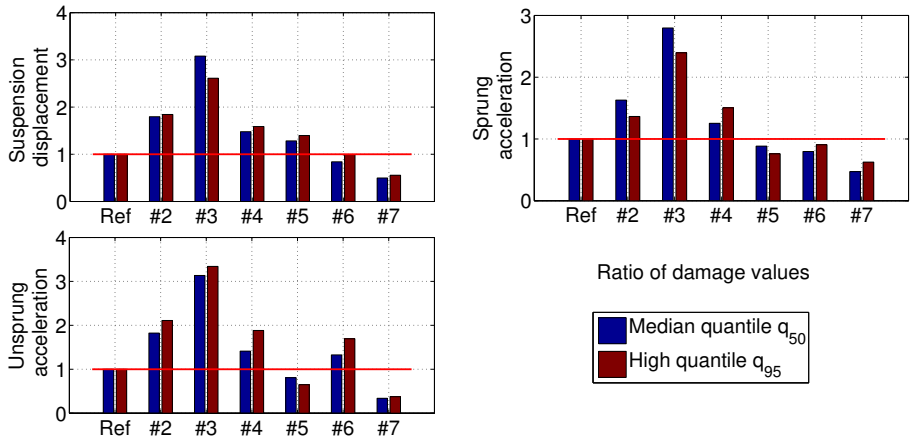

Figure 5.18: Sensitivity of high quantiles to influential factors. The first campaign is taken as a reference. All quantile values are given as a ratio to the reference campaign.

This illustrates that the methodology can be applied to study the effects of modifications in the variation of the different influential factors. **This would be both very long and costly if such analyses were to be done using measurements**, see also the conclusions of subsection 5.4.3.

5.5.3 Modifications of influential factors and reliability assessment

It is supposed that the three considered response signals are representative of the loads that may act on three distinct types of components. For example, the components of the chassis tend to be more related to unsprung accelerations, while the equipments mounted on the vehicle body tend to be more related to sprung accelerations. In order to get an idea on the effect of modifications of the load distribution on the reliability of vehicle components, the probability of failure is calculated using a simple stress-strength approach, see *e.g.* [Thomas et al., 1999]. This type of calculation has already been described in subsection 2.2.3. The following hypotheses are considered.

The strength of a component is rather defined through the load it is able to withstand. It is supposed that the strength of each component (three responses) is a scattered quantity, well represented by a log-normal distribution R. If the pseudo-damage value associated to the load exceeds the strength value of the component, then the latter will experience fatigue

failure. If S is the distribution of pseudo-damage values and if, for simplicity reasons, it is further assumed that S is also distributed according to a log-normal distribution, the probability of failure p_f may be calculated using a closed-form expression:

$$p_f = \text{Prob}(ln(R) - ln(S) < 0) = \Phi\left(\frac{\mu_{lnR} - \mu_{lnS}}{\sqrt{\sigma_{lnR}^2 + \sigma_{lnS}^2}}\right) \tag{5.11}$$

where Φ is the cumulative density function (CDF) of the normal distribution $N(0,1)$, and the load and strength distributions (independents from one another) are characterised by $S \sim LN(\mu_{lnS}, \sigma_{lnS})$ and $R \sim LN(\mu_{lnR}, \sigma_{lnR})$.

It is supposed here that the value $\sigma_{lnR} = 0.4$ is known from experience. Both μ_{lnS} and σ_{lnS} are inferred through the maximum likelihood estimation (MLE) using the result of each stochastic simulation campaign previously described. Lastly, μ_{lnR} is derived in order to reach a target value for P_f:

$$\mu_{lnR} = \mu_{lnS} + \Phi^{-1}(P_f)\sqrt{\sigma_{lnR}^2 + \sigma_{lnS}^2} \tag{5.12}$$

where Φ^{-1} is the inverse CDF of the normal distribution $N(0,1)$. Simply put, **the reliability target can only be achieved if the design** (and validation) **of the component**, *e.g.* choices of material and dimensions (and testing), **guarantees that this component possesses a strength R which mean value is at least equal to μ_{lnR} and which dispersion is no larger than $\sigma_{lnR} = 0.4$.**

Here, the value of μ_{lnR} is calculated using equation (5.12) when μ_{lnS} and σ_{lnS} are identified in relation to the reference campaign. The value μ_{lnR} then remains unchanged for the all the subsequent calculations. To be clear, this means that the design target (in terms of strength μ_{lnR}) for the component is derived from the reference campaign. Then, μ_{lnS} and σ_{lnS} are sequentially identified using the other simulated campaigns (#2 to #7) and the effect on the probability of failure is estimated using equation (5.11). The different probabilities of failure resulting from this calculation are displayed in figure 5.19.

This illustrates the usefulness of the proposed stochastic simulation methodology in order to analyse the sensitivity of the probability of failure of different components to the principal influential factors, namely the variability in road roughness or vehicle speed as well as a modification in the mechanical characteristics of the vehicle.

In practice, the specification of design targets as well as tests for validation are based on the use of deterministic profiles selected in relation with precise measurements using an instrumented vehicle (on the proving ground and for the load measurement campaign), see subsection 2.2.3. This operation is beyond the scope of the present manuscript. Nonetheless, if a design and validation process is applied in order to ensure and verify the reliability of vehicle components, **the stochastic simulation methodology can be used to enquire whether design and validation targets are still appropriate or should be**

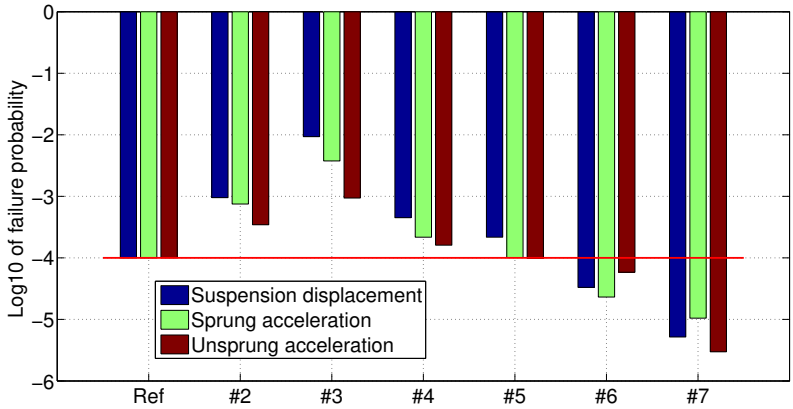

Figure 5.19: Sensitivity of failure probability to influential factors. The strength of the components (linked to the three response types) are selected to guarantee a given reliability target ($P_f = 10^{-4}$) for the reference campaign and remains unchanged for all calculations of P_f (#2 to #7).

adjusted when the variability of influential factors is significantly modified (*e.g.* for a different country/population).

5.6 Synthesis and conclusion

The strong diversity of load lives that may be experienced by a given component within a population of vehicles (associated to a population of customers), makes the issue of load characterisation a formidable statistical challenge. The most natural approach to the latter would be to record the load histories, associated to the said component, on multiple vehicles of that population and across their complete lives. This is obviously neither practical nor economically achievable. Thus, **it is necessary to divide the life of vehicles into shorter segments**.

This division can take multiple forms, but the use of life situations is a very interesting approach to reducing the need to record long histories, if the distribution of the proportion of the different life situations within the population of vehicles can be obtained through simple surveys. In principle, such surveys give valuable information about the diversity of vehicle lives within the population. From this point forward, it rathersbecome necessary to **quantify the load variability associated to each life situation** and the issue is somehow simplified. This latter characterisation is generally done using an instrumented vehicle carrying out measurements in each of these situations.

In this chapter a methodology has been proposed to derive the information on load variability from the statistical information on so-called **influential factors**, namely the

variability of road roughness and the variability of vehicle speed, combined with vehicle dynamics simulation. This former statistical information is stored in a parsimonious form, through so-called **constituting parameters**. The latter fully define stochastic models for road and speed profiles, which mathematical structures have been selected (in chapter 4) so that generated trajectories are as representative as possible of actual road and speed profiles. In this context, the objective of simulation is to convert this data on 'input quantities' into load histories, which are essentially 'output quantities' from the standpoint of the vehicle dynamics issue. Through this methodology, **the characterisation (statistical) effort is focused on 'inputs' rather than 'outputs'**.

The obvious advantages of this approach are that, provided information on influential factors is available, **an arbitrarily large set of load histories may be derived cheaply, rapidly and for a vehicle with any given characteristics**. Acquiring information on influential factors is generally easier and less expensive and the latter is vehicle-independent. Conversely, acquiring samples through measurements is long and expensive, which naturally limits the ability to study load variability extensively and bounds all obtained results to the specific choices of routes, drivers and vehicle.

The usefulness and relevance of this simulation-based paradigm and the expectable quality of the results depend on two elements. First, **one needs to be able to generate random trajectories that are representative of the actual road and speed profiles that can be encountered in real conditions.** Second, **any result of the simulation-based approach depends on the fidelity of the vehicle model used for simulation**, which transforms the road excitation into vehicle-dependent responses, defining in turn the loads acting on the studied components of the vehicle.

Here, the comparison of a simulated campaign with a real measurement campaign has shown that the results of the practical implementation of the methodology, *i.e.* the selected stochastic models for road and speed profiles, show significant deficiencies in terms of precision. Several explanations have been advanced but the most likely contributors are the presence of strongly non-stationary patterns in road profiles, or **transients**, and the natural correlation of the latter with the evolution of the speed model. They induce large amounts of (fatigue) damage and their modelling appears to be a very sensitive issue. On the other hand, simulation errors do not constitute a serious impediment if the methodology is used to make comparison between loading environments, using the same model. For the latter issue, the solution to realise improvements is fairly obvious, namely ameliorating the fidelity of the vehicle model, but nonetheless significantly increases the computational cost of any prediction.

It has simultaneously been shown that the large number of load histories that can be generated proves very useful and efficient for the **study of trends (*e.g* between different countries or vehicles with different characteristics) or of the sensitivity to influential factors**. In the last section, 'sensitivity-related' analyses have been displayed in the practical context of the design and validation of vehicle components. For example, the information they provide can be used to enquire whether deterministic testing profiles based on company-specific proving ground are still adapted if a new vehicle with quite

different characteristics is being designed or if the influential factors have been modified significantly (in the statistical sense), *e.g.* for a different population of customers. It can also be used to get more extensive insights into the effect of modifications of the load variability on the estimated reliability of components. Indeed, this evaluated probability of failure is a quantity that is particularly sensitive to the statistical hypothesis being employed or the statistical data at disposal.

As far as perspectives go, due to the strong complexity of modelling extremely varying and correlated quantities, such as road and speed profiles, or the complexity of the dynamic behaviour of the vehicle, it does not seem relevant to use the proposed methodology to directly perform predictions of load variability (*e.g.* to assess the relative severity between a testing profile and a population of customers). **Increasing the quality of the results would require a large and potentially prohibitive increase in the complexity of stochastic models**, which would in turn imply much more extensive road and speed characterisation than what is available in the context of this research work. Even if improving the vehicle model seems possible (to a non-linear model), thus increasing significantly the computation time, it is not necessarily a guarantee for better results if the randomly generated inputs fed to simulation are not sufficiently representative.

In contrast, the proposed methodology is arguably a very interesting tool to **process large amounts of statistical information one may have collected on influential factors**. Information on influential factors could be gathered in the future through extensive acquisitions, realised for example using the on-board sensors that are increasingly being installed on most commercial vehicles, as well as the road estimation method proposed in chapter 3. **This opens the potential for more extensive and flexible characterisations of load variability and its sensitivity to influential factors than can ever be achieved through standard measurement campaigns**. Another potential application includes addressing the different questions that have been laid out within the framework on this chapter, regarding the issue of extrapolation from small sections and the division of the load life of vehicles. The effects of the latter appear to be often underestimated due to the lack of information but are arguably extremely important.

Simply put, **the stochastic simulation methodology is more a valuable statistical processing and analysis tool rather than a precise instrument of load characterisation as load measurement campaigns are, yet at much larger cost and with much lower flexibility for analysis**.

To remember

- The central principle of the proposed methodology is to concentrate statistical analysis efforts on 'inputs' rather than 'outputs'.
- The proposed methodology of stochastic simulation consists in simulating load histories rather than measuring them through load measurement campaigns. Random road and speed profiles are generated and load histories may subsequently be derived through simulations.
- This allows us to generate rapidly and at a low cost an arbitrarily large set of load histories for any given component and any given vehicle.
- Life situations are an interesting approach to describe the variability of road and speed factors across the life of vehicles within a given population.
- Essentially, the proposed methodology is a combination of stochastic modelling of road and speed profiles, stratified sampling (life situations) and vehicle dynamics simulation.
- The quality of the results depends on the representativeness of the generated road and speed profiles, as well as on the fidelity of the vehicle model.
- The quality of the practical implementation (selected stochastic models) of the methodology has been analysed through two comparisons between simulated campaigns and measurement campaigns (in two different countries).
- The most likely cause for the poor quality of the observed results is that non-modelled transient patterns (and the associated road/speed correlation) account for a significant fraction of the damage. Unfortunately, any attempt to increase the representativeness of stochastic road and speed models would induce a very significant and potentially prohibitive increase in complexity and require more extensive road and speed profile data.
- Conversely, comparisons between the observed and predicted sensitivities to influential factors have shown better and exploitable results.
- The stochastic simulation methodology is more a valuable statistical processing and analysis tool rather than a precise instrument of load characterisation as load measurement campaigns are, yet at much larger cost and with much lower flexibility for analysis.

Chapter 6

Conclusions and perspectives

Summary of the conducted research work and main contributions

The acquisition of statistical information about the large diversity of load lives experienced by different vehicles is an indispensable and critical element for the definition of design and validation targets, during the vehicle development process, or for any assessment of the reliability of vehicle components. In this manuscript, a fundamental change in approach to the quantification of the variability of road-induced fatigue loads within a population of vehicles has been proposed.

Proposed stochastic simulation methodology

Conceptually, the methodology is founded upon the principle of **concentrating statistical analysis efforts on input factors**, or 'influential factors', namely the road excitation applied on the vehicle that depends on the geometry of the road surface and on vehicle speed, **rather than directly on output factors**, namely the dynamic responses generated on a particular vehicle.

It is proposed that numerous random realisations of road and speed profiles are generated through appropriate stochastic models and used to calculate the dynamic responses of the vehicle through simulation. In this framework, **an arbitrary large set of load histories can be obtained rapidly and at a low cost for any response quantity on a vehicle with any given mechanical characteristics**. These latter features represent clear advantages of a simulation-based approach over the conventional, long and costly 'load measurement campaigns' based a particular instrumented vehicle.

It should be strongly emphasized that the efficiency of the proposed methodology depends heavily on the ability to describe the variability of influential factors such as road roughness or vehicle speed and generate representative realisations of road and speed

profiles. **The analysis and modelling of the variability of such factors, across the lives of different vehicles of a population, constitute a central objective of this research work**. Also, any simulation-based results are inevitably dependent on the fidelity of the vehicle model.

Analysis and modelling of the variability of influential factors

Stochastic simulations can only be carried out if there is available statistical information about the variability of influential factors (road and speed). The latter may be collected through multiple means and it is generally possible to acquire such information in a more extensive and yet less expensive manner than load histories. Also, this information is vehicle-independent.

Within this research work, **an efficient road estimation algorithm has been proposed and tested** in chapter 3 and latter **used in view of extracting information on the road excitation from the measured responses of a vehicle**. Here, statistical information about the variability of road and speed profiles has been acquired inexpensively from the processing of existing datasets, gathered by Renault in the context of different load measurement campaigns, see chapter 4.

Different stochastic models have been considered as candidates for the generation of road and speed profiles, either based on existing work available in the literature or based on original propositions formulated within this manuscript. For all candidate mathematical structures, randomly generated trajectories have been compared with real road (obtained as a result of the road estimation method) and speed (measured) profiles, according to both statistical and damage-based relevant criteria. **An extensive study** performed in chapter 4 **has led us to select the most suitable model, with respect to these criteria, among the different candidates**.

The **stochastic road model** eventually selected is extracted from literature, fully described by 4 scalar parameters and based on a **piecewise-stationary Gaussian process** with a PSD in the form of two juxtaposed power laws with negative exponents. The length of the different stationary sections is kept constant and the variance on those sections is distributed according to a Gamma distribution. The selected **speed model** is an original proposition of this work and is also fully described by 4 scalar parameters. It consists of a **piecewise-constant process**, where the length of a constant speed section is distributed exponentially and the value of vehicle speed on a given section is distributed normally. Both distributions are correlated through a linear Gaussian copula. Additionally, the issue of the correlation between road and speed profiles has been analysed in chapter 4.

Inference techniques have been described and applied to identify the 4 scalar parameters determining each model structure, labelled as '**constituting parameters**', based on observed road and speed profiles. All analyses, predictions and comparisons have been realised using $10km$-long profiles. This latter length has been presented as a good compromise when it comes to analysing the variability of influential factors both across the life

of a given vehicle and between different vehicles of a given population. A simplification of the issue has been proposed in this manuscript through the assumption that 'constituting parameters' conceptually represent a 'projection' of continuously varying quantities (on $10km$), namely road and speed profiles, on a vector of limited dimension (here $n = 8$). **It is then much easier to propose a statistical analysis of these constituting parameters across the lives of a population of vehicles.**

Variability of constituting parameters across the lives of vehicles

Provided the selected stochastic models enable us to generate random trajectories that are representative of the segments ($10km$-long) on which constituting parameters have been identified, the description of the variability of influential factors essentially consists in the **description of the variability of constituting parameters**. This latter description thus constitutes a key element of the methodology.

The division of the life of the vehicle based on the concept of **life situations** (*e.g.* city travels, country travels, highway travels) has been introduced here. Using this approach it is possible to gather, through surveys carried out among the studied population of customers (drivers), valuable and extensive information with respect to the variation in constituting parameters across the lives of different vehicles. Indeed, it has been shown that the scatter of these parameters is notably reduced within the boundaries of each life situation. The concept of life situation is already applied in the context of the available measurement data but it is also particularly interesting to apply it in relation with the proposed stochastic simulation methodology, in order to facilitate the description of the variability of constituting parameters.

Essentially, **the proposed methodology is a combination of the stochastic modelling of influential factors** (thus requiring statistical information), the division of 'the population of loads', which can be seen as an application of **stratified sampling**, and **vehicle dynamics simulation**.

Testing of the methodology

In order to test the representativeness of the methodology in its practical implementation form, *i.e.* with the selected stochastic models, **stochastic simulation results have been compared with datasets acquired through standard load measurement campaigns**. Two large measurement campaigns (worth a few thousands of kilometres) based on the use of life situations (stratified sampling) and corresponding to two different countries, have been processed for this purpose. In order to make comparisons based on the same 'statistical information', here stochastic simulations have been performed using values of the constituting parameters that have been randomly sampled from the set of parameters identified from the different estimated road excitations (*i.e.* based on the processing of the measurement campaign).

Three types of response signals have been considered in order to assess the quality of the methodology.

1. Responses measured on the instrumented vehicle

2. Responses obtained through the simulation of the previously estimated road excitations (estimated road profiles and measured speed profiles), using a linear quarter-car model.

3. Responses obtained from stochastic simulations, using a linear quarter-car model.

The comparison between the first and second types of responses is mostly affected by simulation errors and road estimation errors since no stochastic models are involved. The comparison between the second and third types of responses is a better judge of the quality of the methodology as **it directly reflects the representativeness of the selected stochastic models** and since the same vehicle model is used in both cases.

In chapter 5, comparisons between the load variability derived from stochastic simulations and the load variability observed from measurements, have been performed both for each defined life situation and for the complete lives of vehicles. To carry out the latter comparisons, associated to a target mileage value of $200000km$, the same extrapolation rule has been used when processing load histories ($10km$-long) obtained both from measurements and from simulations. Also assessments of the sensitivity of loads to influential factors, based on simulated and observed (measured) load histories, have been compared.

Potential application for the methodology in the industrial context

In the last section of chapter 5 the methodology has been applied on a toy example in order to illustrate its usefulness. Several stochastic simulation campaigns have been carried out with different distributions for the constituting parameters (road and speed) and for vehicles with different characteristics, thus emulating the development process for a different market or a new vehicle. The effect of such modifications on the reliability of vehicle components has been illustrated using a simple stress-strength calculation.

It has been shown that the methodology can be used to anticipate the effect of significant modifications in the loading environment of the vehicle's components and enquire whether design and validation targets should be modified or whether additional (precise) measurement campaigns should be considered. Conversely, analysing trends and sensitivities to influential factors would be very long and expensive when using uniquely a measurement-based approach.

Analysis of the obtained results and main conclusions

Quality of the prediction of load variability

On the one hand, the comparisons between the simulated responses to estimated road excitations and the measured responses on the vehicle illustrate that (as partly expected) the linear quarter-car model is a very crude representation of the dynamics of the actual vehicle on which responses have been measured and that simulated responses are affected by significant errors. Also the estimated road excitation (road + speed) is not fully representative of the actual excitation, due to the (discussed) imperfections in the road estimation method. Consequently, it may not be relevant to use the results of stochastic simulations as a precise description of the loads acting on vehicles' components, *e.g.* for fatigue life calculations or to define validation profiles used on test rigs.

Simply put, even if the selected stochastic models were perfect representations of the estimated road and speed profiles, the precision to which the simulation-based methodology could aspire would be limited by simulation errors. This is in fact a natural consequence of the selection of a very simple model rather suited for statistical analyses of the diversity of road-induced loads. Nonetheless, it is seen that the effect of simulation-based (and road estimation) errors can be somehow circumvented if the methodology is applied to **perform relative analyses and comparisons** (between different results of simulations).

On the other hand, the comparisons, through the same vehicle model, between the responses to randomly generated road excitations and to estimated road excitations, also show significant discrepancies. The latter point to **deficiencies in the representativeness of the selected stochastic models for road and speed profiles**. This represents a more serious and inconvenient issue than the effect of simulation-based errors, as it can induce an erroneous assessment of load variability.

Difficulties related to stochastic modelling

The most significant contributor to the poor quality in the prediction of load variability is expected to be the presence of occasional transient patterns such as potholes or speed-bumps, which are not accounted for by the selected road model, since the stochastic description proposed for transients here has not yielded satisfactory results. It has been shown that such **transients can contribute significantly to the damage accumulation** and also that **proposing a tractable mathematical description for the latter might not be easy** since their frequency, forms and amplitude are arguably quite diverse.

It should also be emphasized that a strong correlation between the road and speed profiles has been observed in the vicinity of transients. Indeed, drivers tend to lower their speed when they detect a severe variation in the road profile. To the author's best knowledge, there is no solution to the issue of the correlation between road and speed stochastic models that can be found in literature. Yet its influence on the damage is

significant. Given the diversity of driver behaviours and the fact that one has to deal with continuous and non-stationary random signals, **it is unlikely that a simple or a generic** (*i.e.* applicable for all situations) **mathematical solution to such a complex problem may be found**. Different populations of drivers can have different behaviours in this respect, which constitutes a very involved statistical challenge.

Statistical analysis of trends and sensitivity to influential factors

The comparisons that have been performed between observed sensitivities (based on available measurements) and predicted sensitivities (based on stochastic simulations), seem to indicate that the methodology provides good descriptions of the overall trends and magnitudes regarding the effect of the different influential factors (constituting parameters) on load histories. Since this result has been derived for mean values of the load distribution (using response surfaces adjusted using least squares approaches), one should remain careful when extrapolating the observed trends for high quantiles of the load distribution.

It has been shown on a toy example in chapter 5, that the proposed methodology represents a particularly efficient approach when there is extensive information available on the distribution of the constituting parameters (variation of influential factors), *e.g.* in different countries, and when it is interesting to analyse overall trends rapidly and objectively.

Perspectives for improvement

Current implementation of the methodology: selected stochastic models and vehicle model

Essentially, in this manuscript, **'reasonably simple' model structures** have been proposed and tested against relatively limited sets of real data (*e.g.* number of cover roads and drivers). More detailed stochastic models could be imagined, in order to describe the inherently complex evolution of road and speed profiles and with the objective of improving the quality of the results of the proposed methodology. However, they would likely imply **a serious and potentially prohibitive increase in complexity as well as a need for more extensive statistical information** (*e.g.* on the diversity of driver behaviours in the vicinity of transients). A **trade-off** necessarily has to be reached between complexity and the level of precision that is needed. It should be noted that very complex statistical models, *i.e.* models based on multiple statistical hypotheses, can naturally raise questions on the confidence one can attribute to the results.

Additionally, it is quite difficult to rigorously **'validate'** (in the conventional sense) **the selection of stochastic models**. The best that can be done (see chapter 4) is to compare random realisations generated from such models with available real data and according to criteria that have been deemed relevant for the application at hand, *e.g.* damage generated

on different points of the vehicle, frequency content of the excitation, etc. Unfortunately, while stochastic models may be sufficiently precise with respect to the prediction of one response quantity, *e.g.* suspension displacement, they may simultaneously be too crude to predict a more 'road-sensitive' response quantity, *e.g.* unsprung acceleration, as observed here when comparing the quality of the results obtained for the different responses.

Conversely, the amelioration of the quality of vehicle dynamics simulation should not be seen as a delicate matter, at least conceptually speaking. A more elaborate and detailed model (described in this manuscript) for the vehicle and its tyres can always be considered but this will significantly **increase the calculation time**. Again, a **trade-off** has to be reached between computation cost/complexity and the level of precision that is needed.

Deeper statistical analyses of the diversity of road-induced loads

Within this manuscript it has been pointed out that certain aspects of the issue of load variability are often disregarded and seldom discussed in literature, due to both the complexity of the issue and the lack and cost of information. The main question that has in particular been revealed and analysed is the following. How can one extrapolate from observed (simulated or measured) short load histories (at best a few thousand kilometres) to the complete life of the vehicle (high mileage values) and for different vehicles? An underlying conceptual question can be formulated: **how are the influential factors evolving across the life of different vehicles within a population of interest**?

It is the opinion of the author that **the key to making progress regarding this formidable statistical challenge is to analyse influential factors (or constituting parameters)** rather than directly loads, which is the central objective of the proposed work. One should be advised that the selected extrapolation rule is in fact extremely influential with respect to the prediction of load variability. Also, any improvement of the process of reliability prediction is strongly dependent on the capacity to acquire representative information about load variability.

In the end, it seems that the leitmotiv for any improvement regarding the description of the load variability is: **'acquire more data'**. The research work presented within this manuscript provides a relevant framework to seek a more extensive description of load variability than could ever be achieved through measurements (where cost and time are a concern).

Conclusion on the industrial applicability

The simulation-based methodology that has been proposed through this research work should essentially be seen as a rapid, inexpensive, flexible and effective statistical processing approach, which can be used to add value to any information about the evolution of road and speed profiles, *e.g.* within a country or population of interest, provided such

information is available. An efficient road estimation algorithm has also been proposed to valorize voluminous existing datasets.

It appears that **the methodology constitutes the first step** (and likely the most relevant approach) **to pursuing more extensive characterisations of load variability**, especially for high mileage values and ultimately **to improve the assessment of the reliability of vehicle components.**

In its current implementation form, care is advised when using the methodology, depending on the level of precision that is sought. However, it clearly represents an interesting tool to rapidly **study overall trends with respect to the influence of certain factors** such as the overall road roughness level of a given country, the stiffness of the suspension or tyre, the driving behaviours of different populations, etc., or certain hypotheses (*e.g.* the extrapolation rule). This is clearly not economically achievable when using measurement campaigns in the industrial context related to the development of vehicles. In consequence, **the methodology can be used to provide objective information and help address certain decision problems** such as the following: should design and validation targets be re-evaluated/modified when designing a new vehicle destined to a different loading environment and should specific and costly measurements be planed in order to adjust these targets?

This research work has also clearly been helpful to better identify conceptual difficulties and limitations associated to a probabilistic description of the loading environment of the vehicle but also to the issue of load characterisation in general.

Published materials and acknowledgements

Within the context of this research work, the following materials have been published. The stochastic simulation methodology proposed within this manuscript has been presented at the Fatigue Design 2015 conference and published in [Fauriat et al., 2015b]. The road estimation algorithm developed within this manuscript has been proposed in view of addressing the issue of road roughness variability in [Fauriat et al., 2016]. A discussion about the issue of extrapolation from short segments of load measurements has been presented at the 'Congrès Français de Mécanique' (CFM) 2015 conference, see [Fauriat et al., 2015a].

The author would like to acknowledge the support of Renault and the French 'Association Nationale de la Recherche et de la Technologie' (ANRT).

Bibliography

[AFNOR, 1991] AFNOR (1991). A03-405 - produits métalliques - essais de fatigue - traitement statistique des données.

[AFNOR, 1993] AFNOR (1993). A03-406 - produits métalliques - fatigue sous sollicitations d'amplitude variable - méthode rainflow de comptage des cycles.

[Andren, 2006] Andren, P. (2006). Power spectral density approximations of longitudinal road profiles. *International Journal of Vehicle Design*, Vol40:p2–14.

[Basquin, 1910] Basquin, O. (1910). The exponential law of endurance tests. In *Proc. Astm*, volume 10, pages 625–630.

[Benasciutti and Tovo, 2005] Benasciutti, D. and Tovo, R. (2005). Spectral methods for lifetime prediction under wide-band stationary random processes. *International Journal of fatigue*, Vol27(8):p867–877.

[Bogsjö, 2006] Bogsjö, K. (2006). Development of analysis tools and stochastic models of road profiles regarding their influence on heavy vehicle fatigue. *Vehicle System Dynamics*, Vol44(sup1):p780–790.

[Bogsjö, 2007] Bogsjö, K. (2007). Evaluation of stochastic models of parallel road tracks. *Probabilistic Engineering Mechanics*, Vol22(4):p362–370.

[Bogsjo et al., 2012] Bogsjo, K., Podgorski, K., and Rychlik, I. (2012). Models for road surface roughness. *Vehicle System Dynamics*, Vol50(5):p725–747.

[Bogsjö and Rychlik, 2009] Bogsjö, K. and Rychlik, I. (2009). Vehicle fatigue damage caused by road irregularities. *Fatigue & Fracture of Engineering Materials & Structures*, Vol32:p391–402.

[Bouyé et al., 2000] Bouyé, E., Durrleman, V., Nikeghbali, A., Riboulet, G., and Roncalli, T. (2000). Copulas for finance-a reading guide and some applications. *Available at SSRN 1032533*.

[Bruscella et al., 1999] Bruscella, B., Rouillard, V., and Sek, M. (1999). Analysis of road surface profiles. *Journal of Transportation Engineering*, Vol125(1):p55–59.

[Burger, 2014] Burger, M. (2014). Calculating road input data for vehicle simulation. *Multibody System Dynamics*, Vol31(1):p93–110.

[Cebon, 1999] Cebon, D. (1999). *Handbook of vehicle-road interaction.*

[Charles, 1993] Charles, D. (1993). Derivation of environment descriptions and test severities from measured road transportation data. *Journal of the IES*, Vol36(1):p37–42.

[De Cuyper et al., 2003] De Cuyper, J., Verhaegen, M., and Swevers, J. (2003). Off-line feed-forward and $h-\infty$ feedback control on a vibration rig. *Control engineering practice*, Vol11(2):p129–140.

[Dirlik, 1985] Dirlik, T. (1985). *Application of computers in fatigue analysis.* PhD thesis, University of Warwick.

[Dodds and Robson, 1973] Dodds, C. and Robson, J. (1973). Description of road surface roughness. *Journal of Sound and Vibration*, Vol31(2):p175–183.

[Doumiati et al., 2014] Doumiati, M., Erhart, S., Martinez, J.-J., Sename, O., and Dugard, L. (2014). Adaptive control scheme for road profile estimation: Application to vehicle dynamics. In *World Congress*, volume 19, pages 8445–8450.

[Doumiati et al., 2011] Doumiati, M., Victorino, A., Charara, A., and Lechner, D. (2011). Estimation of road profile for vehicle dynamics motion: experimental validation. In *American Control Conference (ACC), 2011*, pages 5237–5242. IEEE.

[Dreßler et al., 1997] Dreßler, K., Hack, M., and Kruger, W. (1997). Stochastic reconstruction of loading histories from a rainflow matrix. *ZAMM Journal of Applied Mathematics and Mechanics/Zeitschrift für Angewandte Mathematik und Mechanik*, Vol77:p217–226.

[Dreßler et al., 2009] Dreßler, K., Speckert, M., Müller, R., and Weber, C. (2009). *Customer loads correlation in truck engineering.* Fraunhofer-Institut für Techno-und Wirtschaftsmathematik, Fraunhofer (ITWM).

[Echard, 2012] Echard, B. (2012). *Evaluation par krigeage de la fiabilité des structures sollicitées en fatigue.* PhD thesis, Université Blaise Pascal-Clermont-Ferrand II.

[Fauriat et al., 2015a] Fauriat, W., Mattrand, C., Gayton, N., and Beakou, A. (2015a). Analyse de la variabilité des chargements de fatigue dans l'automobile et influence sur les prévisions de fiabilité. In *Congrès Français de Mécanique 2015.*

[Fauriat et al., 2015b] Fauriat, W., Mattrand, C., Gayton, N., and Beakou, A. (2015b). An application of stochastic simulation to the study of the variability of road induced fatigue loads. *Procedia Engineering*, Vol133:p631–645.

[Fauriat et al., 2016] Fauriat, W., Mattrand, C., Gayton, N., Beakou, A., and Cembrzynski, T. (2016). Estimation of road profile variability from measured vehicle responses (accepted for publication). *Vehicle System Dynamics.*

[Ferris, 2004] Ferris, J. B. (2004). Characterising road profiles as markov chains. *International journal of vehicle design*, Vol36:p103–115.

[Gagarin et al., 2004] Gagarin, N., Huang, N. E., Oskard, M. S., Sixbey, D. G., and Mekemson, J. R. (2004). The application of the hilbert-huang transform to the analysis of inertial profiles of pavements. *International journal of vehicle design*, Vol36:p287–301.

[Gear, 1971] Gear, C. W. (1971). *Numerical initial value problems in ordinary differential equations*. Prentice Hall PTR.

[Genet, 2006] Genet, G. (2006). *A statistical approach to multi-input equivalent fatigue loads for the durability of automotive structures.* PhD thesis, Chalmers University.

[Ghanem and Spanos, 2003] Ghanem, R. G. and Spanos, P. (2003). *Stochastic finite elements, a spectral approach*. Dover Publications.

[Gillespie et al., 1980] Gillespie, T., Sayers, M., and Segel, L. (1980). Calibration of response-type road roughness measuring systems. Technical report, NCHRP Report 228.

[Gonzalez et al., 2008] Gonzalez, A., O'Brien, E. J., Li, Y. Y., and Cashell, K. (2008). The use of vehicle acceleration measurements to estimate road roughness. *Vehicle System Dynamics*, Vol46(6):p483–499.

[Hadamard, 1923] Hadamard, J. (1923). *Lectures on Cauchy's Problem in Linear Partial Differential Equations*. Dover Phoenix, New York, NY, USA.

[Heuler and Klätschke, 2005] Heuler, P. and Klätschke, H. (2005). Generation and use of standardised load spectra and load–time histories. *International Journal of Fatigue*, Vol27(8):p974–990.

[Howe et al., 2004] Howe, J. G., Chrstos, J. P., Allen, R. W., Myers, T. T., Lee, D., Liang, C.-Y., Gorsich, D., and Reid, A. (2004). Quarter car model stress analysis for terrain/road profile ratings. *International journal of vehicle design*, Vol36(2):p248–269.

[Hugo et al., 2008] Hugo, D., Heyns, P. S., Thompson, R., and Visser, A. T. (2008). Haul road defect identification using measured truck response. *Journal of Terramechanics*, Vol45(3):p79–88.

[Idier, 2013] Idier, J. (2013). *Bayesian approach to inverse problems*. John Wiley & Sons.

[Imine et al., 2006] Imine, H., Delanne, Y., and M'sirdi, N. (2006). Road profil input estimation in vehicle dynamics simulation. *Vehicle System Dynamics*, Vol44(4):p285–303.

[ISO8608, 1995] ISO8608 (1995). Iso 8608:1995 mechanical vibration - road surface profiles - reporting of measured data.

[Jeong et al., 1990] Jeong, W., Yoshida, K., Kobayashi, H., and Oda, K. (1990). State estimation of road surface and vehicle system using a kalman filter. *JSME international journal. Ser. 3, Vibration, control engineering, engineering for industry*, Vol33(4):p528–534.

[Johannesson and Rychlik, 2014] Johannesson, P. and Rychlik, I. (2014). Modelling of road profiles using roughness indicators. *International Journal of Vehicle Design*, Vol66(4):p317–346.

[Johannesson and Speckert, 2013] Johannesson, P. and Speckert, M. (2013). *Guide to load analysis for durability in vehicle engineering.* John Wiley & Sons.

[Kalman, 1960] Kalman, R. E. (1960). A new approach to linear filtering and prediction problems. *Journal of Basic Engineering*, Vol82 (1):p35–45.

[Kamash and Robson, 1978] Kamash, K. and Robson, J. (1978). The application of isotropy in road surface modelling. *Journal of Sound and Vibration*, Vol57(1):p89–100.

[Kharoufeh and Gautam, 2004] Kharoufeh, J. P. and Gautam, N. (2004). Deriving link travel-time distributions via stochastic speed processes. *Transportation Science*, Vol38(1):p97–106.

[Lalanne, 2010] Lalanne, C. (2010). *Mechanical Vibration and Shock Analysis, Fatigue Damage*, volume Vol4. John Wiley & Sons.

[LCPC, 2000] LCPC (2000). Mesure de l'uni longitudinal des chaussées routières et aéronautiques, méthode d'essai numéro 46 du laboratoire central des ponts et chaussées.

[Lemaire, 2013] Lemaire, M. (2013). *Structural reliability.* John Wiley & Sons.

[Lourens et al., 2012] Lourens, E., Reynders, E., De Roeck, G., Degrande, G., and Lombaert, G. (2012). An augmented kalman filter for force identification in structural dynamics. *Mechanical Systems and Signal Processing*, Vol27:p446–460.

[Matsuishi and Endo, 1968] Matsuishi, M. and Endo, T. (1968). Fatigue of metals subjected to varying stress. *Japan Society of Mechanical Engineers, Fukuoka, Japan*, pages p37–40.

[Maybeck, 1979] Maybeck, P. (1979). *Stochastic models, estimation and control, volume 1.* Academic Press.

[Miner, 1945] Miner, M. A. (1945). Cumulative damage in fatigue. *Journal of applied mechanics*, Vol12(3):p159–164.

[Neyman, 1934] Neyman, J. (1934). On the two different aspects of the representative method: the method of stratified sampling and the method of purposive selection. *Journal of the Royal Statistical Society*, pages p558–625.

[Ngwangwa et al., 2010] Ngwangwa, H., Heuns, P., Labuschagne, F., and Kululanga, G. (2010). Reconstruction of road defects and road roughness classification using vehicle responses with artificial neural networks simulation. *Journal of Terramechanics*, Vol47:p97–111.

[Oijer and Edlund, 2004] Oijer, F. and Edlund, S. (2004). Identification of transient road obstacle distributions and their impact on vehicle durability and driver comfort. *Vehicle System Dynamics*, Vol41:p744–753.

[Pacejka, 2005] Pacejka, H. (2005). *Tire and vehicle dynamics.* Elsevier.

[Papoulis, 1991] Papoulis, A. (1991). *Probability, random variables and stochastic processes, Third Edition.* McGraw-Hill.

[Parzen, 1962] Parzen, E. (1962). *Stochastic processes.* SIAM.

[Pitoiset, 2001] Pitoiset, X. (2001). *Méthodes spectrales pour une analyse en fatigue des structures métalliques sous chargements aléatoires multiaxiaux.* na.

[Prem, 1988] Prem, H. (1988). A laser-based highway-speed road profile measuring system. *Vehicle System Dynamics*, Vol17(sup 1):p300–304.

[Priestley, 1981] Priestley, M. (1981). *Spectral analysis and time series.* Academic Press, New York.

[Robson and Dodds, 1976] Robson, J. and Dodds, C. (1976). Stochastic road inputs and vehicle response. *Vehicle System Dynamics*, Vol5:p1–13.

[Rouillard, 2009] Rouillard, V. (2009). Statistical models for non-stationary and non-gaussian vehicle vibrations. *Engineering Letters*, Vol17(4):p1–11.

[Rouillard et al., 2000] Rouillard, V., Bruscella, B., and Sek, M. (2000). Classification of road surface profiles. *Journal of Transportation engineering*, Vol126(1):p41–45.

[Rouillard et al., 2001] Rouillard, V., M.Sek, and B.Bruscella (2001). Simulation of road surface profiles. *Journal of Transportation Engineering*, Vol127(3):p247–253.

[Saltelli et al., 2006] Saltelli, A., Ratto, M., Tarantola, S., Campolongo, F., Commission, E., et al. (2006). Sensitivity analysis practices: Strategies for model-based inference. *Reliability Engineering & System Safety*, Vol91(10):p1109–1125.

[Sayers et al., 1986] Sayers, M., Gillespie, T., and Queiroz, A. (1986). The international road roughness experiment. establishing correlation and a calibration standard for measurements. Technical report, World Bank (No. HS-039 586) USA.

[Sayers and Karamihas, 1998] Sayers, M. and Karamihas, S. (1998). The little book of profiling. Technical report, University of Michigan Transportation Research Institute ders notlari, Michigan, USA.

[Shinozuka and Jan, 1972] Shinozuka, M. and Jan, C.-M. (1972). Digital simulation of random processes and its applications. *Journal of sound and vibration*, Vol25(1):p111–128.

[Sobczyk et al., 1977] Sobczyk, K., Macvean, D., and Robson, J. (1977). Response to profile-imposed excitation with randomly varying traversal velocity. *Journal of Sound and Vibration*, Vol52(1):p37–49.

[Steinwolf et al., 2002] Steinwolf, A., Giacomin, J., and Staszewski, W. (2002). On the need for bump event correction in vibration test profiles representing road excitations in automobiles. *Proceedings of the Institution of Mechanical Engineers, Part D: Journal of Automobile Engineering*, Vol216(4):p279–295.

[Sun, 2001] Sun, L. (2001). Computer simulation and field measurement of dynamic pavement loading. *Mathematics and Computers in Simulation*, Vol56(3):p297–313.

[Tarantola, 2005] Tarantola, A. (2005). *Inverse problem theory and methods for model parameter estimation.* Siam.

[Thomas et al., 1999] Thomas, J., Perroud, G., Bignonnet, A., and Monnet, D. (1999). Fatigue design and reliability in the automotive industry. *Fatigue Design and Reliability*, Vol23:p1–11.

[Tikhonov, 1963] Tikhonov, A. N. (1963). Regularization of incorrectly posed problems. In *Soviet Math. Dokl*, volume 4, pages 1624–1627.

[Tudon-Martinez et al., 2015] Tudon-Martinez, J., Fergani, S., Sename, O., Martinez, J., Morales-Menendez, R., and Dugard, L. (2015). Adaptive road profile estimation in semiactive car suspensions. *IEEE Transactions on Control Systems, 2015.*

[Virchis and Robson, 1971] Virchis, V. and Robson, J. (1971). Response of an accelerating vehicle to random road undulation. *Journal of Sound and Vibration*, Vol18(3):p423–427.

[Yousefzadeh et al., 2010] Yousefzadeh, M., Azadi, S., and Soltani, A. (2010). Road profile estimation using neural network algorithm. *Journal of Mechanical Science and Technology*, Vol24(3):p743–754.

[Yu et al., 2013] Yu, W., Zhang, X., Guo, K., Karimi, H. R., Ma, F., and Zheng, F. (2013). Adaptive real-time estimation on road disturbances properties considering load variation via vehicle vertical dynamics. *Mathematical Problems in Engineering.*

Index

augmented Kalman filter, 38, 39, 48

constituting parameters, 117, 119, 128, 137, 143, 155, 156, 173

damage, 11
damage equivalent amplitude, 13, 132

external load, 11, 16
extrapolation, 153
extrapolation rule, 158

frequency response function, 30, 34, 37, 41

influential factors, 33, 92, 104, 135, 143, 172
inverse problem, 35, 39

life situation, 131, 133, 134, 157
load severity, 13, 22, 158

pseudo-damage, 14, 132

regularisation coefficient, 42, 49, 51
relative proportions, 134, 135
reliability, 1, 16
road excitation, 36, 74
road profile, 36, 75
road roughness, 34, 92
roughness coefficient, 94

sampling strategies, 19, 133
stratified sampling, 133, 135

transients, 96, 100, 111, 173

Appendix A

Notations

Notations

Fatigue, load variability and reliability

Notation	Quantity
D	Damage
d	Pseudo-damage
β	Basquin's coefficient
y	Response signal (*e.g.* displacement, acceleration, force, stress, etc.)
y_{eq}	Damage Equivalent Amplitude (DEA)
α_i	Relative proportion of the 'i-th' life situation
S	Load distribution ("Stress")
R	"stRength" distribution
μ_X	Mean of 'X' distribution
σ_X	Standard Deviation of 'X' distribution
q_5	Five percent quantile of the distribution
q_{95}	Ninety-five percent quantile of the distribution
p_f	Probability of failure

Table A.1: Notations: fatigue, load variability and reliability.

Vehicle vertical dynamics and inverse problem

Notation	Quantity
z_s, v_s, a_s	Sprung mass displacement, speed and acceleration
z_t, v_t, a_t	Unsprung (tyre) mass displacement, speed and acceleration
$z_s - z_t$	Suspension displacement
$\mathbf{x}(t)$	State vector
$\mathbf{y}(t)$	Output or 'measurement' vector
$u(t)$	Road excitation
f	Time frequency (Hz)
$u(x)$	Road profile
n	Spatial frequency (m^{-1})
$\mathbf{A}, \mathbf{B}, \mathbf{C}, \mathbf{D}$	Space-State representation matrices
$\Gamma(f)$	Frequency Response Function
$\mathbf{x}^a(t)$	Augmented state vector
$\mathbf{Q}$	State noise auto-covariance matrix
$\mathbf{R}$	Measurement noise auto-covariance matrix
S	'Excitation' noise matrix: regularisation coefficient

Table A.2: Notations: vehicle dynamics and inverse problem.

Stochastic modelling, road and speed

Notation	Quantity
$\{X(t)\}$	Continuous-time stochastic process
$x(t)$	Trajectory (realisation) of the stochastic process
$\hat{x}(f)$	Fourier Transform (FT) of the trajectory $x(t)$
$h(f)$	PSD of the trajectory $x(t)$
$S(f)$	PSD of the stochastic process $X(t)$
σ^2	Variance of the process
$u(x)$	Road profile
$S(n)$	PSD of the stochastic model for road profiles
r_j	Normalized variance (for the piecewise-stationary road model)
$v(t)$ or $v(x)$	Speed profile
v_c	Mean speed of the speed profile

Table A.3: Notations: Stochastic modelling, road and speed.

Acronyms

Acronym	Full designation
PSD	Power Spectral Density
FFT	Fast Fourier Transform
RMS	Root Mean Square value
PDF	Probability Density Function
CDF	Cumulative Density Function
COV	Coefficient Of Variation
MLE	Maximum Likelihood Estimation
ODE	Ordinary Differential Equation
DAE	Differential-Algebraic Equation
DOF	Degree-Of-Freedom
MBS	Multi-Body Simulation
FRF	Frequency Response Function
FE	Finite-Elements
FEA	Finite-Elements Analysis
DEA	Damage Equivalent Amplitude
LC	Level-Cross

Table A.4: Table of acronyms.

Life situations

Route type	Full designation
V type	City route (“Ville”)
R type	Country route (“Route”)
A type	Highway route (“Autoroute”)
M type	Mountain route (“Montagne”)
P type	Off-road or unpaved track route (“Piste”)

Table A.5: Life situations designations.

Appendix B

Additional vehicle models

Throughout most of the manuscript, the quarter-car model of the vehicle described in subsection 2.3.2 is used. First, this is much more convenient to introduce new concepts, methods and the equation that may be related to the latter, *e.g.* the road estimation algorithm presented in chapter 3. Second, as stochastic simulations consist in the repetition of a large number of calculations, more complex models significantly increase the calculation time. Additionnaly, it is not at all straightforward that more complex models are significantly more helpful when performing a statistical analysis or road-induced loads.

In this appendix, the different and more complex vehicle models that are occasionally used within the manuscript are described.

B.1 Non-linear (2-DOF) quarter-car model

While the linear quarter-car model gives a good first approximation of the vertical dynamics of the front suspension system of the vehicle, this suspension system is often highly non-linear. Even if geometrical non-linearities are disregarded, physical non-linearities can be considered.

First, the vertical stiffness of the suspension is non-linear because of bump and rebound stops mounted in parallel with the spring, see figure B.1. These elements naturally limit the amplitude of the suspension displacement and only become active when the suspension is sufficiently extended or compressed. These non-permanent contacts occasionally increase the stiffness of the suspension (addition with respect to the spring stiffness), as displayed in the left-hand side of figure B.2. On the other hand the damper generally exhibits a non-linear functioning, see an example in the right-hand side of figure B.2.

It is not possible to obtain the response of this non-linear model directly in the frequency domain (*i.e.* using FRFs and equation 2.16) and one has to solve the ODE of the system numerically, see equation (2.11). The state vector used for the simulation is the

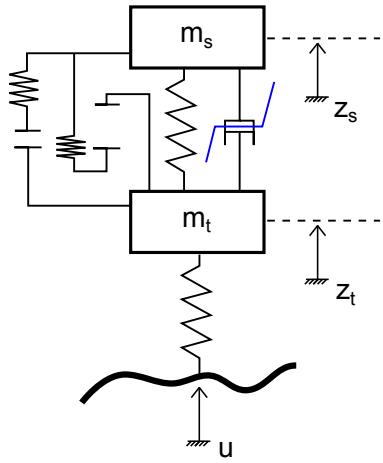

Figure B.1: Non-linear (2-DOF) quarter-car model. The non-linearity is due to bump and rebound stops and to the non-linear characteristics of the damper.

same as in the linear case, namely $\mathbf{x} = [\dot{z}_s, \dot{z}_t, z_s, z_t]$.

B.2 Linear bicycle model

The linear bicycle model describes the dynamics of the front and the rear of the vehicle. It is displayed in figure B.3, where only mass and inertia characteristics are shown.

It is a 4-DOF model constituted by a front unsprung mass, a rear unsprung mass and a sprung mass representing the full body of the vehicle. The latter both has a vertical movement and a pitch movement (*i.e.* rotation around the lateral axis Oy). The state vector of the model is $\mathbf{x} = \left[\dot{z}_{tf}, \dot{z}_{tr}, \dot{z}_s, \dot{\theta}_s, z_{tf}, z_{tr}, z_s, \theta_s\right]$.

The simulation of the response of the vehicle model requires the specification of two road excitations, namely u_f and u_r. In practice here, it is further assumed that the rear road excitation u_r is only a delayed version of the front excitation u_f.

B.3 Linear full-vehicle model

The linear full-vehicle model describes the dynamics of the complete vehicle. It is displayed in figure B.4, where only mass and inertia characteristics are shown.

It is a 7-DOF model constituted by a four unsprung masses representing the four different wheels and a sprung mass representing the full body of the vehicle. The latter has a vertical movement, a pitch movement (*i.e.* rotation around the lateral axis Oy) and a roll movement (*i.e.* rotation around the longitudinal axis Ox). The state vector of the

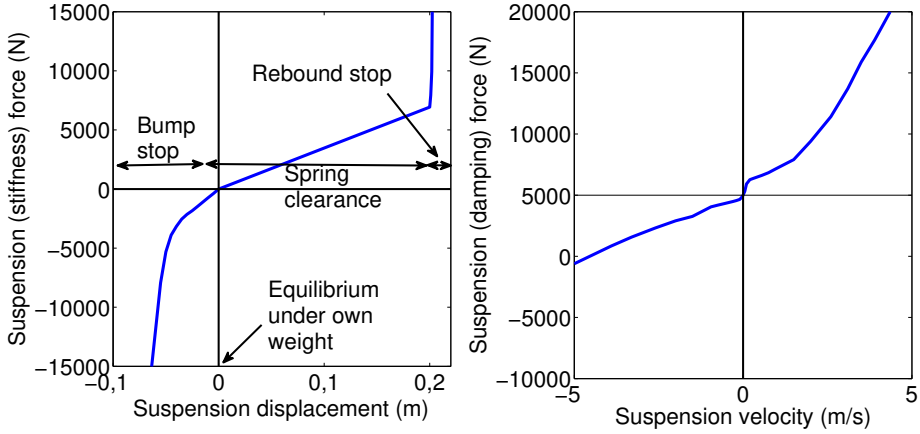

Figure B.2: Characteristics of the non-linear suspension. Non-linear stiffness due to bump and rebound stops (left). Non-linear characteristics of the damper (right).

model is $\mathbf{x} = \left[\dot{z}_{tfl}, \dot{z}_{tfr}, \dot{z}_{trl}, \dot{z}_{trr}, \dot{z}_s, \dot{\theta}_s, \dot{\phi}_s, z_{tfl}, z_{tfr}, z_{trl}, z_{trr}, z_s, \theta_s, \phi_s\right]$.

The simulation of the response of the vehicle model requires the specification of four road excitations, namely u_{fl}, u_{fr}, u_{rl} and u_{rr}. In practice here, it is further assumed that the rear road excitations u_{rl} and u_{rr} are respectively delayed versions of the front excitation u_{fl} and u_{fr}.

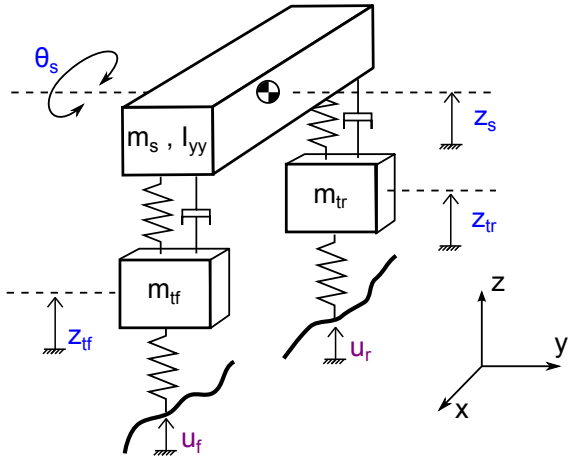

Figure B.3: Linear bicycle model.

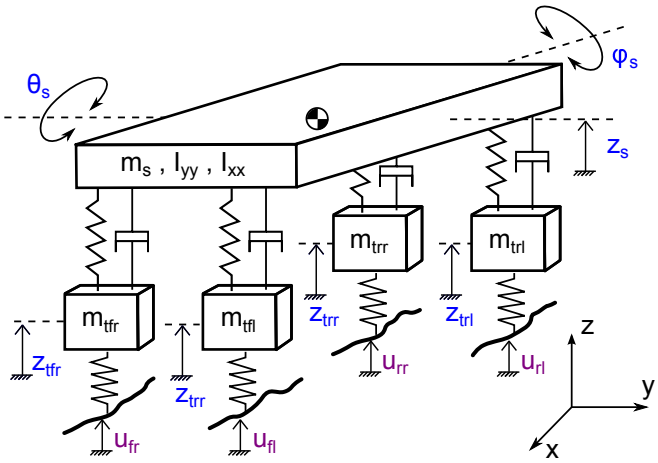

Figure B.4: Linear full-vehicle model.

Appendix C

Modelling and influence of the tyre/road contact

In this appendix, the issue of the contact between the tyre and the road surface is discussed. It has to be considered both when performing estimations of road profiles from a vehicle's responses (in chapter 3) and when carrying out simulations (throughout this manuscript). Indeed, the predicted dynamic response of the vehicle is impacted by the choice of a model for the tyre/road contact.

C.1 Tyre modelling and tyre/road contact

Tyre modelling is a relatively complex issue which forces us to consider a strongly non-linear phenomenon. For a more detailed overview of the existing approaches to deal with tyre modelling see *e.g.* [Johannesson and Speckert, 2013, Pacejka, 2005]. The behaviour of the tyre cannot be described by linear models. Indeed, the contact between the road and the tyre in not necessarily permanent nor necessarily localized around a single point on the tyre. Also this contact represents a unidirectional constraint.

Within this manuscript, the tyre has been replaced by a linear spring that follows rigorously the vertical elevation of the road profile. This is arguably a very strong simplification of the actual problem and it may lead to strong discrepancies between the simulated and real responses of the vehicle, especially in terms of the forces applied on the tyre. The quantity $u(t)$ that represents the so-called 'road excitation' within this manuscript, can either be considered as a resultant of the weighted contributions of the local altitudes within the contact patch, or more simply, the altitude of the central point of the contact patch.

This simplification is nonetheless necessary. Indeed, the focus of the manuscript is rather put on the realisation of statistical analyses and on the study of stochastic models. In this framework, the volume of data to be processed or of simulations to be performed

urges us to consider linear vehicle models so that responses may be calculated extremely quickly. Increasing the complexity of vehicle and tyre models may be a perspective of this research work, but the information of load variability derived from linear vehicle models is still very valuable.

C.2 Limitations of the road estimation method

The estimation method (resolution of an inverse problem) proposed in chapter 3 yields an estimate of the road profile which is 'the most likely from the standpoint of the vehicle'. It is not necessarily a representative image of the road surface geometry. For example, when crossing over a pothole, it is very unlikely that the tyre stays in permanent contact with the road profile or follows exactly the geometry of the latter. Hence, the estimated road profile more likely describes the displacement of a point belonging on the tyre, even if the latter is not in permanant contact with the road geometry.

The transient-laden profile employed to test the estimation algorithm in section 3.6.2, is used here as an example. A filtering is applied on the road profile, thus converting it into a more realistic vertical excitation, by enforcing the following condition. If the tyre rolling on the profile is assumed to be non-deformable, certain evolutions of the vertical contact are geometrically non admissible.

To be more precise the geometrical filtering of the profile is performed as follows. At the current point, the vertical projection of the wheel centre is positioned on the road surface. If there is an interference between the tyre circumference and the forward part of the surface, then the contact point is elevated until there is only a single contact point on the forward part of the road surface and the resulting elevation becomes the new point of the road excitation. Otherwise, the new point of the road excitation is directly taken on the road surface. Then, the following point on the road surface is taken as the new current point and the operation is repeated iteratively. This proposed treatment is not necessarily an optimal solution but it is an easy way to obtain a profile that is more representative of the vertical excitation imposed on the spring representing the tyre in the linear model.

This operation yields the 'filtered profile' (road excitation) that is compared with the exact geometry in figure C.1. Another example of profile filtering is given in figure C.2 for the rough pavement profile described in section 3.6.2.

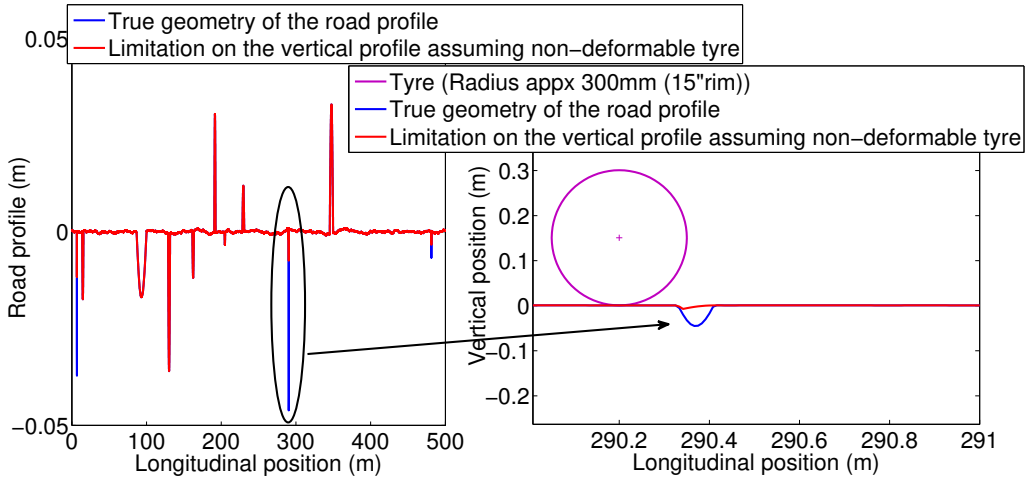

Figure C.1: Comparison of the road geometry with a more realistic vertical excitation. The filtering considers the admissibility of the displacement of the tyre geometry on the road profile.

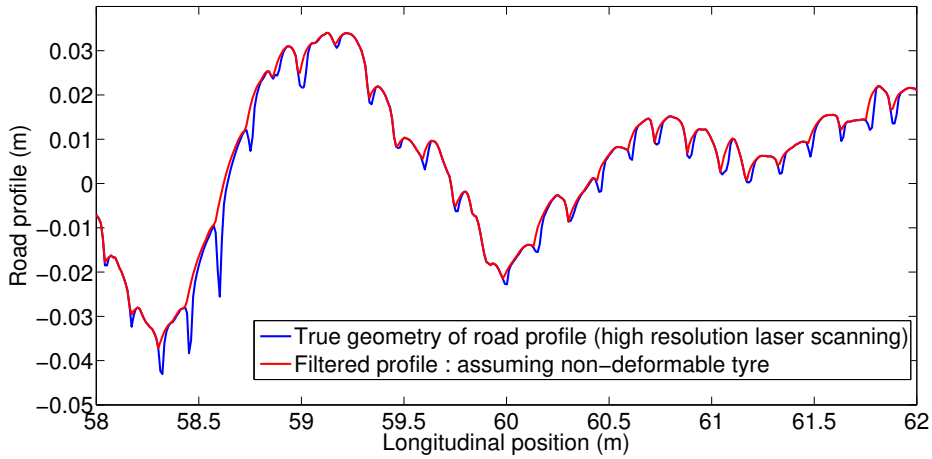

Figure C.2: Geometric filtering of rough pavement track, assuming that the tyre is non-deformable

To asses the quality of the road estimation method in subsection 3.6.2, for any comparison between the real road profile and the estimated profile, it is preferable to transform the real road profile into a more 'realistic' vertical excitation through geometric filtering. This has been done in order to obtain the results in table C.1 (identical to table 3.5). The effect of geometric filtering is illustrated by the results in table C.2 where both the response to the geometric filtered (red profile in figure C.1) and unfiltered (blue profile in figure C.1) road profiles are compared.

Criterion (direct and indirect)	Value for the true (filtered) profile	Value for the estimated profile	Relative error
Road roughness	(power in m^3) $\times 10^{-6}$		
Low band ($0.05m^{-1}$-$0.2m^{-1}$)	54.02	41.45	-23.3%
Medium band ($0.2m^{-1}$-$1m^{-1}$)	14.97	8.12	-45.7%
High band ($1m^{-1}$-$5m^{-1}$)	0.98	0.23	-76.9%
Equivalent damage amplitude	(use of linear quarter-car model)		
Suspension displacement (m)	0.0035	0.0027	-24.2%
Sprung mass acceleration (m/s^2)	0.52	0.40	-23.7%
Unsprung mass acceleration (m/s^2)	5.87	2.48	-57.8%

Table C.1: A 'geometric filter' has been applied on true road profile before carrying out the comparison between the true and estimated profile.

Criterion (direct and indirect)	Value for the true geometry	Value for the filtered profile	Relative error
Road roughness	(power in m^3) $\times 10^{-6}$		
Low band ($0.05m^{-1}$-$0.2m^{-1}$)	54.02	54.02	0%
Medium band ($0.2m^{-1}$-$1m^{-1}$)	18.73	14.97	-20.0%
High band ($1m^{-1}$-$5m^{-1}$)	23.38	0.98	-95.8%
Equivalent damage amplitude	(use of linear quarter-car model)		
Suspension displacement (m)	0.0035	0.0035	0%
Sprung mass acceleration (m/s^2)	1.02	0.52	-48.8%
Unsprung mass acceleration (m/s^2)	15.13	5.87	-61.6%

Table C.2: Comparison of the road geometry with a realistic vertical excitation

To sum up, it is quite obvious that the road profile estimated from data measured on an actual vehicle (inverse method), more likely represents a realistic evolution of the road/tyre contact (or lack thereof) rather than the exact evolution of the road geometry. There is no perfect solution to the road/tyre contact issue when the estimation algorithm is based on a linear tyre model. Nonetheless, care should be exercised when comparing 'real' profiles (*i.e.* exact road geometries) with estimates obtained from the road estimation algorithm, when the objective is to assess the quality of the latter.

C.3 Limitations of the simulation with a linear tyre model

In order to illustrate the differences in vehicle responses when considering both a case where the tyre rolls on the road profile and a case where the tyre is subjected to a time-varying vertical constraint, a calculation is carried out with the detailed vehicle and tyre model. The result is displayed in figure C.3. In the first case (in red) the tyre model covers the geometry of the road surface provided to the MBS software. In the second case

(in blue), a virtual vertical test rig is used and the road profile is directly provided as the displacement constraint applied on the tyre. In both case, the exact same 'road data' is used as in input.

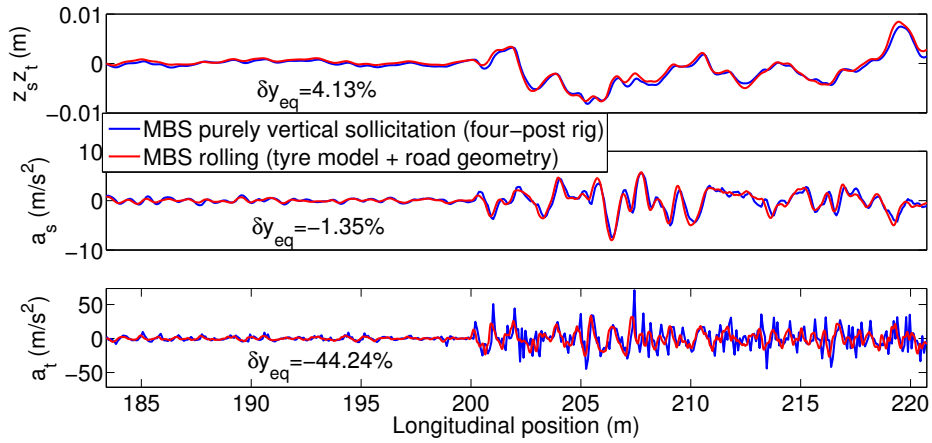

Figure C.3: Comparison between vertical excitation and rolling tyre.

It is seen that while the influence on the DEA value is limited for suspension displacement and sprung acceleration, it is very significant for the unsprung acceleration. Based on this result caution is advised when using the simulated unsprung acceleration based on a linear quarter-car model.

Also, when carrying out a simulation with the linear quarter-car model, it seems preferable to make use of the (geometric) filtered profile that the exact road geometry. Indeed the true road geometry is a poor representation of the vertical excitation that will actually be imposed on the tyre. If no realistic tyre model is used, there does not seem to be a more rigorous way to make the simulation more representative.

Appendix D

Experimentations and testing of the estimation algorithm

For the sake of readability, part of the figures and tables associated with the experimental testing of the road estimation algorithm are gathered in this appendix. Both simulation-based and measurement-based experiments are carried out to test the algorithm, see subsection 3.6.1 for a description of the testing framework.

Simulation-based results are presented in section D.1 and measurement-based results are presented in section D.2. Studies of the influence of diverse factors on the road estimation are then proposed. The influence of tuning parameters, known mechanical characteristics of the vehicle or the speed of the vehicle are detailed respectively in sections D.3, D.4 and D.5. The possibility of improving the results with more complex models is also explored in section D.6.

D.1 Numerical testing of the road estimation algorithm

D.1.1 Experiments involving a 2-DOF non-linear quarter-car model

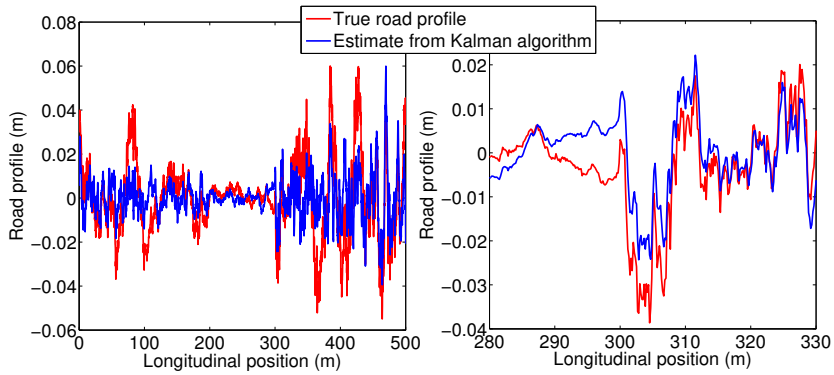

Figure D.1: Road estimate obtained from the application of the algorithm on the data set constructed through simulation using a 2-DOF non-linear model. Complete road profile (left), zoom on a reduced section (right). A high-pass filtering has been applied with a cut-off frequency of 0.5Hz.

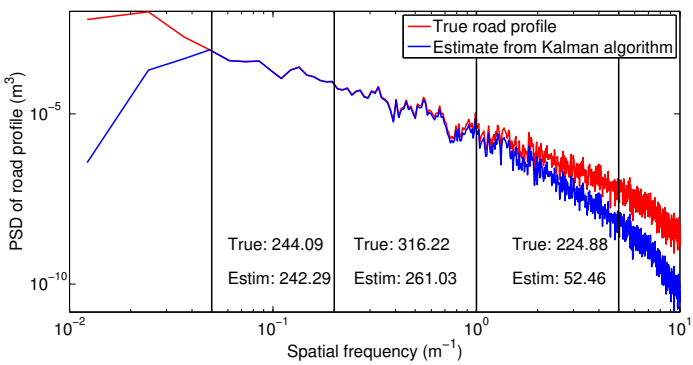

Figure D.2: PSD of road estimate obtained from the application of the algorithm on the data set constructed through simulation using a 2-DOF non-linear model. A high-pass filtering has been applied with a cut-off frequency of 0.5Hz

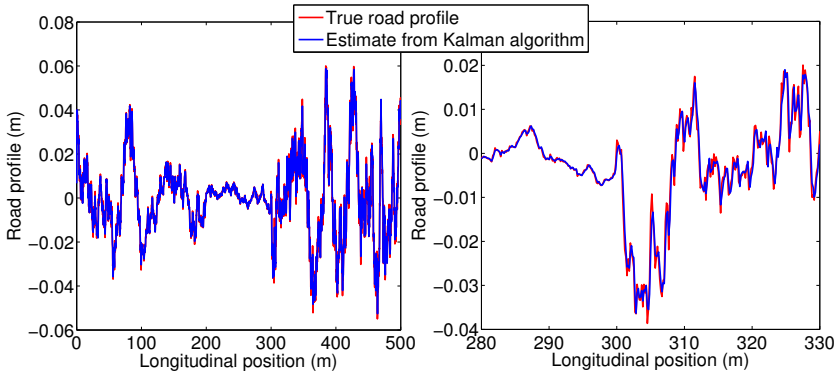

Figure D.3: Road estimate obtained from the application of the algorithm on the data set constructed through simulation, using a 2-DOF non-linear model. No high-pass filtering is applied as the body displacement is directly simulated. Complete road profile (left), zoom on a reduced section (right).

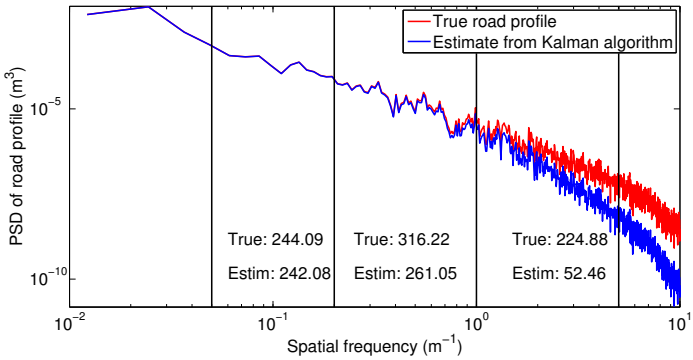

Figure D.4: PSD of road estimate obtained from the application of the algorithm on the data set constructed through simulation using a 2-DOF non-linear model. No high-pass filtering is applied as the body displacement is directly simulated.

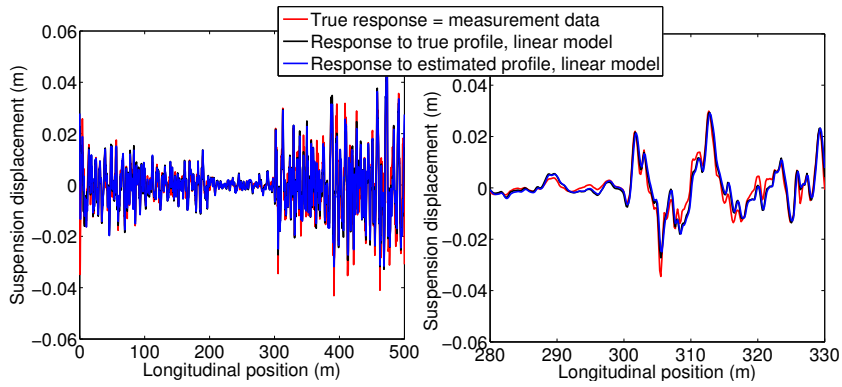

Figure D.5: Suspension displacement. The considered data set is obtained from simulation using a 2-DOF non-linear model. Complete response (left), zoom on a reduced section (right).

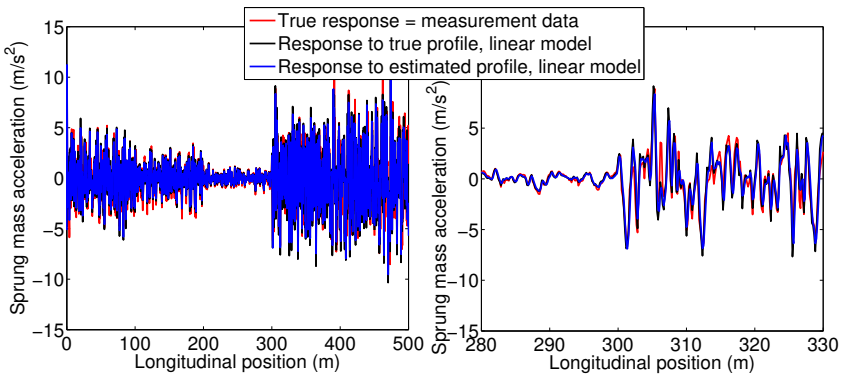

Figure D.6: Sprung mass acceleration. The considered data set is obtained from simulation using a 2-DOF non-linear model. Complete response (left), zoom on a reduced section (right).

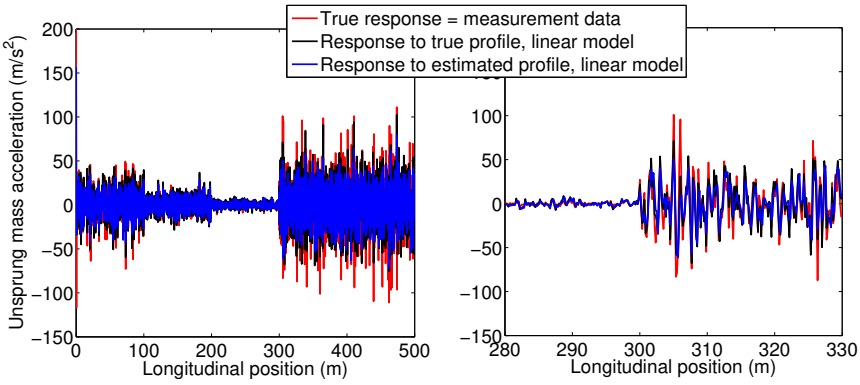

Figure D.7: Unsprung mass acceleration. The considered data set is obtained from simulation using a 2-DOF non-linear model. Complete response (left), zoom on a reduced section (right).

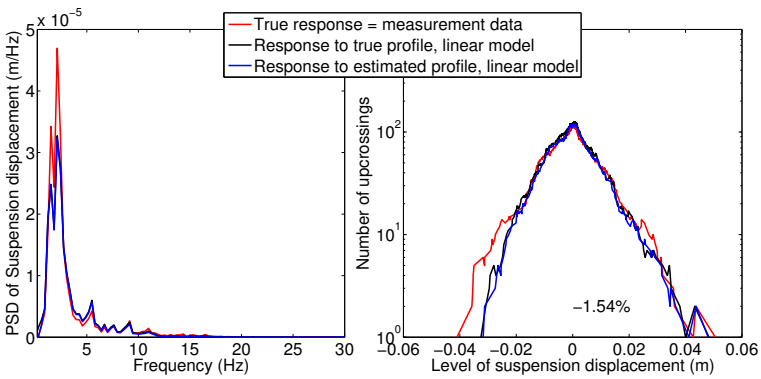

Figure D.8: Suspension displacement PSD and LC. The considered data set is obtained from simulation using a 2-DOF non-linear model.

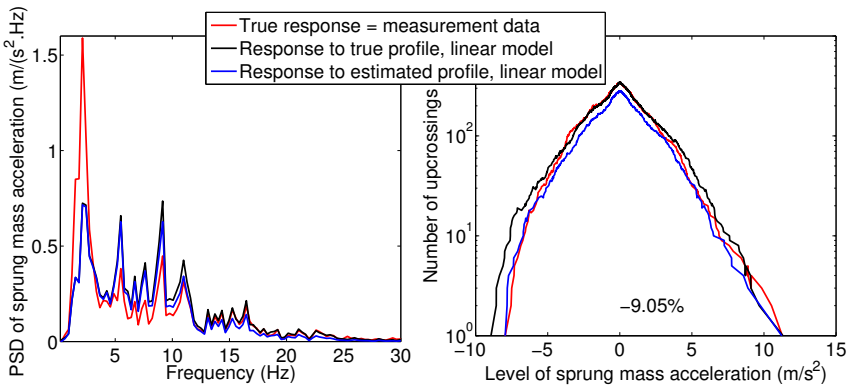

Figure D.9: Sprung mass acceleration PSD and LC. The considered data set is obtained from simulation using a 2-DOF non-linear model.

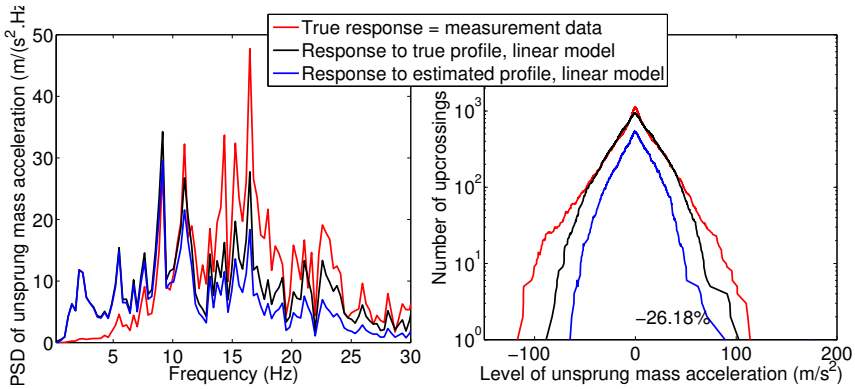

Figure D.10: Unsprung mass acceleration PSD and LC. The considered data set is obtained from simulation using a 2-DOF non-linear model.

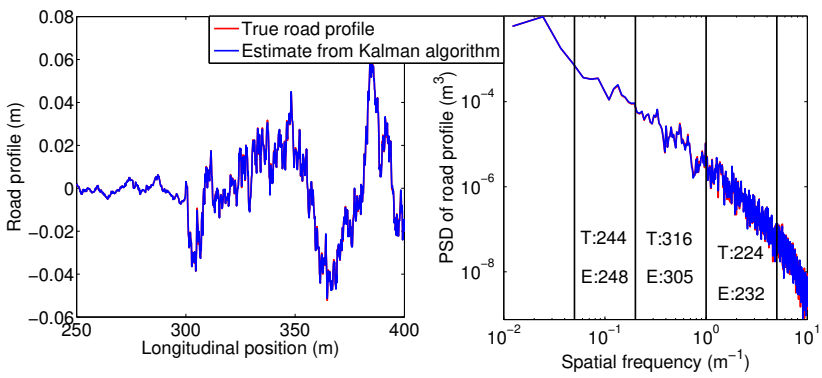

Figure D.11: In this experimental case based on a 2-DOF non-linear model, the estimate converges to the 'true' profile when a weak, if any, regularisation is imposed.

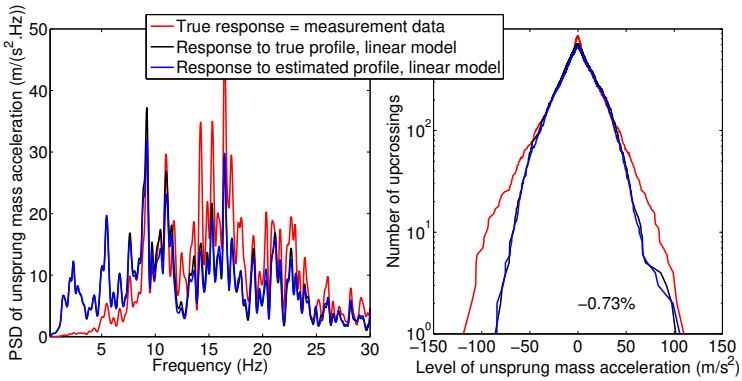

Figure D.12: Unsprung mass acceleration PSD and LC. No regularisation is applied on the estimate.

Criterion (direct and indirect)	Value for the true profile	Value for the estimated profile	Relative error
Road roughness	(power in m^3) $\times 10^{-6}$		
Low band ($0.05m^{-1}$-$0.2m^{-1}$)	244.09	248.80	1.9%
Medium band ($0.2m^{-1}$-$1m^{-1}$)	316.22	305.26	-3.5%
High band ($1m^{-1}$-$5m^{-1}$)	224.88	232.89	3.6%
Damage equivalent amplitude	(use of linear quarter-car model)		
Suspension displacement (m)	0.0053	0.0054	1.5%
Sprung mass acceleration (m/s^2)	1.58	1.57	-0.6%
Unsprung mass acceleration (m/s^2)	15.73	15.62	-0.7%

Table D.1: Result of the estimation for the data set involving a 2-DOF non linear quarter-car model, in terms of scalar criteria. The S parameter is fixed to $S = 10^0 = 1$, which represents an insignificant regularisation.

D.1.2 Experiments involving a detailed Mutli-Body model

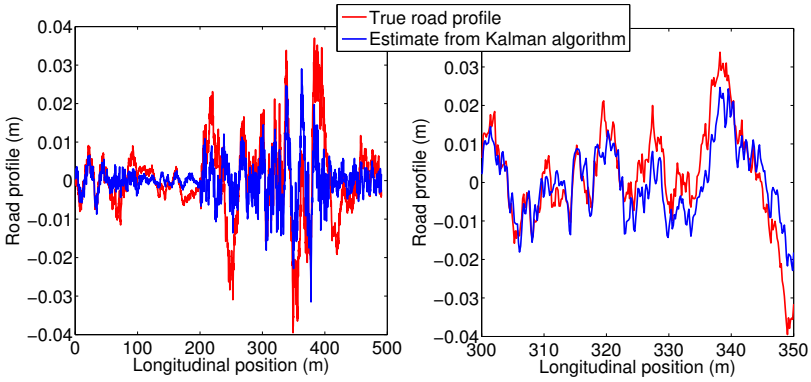

Figure D.13: Road estimate obtained from the application of the algorithm on the data set 1, constructed through simulation using a detailed (MBS) model. The considered road profile is randomly generated.

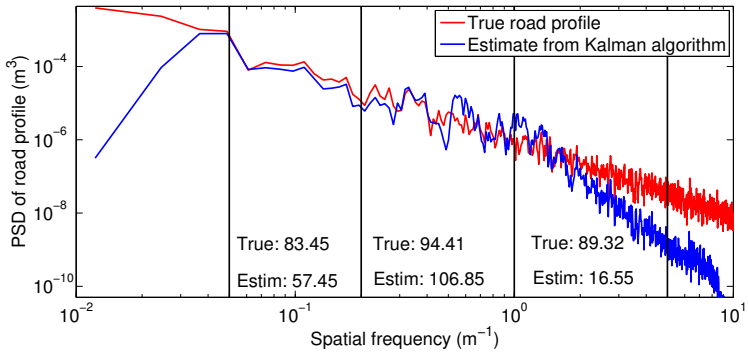

Figure D.14: PSD of road estimate obtained from the application of the algorithm on the data set 1, constructed through simulation using a detailed (MBS) model. The considered road profile is randomly generated.

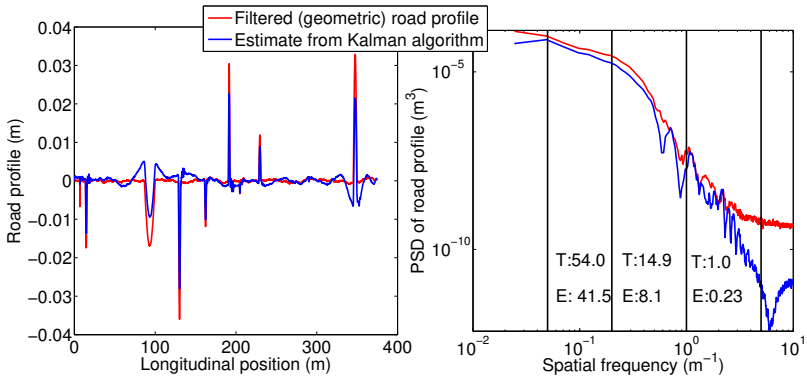

Figure D.15: Road estimate obtained from the application of the algorithm on the data set 2, constructed through simulation using a detailed (MBS) model. The considered road profile is laden with transient obstacles.

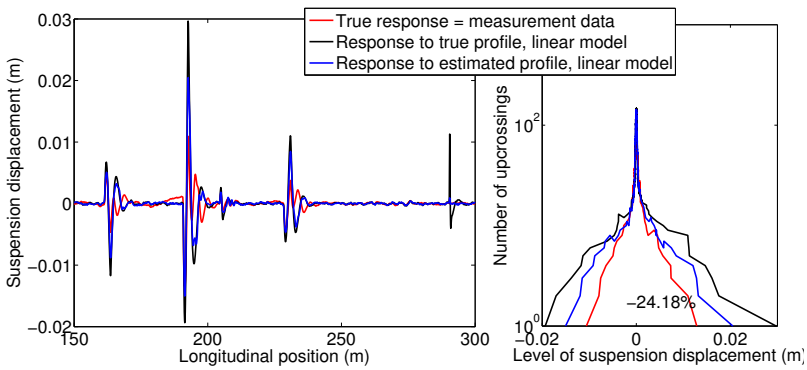

Figure D.16: Suspension displacement (left) and LC (right). The considered data set 2, is obtained from simulation using a detailed (MBS) model. The considered road profile is laden with transient obstacles.

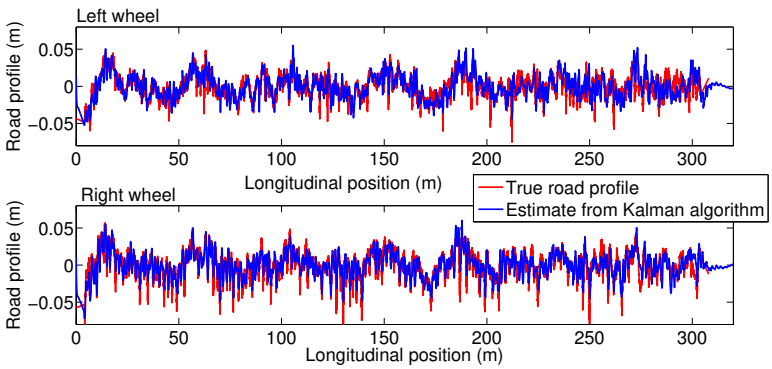

Figure D.17: Road estimates obtained from the application of the algorithm on the data set 3, constructed through simulation using a detailed (MBS) model. The considered road profiles correspond to a real rough pavement track.

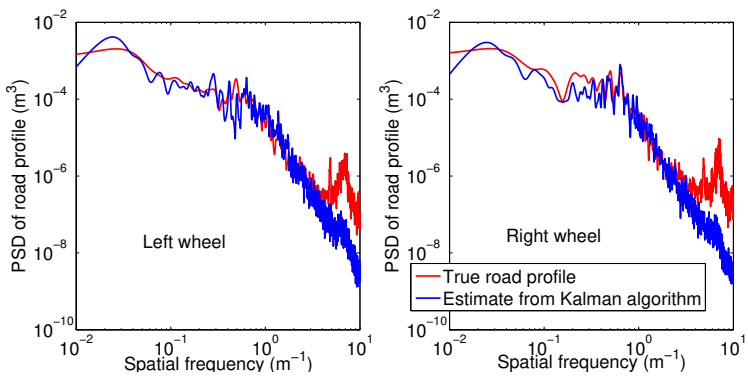

Figure D.18: PSD of road estimates obtained from the application of the algorithm on the data set 3, constructed through simulation using a detailed (MBS) model. The considered road profiles correspond to a real rough pavement track.

D.2 Physical testing of the road estimation algorithm

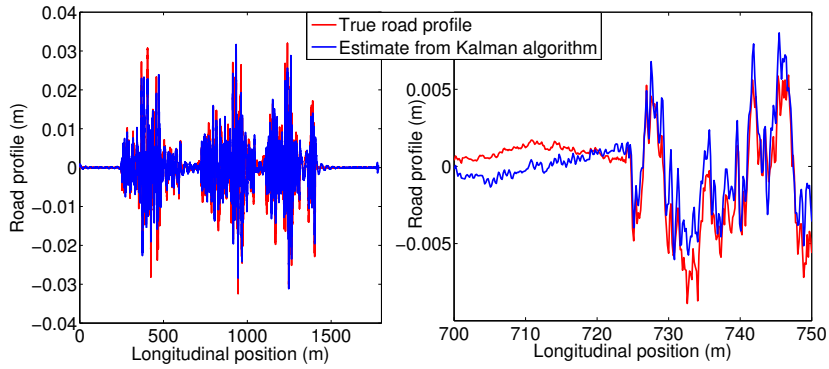

Figure D.19: Road estimate obtained from the application of the algorithm on the data set 1, constructed through a measurement on a vertical test-rig. The considered road profile is randomly generated.

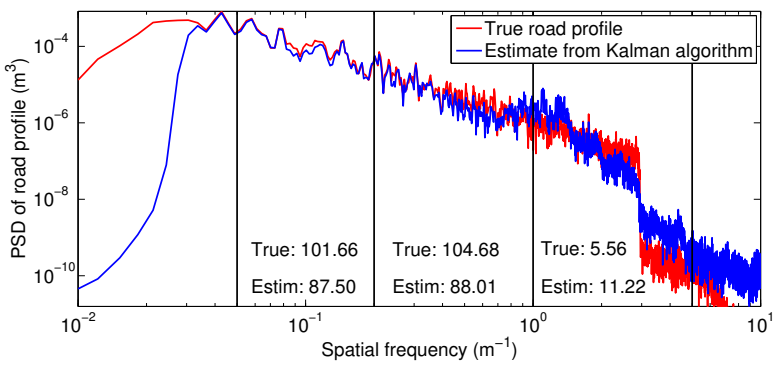

Figure D.20: PSD of road estimate obtained from the application of the algorithm on the data set 1, constructed through a measurement on a vertical test-rig. The considered road profile is randomly generated.

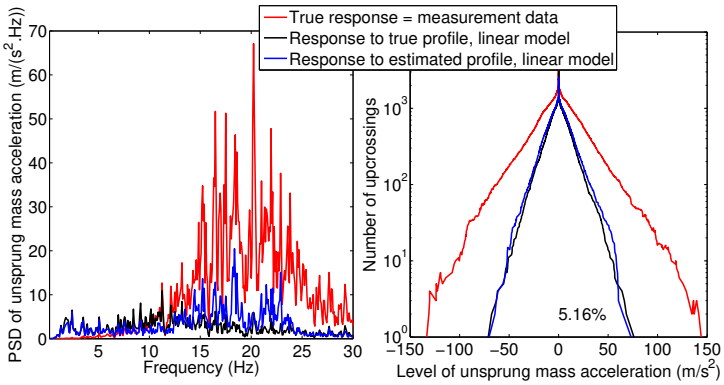

Figure D.21: Unsprung mass acceleration. The considered data set 1, is obtained from a measurement on a vertical test-rig. A significant regularisation is applied, $S = 10^{-7.6}$.

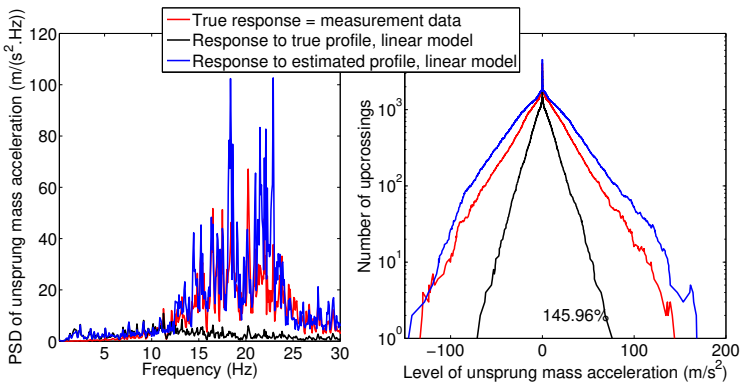

Figure D.22: Unsprung mass acceleration. The considered data set 1, is obtained from a measurement on a vertical test-rig. No significant regularisation is applied, $S = 10^0 = 1$.

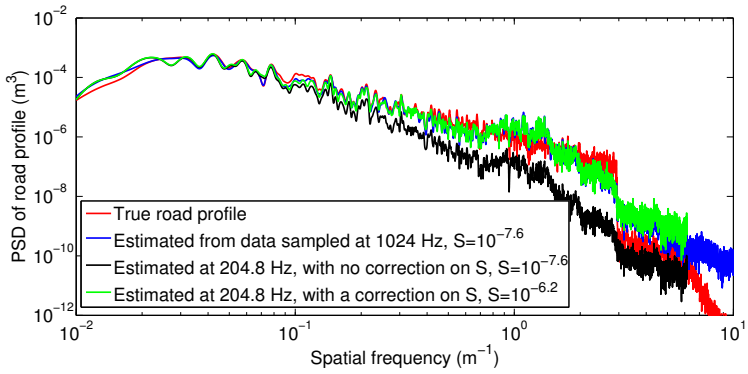

Figure D.23: PSD of the road estimate. The considered road profile is randomly generated. Two sampling time for the input data are considered and the effect of an adaptation of the regularisation coefficient is studied.

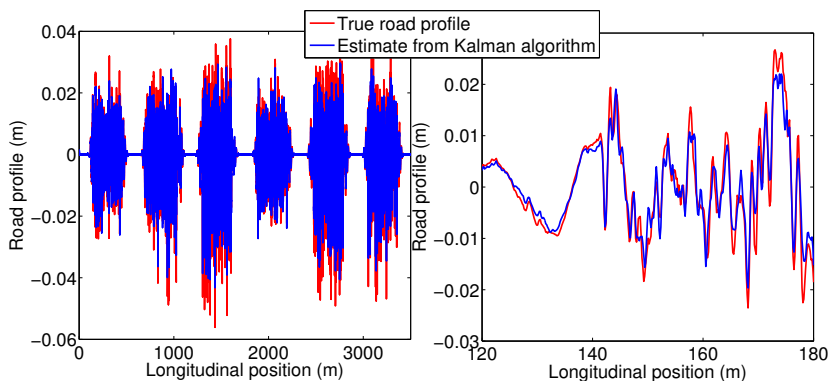

Figure D.24: Road estimate obtained from the application of the algorithm on the data set 2, constructed through a measurement on a vertical test-rig. The considered road profile corresponds to a realistic rough paved track.

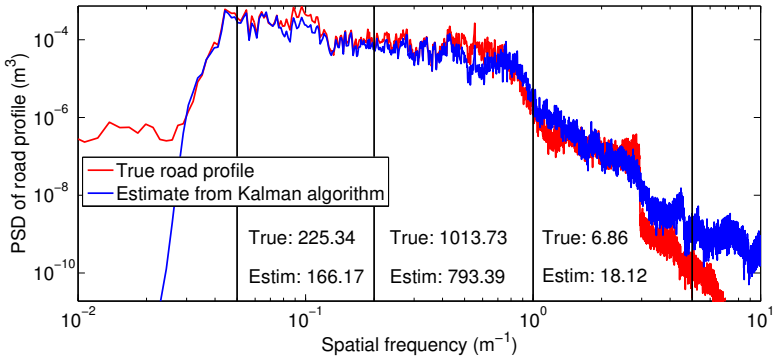

Figure D.25: PSD of road estimate obtained from the application of the algorithm on the data set 2, constructed through a measurement on a vertical test-rig. The considered road profile corresponds to a realistic rough paved track.

D.3 Study of the influence of tuning parameters

In this section different experiments are carried out in order to get insights into the influence of tuning parameters on the results of the estimation algorithm.

Parameter	Reference ($S = 10^{-6}$)	$S = 10^{-6}$	$S = 1$
Q_1	10^{-4}	10^{-2}, 10^{-3}, 10^{-5}	10^{-4}
Q_2	10^{-2}	1, 10^{-1}, 10^{-3}	10^{-2}
Q_3	10^{-8}	10^{-6}, 10^{-7}, 10^{-9}	10^{-8}
Q_4	10^{-7}	10^{-5}, 10^{-6}, 10^{-8}	10^{-7}
R_1	10^{-6}	10^{-4}, 10^{-5}, 10^{-7}, 10^{-8}	10^{-5}, 10^{-7}
R_2	10^{-6}	10^{-4}, 10^{-5}, 10^{-7}, 10^{-8}	10^{-5}, 10^{-7}
R_3	1	10^{2}, 10, 10^{-1}, 10^{-2}	10, 10^{-1}
R_4	10^{2}	10^{4}, 10^{3}, 10, 1	10^{3}, 10

Table D.2: Study of the influence of tuning parameters. This table gives the values of the design of experiments plotted on figures D.26, D.27 and D.28. Calculations are repeated 30 times (vertical scatter) for each arrangement of values.

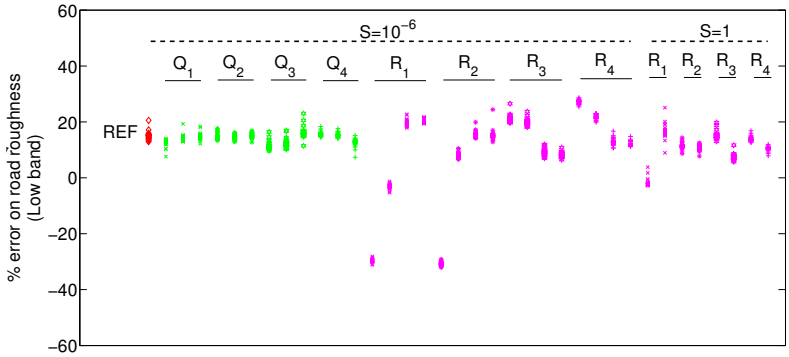

Figure D.26: Influence of the tuning parameters on the quality of the estimate's low frequency content.

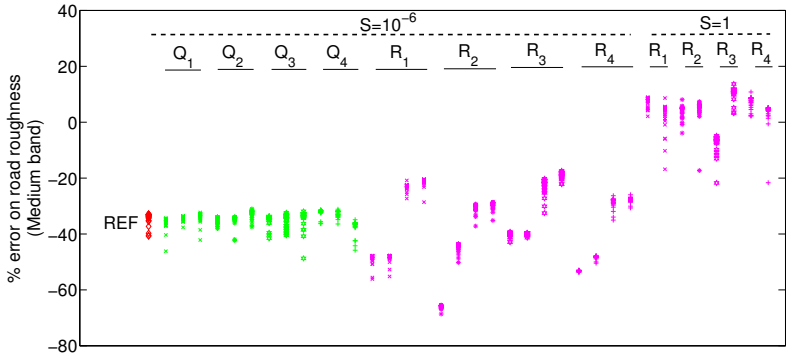

Figure D.27: Influence of the tuning parameters on the quality of the estimate's medium frequency content.

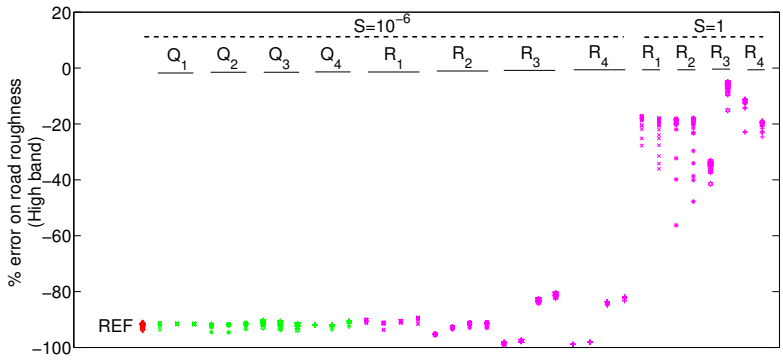

Figure D.28: Influence of the tuning parameters on the quality of the estimate's high frequency content.

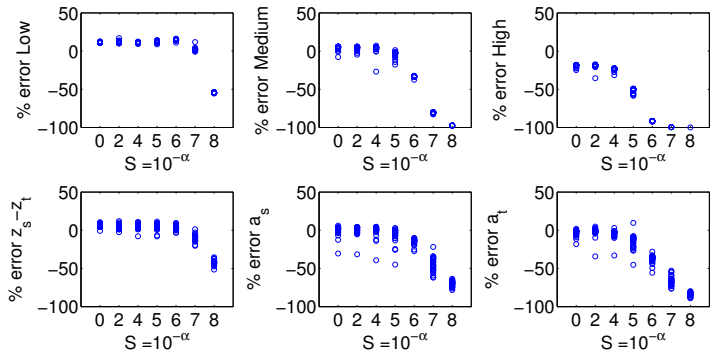

Figure D.29: Influence of the regularisation coefficient on all scalar criteria. Calculations are repeated 30 times (vertical scatter) for each value of the regularisation coefficient.

D.4 Study of the influence of mechanical characteristics

In this section different experiments are carried out in order to get insights into the influence of the knowledge of mechanical characteristics (provided to the estimation algorithm) on the results of the estimation algorithm.

Parameter	Reference ($S = 10^{-6}$)	$S = 10^{-6}$	$S = 1$
m_s	372 kg	Ref -20% -10% +15% +30%	Ref -20% 0% +20%
c_s	3300 N.S/m	Ref -50% -25% +25% +50%	Ref -20% 0% +20%
k_s	36540 N/m	Ref -30% -15% +15% +30%	Ref -20% 0% +20%
m_t	36 kg	Ref -20% -10% +10% +20%	Ref -20% 0% +20%
k_t	242000 N/m	Ref -40% -20% +20% +40%	Ref -20% 0% +20%

Table D.3: Study of the influence of the knowledge on the mechanical characteristics of the vehicle. This table gives the values of the design of experiments plotted on figures D.30, D.31 and D.32. Calculations are repeated 30 times (vertical scatter) for each arrangement of values. The parameters of the reference case are also the parameters used for all simulations.

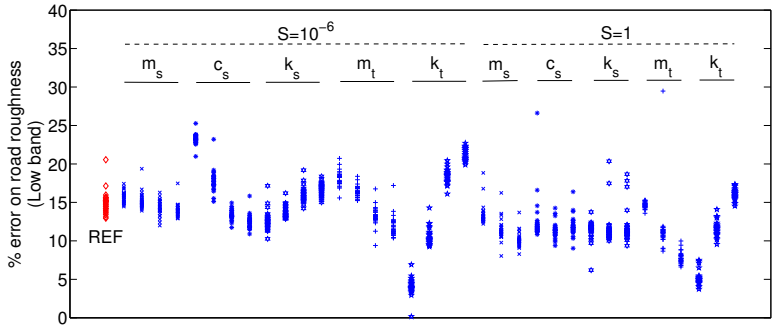

Figure D.30: Influence of the knowledge on the mechanical characteristics of the vehicle, on the quality of the estimate's low frequency content.

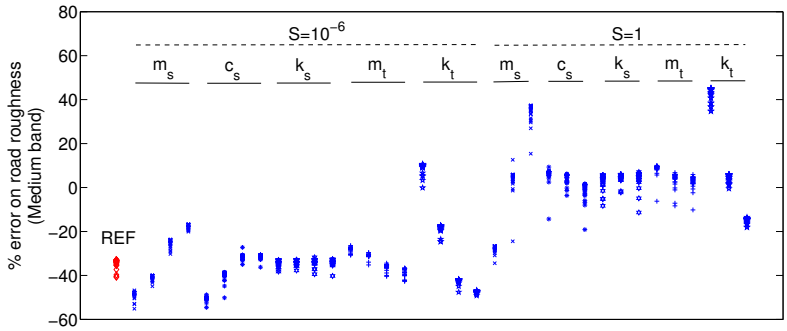

Figure D.31: Influence of the knowledge on the mechanical characteristics of the vehicle, on the quality of the estimate's medium frequency content.

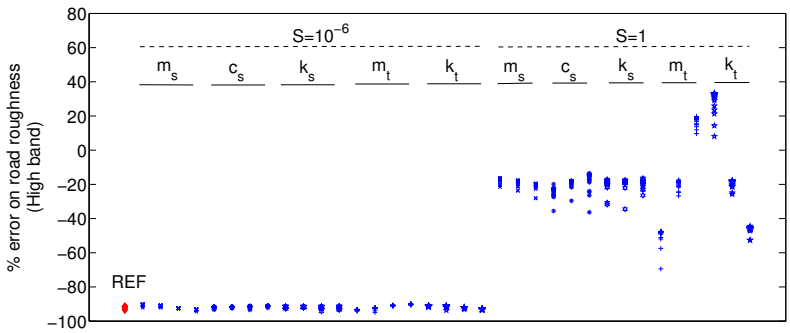

Figure D.32: Influence of the knowledge on the mechanical characteristics of the vehicle, on the quality of the estimate's high frequency content.

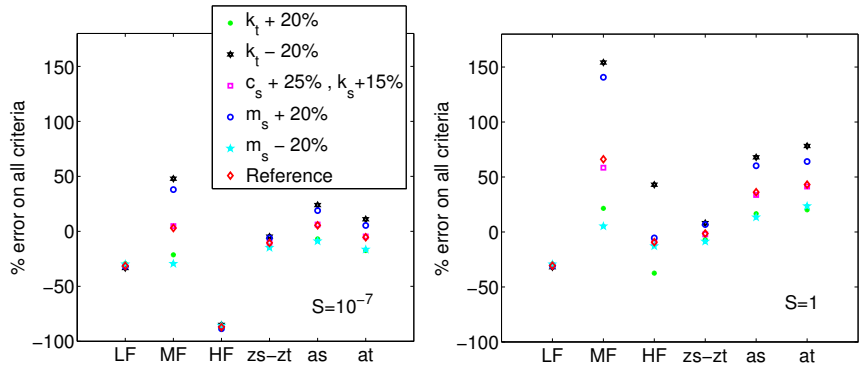

Figure D.33: Influence of the knowledge on the mechanical characteristics of the vehicle. The data set 1 obtained through a detailed MBS is used.

D.5 Study of the influence of vehicle speed

In this section different experiments are carried out in order to draw certain conclusion about the influence of vehicle speed on the quality of the estimation and identify overall trends.

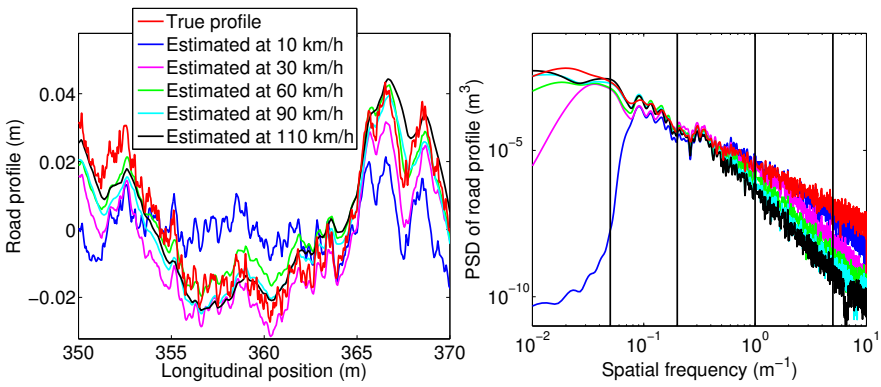

Figure D.34: Influence of the vehicle's speed on the quality of the estimate. The same road profile is covered through simulation at different speeds. The resulting data sets are used to produce different estimates. The latter are compared.

Speed (km/h)	Criterion (direct and indirect)	Value for the true profile	Value for the estimated profile	Relative error
	Road roughness	(power in m^3) $\times 10^{-6}$		
10	Low band ($0.05m^{-1}$-$0.2m^{-1}$)	346.72	65.16	-81.2%
	Medium band ($0.2m^{-1}$-$1m^{-1}$)	327.18	319.07	-2.5%
	High band ($1m^{-1}$-$5m^{-1}$)	327.07	225.93	-30.9%
30	Low band ($0.05m^{-1}$-$0.2m^{-1}$)	347.72	211.81	-38.9%
	Medium band ($0.2m^{-1}$-$1m^{-1}$)	327.18	296.91	-9.3%
	High band ($1m^{-1}$-$5m^{-1}$)	327.07	62.72	-80.8%
60	Low band ($0.05m^{-1}$-$0.2m^{-1}$)	346.72	318.14	-8.2%
	Medium band ($0.2m^{-1}$-$1m^{-1}$)	327.18	197.09	-39.8%
	High band ($1m^{-1}$-$5m^{-1}$)	327.07	17.87	-94.5%
90	Low band ($0.05m^{-1}$-$0.2m^{-1}$)	346.72	322.58	-7.0%
	Medium band ($0.2m^{-1}$-$1m^{-1}$)	327.18	127.56	-61.0%
	High band ($1m^{-1}$-$5m^{-1}$)	327.07	7.91	-97.6%
110	Low band ($0.05m^{-1}$-$0.2m^{-1}$)	346.72	307.48	-11.3%
	Medium band ($0.2m^{-1}$-$1m^{-1}$)	327.18	101.11	-69.1%
	High band ($1m^{-1}$-$5m^{-1}$)	327.07	5.40	-98.3%

Table D.4: Influence of vehicle's speed on road roughness estimation. The estimates corresponding to different measurement speeds are compared.

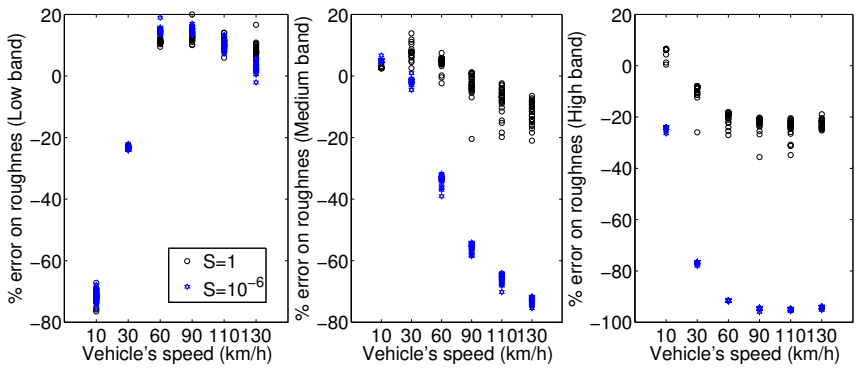

Figure D.35: Sensibility of the estimation to vehicle's speed. Calculation are repeated 30 times (vertical scatter) for each value of speed and for different randomly generated road profiles. Two values are considered for the S parameter.

D.6 Study of more complex models

In this section some attempts to increase the quality of the road estimation algorithm by considering more complex models are presented and analysed.

D.6.1 Models with more DOF

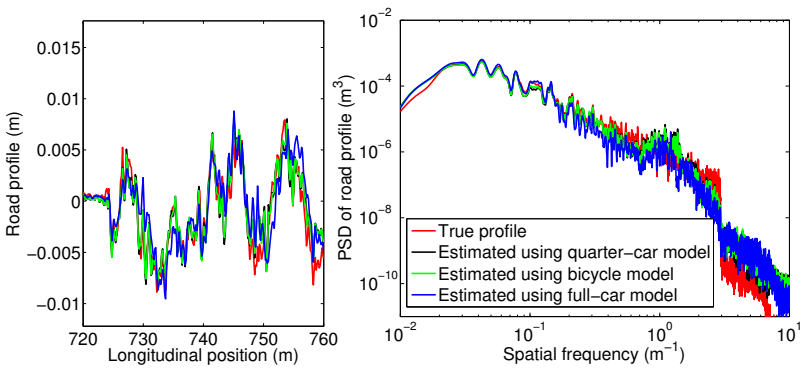

Figure D.36: Comparison of estimates obtained with different vehicle models. The considered input data is taken from the data set 1, constructed through a measurement on a vertical test-rig. The S parameters are fixed at $S_{ii} = 10^{-7.6}$ depending on the size of the $\mathbf{S}$ matrix and state vectors.

Model	Criterion (direct and indirect)	Value for the true profile	Value for the estimated profile	Relative error
Road roughness		(power in m^3) $\times 10^{-6}$		
Quarter	Low band ($0.05m^{-1}$-$0.2m^{-1}$)	101.66	87.50	-13.9%
	Medium band ($0.2m^{-1}$-$1m^{-1}$)	104.68	88.01	-15.9%
	High band ($1m^{-1}$-$5m^{-1}$)	5.57	11.22	101.9%
Bicycle	Low band ($0.05m^{-1}$-$0.2m^{-1}$)	101.66	89.56	-11.9%
	Medium band ($0.2m^{-1}$-$1m^{-1}$)	104.68	81.66	-22.0%
	High band ($1m^{-1}$-$5m^{-1}$)	5.57	12.14	117.9%
Full	Low band ($0.05m^{-1}$-$0.2m^{-1}$)	101.66	96.11	-5.5%
	Medium band ($0.2m^{-1}$-$1m^{-1}$)	104.68	47.16	-55.0%
	High band ($1m^{-1}$-$5m^{-1}$)	5.57	8.92	60.0%
Equivalent damage amplitude		(use of linear quarter-car model)		
Quarter	Suspension displacement	0.0046	0.0042	-9.2%
	Sprung mass acceleration	1.31	1.25	-4.7%
	Unsprung mass acceleration	11.27	11.85	5.2%
Bicycle	Suspension displacement	0.0046	0.0042	-8.9%
	Sprung mass acceleration	1.31	1.21	-7.8%
	Unsprung mass acceleration	11.27	11.02	-2.2%
Full	Suspension displacement	0.0046	0.0041	-9.3%
	Sprung mass acceleration	1.31	1.07	-18.6%
	Unsprung mass acceleration	11.27	8.8	-21.9%

Table D.5: Comparison of estimates obtained with different vehicle models, in terms of scalar criteria. The considered input data is taken from the data set 1, constructed through a measurement on a vertical test-rig. The S parameters are fixed at $S_{ii} = 10^{-7.6}$ depending on the size of the $\mathbf{S}$ matrix and state vectors.

D.6.2 Non-linear model

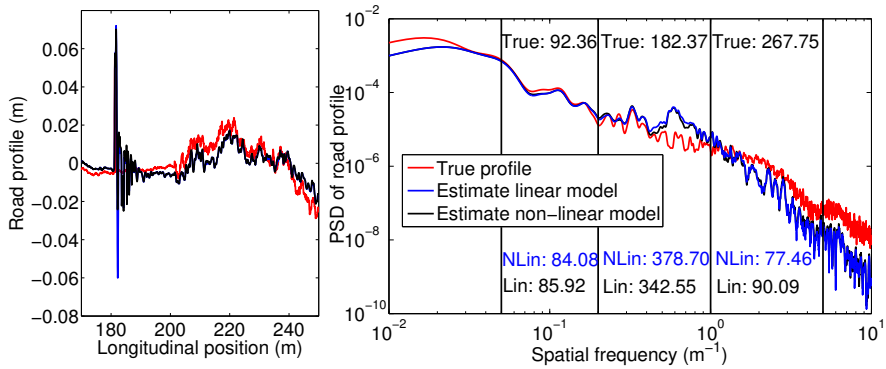

Figure D.37: Comparison of the estimates obtained using a linear and non-linear model, and associated algorithms (including Extended Kalman Filtering (EKF)). The considered input data is taken from a detailed MBS. The S parameter is fixed at $S = 10^{-7}$.

Model	Criterion (direct and indirect)	Value for the true profile	Value for the estimated profile	Relative error
Road roughness		(power in m^3) $\times 10^{-6}$		
N-Lin	Low band ($0.05m^{-1}$-$0.2m^{-1}$)	92.36	84.08	-9.0%
	Medium band ($0.2m^{-1}$-$1m^{-1}$)	182.37	378.7	107.7%
	High band ($1m^{-1}$-$5m^{-1}$)	267.75	77.46	-71.1%
Lin	Low band ($0.05m^{-1}$-$0.2m^{-1}$)	92.36	85.92	-7.0%
	Medium band ($0.2m^{-1}$-$1m^{-1}$)	182.37	342.55	87.8%
	High band ($1m^{-1}$-$5m^{-1}$)	267.75	90.09	-66.4%
Equivalent damage amplitude		(use of linear quarter-car model)		
N-Lin	Suspension displacement	0.0043	0.0073	68.6%
	Sprung mass acceleration	2.80	4.21	50.2%
	Unsprung mass acceleration	30.73	34.08	10.9%
Lin	Suspension displacement	0.0043	0.0061	41.0%
	Sprung mass acceleration	2.80	3.54	26.4%
	Unsprung mass acceleration	30.73	28.08	-8.6%

Table D.6: Comparison of the estimates obtained using a linear and non-linear model, and associated algorithms (including Extended Kalman Filtering (EKF)), in terms of scalar criteria. The considered input data is taken from a detailed MBS. The S parameter is fixed at $S = 10^{-7}$.

Appendix E

Algorithm for the division in constant speed segments

The algorithm that has been used to identify constant speed sections from a measured speed profile is described here. Let $(v_i)_{i=1,\ldots,N}$ be the speed of the vehicle acquired with sample time dt. Let q_f be a threshold above which the speed state switches (that has to be chosen wisely).

```
While
Δ_v(i) ← v(i+1) − v(i), for i = 1, ..., N − 1
i_x = arg min Δ_v(i)
If Δ_v(i_x) < q_f Then
  V_x ← [v(i_x), v(i_x + 1)]
  k = 1, l = 1
  While
    v^+ ← |mean(V_x) − v(i_x + 1 + k)|
    v^− ← |mean(V_x) − v(i_x − l)|
    If v^+ < v^− and v^+ < q_f Then
      V_x ← [V_x, v(i_x + 1 + k)]
      k ← k + 1
    ElseIf v^− < v^+ and v^− < q_f Then
      V_x ← [v(i_x − l), V_x]
      l ← l + 1
    Else
      Break
    End If
  End While
  v(i) ← mean(V_x), for i = i_x − l, ..., i_x, ..., i_x + 1 + k
Else
  Break
End If
End While
```

An example of speed profile decomposition is displayed in figure E.1. The splitting parameter q_f described above is respectively equal to $10km/h$ (top) and to $5km/h$ (bottom).

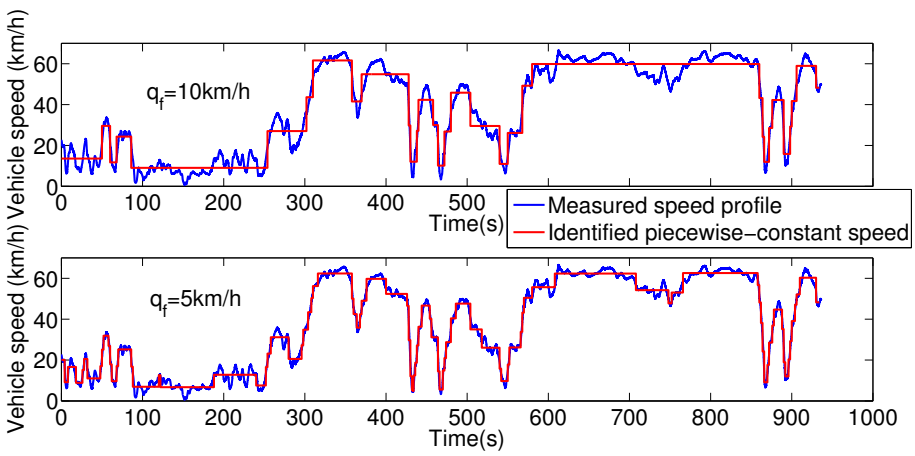

Figure E.1: Identification of constant speed sections using the algorithm presented above.

Appendix F

Testing and validation of stochastic simulation

In this appendix the different figures illustrating the testing of the methodology proposed in chapter 5, are displayed. In section F.1, the results of the comparison between the predicted and observed (measured) load variability are illustrated. In section F.2, the results of the comparison between the predicted and observed (measured) sensitivities of loads to influential factors are shown. Then, in section F.3, comparisons are displayed with respect to predictions corresponding to the complete life of vehicles.

F.1 Comparison of the predicted and observed (measured) load variability

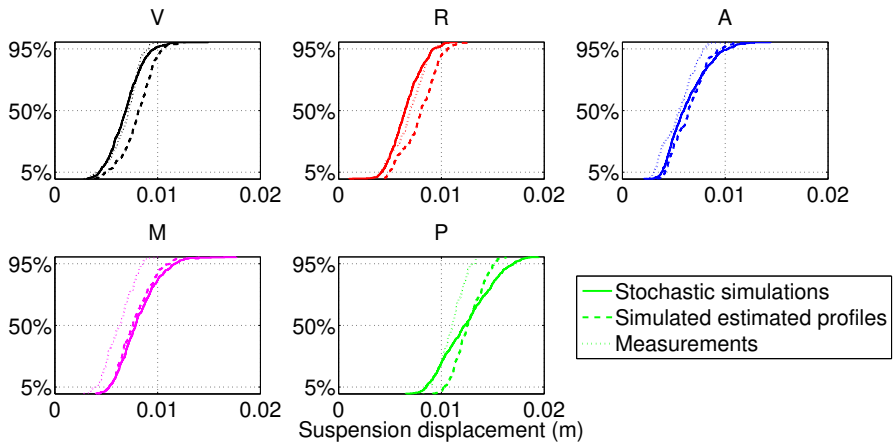

Figure F.1: Comparisons of predicted and measured distributions: Suspension displacement.

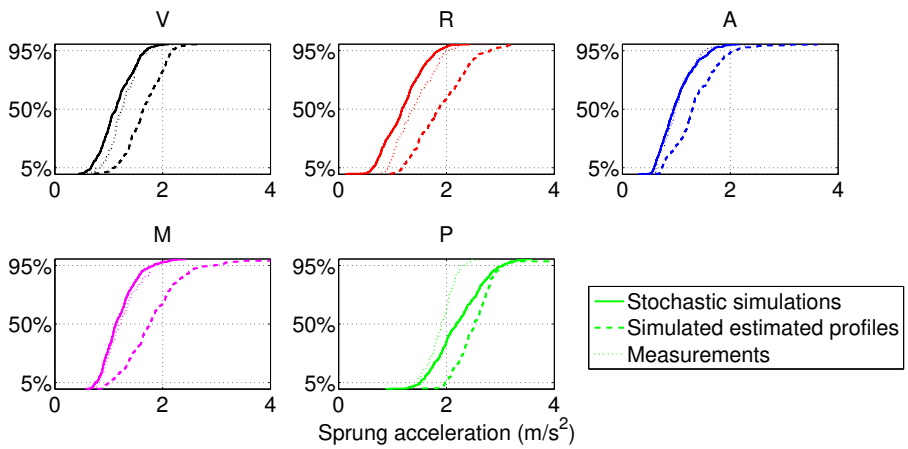

Figure F.2: Comparisons of predicted and measured distributions: Sprung acceleration.

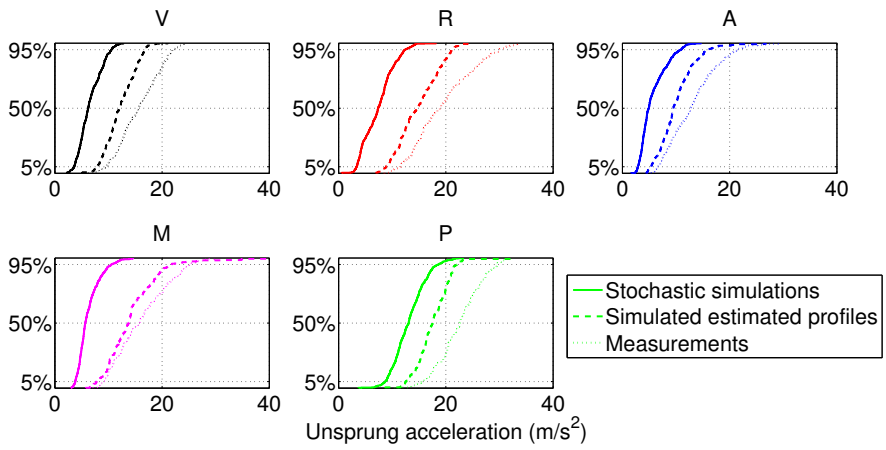

Figure F.3: Comparisons of predicted and measured distributions: Unsprung acceleration.

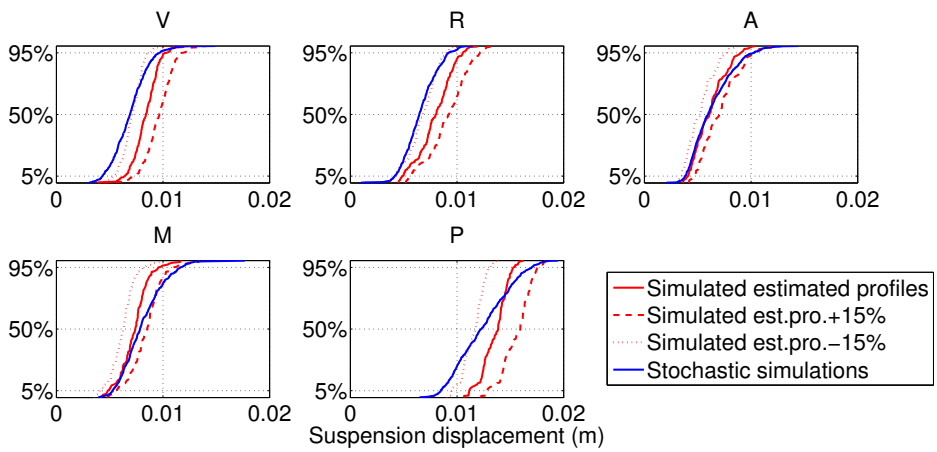

Figure F.4: Overall quality of the methodology: suspension displacement.

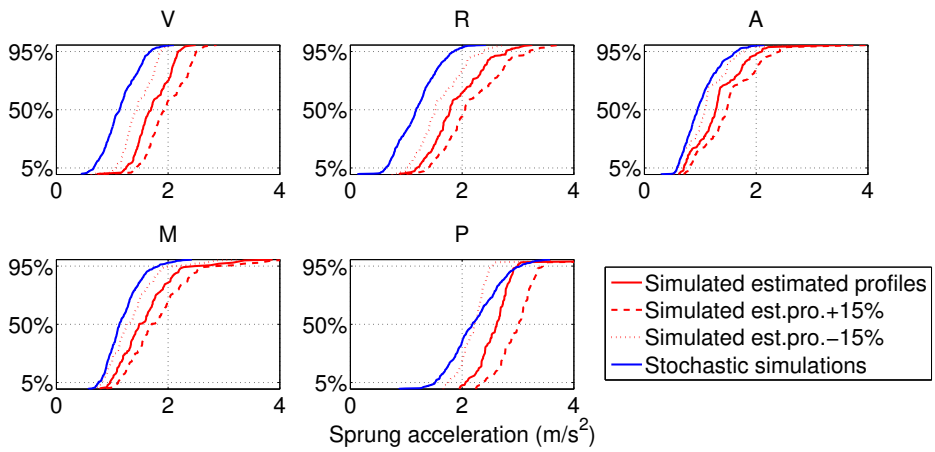

Figure F.5: Overall quality of the methodology: Sprung acceleration.

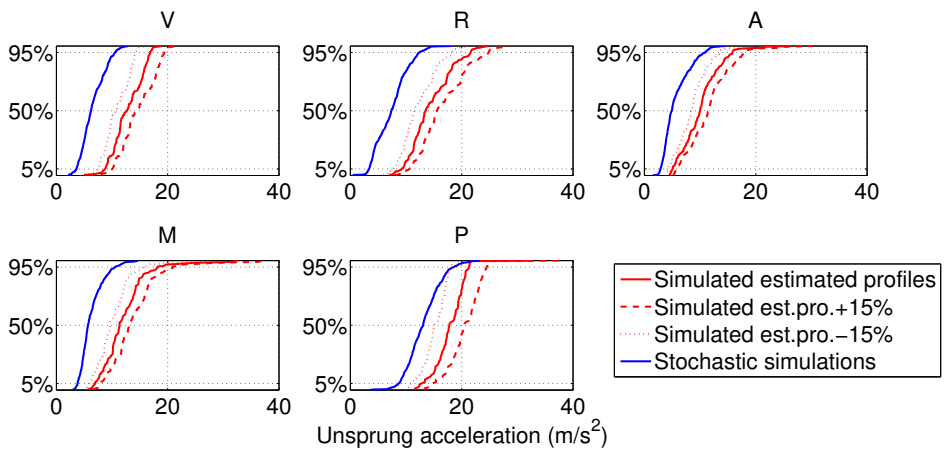

Figure F.6: Overall quality of the methodology: Unsprung acceleration.

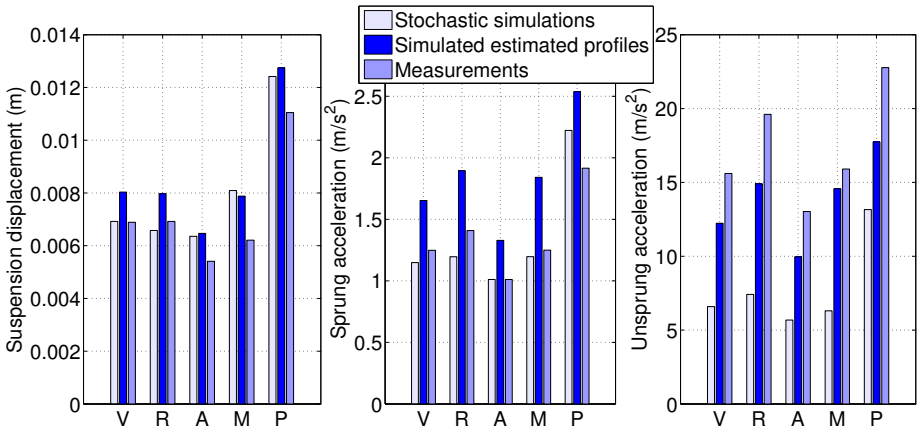

Figure F.7: Testing of the methodology: comparison of mean values, country A.

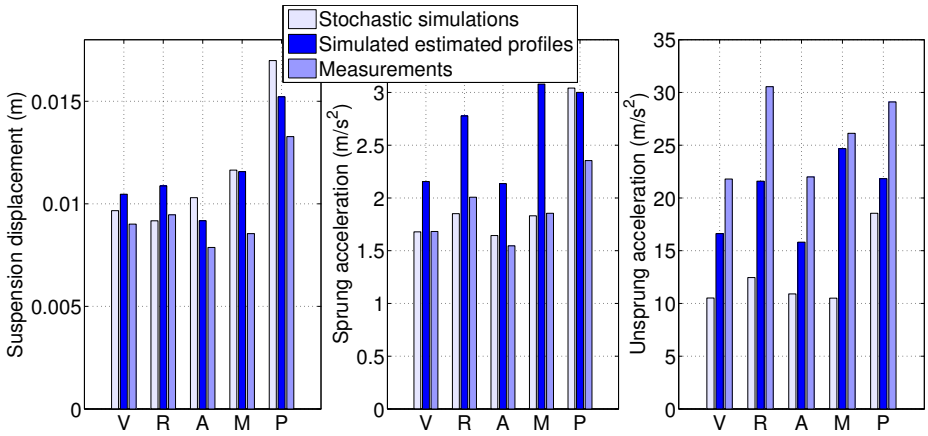

Figure F.8: Testing of the methodology: comparison of 95% quantiles, country A.

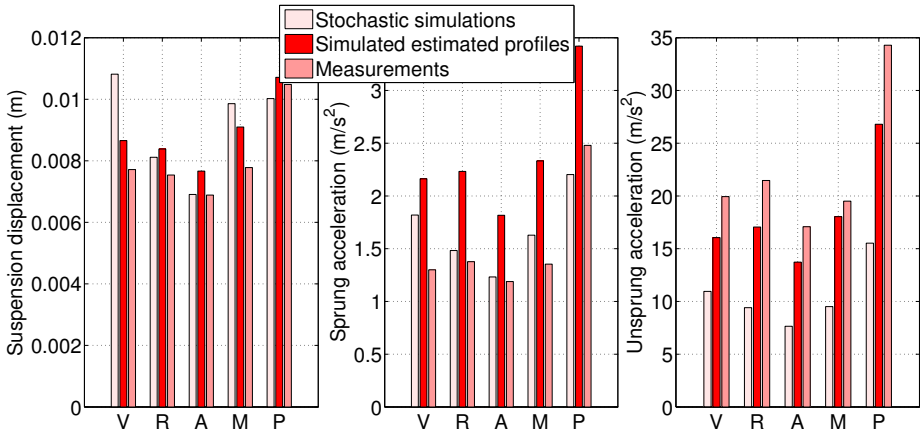

Figure F.9: Testing of the methodology: comparison of mean values, country B.

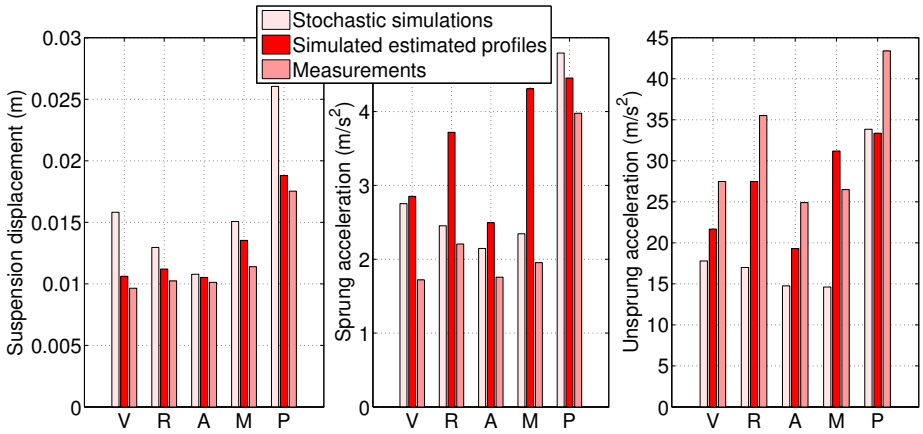

Figure F.10: Testing of the methodology: comparison of 95% quantiles, country B.

Life situ.	Resp.	Stochastic simulations	Simulated est.profiles	Measured loads	% error col1/col2	% error col2/col3	% error col1/col3
V		0.0069	0.0080	0.0069	-13.8%	16.6%	0.5%
R		0.0066	0.0080	0.0069	-17.5%	15.1%	-5.0%
A	$z_s z_t$	0.0064	0.0065	0.0054	-1.7%	19.5%	17.5%
M		0.0081	0.0079	0.0062	2.7%	26.9%	30.3%
P		0.0124	0.0127	0.0110	-2.5%	15.3%	12.4%
V		1.15	1.65	1.25	-30.5%	32.4%	-8.0%
R		1.20	1.90	1.41	-36.9%	34.5%	-15.1%
A	a_s	1.01	1.33	1.01	-23.9%	31.4%	0.0%
M		1.20	1.84	1.25	-35.0%	47.3%	-4.2%
P		2.22	2.54	1.92	-12.4%	32.5%	16.1%
V		6.59	12.24	15.60	-46.5%	-21.6%	-57.7%
R		7.42	14.90	19.61	-50.2%	-24.0%	-62.2%
A	a_t	5.68	9.96	13.03	-43.0%	-23.5%	-56.4%
M		6.31	14.57	15.91	-56.7%	-8.4%	-60.3%
P		13.16	17.74	22.77	-25.8%	-22.1%	-42.2%

Table F.1: Testing of the methodology: comparison of mean values, country A.

Life situ.	Resp.	Stochastic simulations	Simulated est.profiles	Measured loads	% error col1/col2	% error col2/col3	% error col1/col3
V		0.010	0.010	0.009	-7.7%	16.2%	7.3%
R		0.009	0.011	0.009	-15.6%	14.9%	-3.1%
A	$z_s z_t$	0.010	0.009	0.008	12.3%	16.5%	30.8%
M		0.012	0.012	0.009	0.7%	35.4%	36.2%
P		0.017	0.015	0.013	11.6%	14.6%	27.9%
V		1.68	2.16	1.68	-22.1%	28.1%	-0.2%
R		1.85	2.78	2.01	-33.3%	38.4%	-7.8%
A	a_s	1.64	2.14	1.55	-23.0%	38.1%	6.3%
M		1.83	3.08	1.86	-40.5%	66.0%	-1.3%
P		3.04	3.00	2.35	1.4%	27.5%	29.2%
V		10.52	16.62	21.79	-36.7%	-23.8%	-51.7%
R		12.45	21.59	30.55	-42.3%	-29.3%	-59.2%
A	a_t	10.90	15.81	21.99	-31.0%	-28.1%	-50.4%
M		10.50	24.67	26.13	-57.4%	-5.6%	-59.8%
P		18.55	21.83	29.10	-15.0%	-25.0%	-36.3%

Table F.2: Testing of the methodology: comparison of 95% quantiles, country A.

Life situ.	Resp.	Stochastic simulations	Simulated est.profiles	Measured loads	% error col1/col2	% error col2/col3	% error col1/col3
V		0.0108	0.0087	0.0077	24.9%	12.2%	40.2%
R		0.0081	0.0084	0.0075	-3.2%	11.2%	7.7%
A	$z_s z_t$	0.0069	0.0077	0.0069	-9.9%	11.3%	0.3%
M		0.0099	0.0091	0.0078	8.3%	16.9%	26.7%
P		0.0100	0.0107	0.0105	-6.5%	2.2%	-4.4%
V		1.82	2.16	1.30	-15.9%	66.3%	39.9%
R		1.48	2.23	1.38	-33.6%	62.1%	7.6%
A	a_s	1.23	1.82	1.19	-32.2%	52.9%	3.7%
M		1.63	2.33	1.35	-30.2%	72.3%	20.3%
P		2.20	3.42	2.48	-35.6%	37.9%	-11.1%
V		10.95	16.05	19.94	-31.8%	-19.5%	-45.1%
R		9.41	17.05	21.47	-44.8%	-20.6%	-56.2%
A	a_t	7.65	13.73	17.09	-44.3%	-19.7%	-55.2%
M		9.52	18.04	19.51	-47.3%	-7.5%	-51.2%
P		15.52	26.79	34.29	-42.1%	-21.9%	-54.7%

Table F.3: Testing of the methodology: comparison of mean values, country B.

Life situ.	Resp.	Stochastic simulations	Simulated est.profiles	Measured loads	% error col1/col2	% error col2/col3	% error col1/col3
V		0.0158	0.0106	0.0096	49.0%	10.0%	64.0%
R		0.0130	0.0112	0.0102	15.7%	9.4%	26.6%
A	$z_s z_t$	0.0108	0.0105	0.0101	2.4%	3.9%	6.4%
M		0.0151	0.0135	0.0114	11.3%	18.8%	32.2%
P		0.0260	0.0188	0.0175	38.6%	7.2%	48.6%
V		2.75	2.85	1.72	-3.5%	65.8%	60.0%
R		2.45	3.72	2.21	-34.0%	68.6%	11.2%
A	a_s	2.15	2.50	1.76	-14.0%	42.0%	22.1%
M		2.35	4.31	1.95	-45.6%	120.6%	20.1%
P		4.79	4.45	3.98	7.6%	12.0%	20.5%
V		17.79	21.67	27.48	-17.9%	-21.1%	-35.2%
R		16.99	27.48	35.51	-38.2%	-22.6%	-52.1%
A	a_t	14.76	19.30	24.90	-23.5%	-22.5%	-40.7%
M		14.61	31.19	26.49	-53.1%	17.8%	-44.8%
P		33.85	33.36	43.39	1.5%	-23.1%	-22.0%

Table F.4: Testing of the methodology: comparison of 95% quantiles, country B.

F.2 Comparison of the predicted and measured load sensitivity

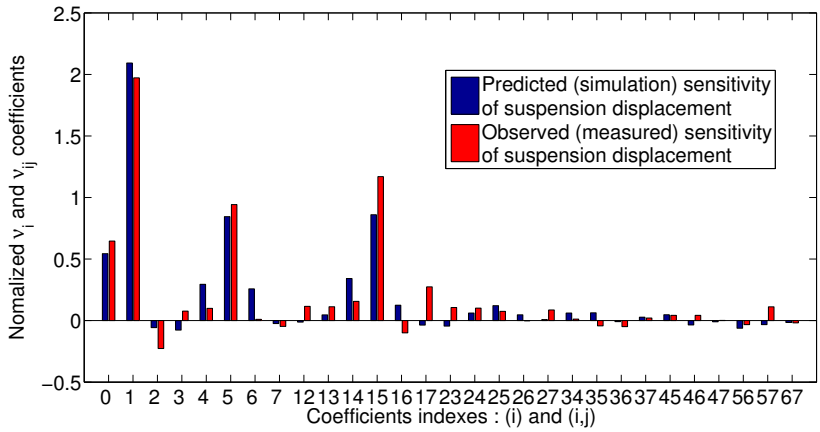

Figure F.11: Coefficients of simulation and measurement-based response surfaces for suspension displacement.

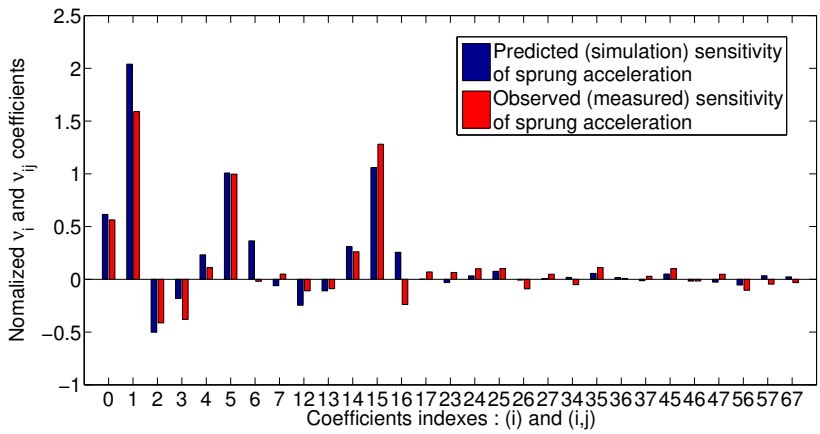

Figure F.12: Coefficients of simulation and measurement-based response surfaces for sprung acceleration.

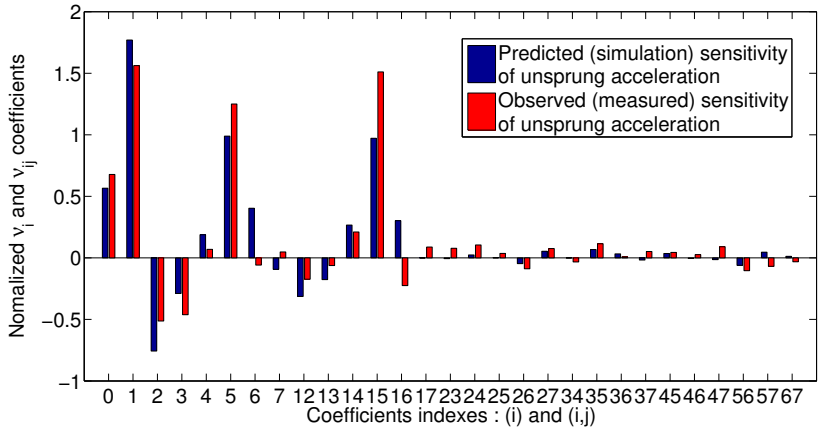

Figure F.13: Coefficients of simulation and measurement-based response surfaces for unsprung acceleration.

F.3 Comparison of the predicted and measured load lives of vehicles

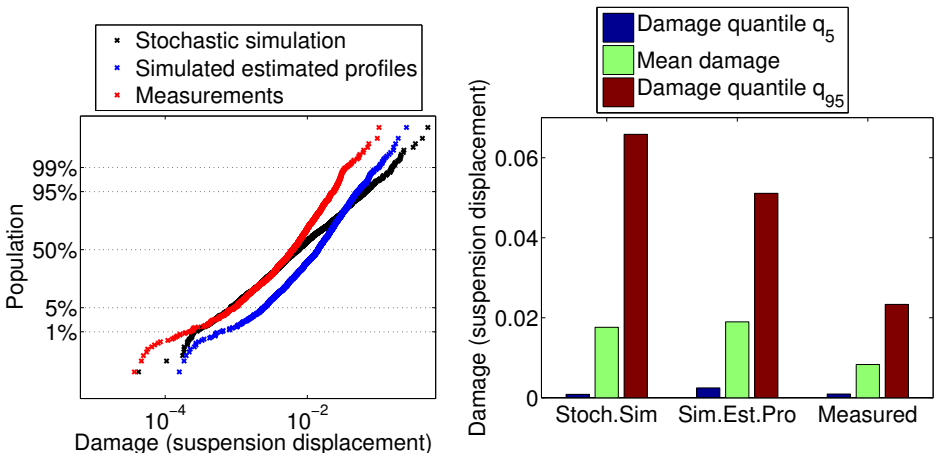

Figure F.14: Predicted variability of the load lives of a population vehicles, for suspension displacement. The three types of responses in figure 5.7 are used as inputs to make the predictions and the comparison is displayed. Country A.

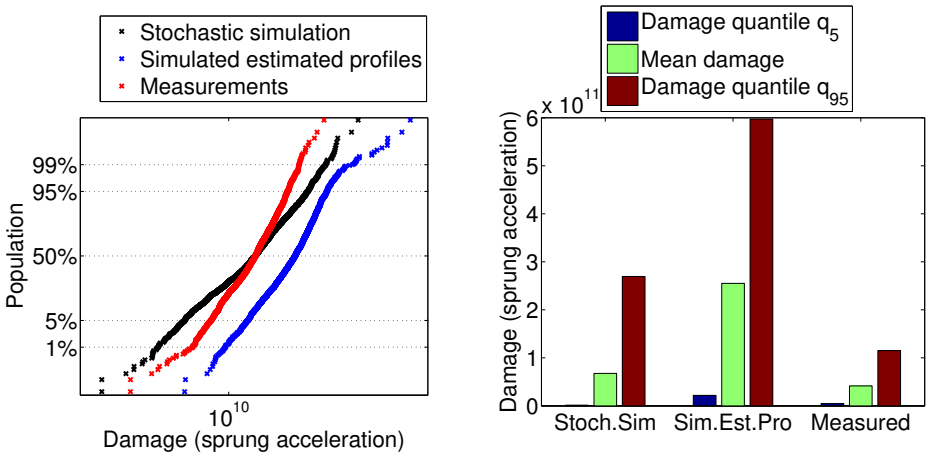

Figure F.15: Predicted variability of the load lives of a population vehicles, for sprung acceleration. The three types of responses in figure 5.7 are used as inputs to make the predictions and the comparison is displayed. Country A.

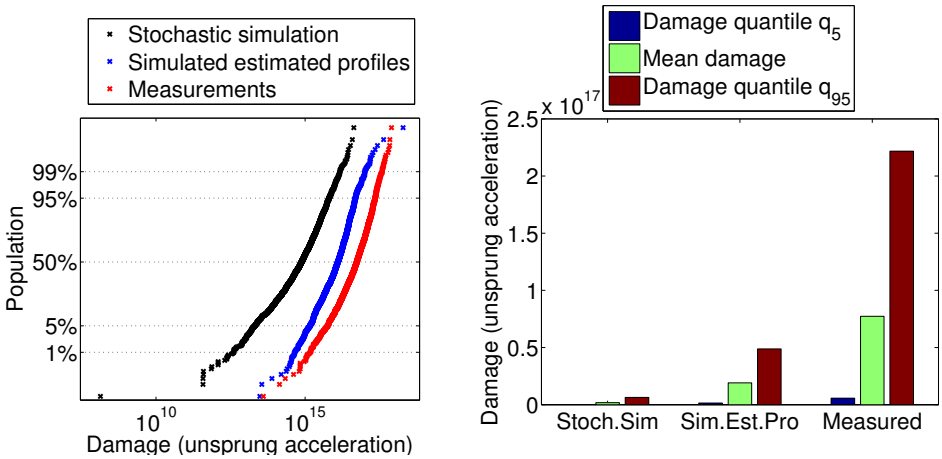

Figure F.16: Predicted variability of the load lives of a population vehicles, for unsprung acceleration. The three types of responses in figure 5.7 are used as inputs to make the predictions and the comparison is displayed. Country A.